THÈSE

En vue de l'obtention du

DOCTORAT DE L'UNIVERSITÉ DE TOULOUSE

Délivré par :

Institut National Polytechnique de Toulouse (INP Toulouse)

Discipline ou spécialité :

Sciences des Agroressources

Présentée et soutenue par :

M. THIBAUD PINTIAUX

le vendredi 27 mars 2015

Titre :

ETUDE D'UN PROCEDE DE MISE EN FORME DE MATIERES NATURELLES LIGNOCELLULOSIQUES PAR THERMOCOMPRESSION UNIAXIALE HAUTE PRESSION

Ecole doctorale :

Sciences de la Matière (SDM)

Unité de recherche :

Laboratoire de Chimie Agro-Industrielle (L.C.A.)

Directeur(s) de Thèse :

M. LUC RIGAL

M. ANTOINE ROUILLY

Rapporteurs :

M. BERTRAND CHARRIER, UNIVERSITE DE PAU ET DES PAYS DE L ADOUR

M. PATRICE DOLE, INRA REIMS

Membre(s) du jury :

Mme CHRISTELE COMBES, INP TOULOUSE, Président

M. LUC RIGAL, INP TOULOUSE, Membre

Table of contents

I Literature review: binderless materials obtained by thermo-compressive processing of lignocellulosic fibers 9
I.1 An overview of the mechanical properties and water resistance of self-bonded materials obtained by thermo-compressive processing of plant fibers 12
I.1.A Mechanical properties of self-bonded thermo-compressed plant materials 12
Boards-type, low pressure molding 14
High pressure, plastic-substitute type, cellulose processing 14
I.1.B Water resistance of self-bonded thermo-compressed plant materials 15
I.2 The effects of plant materials origin on the molded specimens 17
I.2.A Reported Molded Materials 17
I.2.B Different parts of plants 18
Type of plant tissue, cell wall structure and composition 18
Particle geometry and the need of steam treatment 18
Remnants of storage polymers and agroindustrial by-products 19
Mixing / structural associations 19
Contribution of lignin to water resistance 19
Contribution of hemicelluloses to water sensitivity 20
I.3 The use of steam in plant material processing 20
I.3.A The use of steam as a pretreatment: effects and optimal conditions on molded specimens 22
Mild severity optimum for strength 22
High severity decreases MOR and MOE but is positive for IB and water resistance 22
Steam pretreatment, flow behaviour and molding capability 23
I.3.B Steam as a processing aid: effects and optimal conditions 24
Steam atmosphere pressing 24
Steam injection pressing 24
Steam injection pressing, water resistance and boards' thickness 25
I.4 Thermo-compressive process parameters and their effect on properties of molded specimens 26
I.4.A Molding pressure 26
Clarification of the relationship between pressure / density / target density 26
Effect of pressure: Board manufacture with target density 26
Effect of directly applied pressure (pressure control) 27
High-pressure molding 28
Effect of pressure on pure cellulose molding 29
I.4.B Moisture content 29
Temperature gradient, moisture, time and heat transfer 30
I.4.C Temperature 31
Effect of pressing temperature on non-treated and steam treated materials 31
Delamination process a conjugated effect of temperature and moisture content 33
Pressing temperature and steam assisted molding 33
Pressing temperature, time and water resistance 34
Skin effect 34
Effect of temperature in the particular case of free sugars containing materials 34
Effect of temperature in the particular case of bark 34
I.4.D Time 35
I.4.E Granulometry 35
I.5 The physico-chemical changes and mechanisms of cohesion in self-bonded thermo-compressed plant materials 36

I.5.A Physical changes ... 37
Change of color ... 37
Steam treatment and defibration ... 37
Production of fines ... 37
I.5.B Non-lignocellulosic parts chemical changes and effects ... 38
Weight loss, extractives and elimination of degradation products ... 38
I.5.C Cellulose and hemicelluloses changes ... 38
Cellulose and hemicelluloses degradation ... 38
Correlation of cellulose and hemicelluloses content and the physical properties ... 39
Furfural and hydroxymethyl furfural routes hypothesis ... 39
I.5.D Lignin changes ... 40
Observation of lignin flow after steam pretreatment and matrix effect ... 40
Lignin modification / degradation ... 41
Lignin softening and “activation” ... 43
I.5.E Mechanisms of cohesion ... 43
Glass transition of cell-wall polymers ... 44
Cross-linking of lignin-carbohydrate-complex (LCC) ... 45
Hydrogen bonding and cocrystallisation of cellulose as a consolidation mechanism ... 45
II Preliminary discussion about technical considerations ... 49
II.1 Project HYPMOBB: where it all begun ... 49
II.2 Compaction molding, principle, design and terms ... 50
II.2.A Two dimensions molding ... 50
II.2.B Three dimensions molding ... 50
II.3 Limits of compaction molding applied to lignocellulosic fibers ... 51
II.3.A Limited shapes, not actual 3D ... 51
II.3.B Demolding ... 52
II.3.C Homogeneous filling of the mold cavity ... 53
II.3.D Mold filling and flow behavior ... 55
II.3.E Steam explosion, delamination ... 57
II.3.F Shear and steam explosion ... 60
II.4 Transfer molding ... 60
II.4.A Principle ... 60
II.4.B Advantages over compaction molding and drawbacks ... 61
II.5 Other technical locks ... 61
II.5.A Moisture adjustment ... 61
II.5.B Particle size ... 62
II.5.C Machining, thermal dilatation and seizing of molds ... 62
III Study on a model polymer: α-cellulose ... 63
III.1 The different ways to process cellulose into solid material ... 63
III.1.A Native cellulose structure ... 63
III.1.B Cellulose polymer basic properties ... 66
Paracrystalline organization ... 66
Fusion temperature ... 66
Glass transition temperature ... 67
Thermal decomposition ... 67
III.1.C Cellulose to solid materials processing routes ... 68
Paper and other water suspension processes ... 68
Solubilization process ... 70
Compaction molding ... 71
III.2 Behavior of compressed cellulose under various operating condition ... 73
III.2.A Methodology and control conditions ... 73

III.2.B Effect of mass loaded in the mold ... 75
III.2.C Effect of processing time ... 76
III.2.D Effect of cellulose moisture content ... 77
III.2.E Effect of pressurization speed ... 78
III.2.F Effect of temperature ... 79
III.2.G Effect of pressure ... 81
III.3 The cliff behind the hill: investigating the interdependency of temperature and moisture content on the mechanical properties and delamination ... 82
III.3.A Delamination mapping ... 82
III.3.B Color scale ... 84
III.3.C Mechanical properties mapping ... 84
III.4 Correlation of equilibrium moisture content and density of the compressed specimens ... 87
III.5 Humid atmosphere, water and time properties of compaction molded α-cellulose specimens ... 88
III.5.A Humid atmosphere behavior ... 88
III.5.B Water resistance measurements ... 88
III.6 Time stability of compressed specimens ... 89
III.7 Discussion: about the structure / property relationship of compacted cellulose specimens 91
III.7.A The specimens' structure as a result of the compaction process ... 91
A laminated structure ... 91
A marked surface effect ... 93
III.7.B Mechanisms of cohesion ... 97
The structural changes during compaction molding ... 97
The central role of water ... 98
III.8 α-cellulose flowability investigation trials (Nagoya) ... 100
IV Pressure and heat catalyzed esterification for the hydrophobation of compressed cellulose materials ... 105
IV.1 Preliminary results, mapping of fatty compounds ... 105
IV.2 High-pressure driven solvent-free heterogeneous phase esterification of cellulose ... 111
IV.2.A List of Experiments ... 111
IV.2.B Results ... 113
IV.2.C Discussion ... 114
V The processing of native plant materials ... 117
V.1 Physico-chemical analyses of the native plant materials ... 117
V.2 Evaluation of the flowability of the different materials ... 120
V.3 The influence of the volume/surface ratio ... 122
V.3.A 50 x 50 mm square molding as a preliminary study ... 122
V.3.B Dog-bones specimen molding from the native plant materials ... 123
Molding in reference conditions (175°C – 60 % RH equilibrium) ... 123
Molding in alternative conditions (250°C – 0% MC) ... 125
V.4 Analysis of "compaction molding set" results ... 127
V.4.A Summary of results ... 127
Missing values ... 127
Inspection of variable ranges ... 128
V.4.B Statistical analysis ... 129
V.5 Transfer molding or compaction molding: The perspectives of a promising processing route ?134
V.5.A The limitations of compaction molding ... 134
V.5.B Exploratory results on the mechanical properties evaluation of extruded materials 134
Principle ... 134

Results 136
VI Materials and methods 156
VI.1 Starting materials and chemicals 156
VI.1.A Cellulose 156
VI.1.B Hydrophobating agents (Chapter IV, part IV.1) 156
VI.1.C Esterification reagents (Chapter IV, part IV.2) 156
VI.1.D Native plant materials 156
VI.2 Preparation methods 157
VI.2.A Thermo-mechanical refining 157
VI.2.B Grinding 159
VI.2.C Moisture conditioning and dynamical vapor sorption 159
VI.3 Methods of analysis for physic-chemical properties of plant materials 160
VI.3.A Physical parameters 160
Apparent density of the powder (tapped density) 160
Particle size distribution 160
Form factor profile 160
VI.3.B Chemical composition 161
Moisture content 161
Mineral matter 161
Total lipids 161
Protein content 161
Lignocellulosic constituents 162
Total polyphenols 163
Thermo-compressive molding 163
Pressing machines 163
2D molding 163
3D molding 165
Molding cycle 165
Molding pressure 166
Flow test apparatus (Nagoya) – Chapter III 167
Transfer molding and flow tests (Toulouse) – Chapter V 167
VI.3.C Thermo-compressed material specimens evaluation 169
SEM Observations 169
Specific Gravity and moisture equilibrium measurements 170
Tensile and 3 Points Bending Tests 170
VI.3.D Statistical analysis (Chapter V) 172
VI.3.E Methods for performing and studying the esterification in high pressure molding conditions (Chapter IV part 2) 173
Liquid solid separation 173
Materials pretreatments for solid-liquid pre-contact 173
Reactant removal prior to analysis 173
IR Analysis 173
Drop angle determination method 174
Degree of substitution (cellulose) and grafting rate measurements 174

General introduction

The majority of the convenience goods are based on plastics that are produced from fossil oil. Their convenient implementation makes them the perfect material for packaging and short life products. Due to their low density plastic trashes are all over the planet and accumulate because of a low degradability which became a serious source of pollution in the last decades. This, associated to the upcoming depletion of fossil oil in a near future created a need for bio-degradable (reducing pollution) and bio-based (independence from fossil oil) plastic substitutes.

Fragmenting polymers (oxo-fragmenting, bio-fragmenting) have first been designed in order to reduce the visual pollution, but this solution was rapidly criticized because of the dissemination of micro and nano-particles all over the biosphere that could not be recovered from the soil and water they were dispersed in. In the last decades, biodegradable polymers have become a reality with the industrial scaling up of PLA (polylacticacid) production which was furthermore bio-based. With help of the biotechnologies, other bio-based polymers were invented like PHA's (polyhydroxylalkanoates) for instance. These productions were dependent on crops and biotransformation, which took some time to become industry-viable, and by this time, other bio-degradable polymers like PBAT (polybutyleneadipate co terephthalate) were developed from fossil oil, which have rapidly been more easily available, with secured supply and easier processability. More recently, partially or totally bio-based replacement for classic plastics has also been designed with the idea of independence from fossil oil and production of durable material that would be easily recycled for example bio-PVC (polyvinylchloride), bio-PE (polyethylene) and PEF (polyethylenefuranoate, alternative to PET – polyethyleneterephthalate). This tendency considers that in some cases plastic re-use could be more eco-efficient than biodegradation. Finally, native polymers (i.e. polymers naturally occurring in nature) have gain interest especially starch that rapidly found industrial applications, purified or in whole plant version (for example Mater-bi, or the whole plant maize plastic alternative produced by Vegeplast in France). Proteins crops residues like sunflower are also close to find industrial application.

The possibility of finding natural thermoplastic polymers (if verified to be biodegradable) appeared a great opportunity for reducing pollution and fossil oil dependency… until the competition between food and convenient goods (plastic but also fuels) on the food-use was considered. One last possibility could be in the focus on agricultural wastes and non-edible parts of plants like straws and other residues that are mostly composed of ligno-cellulosic compounds.

Paper is a bio-based, bio-degradable material that is known for centuries and which matches most of the eco-requirements although the pollution of wastes due to cellulose extraction (pulping process) is disputable. A modern development of paper conducted to Zelfo, which was obtained upon a more advanced separation of cellulose fibers by Zellform GesmbH in the 1990's (Döpfner et al. 1997). Cohesion is obtained, like paper, by hydrogen bonding established when water evaporates. Micro-fibrillation provides enhanced mechanical properties to Zelfo, but time and/or energy costly drying and consequent shrinkage of objects upon drying are important drawbacks that did not permit an industrialization, even after the glorious work of Omodo Gmbh in the 2000's that conducted to win the "Biomaterial of the year 2011" prize at the Nova institute international congress on bio-plastics (Cologne, Germany).

In 2007, the young company "The Green Factory" bought a license to Omodo with the idea of starting research collaboration in order to develop and possibly industrialize the Zelfo. Omodo and TGF became partner short after and worked together on the production of Zelfo using twin screw extruders for increased efficiency and lowered costs. Another partner was found with the LCA, which has been working for decades on the bio-refinery of agricultural wastes and other biomasses, and with some experience in the thermo-mechanical treatment and thermo-forming of lignocellulosic materials remaining after extractions of other interesting compounds. From this collaboration begun some first experiments and a patent

(WO2012069736, Rouilly et al. 2012) concerning was deposited before the beginning of this thesis in co-ownership between the INPT (National Polytechnic Institute from Toulouse) and The Green Factory. Short after this first collaboration was born this ANRT (French National Agency for promoting Research and Technology) PhD thesis: *Study of a thermo-compression-process for the molding of natural lignocellulosic materials without pretreatments or binders*. The idea was to study the possibilities of thermo-compression as a single step molding technique for the processing of lignocellulosic residues into simple, raw, yet valuable materials and possibly work towards the development of a new molding route for Zelfo. Meanwhile, an ANR (National research agency) project (HYPMOBB, High Pressure Molding of Biopolymers and Biomolecules) started in the laboratory which comprised a PhD thesis directed towards the study of the behavior of starch and cellulose under mechanical pressure (Jallabert 2014, PhD thesis).

Five chapters compose this PhD work thesis:

The first chapter contains a literature review over the thermo-compression molding of lignocellulosic materials which has been published recently (Pintiaux et al. 2015). The analysis of the literature permitted to consider the important parameters to analyze in the processing of plant materials by thermo-compression molding. Some inspiration was also taken for designing apparatus and techniques.

Chapter II presents a technological discussion around the "thermo-compressive molding". This thesis consisted in a lot of prototyping and technological research around the thermo-compression molding, and thus it is important for the reader to take note of this first part before getting to the results.

Although being the major constituent of plant, very few results existed on the processing of pure cellulose by thermo-compression in the literature. Chapter III is an extensive study of the thermo-compression of pure cellulose, chosen as a model polymer in the early stages of this thesis. The influence of the molding parameters have been examined separately, and results published in a first paper (Pintiaux et al. 2013). Based on these first results, following studies were run on the pressure response, water properties and the temperature / moisture couple which was identified as the most impacting parameter. In regard to the results obtained in the PhD thesis of Jallabert, hypotheses are drawn towards the explanation of a new kind of cohesion mechanism.

Chapter IV gathers results obtained towards the improvement of the water resistance of materials obtained by the thermo-compression of cellulose with fatty compounds added as hydrophobating agents. After a first mapping on the potential compounds, a deeper study was performed on a very specific case in order to investigate the actual grafting of one hydrophobic compound on cellulose during the thermo-compression process.

In chapter V, the influence of other compounds than cellulose on the properties of the resulted thermo-compressed specimens was studied, based on a mapping of several plant materials collected on other projects in the laboratory. Although encountering some technical troubles, statistical analyses permitted to draw some conclusions about the necessary features of plant materials for being molded into valuable materials using compaction molding and a methodology was investigated towards the production of these materials using transfer molding.

The references cited, materials and methods chapter and the tables of figures are presented at the end of this manuscript.

Abbreviations

σ_f: Flexural strength at break, bending strength at break (MPa)
σ_t: Tensile strength at break (MPa)
AIST: Aishi Institute of Science and Technology, host laboratory for the JSPS internship.
cont.: is used as an abbreviation for content, when needed
CEF: Cellulose elementary fiber
DMA: Dynamical Mechanical Analysis
DP: Degree of Polymerization
DS: Degree of Substitution
DSC: Differential scanning calorimetry
E_f: Flexural modulus, bending modulus (GPa)
E_t: Tensile modulus (GPa)
GR: Grafting Yield
IB: Internal bonding
LCA: Laboratory of Agroindustrial Chemistry, host laboratory
MC: Moisture Content
MFC: Microfibrillated cellulose
MOR: modulus of rupture, equivalent to bending strength at break.
MOE: modulus of elasticity, most of the time corresponds to the bending modulus
NFC: Nanofibrillated cellulose
OA: Octanoïc acid
OAn: Anhydride octanoïc
PC: Principal Component
PCA: Principal Components Analysis
RH: Relative Humidity
SG: Specific Gravity, also density (g/cm^{-3})
TGA: Thermo-gravimetric analysis
TGF: The Green Factory, financing company, changed name to Zelfo technology
TS: thickness swelling, percentage of thickness increase, measured on a 50 mm square sample after 24 hours dipped in 20°C water
WA: water absorption, percentage of mass increase during the TS test

I Literature review: binderless materials obtained by thermo-compressive processing of lignocellulosic fibers

Plants cell walls can be regarded as being high-end engineered nano-scale composites basically composed of cellulose, lignin, and hemicelluloses (Rose 2003). The supra-molecular organization in the plant cell wall provides fascinating unique mechanical properties (Niklas et al. 2006). Being the basic constituent of plants and because very few organisms can degrade it, cellulose is the most widely occurring polymer on planet earth. This polymer, made of ß-1-4 linked D-hydroxyglucopyranose, has an extraordinarily strong and rigid molecular design. The macroscopic Young's modulus of plant cellulose has been measured at 128 GPa (Page et al. 1971), which is higher than aluminum (70 GPa) or glass fibers (76 GPa) (Lo and Hoa 2006). The Young's modulus of the crystal of cellulose has been estimated to be 138 GPa (Sakurada et al. 1962). With low density and high mechanical performance, it provides amazing strength and growth possibilities to plants e.g. trees of 115 meters height (sequoia sempervirens, Redwood national park, California, USA) and 14.4 meters of diameter (taxodium mucronatum, Arbol del Tul, Oxaca, Mexico) can be found. Bamboo for example is a well-known strong and fast-growing plant widely used for small constructions in Asia. All civilizations have worked with wood or other plant materials to build tools, furniture, housing and many sorts of goods.

A comparison of mechanical properties of synthetic and natural fibers is provided in Table I - 1 (Eichhorn et al. 2001). It shows that plant fibers from diverse origins have various mechanical properties, and they can in some cases compete with glass fibers, if their relative densities are taken into consideration.

Table I - 1: Properties of different plant fibers and synthetic fibers, adapted from Eichhorn et al. (2001)

Fibre	Density (g.cm^{-3})	Elongation at break (%)	Tensile strength (MPa)	Young's modulus (GPa)
Cotton	1.5-1.6	7-8	287-597	5.5-12.6
Jute	1.3	1.5-1.8	393-773	26.5
Flax	1.5	2.7-3.2	345-1035	27.6
Hemp	-	1.6	690	-
Ramie	-	3.6-3.8	400-938	61.4-128
Sisal	1.5	2-2.5	511-635	9.4-22
Coir	1.2	30	175	4-6
Viscose (cord)	-	11.4	593	11
Soft wood Kraft	1.5	-	1000	40
E-glass	2.5	2.5	2000-3500	70
S-glass	2.5	2.8	4570	86
Aramid (normal)	1.4	3.3-3.7	3000-3150	63-67
Carbon	1.4	1.4-1.8	4000	230-240

Furthermore, plant fibers are renewable, biodegradable, and safe for humans and the environment. Using natural fibers instead of petroleum-based material or highly consuming energy materials such as concrete or metal alloys is highly promising for reducing the greenhouse effect and drastic climate change as well as not contributing further to today's immense plastic waste environmental pollution (Lebreton et al. 2012).

Of course, interest in the use of natural fibers for materials has been motivated by raising environmental consciousness. Such interest is revealed by the number of scientific articles related to the introduction of plant fibers in composites using a classical thermoplastic matrix (e.g. PVC, PE), which could also be partially bio-based (biobased PE / PVC) to produce partially bio-based composites (Faruk et al. 2012), and also with a

biodegradable matrix to produce fully biodegradable composites (e.g. PLA, PBAT, PHA's) even on a nano-scale (Reddy et al. 2013).

Another option is the use of plant fibers in a natural bio-based and biodegradable matrix, e.g. starch or proteins to create a 100% bio-based and biodegradable composite product (Rouilly and Rigal 2002). The fact that every thermoplastic biopolymer comes from edible resources for humans has raised ethical problems because of the possible land-use competition between food and convenience goods. Therefore, 100% lignocellulosic fibers materials have to be designed based on agricultural wastes such as cereals straws, oilseed cakes, etc.

Wood is also the input material of another huge industry: paper and its derivatives, wherein water suspensions of wood fibers (pulps) are processed by squeezing and drying. These "wet processes" will not be reviewed here. Neither will the solubilization processes be considered (e.g. Lyocell, Carbamate), on which a review was recently published (Fink et al. 2014). Pharmaceutical tablets that contain cellulose or starch as excipient will also be omitted because of the differences of process (ram compression, cold processing to prevent damage to the active components, and size of the molded objects).

Wood processing includes many technologies to cut, machine, deform, and assemble pieces of wood without any additives, which produce eco-friendly materials, until the wastes (saw dust, useless cuts, etc.) are considered. Saw dust and wood particles used to be mainly burnt and composted (both disposal techniques released CO2 to the atmosphere), but today they more and more enter in processes to be assembled with binders or polymers to form boards or more recently wood-polymer composites (WPC). Thermoset resins are based on fossil resources, and most of them are formaldehyde-based, resulting in emissions of formaldehyde from the final products with potential harm to customers and the environment (Tunga Salthammer et al. 2010). The replacement of resins is also considered for economic reasons because of the increasing part of resins in the cost of particleboard production (Hashim et al. 2010), and even the recycling of the formaldehyde from waste wood-based panels has been considered .

The situation just described provides reasons for the recent spike in researchers' interest in pursuing studies on the processing of various plant materials into boards without the use of additives, binders, resins, or chemical modifications, which is precisely the aim of this literature review. This work will then focus on the thermo-compressive processing of non-modified plant fibers without additives. Because of the interaction of parameters one to the others and with water (which plays a major role) and because of the high diversity of compositions and complicated structures of plant fibers, attention has been placed on isolating parameters and effects, and precise research facts have been reported here in order to highlight past achievements and future directions.

Definitions

In the wood-based panel industry, particleboard (PB) products mainly are made from wood particles (chips) recycled from wastes that are glued together with petroleum-based binders. Oriented strand boards (OSB) are quite similar but the wood particles that compose them are bigger with a particular flat geometry, i.e. like flakes. Fiberboards (FB) on the other hand, are made from wood fibers, thinner elements that have been first separated in a refiner. Finally, hardboards (HB) are produced from steam-exploded wood particles and, if they are subjected to a wet process (Masonite) they do not require binders.

While the materials and processing conditions used in present-day production of particleboard, strand board, and fibreboard products can provide a practical point of focus for this review, some of the best evidence regarding the mechanisms underlying the successful preparation of binderless board products can be found outside of the scope of conventional wood-based panel manufacturing. Indeed, most of the research works gathered during the preparation of this review did not employ wood and had experimental conditions that would

not fit the wood-based panels standards (e.g. higher density, longer pressing time, and higher temperature). This article focus on collecting the technological possibilities to produce self-bonded lignocellulosic materials and explanations about the self-bonding mechanisms, for which it is important to take into consideration all types of boards and confront the results (e.g. differences and commonality between steam pretreatment, steam injection, and no-steam processing). The mechanisms of cohesion in the different types of binderless boards are assumed to be comparable; thus, when possible, the term "binderless particleboards" (no refining) have been used as well as "binderless fiberboard" when a refining step was present. If reported panels do not fit in a category, or when the elements concern all types of boards, the generic term "boards" has been used.

In addition, a distinction will be made between steam-pretreated binderless boards, which in most cases are indeed in the fiberboards type, and those which are not. Most of the examples that enter the category of "non-steamed" boards would be in the particleboards type.

Usually boards are "pressed" (at low pressure) and 3D objects are "molded" (at higher pressure) but, because the mechanisms of cohesion are discussed against pressure and since selfbonding of "pressed" and "molded" materials relies on the same physico-chemical phenomena, the term "molded" will thus be used for comparison when needed.

Delamination refers to the creation of cracks in compressed materials due to excessive steam production within the specimen. Delamination most probably occurs at high temperature and moisture content (MC) when pressure is released within the specimens. An extreme case of delamination can make the materials explode upon depressurization of a mold. Delamination is a casually identified limit in binderless boards' production and is further discussed in the paper.

History of binderless compression-molded plant materials

Binderless boards were born with the Masonite® process (Mason 1928). William H. Mason invented a process for producing wood fibers hardboards, using a steam pretreatment step. The chemo-mechanical action inherent in the pretreatment released components from the fibers on their surface to form an in situ glue. For historical reasons, because of the close interaction of plant fibers and moisture and the very similar chemistry changes occurring upon steam treatment and during hot pressing, steam processing will be considered in this review.

Later, a patent of Runkel and Jost (1956) described a process called Thermodyn for producing binderless boards from plant material without requiring steam. The inventors described two stages in the process: during the first step, degradation gases are produced from plant materials under heat and pressure, and these serve as hydrolyzing agents to produce binders from the plant materials. This first step is very much like Mason's steam treatment, although it occurs in the mold. In a second step that could be separated, the material is molded into the desired shape. Some details are missing in the patent. For example no problems are mentioned concerning steam delamination, rheological behaviour, mechanical properties, or water resistance. Runkel and Jost reported "physical, colloidal, chemical changes of the cell wall components, leading to some sort of thermoplasticity of the material occurring under compression, heat, and in the presence of a little moisture", and there is no doubt that these phenomena are keys to understand the moldability of 100% natural fibers. The interest in this process was probably not sufficient in comparison to petroleum-based thermoplastics so unfortunately the Thermodyn process did not leave behind an imperishable memory.

More recently, Mobarak et al. (1982) published what is today' oldest available academic paper on binderless boards made from unmodified natural plant materials (Mobarak et al. 1982). The paper starts with a very nice overview on the older scientific

works that are in Russian and German, and most of them not easily available. They haven't been taken into consideration for this review.

I.1 An overview of the mechanical properties and water resistance of self-bonded materials obtained by thermo-compressive processing of plant fibers

I.1.A Mechanical properties of self-bonded thermo-compressed plant materials

The concept behind binderless molded objects probably appeared with the idea of avoiding the use of environmentally harmful binders. It is reasonable to assume that at first, available production tools (pressing machines) were used; therefore, a first "boards" category can be made, for which the process uses available and relatively low pressure. Researchers working on binderless boards have the standard wood-based panels' properties as reference and not the processing conditions. Most of the time, the idea of binderless boards research is to reach the industrial wood–based panels properties (with adhesive) without using binders. However, the higher temperatures and much longer times required to meet quality standards may fall outside of the norms for commercial production.

Table I - 2: Summary table of mechanical performances of binderless boards and compared properties obtained by steam pretreatment, steam injection pressing and without treatment*

		Steam pretreated materials												Steam injection					No steam												
Reference		Howard and Sandborn 1937	Suchsland *et al.* 1987	Suzuki *et al.* 1998	Suzuki *et al.* 1998	Laemsak and Okuma 2000	Anglès *et al.* 1999	Anglès *et al.* 2001	Velasquez *et al.* 2003	Salvado *et al.* 2003	Gao *et al.* 2011	Nachari *et al.* 2013	Saari *et al.* 2014	Xu *et al.* 2006	Xu *et al.* 2003	Xu *et al.* 2004	Widyorini *et al.* 2005b	Widyorini *et al.* 2005b	Mobarak *et al.* 1982	Shen 1986	Hashim *et al.* 2010	Hashim *et al.* 2010	Hashim *et al.* 2011a	Hashim *et al.* 2011b	Nachari *et al.* 2013	Boon *et al.* 2013	Saadaoui *et al.* 2013	Okuda and Sato 2004	Okuda and Sato 2006	Nonaka *et al.* 2013	van Dam *et al.* 2004b
Plant material		Wood	Green hardwood	Oil palm tree fronds	Oil palm tree fronds	Oil palm tree fronds	Spruce and pine residues	Spruce and pine residues	*Miscanthus sinensis*	*Miscanthus sinensis*	Black spruce bark	Oil palm trunk	Oil palm trunk strands	Kenaf core	Kenaf core	Kenaf core	Sugar bagasse pith	Sugar bagasse rind	Bagasse pith	Bagasse	Oil palm trunk fines	Oil palm trunk strands	Oil palm trunk core	Oil palm trunk	Oil palm trunk	Oil palm trunk	Palm date tree fibrillum	Kenaf core	Kenaf core	Bagasse	Coconut husk
Density (g.cm^{-3})		1.44	1*	1.2	1.2	1.2	1	1.07	1.18	1.27	0.98	0.8*	0,8*	0.5*	0.7	0.25	0.75	0.75	1.35	0.75	0.8*	0.8*	0.8*	0.8*	0.8*	0.62	0.97	1*	0.7	0.75	1.35
Properties (MPa)	IB	-	2.5	1.85	0.59	1.8	1.8	1,8	1.2	3.76	1.77	0.49	1.4	0.55	0.6	0.15	0.2	0.2	-	0.74	0.47	0.93	0.71	0.93	0.49	0.6	0.02	5.7	4.9	1.2	-
	MOR	50	20.7	20	20	22.4	24	35	48.2	61	20.3	8.18	25.8	18	16	2	10	5	130	23.5	3.99	25	13.4	5.73	8.18	15.8	12.9	36.1	35	17	50
	MOE	-	3709	4227	7610	-	4000	7500	6050	6600	2360	-	-	2300	3000	500	1500	1000	-	5240	-	-	-	-	-	-	1257	5500	5500	3500	5000

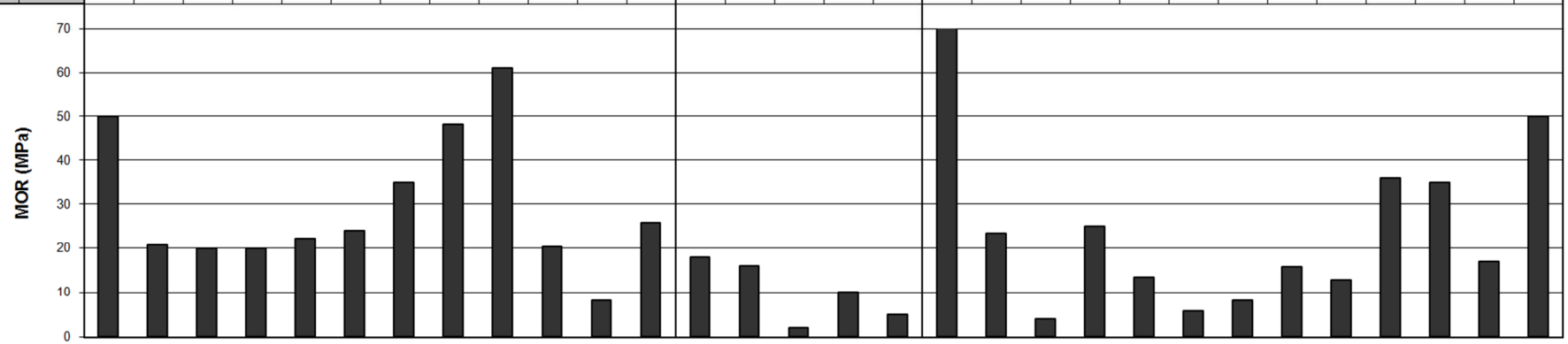

An asterix (*) in the density line means that target density is reported and not the actual density measured.

Boards-type, low pressure molding

Mechanical properties of boards are commonly expressed with the use of three variables, the modulus of rupture (MOR), the modulus of elasticity (MOE), and internal bond (IB). Somehow, these three parameters are correlated. Plant materials do not produce rubber-like materials (high MOR and low MOE), and the IB is also somehow correlated with the bending properties. As the most common usage of boards (e.g. flooring, furniture) relies on strength of the boards, the MOR is the first criterion.

Table I - 2 presents a quick comparison of the performances of steam-pretreated, steam-injection pressed, and non-treated-materials binderless boards. All of the values reported in this table come from the highest MOR obtained by researchers, with the MOE and IB reported on the same specimen. It can be observed that steam pretreatment always produces relatively strong products with decent MOR, whereas direct hot pressing without any treatment of the starting materials can produce either low or high mechanical properties. This basically means that the molding of natural fibers without any treatment is more sensitive to the nature of starting material. Some materials would be suitable for direct molding and do not need steam treatment, whereas some others would require it.

High pressure, plastic-substitute type, cellulose processing

Research involving new materials as well as the need for understanding the chemical changes and processing possibilities of lignocellulosic materials have led some researchers to work at higher pressure. In this review, the "high pressure" range would start at around 30 MPa. But more than the value, "high pressure" is defined by the intent from the authors to mold products towards the creation of new materials, with higher density and properties, usually at a smaller scale. This would not be with the idea of producing boards, but more likely plastic materials, which potentially can be three-dimensional, extrusion tests, or transfer molding. Raw lignocellulosic materials have been processed at high pressure (Miki et al. 2003), sometimes together with steam (T. Miki et al. 2007; Takahashi et al. 2010), and pure cellulose compression molding was also studied (Nilsson et al. 2010; Rampinelli et al. 2010; Zhang et al. 2012; Pintiaux et al. 2013; Privas et al. 2013). The “ECAP” process (Equal Channel Angular Pressing) of Zhang et al. (2012) comes from metallurgy and involves the material being subjected to high shear stress; this approach is comparable to transfer molding as experimented by Miki et al. (Yamashita et al. 2007) yet quite different from compaction molding (low and high pressure), wherein shear is limited. The influence of shear is an interesting parameter, however not very much described in molding, but well known in the wood welding process from the group of Pizzi et al. (Gfeller et al. 2003).

Obviously, as can be seen in Table I - 3, high pressure can result in considerably higher MOR than low-pressure molding, and the resulting densities fall in a narrow range of 1.4 to 1.5 g/cm^3. Results obtained on pure cellulose are quite disappointing compared to lignocellulosic materials unless the material has been refined (micro-fibrillation).

Table I - 3: Summary table of mechanical performances of high pressure molding experiments for producing self-bonded plant materials

		Steam pretreated materials	Steam atmosphere pressing	Non steam treated			
Reference		Takahashi *et al.* 2010	Miki *et al.* 2008	Miki *et al.* 2003	Rampinelli and Di Landro 2010	Zhang *et al.* 2013	Pintiaux *et al.* 2013
Plant material		Beech wood	Cypress and cedar wood (1:1)	Cedar wood	Micro fibrillated cellulose (*i.e.* refined)	Coton linters microcristalline cellulose	α-cellulose
Pressure (MPa)		30	36.5	178	120	-	267
Density (g.cm^{-3})		1.45	1.4	1.4	-	-	1.51
Properties (MPa)	MOR	63	70	100	185	7.6	43.2
	MOE	11000	8000	-	-	3215	7170

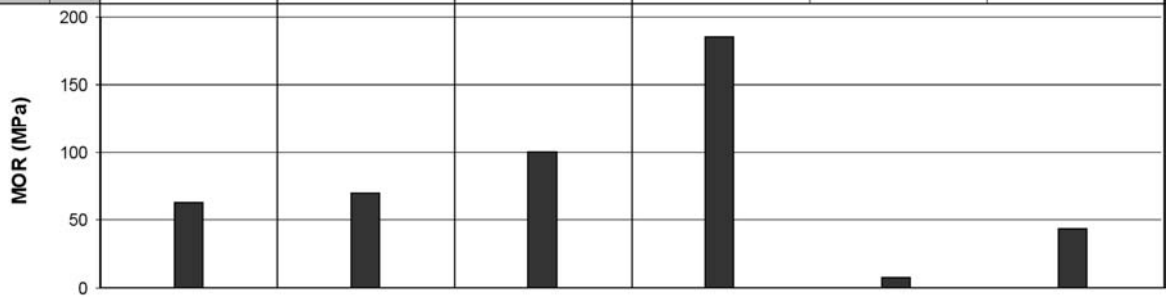

I.1.B Water resistance of self-bonded thermo-compressed plant materials

Water resistance is classically evaluated by measuring the water absorption and thickness swelling of 5x5cm specimen samples, which is convenient for comparisons. Different standards are to be found in different parts of the world. The European system (EN standards), for example, is quite complicated. TS requirements are specific depending on the type of panel (particleboards P1 to P7, EN 309 – medium density fiberboard, EN 622-5 – oriented strand board types 1 to 4, EN 300). Particleboards of type 3 to 7 have requirements of TS depending on specifications (humid environment or not). Medium density fiberboard and oriented strand board also have increasing specification of resistance against water, and all the values required by the standards vary as a function of the boards' thickness. Japanese standards, however, are much more convenient, requiring that any type of boards should have a TS lower than 12% (according to JIS A 5908 2003). The explanation for application of such a broad standard probably arises from the very humid Japanese weather. The 12% maximum TS from the Japanese standards is found as a reference in many publications and has been reported here in Table I - 4. In this table, it can be observed that binderless boards have difficulties to achieve water resistances good enough to pass the standards. The use of steam, however, appears to significantly increase the water resistance.

Okuda and Sato (2004) reported that the mechanical properties of their binderless boards made from kenaf core became reduced to (only) 1/3 of their dry value when placed in wet conditions (Figure I - 1) for specimens in the high range of IB. Another promising value of 87% was reported upon high-temperature molding of bagasse (Nonaka et al. 2013). Mechanical properties in the wet state are very rarely reported, and these two examples are actually excellent values; sometimes, water resistance tests (TS / WA) are not even reported because the specimens swelled and broke down in water.

Table I - 4: Summary table of water resistances of self-bonded thermo-compressed plant materials and comparison between steam pretreatement, steam injection and without steam*

	Steam pretreatment												Steam injection pressing					Without steam												
Reference	Howard and Sandborn 1937	Suchsland *et al.* 1987	Suzuki *et al.* 1998	Laemsak and Okuma 2000	Anglès *et al.* 1999	Anglès *et al.* 2001	Velasquez *et al.* 2003	Salvado *et al.* 2003	Gao *et al.* 2011	Nadhari *et al.* 2013	Saari *et al.* 2014	Takahashi *et al.* 2010	Xu *et al.* 2006	Xu *et al.* 2003	Xu *et al.* 2004	Widyorini *et al.* 2005b	Widyorini *et al.* 2005b	Mobarak *et al.* 1982	Shen 1986	Hashim *et al.* 2010	Hashim *et al.* 2010	Hashim *et al.* 2011a	Hashim *et al.* 2011b	Boon *et al.* 2013	Saadaoui *et al.* 2013	Okuda and Sato 2004	Okuda and Sato 2006	Ando and Sato 2010	Nonaka *et al.* 2013	van Dam *et al.* 2004b
Starting material	Fine materials after masonite gun	Hardwood	Oil palm tree fronds	Oil palm tree fronds	Softwood (Spruce and Pine) residues	Softwood (Spruce and Pine) residues	Miscanthus sinensis		Bark + Wood sandwich structure	Oil palm trunk	Oil palm trunk strands	Japanese beech	Kenaf core	Kenaf core	Kenaf core	Sugarcane bagasse Pith	Sugarcane bagasse Rind	Bagasse pith	Bagasse	Oil palm trunk	Oil palm trunk	Core part of oil palm trunk	Oil palm trunk	Oil palm trunk	Palm date tree leaflets	Kenaf core	Kenaf core	Sugi Heartwood and sapwood	Bagasse	Whole coconut husk
Density ($g.cm^{-3}$)	1.44	1*	1.20	1.20	1.00	1.07	1.18	1.27	0.98	0.8*	0,8*	1.45	0.5*	0.35	0,15	0.75	0.75	1.35	0.75	0.8*	0.8*	0.8*	0.8*	0.62	0.97	1*	0.70	1*	0.75	1.35
TS (%)	-	23	-	-	12	18	15	9	9	22	32	12	11	11	10	200	10	7.5	7	47	42	20	18	25	150	20	35	20	14	8
WA (%)	1	43	5	11	40	45	26	23	-	51	59	8	23	-	300	-	-	11	-	105	80	60	70	-	100	41	20	45	-	8

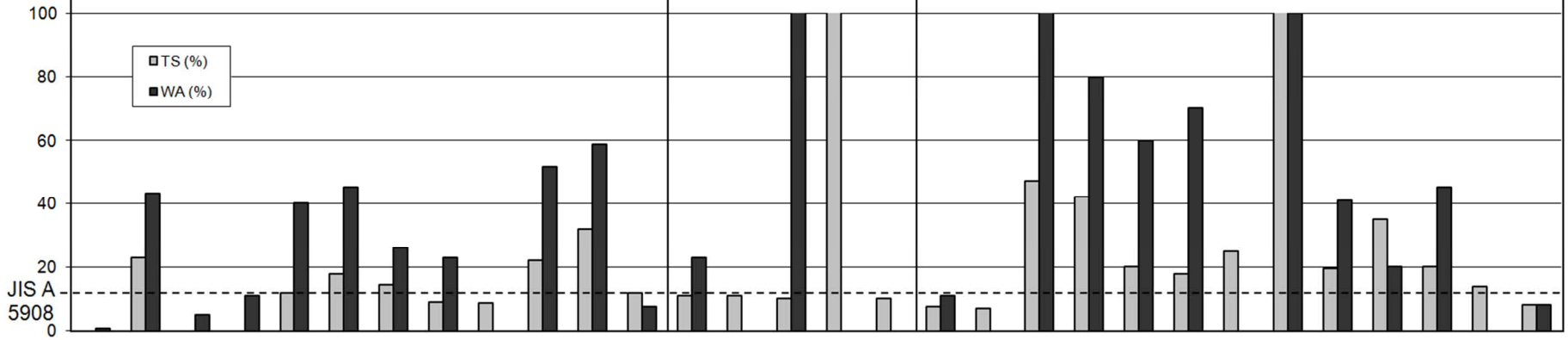

Note: An asterisk (*) in the density line means that target density is reported and not the actual density measured.

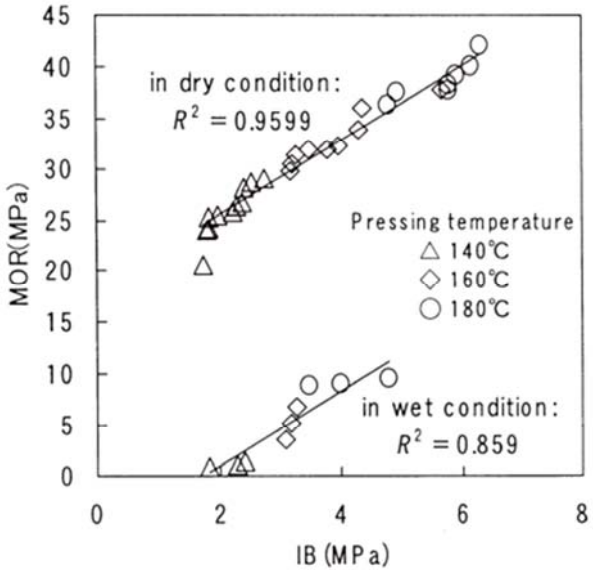

Figure I - 1: Comparison between dry and wet mechanical properties (Okuda and Sato 2004, republished with the kind permission of the Japan Wood Research Society)

I.2 The effects of plant materials origin on the molded specimens

I.2.A Reported Molded Materials

The effect of the nature of plant material is a very delicate parameter to study because materials and methods are rarely comparable between different studies reported in the literature, and most of the time researchers tend to focus on just one plant. Also, comparison focusing on one plant from one study to another cannot be considered 100% reliable, as plant varieties, harvesting season, growing sites, etc. will create heterogeneity (Saito et al. 2013).

Mason indicated that the Masonite disintegration process could work with pretty much whatever "ligno-cellulose material" (Mason 1926a). Then for molding Masonite®, it is reported that lignin is necessary for cohesion; therefore only materials containing sufficient amounts of lignin after steam explosion would be suitable (Mason 1928).

Although wood is the only material present in the examples given in their patent, Runkel and Jost (1956), considered that whatever "substances of vegetable origin which contain resinogene groups and active carbonyl compounds or which can form such groups" could be molded without using a pretreatment. On the other hand, Anglès et al. (2001) mentioned that boards from non-pretreated residual softwood could not be molded, and that thus steam pretreatment was needed. Other wood materials were successfully molded using steam pretreatment (Suchsland et al. 1987) or not (Ando and Sato 2010). The groups of Miki and Takahashi also investigated the possibility of molding wood at high pressure using steam (Miki et al. 2003; Takahashi et al. 2009) and bulk bamboo (Yamashita et al. 2007). Also cedar wood, bamboo rice straw, ginkgo biloba leaves, and coffee bean residues were densified into pellet fuels by high pressure molding (Matsuura et al. 2012)

The oil palm tree is a vastly studied biomass. Suzuki et al. (1998) and Laemsak et al. (2000) molded steam-exploded particles of oil palm tree fronds, and Nadhari et al. (2013) studied trunk particles treated in an autoclave. Different parts of oil palm tree (Hashim, Nadhari, et al. 2011) and date palm tree (Saadaoui et al. 2013) were also molded without steam.

The pith fraction of sugarcane bagasse was successfully molded without steam treatment, and satisfactorily results were obtained (Mobarak et al. 1982; Widyorini et al. 2005).

Kenaf core is another quite extensively studied material that was successfully molded without steam (Okuda and Sato 2004) and also using steam injection pressing, which made it possible to obtain low-density boards (Xu et al. 2004).

Miscanthus and banana bunches were also molded into boards with the help of steam pretreatement (Velasquez et al. 2003; Quintana et al. 2009).

As a conclusion, no general trend can be extracted from these results. The availability of waste plant material in one region often appears to guide the selection of materials to be studied and comparisons between plants remains rare.

I.2.B Different parts of plants

Type of plant tissue, cell wall structure and composition

Hashim et al. (2011a) compared the moldability of different plant tissues from the oil palm tree. In the same processing conditions, without pretreatment, the bark and leaves performed poorly, while fronds and trunk were much better. Bark cells had thick and rigid cell walls and were not deformable enough to be molded. On the opposite, parenchyma is a spongious tissue of plants, consisted of living cells with a high lumen to cell wall dimension; this structure was claimed to be responsible for good molding capacity of fronds and core part of the trunk of oil palm tree. Consistent results were also reported on date palm tree (Saadaoui et al. 2013).

Mobarak et al. (1982) also observed that bagasse pith (parenchyma cells) had better molding capacity than depithed bagasse (less parenchyma cells). Also the pith part reacted to pressure (higher pressure increased the bending strength), although depithed bagasse had the same poor properties with higher pressure. The same conclusions were reported on kenaf core (Okuda and Sato 2004) or coconut husk (van Dam et al. 2004).

On the other hand, it was shown that whatever the conditions, sugi heartwood had more than twice better mechanical properties compared with sugi sapwood on 1 mm powder binderless boards processed without steam (Ando and Sato 2010). Heartwood is the center, older, tougher part of the trunk, constituted of dead cells of higher lignin content. This result appears quite contradictory compared to the previous ones unless chemical differences (probably lignin and extractives) are considered. No difference was observed between heartwood and sapwood when ground to 10 µm and used as a binder for plywood for what was concluded that the grinding treatment cancelled the differences of cell wall structure.

Particle geometry and the need of steam treatment

A comparison of hot pressing and steam injection pressing on the parenchyma part (pith) and non-parenchyma part (rind) of bagasse showed no effect of steam for the pith fraction but a positive effect of steam for the rind fraction (Widyorini et al. 2005). This would explain the results of many researchers who necessarily employed steam for molding non-parenchyma tissue and also the good properties and many studies showing a high interest for kenaf core and other parenchyma parts of plants.

Remnants of storage polymers and agroindustrial by-products

Different agricultural or industrial plant residues are to be found in different countries, but a certain attention can been directed towards agroindustrial byproducts that would contain significant amounts of storage polymers, namely starch and proteins. Hashim et al. for instance worked on oil palm tree residues containing small amounts of starch. They first managed to obtain satisfactory mechanical properties using strands of 3 to 5 cm long, and the SEM photographs showed an homogeneous blend of the cells and melted and compressed starch granules (Hashim et al. 2010). In a second study on different parts of oil palm tree, the IB was quite well correlated to the starch content; starch was able to melt and provide a matrix effect, bonding the fibers together like in a composite material (Hashim et al. 2011). The starch granules were seen to fill the cell voids, sometimes unmelted in the compressed material even at an elevated temperature of 200°C; nevertheless, they were able to provide a bonding effect (Hashim et al. 2011; Lamaming et al. 2013). The melting of starch granules was confirmed after the materials had been steam-pretreated and molded at 220°C (Nadhari et al. 2013) or 180°C (Saari et al. 2014). The effect of starch as thermoplastic in situ binder has been reported to be significantly lower than sugars upon molding (Lamaming et al. 2013). Another example is to be found in the papers of Evon et al. (2010, 2012) who worked on sunflower cake, (which contains proteins) and reported on thermo-compressive molding of sunflower cake, and 3-D molding is easily accessible due to the thermoplastic behaviour of proteins. In this case, studied material is truly an agro-industrial byproduct, wherein the thermo-mechanical extraction of sunflower oil may play a role. Binderless boards were also successfully molded on jatropha seed oil cake (Hidayat et al. 2014).

Mixing / structural associations

Reports on mixing of materials are rare, and so are reports based on structural association of several plants. For instance, in order to counter-balance the poor flexural properties of bark fibers, Gao et al. (2011) introduced a mix of wood fibers (30%) and bark (70%) and tested different structural associations. They concluded that a homogeneous mixture added lot of strength compared to the control (100% bark), but the highest mechanical properties were achieved when they sandwiched bark between two layers of wood fibers. When using such a construction, the MOR and MOE were almost doubled compared with the control.

Contribution of lignin to water resistance

Many authors have made the hypothesis that lignin, on account of its hydrophobic nature, was responsible for most of the water resistance observed on specimens (e.g. van Dam et al. 2004a; Howard and Sandborn 1937; Okuda and Sato 2004). The addition of lignin was reported to drastically increase water resistance, which supports the previous hypothesis (Anglès et al. 2001). Additionally, it has sometimes been observed that lignin degradation was correlated with decrease of TS, showing that hydrophobic degradation products could work as native lignin; such observations could also support a hypothesis proposed by Ito et al. (1998b) to the effect that lignin was not responsible for the dimensional stability triggered by the high-severity steam pressing treatment. Also, the link with steam treatment could be made, as it was reported that steam treatment increased the relative lignin content by degradation of other components, and the correlation to the increase of lignin was made with an improvement of the mechanical properties (Quintana et al. 2009). More elements about this are reported later.

Contribution of hemicelluloses to water sensitivity

The fact that hemicelluloses must be eliminated for better water resistance was already mentioned in the pioneering works of Mason. The reduction of hemicelluloses content was performed thanks to a washing step prior to steam explosion, which effect was later confirmed by others (Howard and Sandborn 1937; Suchsland et al. 1987; Nadhari et al. 2013; Saadaoui et al. 2013).

Steam pretreatment and hot water extraction have been widely studied as a way to improve water properties of classical adhesive containing wood-based panels (Hsu et al. 1988). This effect relies on an improved deformability of wood particles and reduction of springback effect, both of which mainly can be attributed to the reduction of hemicellulose content (Pelaez-Samaniego, Yadama, Garcia-Perez, Lowell, and Amidon 2014). Comparable results were obtained in binderless pressing (Anglès et al. 2001). The hypothesis was also formulated that hemicelluloses' bonding effect could be responsible for water sensitivity of the molded products because of the hydrophilic nature of such bonds (Okuda and Sato 2004).

Finally, in the same way as the increase of lignin, the link between severity of pretreatment and a decrease of the relative content of hemicelluloses was made (Figure I - 2), and a correlation was established with an increase of the water resistance (Velasquez et al. 2003). The correlation between a decrease of TS and hemicelluloses content was verified by others (Widyorini et al. 2005; Quintana et al. 2009), which could possibly explain the improvement of water resistance observed by Ito et al. (1998a,b).

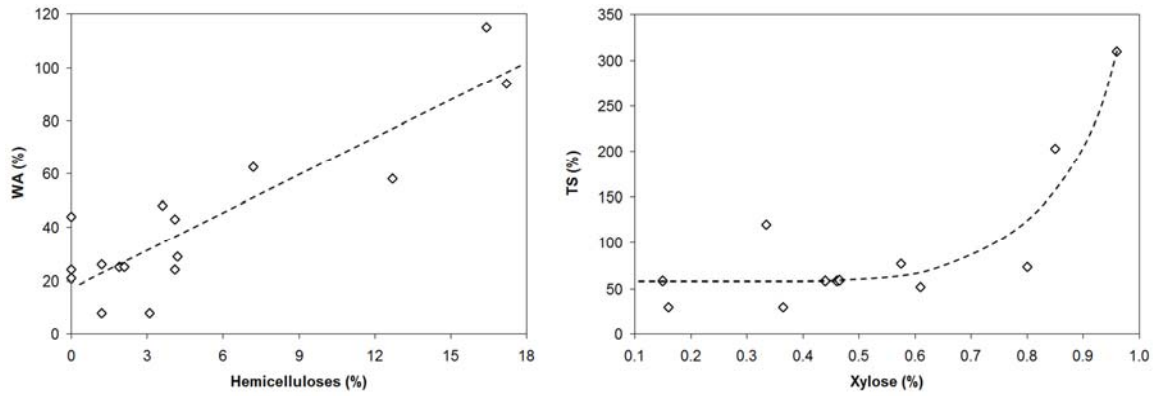

Figure I - 2: Correlation between loss of hemicelluloses and improvement of water resistance in binderless fiberboards, WA on the left (steam exploded miscanthus, adapted from Velasquez et al. 2003), TS on the right (steam exploded banana bunch, adapted from Quintana et al. 2009)

I.3 The use of steam in plant material processing

The first widespread usage of steam treatment for producing materials from natural fibers was in the manufacture of Masonite® (Mason 1928). Mason developed an apparatus called the Masonite gun (Mason 1926a; Mason 1926b) within which wood chips are steam pressurized during a certain time before rapidly releasing the pressure, and the material through a nozzle. A mechanical effect that breaks the structure of the fibers and leads to what is described as a defibrated and fluffy state is produced, cell walls are damaged, and inner plant cell wall chemical components made more accessible.

Steam-exploded wood fibers were processed into wet processed hardboard without binders, and Masonite® was industrially produced. Multiple applications were possible due to its high density, low cost, and relatively good water resistance. The product was also known as isorel, hernit, karlit, torex, or treetex. It was already claimed in the patent that

lignin and its accessibility were responsible for good mechanical cohesion and water resistance of the materials (Mason 1928).

The steam pressure, in the range of a few MPa (Table I - 5), is directly linked to its temperature. So basically, time and temperature (or pressure) are the 2 main parameters. A higher pressure and/or a longer time will produce more "changes" in the natural fibers, for which "severity" is a consensus term. Different materials can be produced by varying the severity (Mason et al. 1937). The time – temperature equivalence is described in the patent (Table I - 5), but it is also mentioned that a critical temperature should be reached.

The low energy requirements and eco-compatibility of steam explosion made it an interesting process for other applications than binderless boards, for instance for reinforcing the water resistance of the adhesive based panels (Hsu et al. 1988; Pelaez-Samaniego et al. 2013). Steam treatment was reported to increase the ethanol yield, lignin solubilization (Bundhoo et al. 2013), and also biogas yield production (up to 40%) despite some negative effects due to the generation of compounds inhibitory to micro-organisms (Zheng et al. 2014).

Table I - 5: First report of a time-temperature equivalence for steam pretreatement adapted from US patent 1,824,221 (Mason et al. 1937)

Time held at pressure	Temperature (°C)	Steam pressure (MPa)
30 minutes	216	2.1
5 minutes	231	2.8
105 seconds	244	3.4
60 seconds	254	4.1
30 seconds	271	5.5
15 seconds	285	6.9

Later, the time – temperature of treatment equivalence was formalized, and a combining variable called "severity factor" was created for more convenient comparison (Overend et al. 1987). This severity factor (also called R_0) has the following expression:

$$R_0[\text{min}] = \int_0^{t[\text{min}]} \exp\left(\frac{T[^\circ\text{C}] - 100}{14.75}\right) dt.$$

The consideration of the log R_0 imposes the prerequisite of the time - temperature equivalence, which remained an hypothesis that was questioned (Velasquez et al. 2003).

There are basically two ways of using steam in the processing of binderless 100% plant fibers materials:

As a pretreatment on the starting material separately from the pressing stage: In this case the very large majority of research works employed Mason's steam explosion approach (Mason 1926a; Suchsland et al. 1987; Velasquez et al. 2003). Some groups used a simple steam pretreatment in an autoclave without the mechanical effect of steam explosion, (Howard and Sandborn 1937; Takahashi et al. 2009; Nadhari et al. 2013). Others used steam in addition to more mechanical refining processes using disks or rolls (Xu et al. 2003; Gao et al. 2011).

As a processing aid, integrated in the pressing process, using a steam atmosphere surrounding a pressing machine (Ito et al. 1998; Widyorini et al. 2005; Miki et al. 2007) or injecting steam in the mold during pressing (Xu et al. 2003).

The benefits of steam treatment as a first step are often reported to be tremendous with respect to the mechanical properties. Anglès et al. (1999) for instance reported that steam-treated biomass succeeded, whereas non-treated biomass compressed materials were so weak they could not even be tested.

I.3.A The use of steam as a pretreatment: effects and optimal conditions on molded specimens

Mild severity optimum for strength

Optimal values of pretreatment (in order to maximize the MOR) are reported in Table 6, which shows that the average optimal value for log R_0 is about 4. Except for the last two examples in Table I - 6, the optimal value was quite uniform, despite the fact that different plant materials were being studied, including hardwood (Suchsland et al. 1987; Takahashi et al. 2010), fronds of oil palm tree (Suzuki et al. 1998; Laemsak and Okuma 2000; Nadhari et al. 2013), softwood (Anglès et al. 2001; Gao et al. 2011), and Miscanthus (Salvado et al. 2003; Velasquez et al. 2003), etc.

Velasquez et al. (2003) optimized temperature and time separately, and concluded that a lower temperature of pretreatment (200°C) and long time (6 minutes, log R_0 = 3.72) were the best conditions, and in doing so questioned the time - temperature equivalence (Overend et al. 1987). The pretreatment step was seen to have a higher impact than the other parameters during the compression-molding, statistically. Using the same methodology, similar conclusions were reported on steam pretreated banana bunches binderless boards, and it was also observed that higher severity led to a decrease of the bending properties (Quintana et al. 2009).

Table I - 6: Summary table of optimal steam pretreatment severity for producing self-bonded materials

Reference	Suchsland *et al.* 1987	Suzuki *et al.* 1998	Laemsak and Okuma 2000	Anglès *et al.* 1999	Velasquez *et al.* 2003	Salvado *et al.* 2003	Gao *et al.* 2011	Takahashi *et al.* 2010	Nadhari *et al.* 2013	Saari *et al.* 2014
Pretreatement type	Masonite gun + refiner	Batch steam explosion	Steam explosion	Continuous steam treatment	Batch steam explosion	Batch steam explosion	Mechanical refiner + steam	Autoclave	Autoclave	Autoclave
Steam temperature (°C)	229	224	224	217	216	203	188	180	120	130
Treatment time (min)	2.5	5	5	2.8	5	7.3	3.5	20	46	30
log R_0 (min)	4.2	4.35	4.35	3.89	4.11	3.9	3.14	3.66	2.25	2.36

High severity decreases MOR and MOE but is positive for IB and water resistance

Some papers have reported that severe conditions of pretreatment lead to lower bending properties (Suchsland et al. 1987; Suzuki et al. 1998; Laemsak and Okuma 2000). Suchsland et al. (1987) also reported that high severity of pretreatment appeared to increase the bonding ability, but the hypothesis was made that the shortening of the fibers could hinder this effect, which would explain a decrease on the bending properties. The mechanism was clarified later, with the measurement of a reduced cellulose content and lower degree of polymerization, which made it possible to conclude that the partial hydrolysis of cellulose caused by an excessive severity of treatment was responsible for the lower mechanical properties (Anglès et al. 2001). Later, the IB was actually confirmed to be maximized at high severity of pretreatment, and a higher proportion of fine particles produced during

pretreatment at high severity was suggested as an explanation to higher IB values (Velasquez et al. 2003). Low temperature of pretreatment was claimed to preserve the integrity of the fibers during pretreatment, although high temperature during the pressing stage for a short time was seen to be the best strategy for triggering the bonds without degrading the material too much. This was verified by optimization experiments, which were conducted to achieve a maximum IB for higher values of severity than for MOR / MOE, with the maximum value of 3.7 MPa (245°C) for 7.3 minutes (log R_0 = 5.13) (Salvado et al. 2003). Consistent results were obtained on banana bunches, wherein the IB was also demonstrated to be statistically dependent only on the pretreatment severity (in related experimental conditions) (Quintana et al. 2009). The maximum IB would be with a pretreatment severity factor of 3.55, which is lower than values reported by the other authors. The same kinds of results were reported using a steam-pressurized disk refiner, for which high pretreatment severity maximized the IB, while at the same time the MOR was decreased (Xu et al. 2006).

Positive effects of steam explosion on the water resistance is a classic of the adhesive bonded panels (Sekino et al. 2005). Mason reported good properties of Masonite (binderless hardboard) against water (Mason 1928), and had another patent on an more intensive use of steam explosion to produce water-resistant materials (Mason et al. 1937). The highest severity levels of pretreatment are uniformly reported to confer the highest water resistance (thus lowest TS and WA values). There is certainly a link to establish between self-bonding ability (IB values) and the water resistance (WA and TS values), as the optimal parameters for these variables are similar.

Unsurprisingly, steam autoclave treatment was also reported to provide good water resistance. A steam temperature of 180°C was reported to have a high impact, although further increase of temperature did slightly further increase the water resistance (Takahashi et al. 2010). In a lower range of temperature treatment, Nadhari et al. (2013) also reported the improvement of autoclave treatment on water resistance but concluded that optimal conditions of treatment should be 120°C and 46 minutes.

Steam pretreatment, flow behaviour and molding capability

Steam pretreatment has also been considered as a way of dramatically increase the flowability of plant materials, which is of great interest towards the production of objects of complicated forms in high pressure molding experiments.

A temperature higher than 160°C made it possible to measure the flowability of Japanese beech using a commercial capillary rheometer. The fluidity increased with temperature of pretreatment until 200 °C (Takahashi et al. 2009). Steaming temperature was demonstrated to first allow flow and secondly to lower the temperature at which the flow occurs. It was demonstrated that 200°C was an optimal temperature to impart fluidity, and the material could be made to flow at only 9.8 MPa of extrusion pressure. At 180°C of treatment, 29.4 MPa of pressure were needed to trigger flow. More generally, the lower the temperature of steaming, the higher has to be the pressure to trigger the ability to flow. A limit of temperature may exist, considering that the results at 220°C were worse than those at 200°C. The same conclusion was reached regarding the time of pretreatment, and the authors concluded that 10 minutes were sufficient at 200°C to trigger fluidity but increasing this time increased the temperature required for flow.

In a later study, Takahashi et al. (2010) correlated these results with the bending properties of their boards, which showed that molding in conditions over the flowing temperature / pressure of the material enhanced all of the mechanical properties that were considered.

I.3.B Steam as a processing aid: effects and optimal conditions

Steam atmosphere pressing

The steam atmosphere pressing technique involves use of a pressing machine wherein the mold is surrounded by a pressurized chamber where heated steam can be injected. A prototype built by HISAKA corporation was used in several studies (e.g. Ito et al. 1998a; Miki et al. 2007a). According to Miki et al. (2007a,b, 2008), the main difference and explanation of the better results of steam atmosphere pressing results from the steam saturation of air surrounding molded materials, which prevents moisture from escaping. The prevention of loss of moisture during the molding process would therefore be a major advantage to this technique. Steam atmosphere pressing also produced improved water resistance (Ito et al. 1998; Miki et al. 2008).

Widyorini et al (2005b) used a custom-designed porous metal pressing machine in an autoclave chamber, gluing together 2 veneers of kenaf core. At 1 MPa (=> 180°C) of steam pressure, 10 minutes was an optimum bonding time, whereas at 1.5 MPa (=> 198°C), 1 minute was optimum. However, best mechanical bonding was achieved with 0.8 to 1 MPa for 10 to 15 minutes.

Steam injection pressing

Steam atmosphere pressing entails a high cost of time and energy, as the whole chamber needs to be pressurized and depressurized at each cycle. Alternatively, as airtight molds are quite easy to build, another possibility is to inject steam directly into the material while it is being pressed in the mold. Originally, steam injection pressing was designed with the idea of maintaining a certain moisture inside the mat to improve thermal conductivity and heat transfer from the plates (Kelly 1977; Back 1987).

The group of Kawai et al. (main results in Table I - 7) first studied the possibility of molding binderless particleboards from kenaf core using a steam-injection pressing method (Xu et al. 2003). Steam is injected in the mat at a pressure from 0.6 to 1 MPa during the whole pressing stage. The IB and bending properties were reported to be much higher compared to hot pressing, and these properties increased with steam pressure. Treatment time had a low impact.

Table I - 7: Examples of conditions and mechanical properties of steam injection pressing experiments for production of self-bonded materials

Reference		Xu *et al.* 2003	Xu *et al.* 2004	Widyorini *et al.* 2005b	Xu *et al.* 2006
Plant material		Kenaf core	Kenaf core	Sugarcane bagasse rind	Kenaf core (pretreated)
Steam injection (MPa)		1	1	1	1
Time (min)		10 - 15	7 - 10	6	10
Target density ($g.cm^{-3}$)		0.7	0.1 - 0.3	0.8	0.5
Apparent density ($g.cm^{-3}$)		0.65	0.15 - 0.25	0.75	-
Properties (MPa)	IB	0.6	0.15	0.2	0.55
	MOR	16	2	5	18
	MOE	3	0.5	1	2.3

In the first paper (Xu et al. 2003), delamination was reported in the case of higher density boards, which was explained by a steam pressure imprisoned in the material that exceeded the IB of the material, making the boards explode when opening the press. Usually, binderless boards with density lower than 0.7 are not reported because of insufficient mechanical properties. Yet, Xu et al. (2003) reported a good correlation between density and the mechanical properties on binderless particleboards with density from 0.35 to 0.65 g/cm^3. Other results at lower density (0.15 to 0.3 g/cm^3) (Xu et al. 2004) followed the same mathematical law as previously reported data, as can be seen in Figure I - 3. The addition of a pretreatment step with a steam-pressurized disk produced fiberboards of very good properties with a low density of 0.5 g/cm^3 (Xu et al. 2006).

Steam pressing produced specimens (bagasse binderless particleboards) with values of TS mostly within the range 150 to 200% for conventional pressing and under 25% for materials made by steam pressing (Widyorini et al. 2005). Dramatic benefits of steam-injection pressing were reported elsewhere, e.g. for kenaf core binderless particleboards (7.47% to 11% of TS were obtained compared to 169% without steam) (Xu et al. 2003; Widyorini et al. 2005).

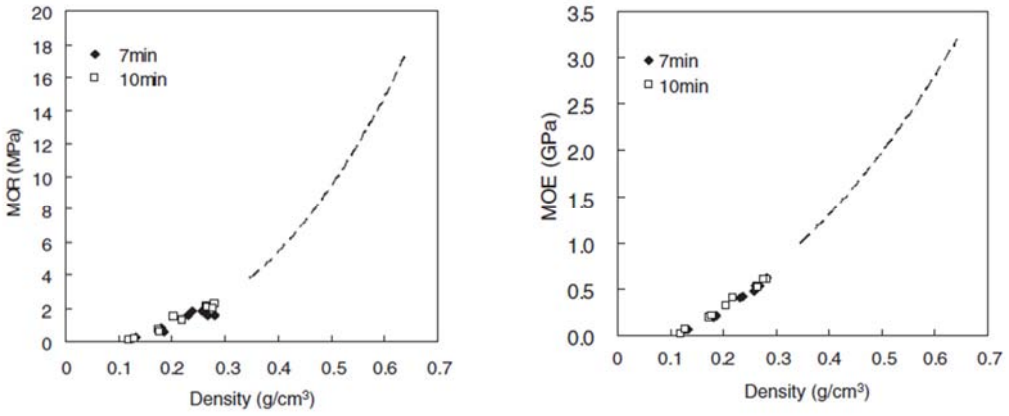

Figure I - 3: Example of correlation between MOR / MOE and density on a wide range of density from Xu et al. (2004), where the dotted line is modelling from Xu et al. (2003), all results on steam injected binderless particleboards from 5mm chips of kenaf core. Figures republished with the kind permission of the Japan Wood Research Society

Steam injection pressing, water resistance and boards' thickness

In the industry of wood-based panels with adhesive, it is well known that the volume / surface ratio has an effect on the WA and TS values. Under the same processing conditions, thicker binderless boards are reported to have better TS values, and thinner boards better WA (Suzuki et al. 1998; Laemsak and Okuma 2000). The explanation relies in the fact that the density gradient is generally less in thin boards, and higher porosity on thicker boards allows more water to infiltrate without making the board swell, which is why the comparison of water resistance is reliable only for boards of similar thickness (Okuda and Sato 2006).

A consistent observation was made on low-density steam-injection pressed binderless boards made from kenaf core, because of low density (0.25 g/cm^3), high WA values of 290% can be obtained on boards with very low TS of 9% (Xu et al. 2004), which would pass the JIS standards if the standard covered this sort of special boards (JIS A 5908, 2003).

I.4 Thermo-compressive process parameters and their effect on properties of molded specimens

I.4.A Molding pressure

Clarification of the relationship between pressure / density / target density

In the industry of wood-based panels, woods with bulk density lower than the resulting particleboards should be used because there is a direct correlation between the compression ratio and the boards strength (Kelly 1977). The purpose of pressing is to bring the particles close to each other while the resin is being cured, which provides thickness control. A "target density" is thus considered, when the mass of material introduced in the mold and the thickness of the product are controlled. This can be achieved, for example, in old presses by use of a metal frame (often called stop bars) that prevents the pressing machine from compressing further than the desired thickness. In classical particleboards densities range from 0.6 to 0.7 g/cm^3, while in classical fiberboards the values range from 0.65 to 0.85 g/cm^3, for instance.

When no glue is used, the generation of an in-situ binder or some other interparticle bonding phenomena is necessary for the product to keep its shape. In fact, because of the lack of binder, a springback effect is often observed in much higher proportions in binderless molding than in traditional resin-based wood-panels (Boon et al. 2013). When unloading the press, the material expands, depending on whether its IB is sufficiently high to retain the particles in their compressed form. Residual mechanical stress remains and produces boards with final density lower than the targeted one. This is why these have to be considered separately. The final densities observed in binderless boards (in general) are higher, ranging from 0.8 to 1.35 g/cm^3. In the industry of wood-based panels with adhesives (thickness control), the initial pressure is impacting the pressurization speed, that has an important effect on the vertical density profile (Kelly 1977) which is different than directly applied pressure. In this case, material can be compressed more than the desired density, but with the springback effect it was possible to obtain a satisfactory density; a good explanation of this effect can be found in the work of Gao et al. (2011).

Effect of pressure: Board manufacture with target density

Common sense suggests that higher density boards will express better mechanical properties (Suchsland et al. 1987). Even though this seems like an easy relationship, some tricky results can be found in the literature. The same author, for instance, once reported a good correlation (Anglès et al. 1999) and elsewhere did not observe any correlation (Anglès et al. 2001) when boards with about the same density exhibited variable mechanical performances. Also, in different studies of Hashim et al. (2010, 2011a,b) the authors suggested that increasing pressure could help to achieve better bonding properties. But while 5 MPa of pressure was used in two studies (Hashim et al. 2010; Hashim et al. 2011), 12 MPa of pressure were later used (Hashim et al. 2011), leading to better properties. Possibly, the 5 MPa of pressure was not sufficient to reach the target density, and the correlation should have been established based on density measurements. In parallel, when the resulting density is correlated to the mechanical properties, very good correlation has been observed (Okuda and Sato 2004; Okuda and Sato 2006; Ando and Sato 2009; Boon et al. 2013). In one paper (Figure I - 4) a non-linear correlation is reported; particleboards had low properties at low density, but after a certain threshold of density, properties increased and there was a linear correlation with density (Ando and Sato 2010). In this last case, an explanation was proposed concerning the improvements of the properties coming from the reduction of porosity when increasing density, which increased the thermal conductivity. One parameter

that has been barely studied is the pressurization speed, which is well known to modify the vertical density profile, classical in the wood-based panels with adhesive but almost never reported in articles concerning binderless molding. For instance, it was reported that thicker binderless boards had much lower IB than thin ones at comparable target density (0.8, 1, and 1.2 g/cm^3) (Suzuki et al. 1998; Laemsak and Okuma 2000) and the explanation to this probably resulted in the different density profiles, induced by thickness differences.

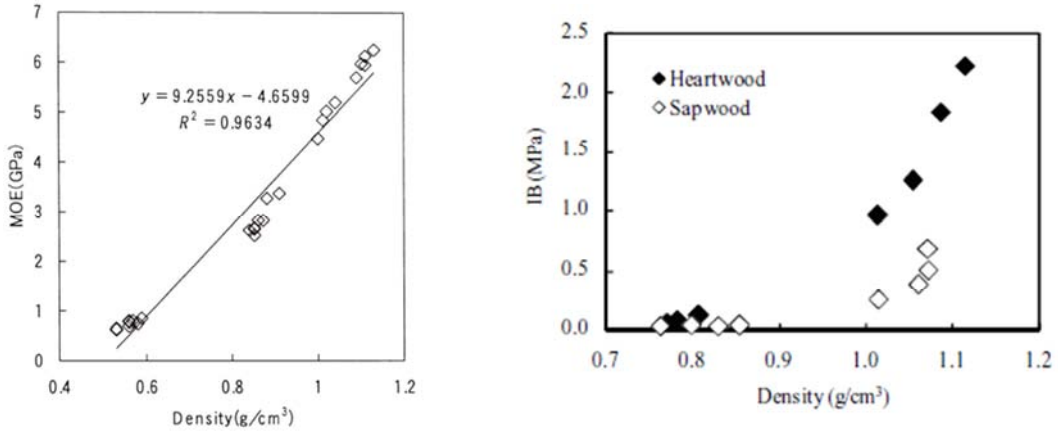

Figure I - 4: Example of correlation between mechanical properties and density of boards. Left graph (Okuda and Sato 2004) binderless particleboards from fine powder (53 µm) bagasse with a linear correlation, right graph (Ando and Sato 2010) particleboards from Japanese cedar milled through 1 mm screen with a non-linear correlation, republished with the kind permission of the Japan Wood Research Society

Effect of directly applied pressure (pressure control)

As opposed to "target density" experiments, pressure directly applied on the material without stopbars has been reported: Mobarak et al. (1982) were the first in the "modern area" to report on binderless boards. This paper first described a major effect of pressure on binderless boards manufacturing from bagasse pith and reported that mechanical strength of the boards was best at higher pressure (25.5 MPa) which is about 7 fold the usual pressure in the production of wood based panels (Figure I - 5). An effect of pressure was only observable for the pith part of bagasse, which is a non-fibrous tissue made of parenchyma cells. On every attempt, the density of the products was 1.35 g.cm^{-3} (about twice the usual density of traditional wood based particleboards), and it did not increase with increasing molding pressure showing that not only density (i.e. compaction) was responsible for the mechanical properties. But in addition, pressure must be triggering some destructuration and chemical reactions that bind the fibers together (e.g. switching the glass temperature transitions of polymers, increasing hydrolysis kinetic).

Ando and Sato (2009) used Kenaf core powder as an adhesive in plywood manufacture and showed that an increased pressure in the production of plywood gave better shear strength, as well as a quicker heating up of the veneer stack when wood cells were compressed. This was mainly caused by the significant increase of the board density when working without stop bars and, hence, producing boards with accordingly lower thickness at higher pressure. If the pressure exceeded a certain even higher limit, delamination occurred, because steam pressure created during the hot press cycle was not able to escape due to the tight material structure.

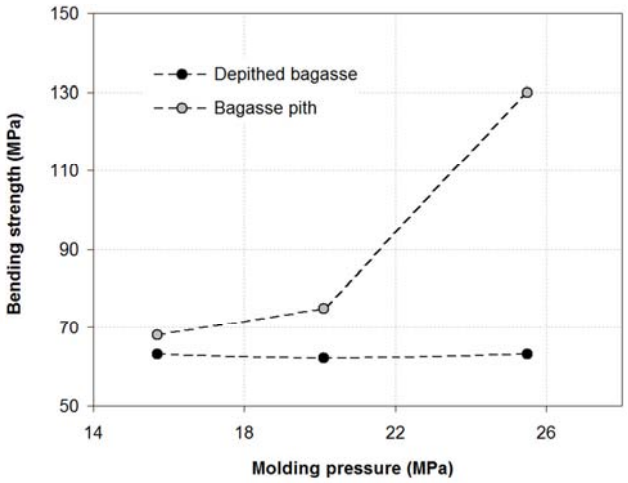

Figure I - 5: Correlation between pressure and bending strength (adapted from Mobarak et al. 1982)

High-pressure molding

Very high pressures cause a certain flow behaviour of pure plant materials. Extrusion tests on Japanese cedar powders were performed without any treatment (Miki et al. 2003). It was demonstrated that extrusion was possible at pressures starting from 70 MPa, whereby extrusion pressures close to 300 MPa were achieved in these experiments. Increasing temperature made it possible to reduce extrusion pressure. The relationship between pressure and bulk density of the extruded product follows a logarithmic curve with an inflexion point around 100 MPa (where obviously most of cell lumens have already collapsed) and a density limit tending to 1.4 g/cm^3 (Figure I - 6), which is close to the density of wood cell wall. The higher the pressure and the density, the higher are the mechanical properties.

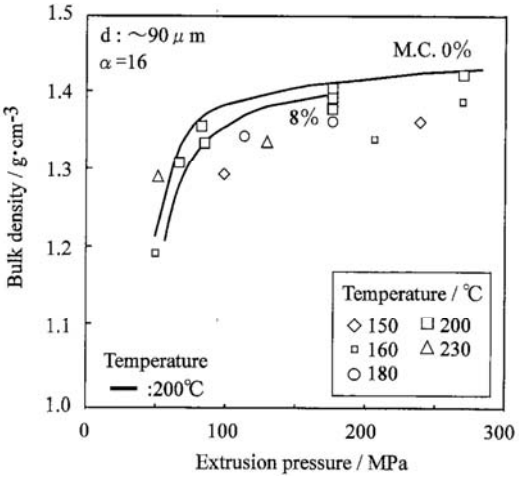

Figure I - 6: Correlation between extrusion pressure and density at high pressure extrusion of wood powders (reproduced from Miki et al. 2003, with kind permission of the Japan Society of Mechanical Engineers)

Later, wood powder was molded using high-pressure molding under a steam atmosphere, and pressure had a clearly positive effect on the shock-resistance properties (dynamic bending or Charpy impact) (Miki et al. 2007) whereas static bending tests, showed

a limited effect (Miki et al. 2008). Figure I - 7 summarizes these two results. The authors also noticed that using steam atmosphere pressing made it possible to reduce the pressure needed to mold wood powder into materials and got excellent bending strength up to 70 MPa with only 36.5 MPa of pressure. Using only 10 MPa of molding pressure resulted in 60 MPa of bending strength specimens.

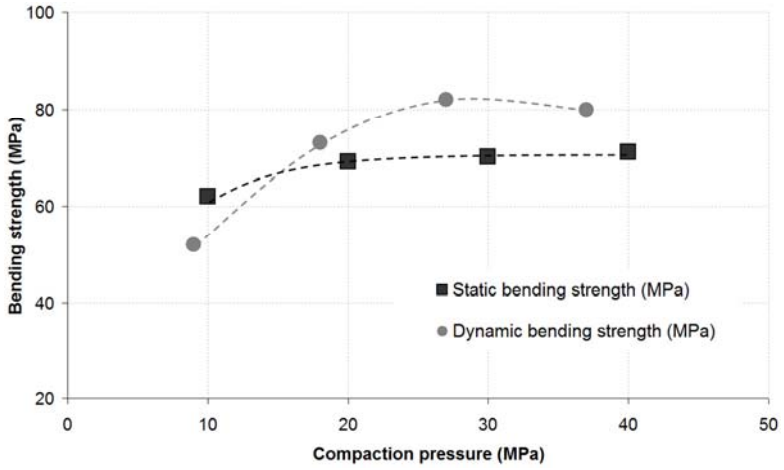

Figure I - 7: Correlation between pressure and bending strength in dynamic test (gray dots) and static (black squares) (adapted from Miki et al. 2007a and Miki et al. 2008)

Effect of pressure on pure cellulose molding

Recent papers have reported pure cellulose compression molding trials and the effect of pressing pressure. Within the range of 40 to 200 MPa, an optimal at 120 MPa was reported for maximizing bending strength (Rampinelli et al. 2010), whereas elsewhere no statistical difference was observed between 134 and 267 MPa of pressure (Pintiaux et al. 2013). Good results with a cold / hot two stages process were reported when using only 45 MPa of pressure (Nilsson et al. 2010). Pressing values from 0.7 to 2.5 GPa (Privas et al. 2013) were reported, but the researchers had to conclude that the pressure range was too high to observe any significant effect. Thus, a pressure bellow 0.7 GPa was sufficient to achieve the maximum density.

I.4.B Moisture content

Natural fibers are highly hygroscopic, and the water content modifies structural parameters such as crystallinity and lowers the glass transition temperature of its polymers (Célino et al. 2014). It is therefore an essential parameter.

Historically, according to the patent of Mason (1937), MC should be adjusted to 5% before pressing. A coproduct of the Masonite process was reported to have an optimal moisture content of 4% for molding (Howard and Sandborn 1937). Without using steam, an optimal moisture for producing compression-molded objects is reported as being between 5 and 25% and preferably between 8 and 17%, according to the patent of Runkel and Jost (1956), which suggests that moisture can be adjusted in quite a wide range. It was then reported that increasing MC had a negative impact on the mechanical properties (Table I - 8), but a minimum moisture was necessary to successfully mold products from bagasse (Mobarak et al. 1982).

Table I - 8: Moisture content and effect on the mechanical properties of molded bagasse products (density 1.34-1.36 g/cm^3) - (adapted from Mobarak et al. 1982)

Initial moisture	%	7.1	9.2	11.8	14.2
Moisture after pressing	%	6.6	6.2	6.4	5.9
Bending strength	MPa	67.8	66.1	63.8	60.6
Water absorption	%	13.3	15.1	18.2	21.7
Thickness swelling	%	10.5	12.9	15	17.2

Molding of dried (0% MC) plant material is generally unsuccessful, and many papers have reported that there is a need for a minimum MC, which is 3% according to Nadhari et al. (2013), but changing MC in the range ~10 to 30% seemed to have less effect on the resulting mechanical properties (Okuda et al. 2006a; Ando and Sato 2009). Nevertheless, high MC was reported to trigger delamination due to steam accumulation in the material during hot pressing (Ando and Sato 2009). The interaction between moisture and temperature is very important; for instance, in a high temperature range (200 to 280°C) the adjustment of MC to lower values (2 to 3%) produced good properties with a maximum at 260°C (Nonaka et al. 2013). In this study, the 200°C values were quite low, necessarily because of the low MC. These last results can be compared with the classical process in the industrial wood-based panels' production in which moisture is reduced in order to prevent reactions with the resin. In the industry, moisture is known to be impacting the density distribution which has never been studied in binderless boards experiments (Kelly 1977).

An increased MC was also reported to facilitate the flowability of wood powders (Miki et al. 2003) and bulk bamboo (Yamashita et al. 2007). Miki et al. (2003) also demonstrated that the increase of moisture shifted the temperature at which the bending strength was maximum: at 0 and 8% the optimum temperature was 195°C, although at 43% moisture 175°C was the optimal temperature. Finally, higher moisture produced significantly weaker materials.

The state of the plant cells has been reported to be different after extrusion (transfer molding), based on SEM observations; the cells were barely observable and had a "matrix" look, although with moisture the cells were still identifiable after molding (Yamashita et al. 2007). Moisture was concluded to ease the separation of the cells during flow testing at high pressure. The same observations was made later on different materials (Yamashita et al. 2009).

Okuda and Sato (2006) reported that the water resistance increased drastically with increasing MC of the initial material, because of a lower softening point of lignin (plasticization) and better heat transfer (Xu et al. 2006). The MC effect also was diminished at higher temperature of molding because softening point of lignin was already reached (Okuda and Sato 2006). However higher MC caused delamination on 0.7 g/cm^3 density boards (although 0.5 g/cm^3 density boards were correct).

Concerning pure cellulose molding, the authors' group has reported consistent results. Dry cellulose performed poorly, whereas 6, 8, and 10% MC cellulose had good and comparable mechanical properties (Pintiaux et al. 2013). Privas et al. (2013), on the contrary, reported higher modulus for dry samples, suggesting that, with very high pressure, moisture was prejudicial to the cohesion.

Temperature gradient, moisture, time and heat transfer

In the classical wood-based panels process, temperature is the energy source to cure the resin. Moisture has the role of facilitating the heat transfer from the plates to the inside of the mat and keeping the particles deformable (lower softening temperature of wood polymers in presence of moisture) for adequate resin/wood particles-fibers contact and target density (Kelly 1977). Temperature and moisture gradients exist inside the mat which has

been fully described in the industry standards but rarely reported in binderless boards experiments (Bouajila et al. 2005). In the surface layers, a certain evaporation takes place during the press cycle which permits to get close (~80%) to the plate temperatures (i.e. skin effect), whereas in the core layer, temperature remains close to the water evaporation temperature (depending on pressure, 105 to 115°C). Increasing pressing time increases the temperature inside the mat but the pressure increases, which can cause delamination. The same way, moisture reduction will reduce steam pressure but also heat transfer, this explains why these parameters have to be optimized together; this has been done in thousands of papers in the wood-based panels with adhesive, but characterization of such phenomena are still incomplete in the field of binderless boards processing.

I.4.C Temperature

Effect of pressing temperature on non-treated and steam treated materials

Temperature is often described as the most important factor in the production of binderless natural fibers moldings (van Dam et al. 2004). Thermal treatments are also crucial in the improvement of properties of wood composites, adhesive containing wood-based panels and self-bonded plant materials (Pelaez-Samaniego et al. 2013).

As can be seen in Table I - 9 which summarizes the conditions for which highest MOR was observed in different studies, research papers on non-steam treated binderless boards and high pressure molding are often reporting an optimal temperature between 180 and 200 °C, except for Shen (1986), who's material contained a high proportion of free sugars and Nonaka et al. (2013), who lowered the MC. Over this favorable range of temperatures, the mechanical properties are decreasing and/or delamination occurs (Ando and Sato 2009; Ando and Sato 2010; Hashim et al. 2011).

Some reports have concluded that increasing temperature had a high impact on increasing the IB of particleboards, which consequently led to the increase of the bending properties (Okuda and Sato 2004; Hashim et al. 2011).

A high temperature of pressing was reported to increase the water resistance and to be the most impactful molding parameter (Anglès et al. 1999; Velasquez et al. 2003; Ando and Sato 2009; Ando and Sato 2010; Hashim et al. 2011; Boon et al. 2013; Nadhari et al. 2013). Better results than equivalent UF or UMF bonded boards were once reported (Okuda and Sato 2006). The TS value went under 10%, which matches particleboards standards.

A higher range of temperature has been reported for steam-pretreated plant fibers (Table I - 10) than for non-treated materials. Low temperature molding processes are reported only for steam-pretreated fibers. In the absence of pre-treatment there is no or reduced possibility to produce objects at low temperature of, for example, 125°C (Suzuki et al. 1998; Laemsak and Okuma 2000). Still, a high temperature of pressing is also reported to have a positive impact on the mechanical properties of compressed specimens after plant fibers have been steam treated (Anglès et al. 1999; Velasquez et al. 2003). One report (Salvado et al. 2003) mentioned however that temperature had a limited impact on the mechanical properties from 195 to 245°C (which is still in a high range). Another report mentioned no effect of temperature on the IB but a drastic and positive effect on the MOR (Nadhari et al. 2013). Confronting these results, it seems difficult to present a general trend; also, for an unknown reason, most of the research works on steam pretreated material tended to use higher temperatures and reduced molding times (the time / temperature of molding equivalence is a classic for standard panels production).

Table I - 9: List of optimal temperature as reported in the literature for producing self-bonded plant materials without steam

Reference	Plant material	Process	Object	Target thickness (mm)	Final density (g/cm3)	Time (min)	Optimal temperature (°C)
Mobarak et al. 1982	Bagasse pith	Hot pressing 25.5 MPa	Particleboard	4	1.35	5	**175**
Shen 1986	Bagasse	Hot pressing 3.4 MPa*	Multipurpose	11.1	0.75	20	**240**
Nonaka et al. 2013	Bagasse	Hot pressing	Particleboards	9	0.8**	10	**260**
Hashim et al. 2010	Oil palm trunk	Hot pressing 5 MPa*	Particleboards	4.8	0.8**	20	**180**
Hashim et al. 2011a	Oil palm trunk	Hot pressing 12 MPa*	Particleboards	4.8	0.8**	20	**180**
Hashim et al. 2011b	Oil palm trunk powder	Hot pressing 5 MPa*	Particleboards	4.8	0.8**	20	**200**
Boon et al. 2013	Oil palm trunk	Hot pressing 5-10 MPa*	Particleboards	5	0.6**	20	**200**
Okuda and Sato 2004	Kenaf core	Hot pressing 5.3 MPa*	Particleboards	5	1**	10	**180**
Okuda and Sato 2006	Kenaf core	3 steps hot pressing 6+4+2 MPa*	Particleboards	5	0.8**	4+3+4	**200**
van Dam et al. 2004b	Whole coconut husk	Hot pressing	Multipurpose	N/A	1.4	3-30	**180**
Ando and Sato 2010	Japanese cedar	Hot pressing 5 MPa*	Plywood	4	0.8-1**	10-30	**200**
Miki et al. 2003	Japanese cedar	Extrusion at 178 MPa	Extrusion tests	N/A	1.4	N/A	**200**
Miki et al. 2008	Japanese cedar / cypress	Steam pressing 36.5 MPa	Multipurpose	N/A	1.4	45	**160**

Note: An asterisk (*) in the process line indicates the presence of stop bars, Two asterisks (**) in the density line means that the target density is reported and not the actual density measured.

Table I - 10: List of optimal temperature as reported in the literature for producing self-bonded plant materials with Process involving steam

Reference	Plant material	Pretreatment	Object	Molding	Target thickness (mm)	Final density (g/cm3)	Time (min)	Optimal temperature (°C)
Howard and Sandborn 1937	Masonite by-product	Masonite gun + grinding + washing	N/A	Hot pressing 13.8 MPa	N/A	1.44	10	176
Suchsland et al. 1987	Hardwood	Masonite gun + refiner	Particleboards	Hot pressing 2.76-5.52 MPa*	3.2	1**	1.3	215-226
Suzuki et al. 1998	Oil palm tree fronds	Steam explosion	Particleboards	Hot pressing 20-40 MPa*	6	1.2**	0.3	125-150
Nadhari et al. 2013	Oil palm trunk	Autoclave	Particleboards	Hot pressing 12 MPa*	5	0.8**	29	215
Anglès et al. 2001	Softwood residues	Continious steam treatment	Particleboards	3 stages hot pressing 4.2 MPa*	3.5	1.07	5-1-5	230
Velasquez et al. 2003	Miscanthus	Steam explosion	Particleboards	3 stages hot pressing 12 MPa*	3	1.18	5-1-18	180
Salvado et al. 2003	Miscanthus	Steam explosion	Particleboards	3 stages hot pressing 12 MPa*	3	1.1**	7.4	195-245
Gao et al. 2011	Bark + Wood	Steam thermomechanic. refinig	Particleboards	2 stages hot pressing 2.8-1.2	6.5	0.98	8	260
Takahashi et al. 2010	Japanese beech	Autoclave	Multipurpose	Hot pressing 30 MPa	N/A	1.45	10	180

Note: An asterisk (*) in the process line indicates the presence of stop bars, Two asterisks (**) in the density line means that the target density is reported and not the actual density measured.

As far as high pressure molding is concerned, temperature was demonstrated to increase the flow ability of wood powder but also increased the stiffness of the extruded products, with a maximum reached at around 180 to 200 °C (Miki et al. 2003). The thermal decomposition was thought to be responsible for better flowability during extrusion (Yamashita et al. 2007). In the case of high-pressure molding under steam atmosphere, 160°C was reported as the optimum temperature (Miki et al. 2007; Miki et al. 2007; Miki et al. 2008). As for cellulose molding, optimal temperatures have been reported at around 160 to 180 °C (Nilsson et al. 2010; Rampinelli et al. 2010).

Delamination process a conjugated effect of temperature and moisture content

The 180 to 200°C limit of pressing temperature, as reported previously, usually comes from delamination. It could be density dependent (Ando and Sato 2009) because low-density products would have sufficient porosity for the steam to escape. Delamination can occur in all sorts of plant material molding: particleboards, fiberboards, and high pressure molding (Rampinelli et al. 2010). In cellulose high pressure molding, the delamination limit was reported to be around 200°C (Pintiaux et al. 2013). Similar phenomenon was observed in high pressure extrusion of wood: lower density and lower mechanical properties are reported, and SEM observations showed cracks and bubbles (Miki et al. 2003).

To some extent, pressure can be released in the process by using a degassing phase, which is a classical procedure for standard panels production, described as a 3-step-process (i.e. compression degassing compression) e.g. used by Anglès et al. (1999) on steam exploded softwood for binderless fiberboards. The degassing phase made it possible for some authors to mold at temperatures exceeding a previously established temperature limit (Okuda et al. 2006a; Okuda and Sato 2006). With higher MC (20%) at 120°C of pressing temperature, the degassing could not prevent delamination. This showed that first, the degassing step is a limited solution, and secondly confirmed that the delamination phenomenon is caused by an interaction between moisture and temperature of pressing. The adequate control of MC and temperature and the understanding of their interaction is a key parameter (Nonaka et al. 2013). It was also demonstrated that sometimes cracks are not obvious (not observable on the outside of the material), and MOE and MOR values can be high whereas at the same time IB can be drastically reduced. Likewise, the water resistance and especially WA (increased) can be reduced under such situations, because water can more easily infiltrate into the samples. This observation is also a classic finding associated with standard panels production.

The cooling down of the specimen prior to releasing the pressure has been reported to work for preventing delamination (Yamashita et al. 2007; Miki et al. 2008). In some cases the cooling step was not sufficient to prevent cracks and bubbles, which were still observed on the materials. The cooling down of the mold between two pressing cycles is obviously a marginal option, as it is time and energy consuming.

Some papers have reported the application of vacuum to boards before unloading the pressure, which is easy in the case of a steam injection pressing apparatus, but the results were not satisfactory (Widyorini et al. 2005).

Pressing temperature and steam assisted molding

The examples of steam injection pressing all reported a molding temperature of 190°C, but such results have been limited to a few publications, all from the same research team. Actually, this value is the result of 1 MPa of injected steam pressure (183°C) plus a few degrees in order to prevent the water for condensing in the mold (Xu et al. 2003).

Pressing temperature, time and water resistance

The classic time / temperature equivalence suggests that the optimal pressing conditions could be either a moderate temperature of molding during a long time or a higher temperature for a short time. The effect of time was reported to decrease at high temperature (Anglès et al. 1999). Elevated temperature is also reported to allow the reduction of molding time at comparable board properties (Ando and Sato 2010). It was also observed that higher temperature resulted in boards having lower density, which was correlated to lower mechanical properties (Okuda and Sato 2006). But, this higher temperature improved the mechanical properties in the humid state, despite the fact that density was lower. More precisely, it was observed that increasing temperature led to increasing the WA but reducing the TS; this indicates that bond quality was better with a lower TS, but voids (cracks) were created in the inner structure, therefore increasing WA. Overall, and in a way comparable to the severity of steam treatment, it can be observed that optimal conditions for bonding (i.e. favorizing the IB) will also maximize the water resistance (Boon et al. 2013).

Skin effect

A special effect on the surface of materials obtained by compression molding is often reported (Runkel and Jost 1956; Mobarak et al. 1982; Suzuki et al. 1998; Laemsak and Okuma 2000; Anglès et al. 2001; Okuda and Sato 2004; Xu et al. 2004; Hashim et al. 2011; Nadhari et al. 2013). The inner part of this kind of material appears rough and mat-like, but the surfaces are, under certain conditions (elevated temperature but not exclusively), smooth, plastic-like, and shiny. The vertical density profile is a classical from the industry of wood-based panels with adhesive, but unfortunately it has been poorly investigated in the research works concerning binderless molding.

Effect of temperature in the particular case of free sugars containing materials

A free sugars binding system requires 180°C or more to achieve thermoset bonding (Shen 1986), and higher temperature leads to the best mechanical properties and water resistance of boards. According to Mobarak et al. (1982) and their trials on bagasse pith, highering temperature from 175 to 185 °C increased the bending strength by 9% but lowered water resistance, which could be explained some delamination as observed by many others. In this later paper, the best specimens had a WA of 11% and a TS of 7.5%, which are excellent values way over the average results. Sugar was also thought to be responsible for the good properties of bagasse molded at high temperature and lower MC (Nonaka et al. 2013). Consistently, the addition of sugars in oil palm trunk particleboards was reported to drastically improve the properties with twice lower TS and WA (Lamaming et al. 2013). Even more impressive, similar products were reported to be resistant to boiling in water (Shen 1986). This very particular behavior is certainly attributable to the in situ resin generated by reactions (decomposition and recondensation) of free sugars induced by high temperature. These include thousands of reaction oligomer products having up to 6 carbohydrates units and reactive furfural derivatives units (Golon and Kuhnert 2012).

Effect of temperature in the particular case of bark

The binderless molding of bark has been successfully reported between 205 and 300 °C (Chow 1975; Mobarak et al. 1982). The molding of bark at "classical" temperatures (180°C) consistently produced boards with very low properties (Hashim et al. 2011). A more recent study reported 240°C and 20 minutes as optimal conditions of pressing refined spruce

bark into boards, whereas 260°C was the best temperature for maximizing IB (Gao et al. 2011). These authors performed TGA analysis and showed that temperature was responsible for a higher weight loss in the material during pressing (up to 33%). In this paper, nothing more precise than "components were produced and responsible for selfbonding" was mentioned but if higher temperature is necessary for molding bark parts, the explanation may be the high content in polyphenolic compounds than can undergo radicalar polymerization.

Elsewhere, tannins have been investigated to serve as a binder for particleboards: Good results were reported with laccase assisted oxidation of tannins, wherein thermomechanical pulp was successfully bonded (Euring et al. 2011), and hydrolyzed tannins were reported to perform better than condensed tannins (Widsten et al. 2009). Ionic interaction and radical coupling were reported between tannins and wood fibers as bonding mechanisms (Widsten and Kandelbauer 2014).

I.4.D Time

Time of molding is quite often reported to be an interesting parameter for improving the mechanical properties, although it is quite tempting to try to reduce the time as much as possible to increase production speed. Some reports indicated that increased time is preferable for mechanical properties (Anglès et al. 1999) and water resistance (Okuda and Sato 2004; Nadhari et al. 2013), although a certain limit was reported to exist after 20 minutes in the bonding ability of kenaf core powder for a 4mm plywood (Ando and Sato 2010). Contradictorily, some researchers have reported that a short time of molding was preferable (Velasquez et al. 2003), which was associated with a high temperature of molding. Other reports showed that time has a limited impact on the mechanical properties (van Dam et al. 2004), which is consistent with high pressure molding of cellulose (Pintiaux et al. 2013). Another report mentioned 6 minutes to be an optimal time for a 1 mm thick cellulose plates (Rampinelli et al. 2010).

I.4.E Granulometry

Grinding is an energy-costly step, but lower particle size increases specific surface area and accessibility to inner cell wall components, which is positive for molding. Molding smaller particles also means that the strength of individual elements has less effect, and the bonding between the particles is responsible for most of the strength. Generally, reducing particle size is reported to have a positive effect on the mechanical properties (Shen 1986; Okuda and Sato 2004). The good effect of steam explosion could also partly rely on the generation of fines and global decrease of particle size because of the treatment (Suchsland et al. 1987). Molding bigger particles was confirmed to decrease the mechanical properties (Mobarak et al. 1982; Okuda and Sato 2006). Also, the introduction of bigger particles in fine powder was reported to degrade the mechanical properties, which were then comparable to 100% bigger particles (Mobarak et al. 1982).

Gao et al. (2011) obtained the best IB with finer particles (from 0.356 to 1 mm), but larger particles (> 1 mm) gave rise to higher MOE and slightly higher MOR boards. Consistent results were obtained elsewhere (Xu et al. 2006). The good adhesive strength of very fine powder (10 µm) was reported (Ando and Sato 2009) to be better than 1 mm particles, but the production of boards made of 10 µm powder failed (Ando and Sato 2010). This shows that a limit in the reduction of particle size may exist.

In some cases, bigger particles were reported to produce interesting properties (Hashim et al. 2010; Saari et al. 2014). In this particular case, strands of several mm long were compared to small particles (< 1 mm) under similar conditions of process and target density, but only bending properties were tested. Elsewhere, better water resistance was

obtained from chips compared to powder under the same operating conditions (Okuda and Sato 2006), but overall, few results can be found about the particle size effect. Conditions favoring higher IB usually have been shown to increase water resistance, but this seems not be the case for reduced particle size.

Concerning high pressure molding, Miki et al. (2003) demonstrated that higher particle size needed more pressure to be extruded. However, the bending strength of the products of 180 to 250 µm (small particles) and 90 µm (powder) was not significantly different. High shear subjected to the material might be responsible for leaving no effect of granulometry, as the particles were really deformed and rubbed one against the others. The same research group later reported an important result on the effect of granulometry in a steam atmosphere pressing process. The very fine particles did not perform strongly, and an optimum was observable around 100 µm particle size (Figure I - 8, Miki et al. 2007a). This somehow confirmed that a limit in reducing particle size would exist for optimal properties.

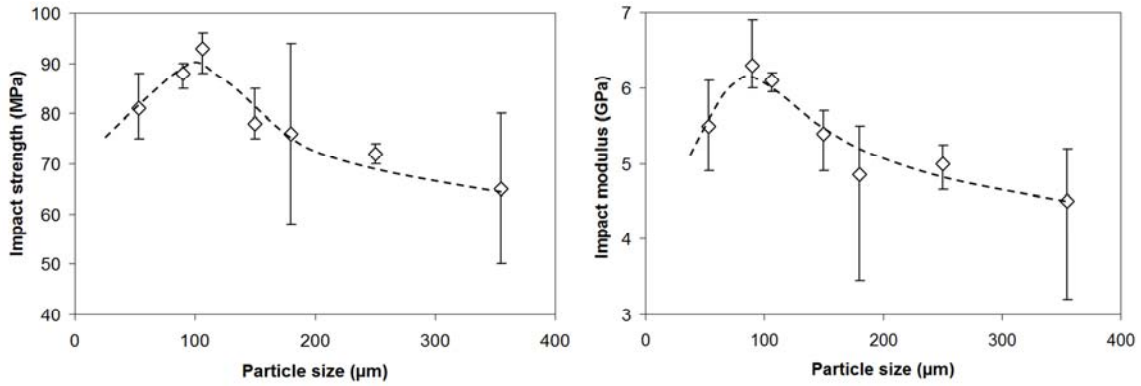

Figure I - 8: Effect of particle size on mechanical properties in high pressure molding under steam atmosphere (adapted from Miki et al. 2007a)

I.5 The physico-chemical changes and mechanisms of cohesion in self-bonded thermo-compressed plant materials

The molding phase is usually conducted at air equilibrium MC (between 5 and 12% and often 8 to 10% MC with room equilibrium) and temperature over 100°C; steam is thus created in the mold. Chemical changes occurring during hot pressing can thus be compared with steam pretreatements. The first thing to notice is that the molding time can be very fast if material has been pretreated (Suchsland et al. 1987; Suzuki et al. 1998), although short times of molding have not been reported on non-treated plant material. The pretreatment, however, takes some time to operate, and both processes, pretreatment + molding, or molding without pretreatment, can take about the same time. Runkel and Jost (1956) actually mentioned 2 phases in the molding of untreated natural fibers, considering a first step of production of gases from the material and their action on the material itself, and a second step of actual molding. The chemical modifications, however, were not reported in these early publications. Recent results have been bringing new data and highlights over the chemical changes occurring to explain the self-bonding ability of binderless plant materials which will be examined in this section.

I.5.A Physical changes

Change of color

During steam explosion of plant materials, a change of color, darker with higher severity of treatment, has been systematically reported, which suggests chemical changes (Mason 1926a; Hsu et al. 1988; Anglès et al. 1999). The same phenomenon is also observed as a result of an autoclave treatment (Takahashi et al. 2010) and on specimens produced by steam atmosphere pressing (T. Miki et al. 2007) and steam injection pressing (Widyorini et al. 2005). The same observations are made during classical compaction molding, darker with higher temperature and time of molding (Runkel and Jost 1956; Ando and Sato 2009; Boon et al. 2013). Obliviously, the change of color is a sign of degradation: the TGA analysis of plant fibers shows that hemicelluloses are the first to be completely degraded (240 to 300°C). Lignin starts to degrade at about the same temperature (240°C), but its degradation slowly proceeds until 700°C; cellulose on the other hand degrades in a narrow range of 320 to 380°C (Yang et al. 2007). The degradation occurring during hot pressing or steam treatment takes place at much lower temperature than the TGA results but conditions are too different (pressure, moisture, air) to conclude. Yet, degradation reactions and the change of colour are often associated with better mechanical performance and water resistance and common explanation for this is the generation of reactive compounds reacting on the fibers, with cross linking and condensation reactions.

Steam treatment and defibration

Pretreatment with steam is called "steam explosion" and "wood disintegration" (Mason 1926a; Mason 1926b), "steam treatment" (Anglès et al. 1999; Velasquez et al. 2002; Velasquez et al. 2003), or a certain type of "pulping process" (Suchsland et al. 1987), which name originates from the paper industry and the aspect of the fibers after treatment. Mason also used the term of "fibration" of wood (Mason 1926a) and described a "highly divided fibrous state" (Mason 1926b). The use of steam for defibrating has been since widely developed as refining method (also in a thermo-mechanical refiner) for the production of industrial wood-based panels (fiberboards and hardboards).

A low severity factor (e.g. 2.6) steam treatment does not bring any observable difference from the original fiber to the steam pretreated, but a higher (e.g. 3.8) severity factor produced fibers with similar length but smaller witdh, as can be seen in SEM photographs of Anglès et al. (1999). An individual fiber will be turn into a network of thinner single fibers with pretty much the same original length, thus increasing the aspect ratio length to width (Xu et al. 2006). The defibration is time and temperature dependent and mild conditions are considered the best option, as the fibers were described as becoming “long, light and fluffy” and not too much damaged.

Production of fines

After a Masonite gun treatment, 5 to 8% of fine solid material is discarded because this material would create defects on the surface of the Masonite boards; this fine material was molded and patented as a potential replacement for backelite (Howard and Sandborn 1937). Suchsland et al. (1987) reported about average fibers length and fines generation; steam treatment is not only increasing the aspect ratio, but also breaking down the fibers assembly, generating smaller particles. As seen earlier in this review, smaller particles (fines, i.e. ~ 0.2 mm and less) were seen to bring better performances (Shen 1986; Okuda et al. 2006b) and more precisely the IB (Xu et al. 2006; Gao et al. 2011), which is consistent with the steam effect on fines generation.

I.5.B Non-lignocellulosic parts chemical changes and effects

Weight loss, extractives and elimination of degradation products

The weight loss occurring during conventional hot pressing has not been clearly investigated, and it is in fact quite difficult to measure the weight loss due to degradation separately from a MC change. Hydrolytic reactions producing acetic and forming acids were reported (Mobarak et al. 1982), and autohydrolysis of plant materials has been described as a result of acids generated from their own degradation (Li et al. 2007).

The presence of high amounts of extractives (in the leaves) was thought to be prejudicial for mechanic performances, even if a high lignin content was measured (Hashim et al. 2011a). The authors made the hypothesis that extractives (e.g. chlorophyll) could hinder the bonding mechanisms. Other reports showed that removal of extractives prior to molding lowered the mechanical properties and the water resistance (Lamaming et al. 2013; Saito et al. 2013).

According to the Masonite corporation patents (Howard and Sandborn 1937), hemicelluloses are degraded with steam pretreatment, and products resulting from degradation are water-soluble. Therefore they can be rinsed out, which increases the strength and water-resistance of the products which is a classic of adhesive containing wood-based panels or composites (Pelaez-Samaniego et al. 2013). Hsu et al. (1988) reported that steam pre-treatment of wood chips increased the amount of water extractives, and a correlation of the "total solubilization" and log R_0 (scale for severity of steam pretreatment) was established (Table I - 11) (Anglès et al. 2001). Consistent results are found in other studies (Widyorini et al. 2005; Takahashi et al. 2010).

Table I - 11: Degradation and weight loss measured upon steam pretreatment severity (adapted from Anglès et al. 2001)

Exp. conditions											
Temperature (°C)	176	187	191	198	215	221	225	223	221	227	229
Time (min)	2.5	3.1	3.1	2.9	3	2.1	2.9	4.3	5.4	4.8	4.8
log R_0	**2.6**	**3.1**	**3.2**	**3.4**	**3.8**	**3.9**	**4.1**	**4.3**	**4.3**	**4.4**	**4.5**
Total solubilisation	**17.5**	**23.8**	**26.03**	**28.6**	**29.3**	**31.4**	**31.4**	**32.1**	**32.3**	**34.8**	**35.5**

A similar result was obtained with steam-injection pressing, and again the weight loss was correlated with steam pressure and time, which was an indication of degradation reactions during the treatment (Widyorini et al. 2005). A correlation was also established between IB and the weight loss (Xu et al. 2006).

I.5.C Cellulose and hemicelluloses changes

Cellulose and hemicelluloses degradation

Hydrolysis reactions leading to partial depolymerization of hemicelluloses and lignin are most likely to occur (Yang et al. 2007), and degradation products of hemicelluloses and lignin are confirmed in the water extractives from steam pretreated biomass (Sun et al. 2005). This was already mentioned in the work of Howard and Sandborn (1937), Suzuki et al. (1998), Tanahashi (1990). This hypothesis was also made for autoclave treatment of wood pieces (Ito et al. 1998).

Actual data confirmed the effective degradation of hemicelluloses and the positive correlation with severity upon steam explosion (Hsu et al. 1988; Quintana et al. 2009), steam injection pressing (Xu et al. 2006) with confirmation of xylose being measured in the water

extractives (Widyorini et al. 2005), and also concerning autoclave treatment (Takahashi et al. 2010). Degradation of hemicelluloses was also confirmed for classical hot pressing (Xu et al. 2006). For instance, Xu et al. (2006) measured 26.7% of hemicelluloses on refined fibers, 25.5% on the fiberboard resulting from hot pressing, and 20.2% when using steam injection pressing.

Cellulose is also thought to be degraded during steam treatments. The relative cellulose content was reported to decrease with increasing severity of steam explosion (Anglès et al. 1999). The alteration of cellulose was also demonstrated in another study (Anglès et al. 2001) where the DP_v (viscosity measurements of the degree of polymerization) was reported to decrease. Steam injection pressing was also reported to decrease alpha cellulose content, even though glucose residues were not significantly more extracted (Widyorini, Xu, Watanabe, et al. 2005). Consistently, the decrease of holocellulose content was reported using an autoclave treatment and confirmed as being positively temperature dependent (Takahashi et al. 2010). Cellulose degradation was not always observed, and some reports indicated a constant holocellulose content after steam explosion (Quintana et al. 2009).

Correlation of cellulose and hemicelluloses content and the physical properties

The basic idea is that hemicelluloses and lignin can undergo glass transition and will, hence, be responsible for the adhesion. Cellulose would not actively participate in the molding but rather serve as "reinforcement" for the lignin/hemicellulose matrix (Saito et al. 2013). But on the contrary, Ito et al. reported an important role of cellulose in the mechanisms of cohesion especially for water resistance. Steam treatment was observed to hydrolyze amorphous domains and turn cellulose crystal Iα into Iß (Ito et al. 1998a). In a second paper (Ito et al. 1998b) the authors concluded that steam treatment partially hydrolyzed even paracrystalline region of cellulose and that novel crystals were responsible for the shape fixation and water resistance. This findings were also confirmed by Tanahashi (1990).

Furfural and hydroxymethyl furfural routes hypothesis

When weak acid or water at 130 to 170°C is added to hydroxymethyl furfural, polymerization occurs (Mobarak et al. 1982; Shen 1986); this reaction could take place during hot pressing of natural fibers after some degradation of hemicelluloses, which is an old and motivating hypothesis (Suzuki et al. 1998, Runkel and Jost 1956). The furfural hypothesis has been often questioned and debated (Anglès et al. 1999; van Dam et al. 2004). However, few reliable chemical analyses have been published so far.

Okuda and Sato (2004) added 5 to 15% of furfural in their binderless boards, and they observed a small increase of IB. However, they could not prove a correlation between IB and amount of furfural addition. In a further study the authors suggested that furfural polymerization would not occur significantly (Okuda et al. 2006b).

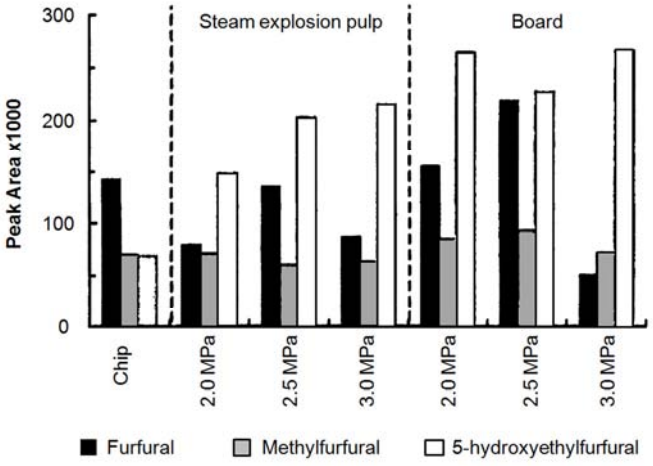

Figure I - 9: Furfural (and derivatives) content changes during steam pretreatment and molding (adapted from Suzuki et al. 1998)

Figure I - 9 shows that 5-hydroxymethyl furfural (HMF) content increased with pretreatment and was also higher in the board than in the steamed fibers (Suzuki et al. 1998). These results tended to verify the furfural hypothesis for the pretreatment step, but as furfural content increased after pressing, a possible polymerization remained uncertain. New results were reported recently which confirmed the formation of furfural and HMF during hot pressing from respectively pentoses and hexoses, and high temperature pressing made the HMF react to form new products (Cristescu and Karlsson 2013; Lamaming et al. 2013).

I.5.D Lignin changes

Lignin, according to Mason (1928), is the most important chemical for self-bonding and for water resistance of fiber-based binderless molded objects, Mason mentioned that during the molding operation, lignin melts and creates a welding effect.

Observation of lignin flow after steam pretreatment and matrix effect

The industrial thermomechanical refining process produce fibers bundles wherein the surface of the fibers is covered by lignin; the wet hardboard production process takes advantage of it by using lignin to form intra-fiber bonding (Back 1987). The explanation to this is in the moisture temperature conditions of thermomechanical refining over the softening point of lignin which preferably breaks wood structures within the lignin-rich middle lamella (up to 70% lignin content) producing holocellulose-rich units (fibers) encased in lignin (Irvine 1985). In binderless boards production, the use of steam-exploded materials other than wood was explored to produce fiberboards-like materials with the hypothesis of using lignin on surface of the fibers to create a matrix effect, the same way than in wet processing of hardboard, but at lower target density and in dry processing (Suzuki et al. 1998).

Lignin droplets were effectively observed on the surface of steam-treated fibers (Anglès et al. 1999). These lignin droplets came from the coalescence of lignin resulting from hydrolytic cleavage at high temperature which largely eliminates the lignin/cellulose interface (Marchessault et al. 1982). Their size was evaluated to be in the range 100 to 400 nm.

The conditions that made it possible to observe lignin on the surface of fibers also produced the best IB on the binderless fiberboards (Anglès et al. 1999; Gao et al. 2011). Consistently, a black matrix embedding the fibers, assumed to be the result of cross-linking of degradation products of hemicelluloses and lignin, was observed as a results of an autoclave treatment and during the pressing step; heat further allowed matrix components to flow out of the cell wall to fill the gaps between the particles (Takahashi et al. 2010). In the context of wood torrefaction study, recent results demonstrated that liquid lignin intermediate (LLI) migrated from the middle lamella upon thermal treatment and deposit on the fiber surface (Pelaez-Samaniego, Yadama, Garcia-Perez, Lowell, and McDonald 2014).

Lignin modification / degradation

Lignin polymer is reported to obtain an increased polydispersity upon steam treatment; the influence of refining temperature on the chemical changes on lignin is well known (Marchessault et al. 1982). Other literature reports (e.g. Figure I - 10 have indicated an increasing lignin content (Klason method) with severity of pretreatment (Lamaming et al. 2013; Quintana et al. 2009; Takahashi et al. 2010).

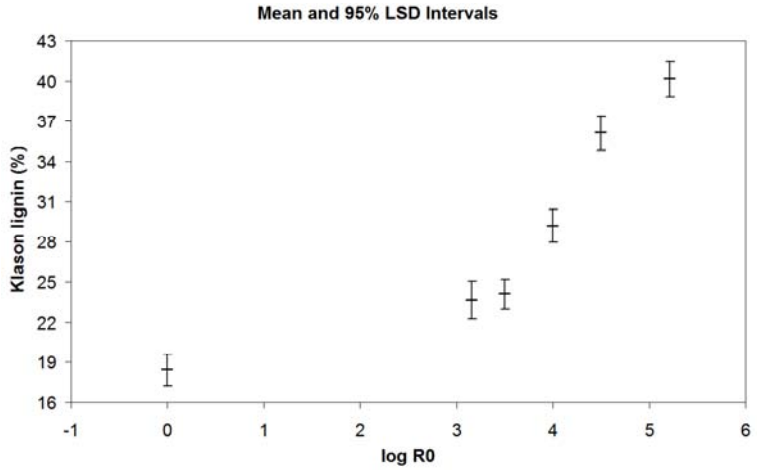

Figure I - 10: Link between the increase of lignin content and pretreatment severity (adapted from Quintana et al. 2009)

A particularly high Bjorkman yield (Björkman 1956) was reported after steam pretreatment, which suggested an increase of the relative apparent lignin content, including a lot of "esterified and etherified phenolic compounds" (Suzuki et al. 1998). According to the authors, those compounds are less likely to form covalent bonds; therefore they should not be responsible for adhesion. The cleavage of the aromatic nuclei of lignin was also reported at high severity, where the mechanical properties of molded products are decreasing. Lignin modifications due to steam pretreatment were confirmed by use of FTIR and NMR analyses (Suzuki et al. 1998; Laemsak and Okuma 2000).

Contradictorily, Klason lignin has been sometimes reported to decrease slightly with severity of steam pretreatment, while organic soluble components (soluble lignin) increased (Anglès et al. 1999). This fact was supported by steam injection experiments, as Klason lignin was reported to be degraded proportionally to steam pressure and time of steam pressing, while the relative composition in acid soluble lignin increased (Widyorini, Xu, Watanabe, et al. 2005). As far as hot pressing is concerned, degradation of lignin has been reported to increase with temperature, showing an increasing methanol yield (Okuda et al. 2006b). In this same paper, FTIR measurements showed cleavages of lignin intermonomer

linkages during hot pressing, demonstrating the degradation of some parts of lignin, which were thus more extractible with methanol and did not appear in the residue. This shows that these molecules did not create covalent bonds; they might nonetheless be plasticizers for lignin (Bouajila et al. 2005).

According to Widyorini et al. (2005c) the syringyl / guaiacyl (S/G) ratio decreased with severity of steam treatment, whereas in hot pressing conditions (without steam) the S/G ratio remained similar to the starting material. This showed that steam treatment degraded syringyl groups more than hot pressing. They also reported that the cinnamic acid / guaiacyl ratio (C/G) decreased with increasing severity of treatment and was well correlated to the strength of the composites. Tanahashi et al. (1990) proposed a complete degradation mechanism of lignin during steam explosion by treating extracted lignins, but the methodology remained unclear and no explicit conclusions were drawn.

Okuda et al. (2006a, 2006b), observed that the benzaldehyde yield of extraction decreased during hot pressing, showing that some lignin residues experienced condensation reactions. The authors claimed that guaiacyl acid could be the favorite molecule for condensation reactions. FTIR showed that new compounds were created, which confirmed reactions on lignin. However the crosslinking was not demonstrated in the cited work, and the authors mentioned that the condensation may occur to form small molecules instead of a real network necessary to obtain a matrix effect and thus explain the better bonding properties. Cristescu and Karlsson (2013) reported recently that beta ether and methoxyl groups subjected to condensation reactions corresponded to good adhesion properties and water resistance.

According to Ito et al. (1998a) the lignin content changes were not correlated to the water resistance of the square compressed wood logs materials. According to the authors, the mechanism of shape fixation against water relied more on cellulose crystallization than on lignin. Except for rare reports like the previous one, the hypothesis according to which lignin is important for selfbonding and strength of molded products is vastly supported (Mason 1928; Howard and Sandborn 1937; Suzuki et al. 1998; Bouajila et al. 2005; Imanishi et al. 2005; Okuda et al. 2006b; Yamashita et al. 2007). For instance, the addition of methanol extractives in fibers prior to molding increases the IB, while the material from which they have been extracted had a lower IB (Figure I - 11) (Okuda et al. 2006a). In this example, kenaf core powder with an average particle size of 53 µm was used and pressed into 0.8 g/cm^3 density binderless boards. The water properties also decreased with removal of those extractives, and improved upon addition. The addition of periodate lignin also enhanced the IB, while adding extracted holocellulose (therefore "diluting" lignin) led to its decrease (Okuda et al. 2006a).

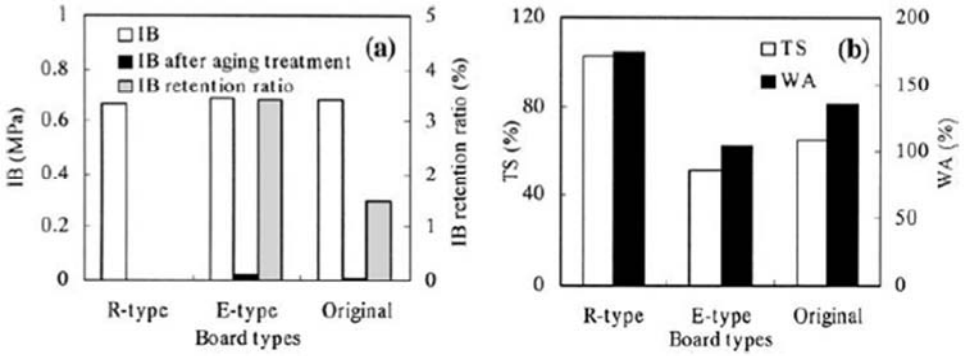

Figure I - 11: Experiment of methanol extractives (lignin components) addition (E-type) and removal (R-type) compared to original kenaf core powder (republished from Okuda et al. 2006a, with kind permission of the Japan Wood Research Society)

Lignin softening and "activation"

As mentioned by van Dam et al. (2004b) based on literature reports, steam explosion lignin and organosolv lignins are very reactive and can be used as adhesives for particleboards. They could replace up to 50% of synthetic binders (phenol / phenolic based resins, based on which an uncountable number of patents have been published), although the effective use for it remains uncertain on an industrial scale (Gosselink et al. 2011). The endotherm at 140°C that disappeared on a second heating was attributed by some authors to the softening of lignin, during which they believed irreversible condensation (dehydratation + crosslinking) happened (van Dam et al. 2004). Recent work on thermal analysis of lignin seems to attribute this first endothermic event around 150°C to the fusion of lignin. Some other high endothermic peaks above 180°C were associated with physical or/and chemical changes of lignin but are difficult to explain completely because of the structural complexity of lignin (Murugan et al. 2008; Kim et al. 2014). This irreversible change in lignin occurring after being heated over a certain temperature (180°C) would possibly be related to the "lignin activation" phenomenon previously reported (Mobarak et al. 1982). Activation is a term inherited from chemical (oxidant and/or alkali) wood treatments that would involve the partial depolymerization (modification of active sites) to obtain new linkage capability. Activated lignin would have a reduced melting point, and capacity to "polycondensate".

The effects of crossing the T_g value (softening point) by adjusting moisture and temperature have tremendous potential in increasing board properties. Bouajila et al. (2005) extensively studied the evolution of T_g of lignin in samples during hot pressing and reported that the mechanical properties mostly depend on the possibility for the molding temperature to exceed the T_g of lignin according to the local moisture in the material. Such experiments that are classical in the industry of wood-based panels with adhesive have been too rarely applied to binderless board production.

I.5.E Mechanisms of cohesion

In the industry of wood based panels, "adhesion" refers to the cohesive interaction between fibers and the adhesive, "bonding" refers to interactions within the adhesive, and "cohesion" is the sum of bonding and adhesion. In the case of hardboard, fibers/fibers cohesion only is responsible for the cohesion. In the case of binderless boards, the sum of fiber/fiber adhesion and insitu matrix adhesion and bonding is responsible for the cohesion and the science behind is still unclear compared to the classical wood-based panels technology. These differences appear to be important:

Plant materials have specific compositions, organization, and morphology that influence the molded objects properties in a much wider variety than wood.

Processing is generally made at higher temperatures for a longer time; thus many chemical reactions are possible: hydrolysis, degradation, oxidation, and recombination. These chemical changes that are undesirable in classical wood panels processing are in binderless necessary preconditions for self-bonding.

Compression of wood particles in the case of wood-based panels with adhesive is necessary, but pressure is an even more crucial parameter in the case of binderless boards processing: densities vary in a wide (mostly higher density) range although the density of wood based panels is calibrated (0.6 to 0.7 g/cm^3 for particleboards, 0.65 to 0.85 g/cm^3 for fiberboards).

In the classical wood panels industry, processing (i.e. pressing) is adjusting pressure time and temperature to evaporate excess of water and cure the resin. In the case of binderless molding, processing must be adjusted in order to trigger the bonding wherein all main parameters are interdependent: for example composition and structure of starting material will determine equilibrium moisture content, which will be determinant on the physico-chemical properties of fibers (glass transition temperature, flowability, crystallinity)

but also on the mechanisms of degradation of lignocellulosics components, and all this will be impacted by processing parameters especially time and temperature.

The comprehensive understanding of the exact mechanisms that would fully explain the properties of binderless plant materials is difficult, but there are some concepts and ideas that can help to improve their properties. There are some parallels to make between selfbonded plant materials and wood welding on the one hand, and thermal wood treatment in the other hand:

Glass transition of cell-wall polymers

The importance of glass transition in wood-based materials inherited from the polymer science and was extended to biopolymers in the early work of Slade and Levine (Slade and Levine 1991). All polymers undergo a transition from a glassy state to a rubbery state at a specific temperature, which is extremely dependent on their moisture content (Figure I - 12).

In the rubbery state, polymers acquire enough molecular motion to deform. They adapt to the mechanical constraints, which increases surface contact and creates a matrix effect inside the composite. Depending on their molecular structure and hygroscopicity (depending on the polar character of the polymer), the glass transition temperature (T_g) varies from around 200°C in the dry state to around 0°C for 20% MC for most carbohydrates. The T_g's of wood polymers in the dry state are reported to be 220°C (cellulose), 170°C (hemicellulose), and 200°C (lignin) (Back 1987). An illustration of the the T_g-moisture dependence is the possible molding of hardboard in wet process without using binders although binders are necessary in the dry state because core layer cannot reach the T_g of wood polymers.

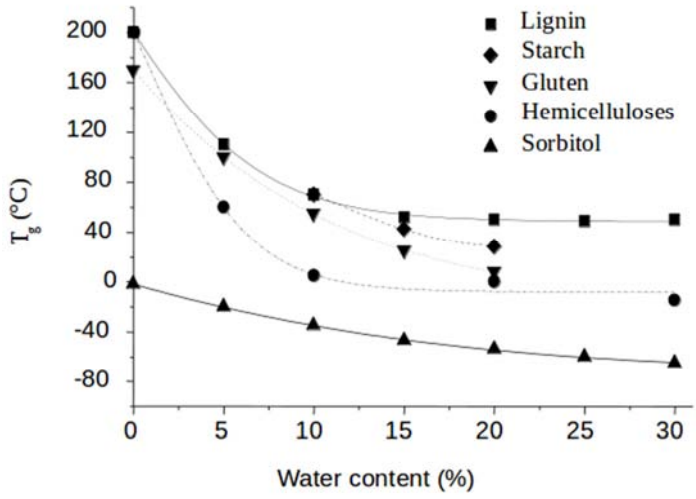

Figure I - 12: Glass transition temperature of biopolymers according to their water content (adapted from Gaudin et al. 1999; Micard et al. 2000; Slade and Levine 1991)

Yet, although isolated lignin and hemicelluloses are amorphous and exhibit glass transitions, their behavior inside the organized cell-wall structure is not as obvious (Irvine 1985), and it becomes even more complicated when they are partially or completely degraded into low molecular weight compounds, for which no thermoplastic effect could be reasonably taken into account. In many cases, the effect related to the glass transition depends on raw material structure, mechanical, chemical, and enzymatic pre-treatments (Álvarez et al. 2011), as all these effects influence molar mass and molar mass distribution of the material as well as secondary forces additionally responsible for the integrity of the material. Nevertheless,

the presence of lignin, free enough to show a relaxation peak when tested in DMA, is determinant to improve mechanical properties (Bouajila et al. 2005). The compression process on lignocellulosic fibers at a temperature above lignin glass transition temperature (which can go above 150°C when water is evaporated) gave the best properties. A parallel can be made with thermomechanical refining of wood that requires to place the fibers in moisture / temperature conditions above the T_g's of polymers (hemicelluloses, amorphous part of cellulose, lignin) in order to separate the fibers along the tangential orientation of other fiber direction and obtain higher surface development (Irvine 1985).

The thermoplastic behavior of biopolymers from plant cells have also been described for fibrous raffinate of sunflower containing residual proteins (Evon et al. 2010) and on wheat straw for the production of pellet by dry extrusion (Stelte et al. 2011).

Similar conclusions have been reported concerning the cohesion obtained by wood friction welding. Temperatures around 200°C are reached in the glue line, which is densified, and the thermoplastic effects of lignin and hemicelluloses are predominant (Gfeller et al. 2003).

Cross-linking of lignin-carbohydrate-complex (LCC)

In the field of wood treatment in order to increase its durability many research works have attempted to explain the mechanisms of chemical changes during a thermal treatment depending on the operating conditions. Factors considered have included the presence or not of oxygen or of water vapor, temperature, and time. These processes involve then clearly the same kinds of modifications as hot-pressing or wood welding.

Some of these findings are similar to those discussed in the previous part on the heat-induced degradation of lignocellulosic components: a reduction of free hydroxyl groups through the degradation of hemicelluloses (Srinivas and Pandey 2012; Singh et al. 2013; Liu et al. 2014), a decrease of cellulose content, like determined on bamboo samples (Y. M. Zhang et al. 2013), a change on lignin structure with an increase of the aromaticity (Park et al. 2013), but also some physical effects such as a decrease of nano-pore shares and fiber saturation point (Zauer et al. 2014).

The increase of durability of heat-treated wood (two stages, first in excess of water vapor then in a dry state under an inert atmosphere, temperature below 200°C) is mainly induced by cross-linking mechanism (Tjeerdsma et al. 1998; Boonstra and Tjeerdsma 2006). First the hemicelluloses are degraded, producing acids that further increase the depolymerization rate of carbohydrates (of the remaining hemicelluloses and the amorphous cellulose); then lignin is cleaved and activated with an increase of free reactive sites. In a second step, the cross-linking of the lignin network occurs, involving some products of hemicelluloses degradation such as furfural or methyl-furfural, which was confirmed in binderless particleboard production (Cristescu and Karlsson 2013; Lamaming et al. 2013). Polycondensation reactions are not completely elucidated but are thought to be responsible for the lignin content increase after heat treatment and obviously related to the improvement of water resistance.

Hydrogen bonding and cocrystallisation of cellulose as a consolidation mechanism

The most admitted hypothesis in binderless board production is that cellulose does not play an important role in bonding (Anglès et al. 2001). But, looking at the results obtained by hot pressing of pure cellulose, there might be a possibility of pressure-driven selfbonding in cellulose, as some mechanical properties obtained by direct compression at high pressure of cellulose powder have been reported (e.g. Pintiaux et al. 2013). The mechanisms of cohesion are thought to rely on fibril aggregation through hydrogen bonding (Nilsson et al. 2010) or other interactions, which has been recently debated (Glasser et al.

2012). Crystallinity changes were also observed (Vaca-Medina et al. 2013), which could confirm the importance of cocrystallization mechanisms (Newman 2004).

Conclusion and future directions

Production of binderless material by thermo-compression of lignocellulosic fibers is a very simple technique in front of a very complicated science: it requires studying many concomitant phenomena involving the disorganization and re-organization of complicated multi-components of biological structures. Most of the time, research studies on binderless boards do not take advantage of the classical phenomena that have been vastly investigated in the thermocompression of industrial wood-based panels with adhesive. In many studies, it is clear that the bridge between these two different worlds of science has not been crossed. Lots of improvements for this new kind of materials are still possible, and although the complete understanding of the occurring transformations remains unachieved to date, some elements that have been highlighted in this review will help to guide researchers who would like to study these fascinating transformations and improve future materials.

From the analysis of the literature, it appeared that correct mechanical properties can be obtained without pretreatment (i.e. particleboards type) in the case of certain raw materials, but when steam treatment is involved it seems that any lignocellulosic material would be moldable (i.e. in fiberboards type) and would result in suitable mechanical properties. Water resistance, however, remains low and does not match the standards on industrial wood-based panels. Regarding the choice of raw materials, the use of by-products is preferred and the presence of lignin (and eventually of storage biopolymers even in small quantities) is definitively favorable. Mixing plants together and structural associations (layers etc.) have been barely studied and could be of great interest.

The eco-friendly argument is very often offered as a competitive feature of such materials, but looking more precisely at the energy cost of such processing is necessary to qualify its eco-compatibility. There is a lot of room for Life Cycle Analysis of this kind of materials and processes, which should produce interesting and innovative studies.

Temperature of molding is undoubtedly the most important processing parameter for which the limiting factor is delamination. High temperatures are favorable to improve water-resistant properties and are responsible for the skin-effect and "plastic" touch. A minimum of moisture is necessary in order to obtain satisfactory mechanical properties, but this minimum value and the effect of higher moisture are still unclear. During compression at elevated temperature, steam is generated from the initial moisture, and effects can be compared to changes occurring during steam pretreatments. Some technological tricks can be applied to prevent delamination, but more research is needed in order to better understand the relation between moisture / temperature and delamination, because molding conditions that give the best properties are very close to those triggering delamination.

Steam treatment involves a combination of defibration, degradation (of hemicelluloses and part of lignin mainly), and lignin modifications (plasticization i.e. decrease of T_g, partial depolymerization, flowability, and condensation to a lower extent). Moderate severity of steam treatments generally provides the best bending properties. The highest severity of steam treatment was reported to increase water resistance and IB: these two parameters seem to be correlated, which could be further studied. In our opinion, a moderate severity of pretreatment in one hand and a higher severity in the other hand would favor two different mechanisms, that we named "thermoplastic" and "thermoset", respectively. These two main bonding mechanisms would happen in thermal treatment and any kind of thermocompressive molding of natural fibers, even at moderate pressure, which is not the case of the quite unknown cocrystallization phenomenon reported on high pressure molding of pure cellulose; and for this reason, is considered apart.

Thus, it makes sense to think in terms of a "thermoplastic" mechanism, which would mostly occur under mild conditions of processing (temperatures below 160 to 180°C), during which the glass transition temperature of lignin and hemicelluloses (and also starch and

proteins if concerned) is passed. In the resulting rubbery state, polymers would deform, filling the voids in and between particles, and giving the highest mechanical properties (MOR, MOE). The "thermoplastic" mechanism can be expected to occur more easily if polymers are freed up by chemo-mechanical destructuration and plasticization brought about by pretreatments because of the highly organized native state in the plant's cell-wall.

Secondly, one can envision a "thermoset" mechanism, which involves chemical reactions at higher temperature (over 200°C), with more important depolymerization / degradation of the polymers, leading to the production of weak acids and contributing to even more degradation by autohydrolysis. Highly reactive degradation products, especially aldehydes (particularly furfural and hydroxymethyl furfural), would participate (together with lignin) in the creation of new compounds (e.g. lignin-cellulose complexes) and in the cross-linking of the composite matrix, which brings about bonding between the cellulosic particles and gives rise to water-resistant properties.

Because of the gradients (density / moisture / temperature) occurring within the processed material, depending on product shape (e.g. thickness), temperature, moisture and time have to be adjusted together to control the thermoplastic/thermoset balance. Lignin for instance, which is reported to be the most important polymer for the development of bonding in the absence of an added adhesive, would have different behaviors: in the "thermoplastic" mechanisms lignin would be "activated", plasticized, and experience flow and some degradation, whereas in the "thermoset" mechanisms, condensation reactions would result in complexes with the other polymers. The "thermoplastic" / "thermoset" limit, however, remains unclear also because it is extremely complicated to study lignin itself, as extracted lignin is always degraded and would not behave as native lignin (as it is inside the cell wall).

Surely, the "thermoplastic" and "thermoset" mechanisms coexist, and no limit can be precisely set. Yet, delamination is thought to occur at the transition from "thermoplastic" to "thermoset". This is because of the loss of native structure due to thermoplastic flow and disorganization of the cell wall structure and the release of volatile compounds and water. At the same time more polymer/polymer interactions take place during the compression in the rubbery state, and these involve organic compounds produced in the course of thermal degradation. When the "thermoset" mechanism is predominant, water would be consumed by hydrolysis and volatile compounds would be condensed into bigger non-volatile structures. Much further work is needed towards the understanding of these physico-chemical reactions for these simple but elegant materials to find a real industrial market.

II Preliminary discussion about technical considerations

This chapter is an appendix of the experimental part (Chapter VI) yet a necessary preliminary to understand the techniques employed in this thesis to acquire the results and their evolution.

As seen in Chapter I, most of the literature about the thermo-compression of plant fibers concern industrial wood-based panels with adhesives or their alternatives that are focusing on replacing either the starting material (wood) or the binder system (different binder, or binderless molding). In the field of industrial wood-based panels and related materials, thermo-compression can be very restrictive because panels of fixed density and thickness are produced. Yet, this technic is not commonplace, and leaves a lot of room for innovations and imagination. Thus, the description of the molding process, definition of terms and some highlights on the technological locks are necessary for the reader to understand the problematic and all the complexity of this subject, and subsequent choices made in this work.

II.1 Project HYPMOBB: where it all begun

The LCA has been working with constituent's separation and treatments and modifications of biomass such as wheat straw for decades. The laboratory has gained a high expertise on the use of twin-screw extruders. When mechanically pretreating vegetable matters in a twin-screw extruder and investigating conditions, low solid/liquid ratio have been tested which conducted to the blockage of the extruder, usually in front of the dies which didn't let the material out. In this situation, pressure is increased, and friction occurs between the rotating screws and the extrusion chamber, which leads to rapid heat generation while the material keeps arriving, increasing shear and torque on the machine, that eventually stops. When disassembling the extruder, highly densified vegetable matters was found with a shiny plastic-like surface effect, perfectly fitting the shape of the screws (Figure II - 1).



Figure II - 1: Remains of wheat straw extrusion blockage

The hypothesis was made that 100% plant fibers self-bonded objects with a plastic finish high molding capacity could result from heat and pressure treatment. Thereafter was born the idea of project HYPMOBB to reproduce this extruder failure phenomenon, study and possibly exploit it.

II.2 Compaction molding, principle, design and terms

Compaction molding is defined as the technique which uses two complementary "male" and "female" shapes to form a molded object upon applying pressure between the two complementary shapes. It is commonly used in reinforced systems with thermosetting resins and glass fibers or more recently plant fibers.

II.2.A Two dimensions molding

In 2D molding, the two complementary shapes are flat and the starting material is loaded in the lower part called "frame". The upper part is called "punch" and enters the frame to apply pressure and form the compacted material (Figure II - 2).

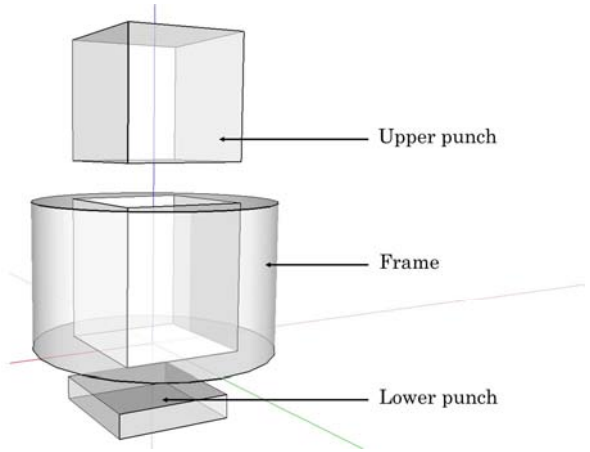

Figure II - 2: Drawing of a 2D mold (5x5 square shape)

II.2.B Three dimensions molding

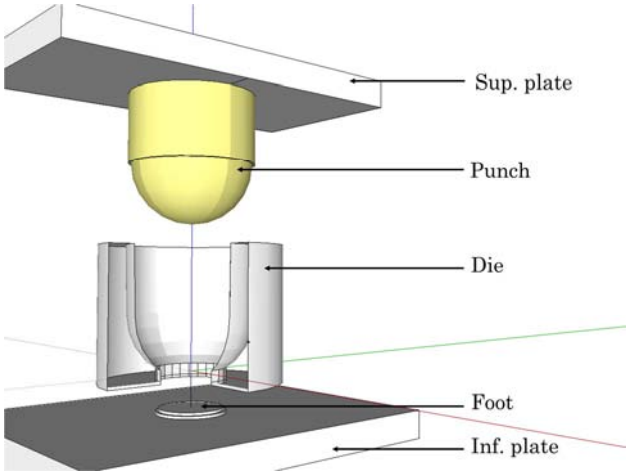

Figure II - 3: Drawing of a 3D mold (bowl shape)

In 3D molding, the female part is called "die" because it includes a prolonged part where the material is loaded before compaction. This prolonged part is necessarily an extruded length of the maximum diameter of the male part which is called “punch”. The part over this maximum diameter will thus be “printed” by the upper punch, whereas the die will be responsible for the shape of what is under the maximum diameter. For example, parts like bowls can be molded (Figure II - 3). For the need of demolding, the die should have an open part in order to help release the molded object from the mold. In the case of a bowl, the open part is on the foot of the bowl, and for stability reason, a relief is machined on the inferior plate in order to mold a hollow disk in the molded object.

II.3 Limits of compaction molding applied to lignocellulosic fibers

Direct compaction molding is a technique that has the advantage of being easy to set up, using simple and relatively light molds, simple pressing machines, allowing versatile experiments but also has some limits. Highlighting and understanding these limits is essential for considering technical applications and improvements.

II.3.A Limited shapes, not actual 3D

Because of this "die and punch" conception, only “semi-3D” shapes can be achieved. For instance, an "hourglass" shape cannot be molded in compaction-molding because, in the direction of the hourglass standing, the cross section (diameter for a round shape) goes through a minimum between 2 maximum thus it cannot be removed from the mold (Figure II - 4). On the contrary, a "bowl" shape is possible (the diameter has only one maximum).

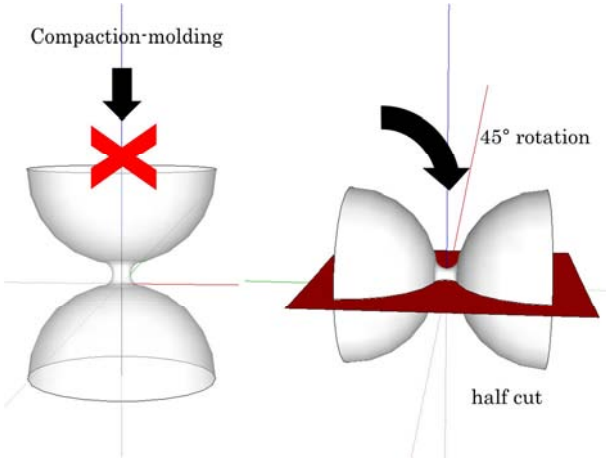

Figure II - 4: Semi 3D compaction molding, the hourglass example

The hourglass can be molded in the direction of the hourglass lying (alongside) which would require to precisely adjust the height (therefore the quantity and density of the material) very carefully.

Considering a perfect control is achieved on quantity and density of the material after compression, the machining of the punch would still be really uncertain as very tight edges are needed (in theory, infinitely tight) with the requirement of resisting to the high pressure (Figure II - 5). Even if these requirements are completed, the demolding would still be difficult; these considerations put on the light on the shape limitations of compaction molding.

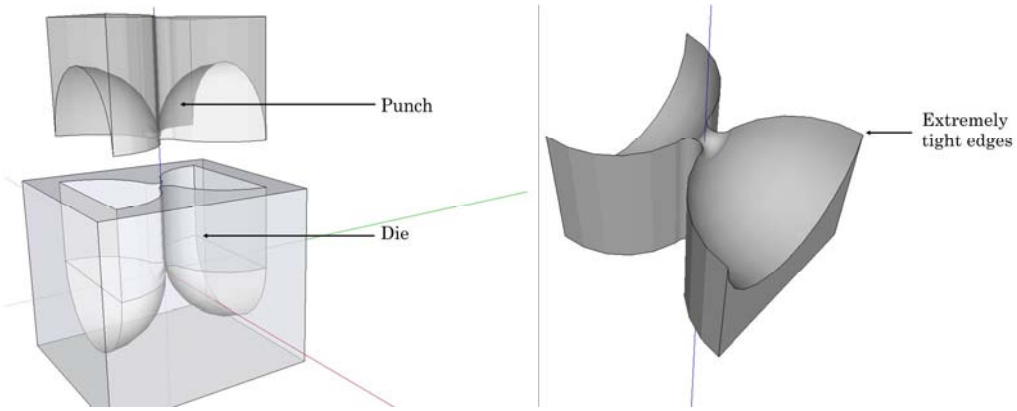

Figure II - 5: Drawing of an hourglass shape mold alongside and punch

II.3.B Demolding

Because of the conception of the molds, the molded part remains in the die (female part) and demolding has to be carefully designed. Manual ejection is possible if the mold can be put apart easily but it would take much time, what, for industrial application is limiting. Casual mechanical ejection technology (e.g. compressed air driven ejectors) cannot be used because the parts needs to be lifted up at least the height of the female part.

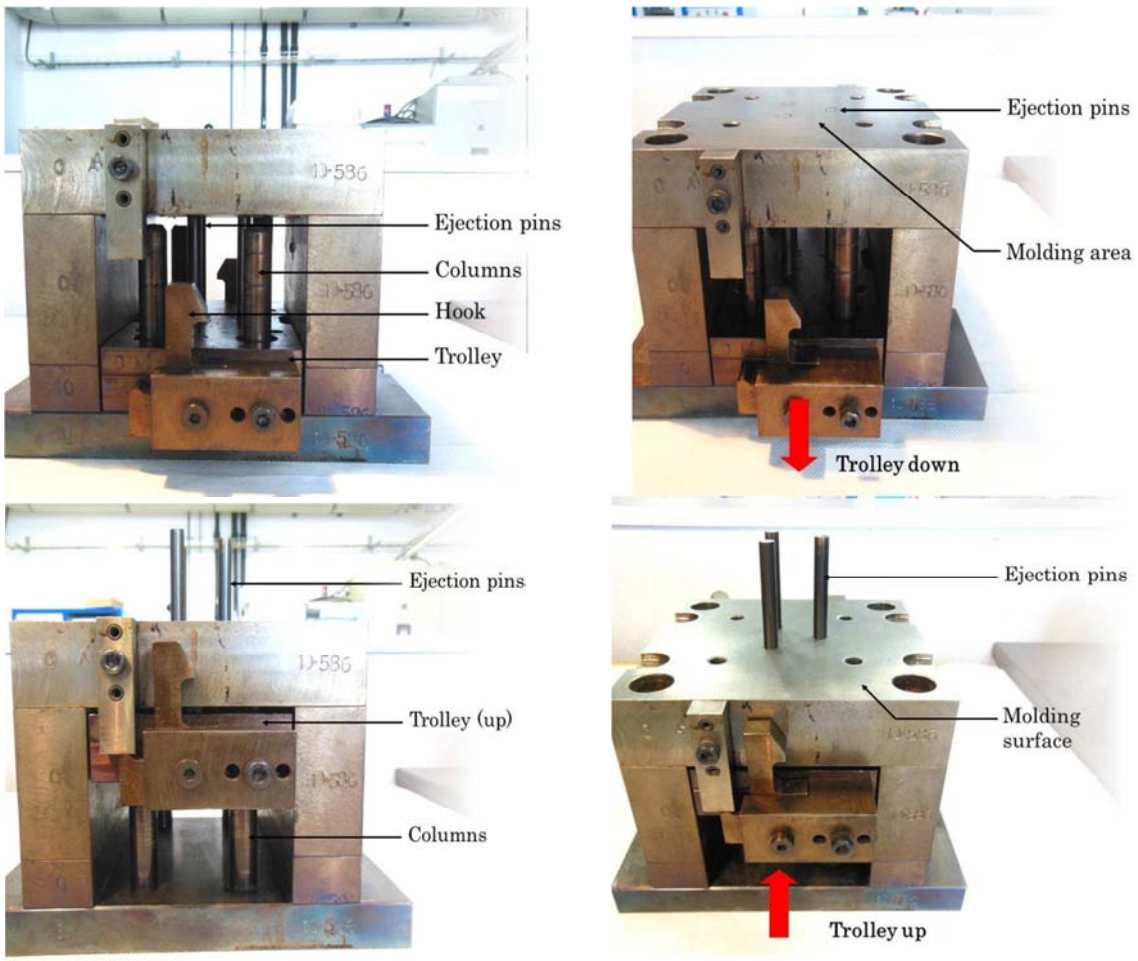

Figure II - 6: 2ROP mechanical ejection system

Available systems would also suffer from high pressure and temperature. Therefore special ejection techniques are required for industrial application, a prototype of mechanical ejectors driven by the pressing machine were designed by 2ROP (Revel, France). Figure II - 6 and Figure II - 7 explains its functioning. The bottom of the die has ejectors going through connected to a trolley that can moves up and down, driving the ejectors through the molding area.

With the die on, the ejectors are down for the molding phase, material is filled and compaction can begin. As the upper part of the mold (punch holder) goes down, a hook connects to the trolley. Upon opening the pressing machine, the trolley goes up with the upper part until a stop disconnects the hook releasing the upper part and letting the trolley up with the part accessible for removing.

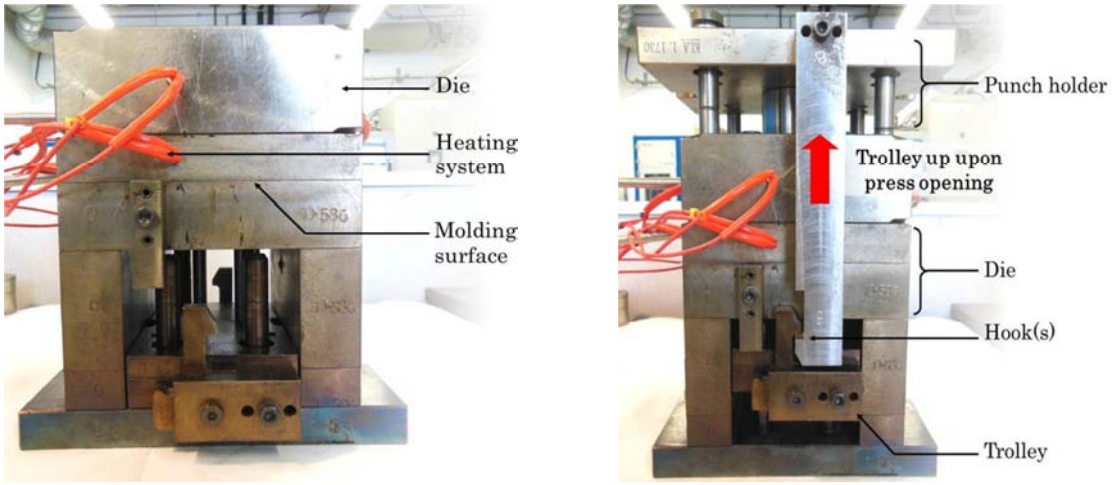

Figure II - 7: 2ROP mechanical ejection system (full setup)

The system works perfectly but long time reliability remains uncertain, notably because of the direct metal-metal friction of ejectors parts through the mold.

II.3.C Homogeneous filling of the mold cavity

The filling of the mold has been a constant source of concern: for example in 2 dimensions, a homogeneous spreading of the material has to be managed, because density will be directly affected by the local thickness of material filled in the mold. Areas were quantity of material is higher (hills) will be more compacted as a result of pressure applied only on part of the surface, thus less compaction on areas were quantity of material is lower (valleys), creating weak points of lower densities.

An experiment was carried out in order to verify the impact of the heterogeneous filling on the mechanical properties of 2D compaction-molded specimens: A first set of dog bone specimens were molded in the control conditions, i.e. manually filling the mold as well as possible, and a second was molded with a 6 mm metal cylinder in the center of the mold during the filing step and normal equalization of the material in the mold. The bar was removed and a normal press cycle was run (Figure II - 8) which created a lower density weak spot (Figure II - 9).

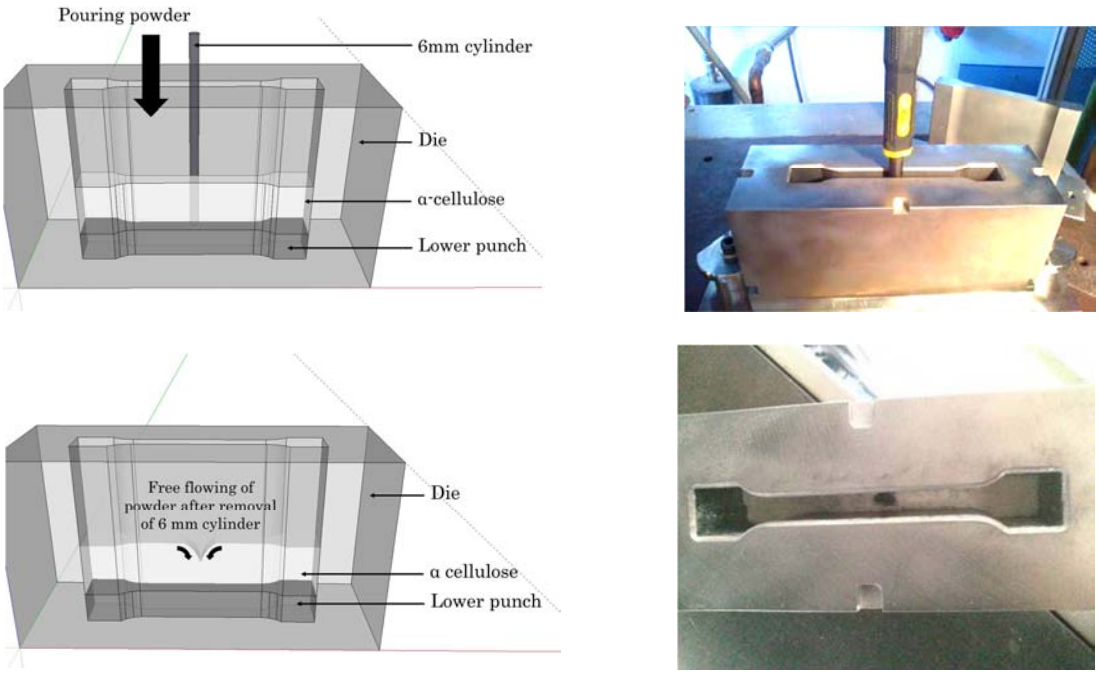

Figure II - 8: Forced heterogeneity of filling experiment

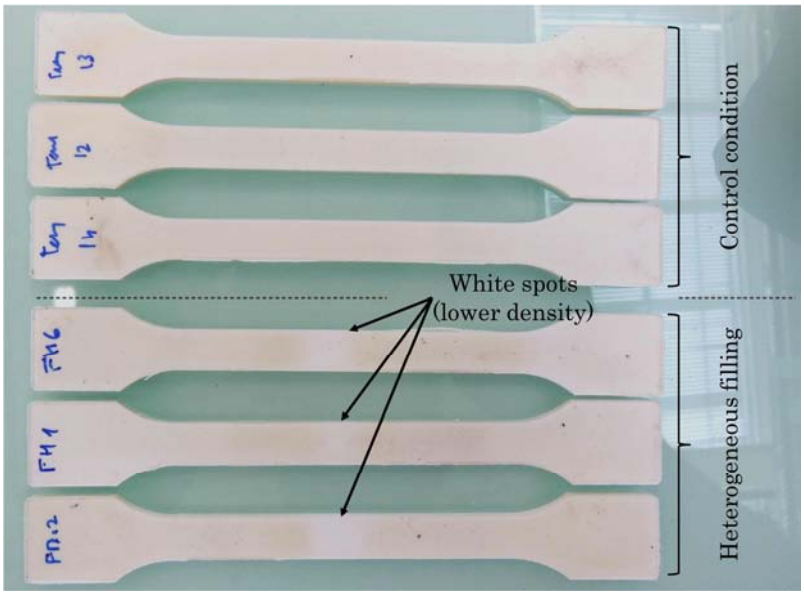

Figure II - 9: Weak spot (whiter) in the centre of dog-bone compacted in forced heterogeneity experiment

Table II - 1: Properties of specimens obtained with forced heterogeneity compared to control

	Thickness (mm)		Bending stress at break (MPa)		Bending modulus (GPa)		Tensile strength at break (MPa)		Tensile modulus (GPa)	
	Mean	St. dev.	Mean	St. dev.	Mean	St. dev.	Mean	St. dev.	Mean	St. dev.
Control	2.73	0.10	35.9	3.6	5.25	0.41	15.5	2.2	1.45	0.12
Heterogeneity	2.71	0.08	5.8	3.9	2.49	1.03	2.0	1.3	1.37	0.62

As seen on Table II - 1, the stresses at break (bending and tensile) are tremendously reduced when heterogeneity was provoked. On the other hand, the moduli are not that much affected showing that the heterogeneity will affect the stresses at break more than the moduli.

Even if great attention was paid to filling the mold as homogeneously as possible, mechanical properties (especially strengths at break) would be greatly affected by filling. Some trials were made in this sense:

- A vibrating table available in the laboratory was used but the rotational movement of the vibration due to the camshaft construction of the apparatus led to the accumulation of the material on one side. Making the mold rotate on the surface of the table was improving the spreading but the irregularities remained due to compaction in the same way than in a tap density apparatus. Temperature decrease during the vibration step was also inevitable.
- Another setup was made in order to hold the lower punch about the thickness of the non-compacted powder, poor the powder in excess in the mold and sweep the excess on surface of the die. Results were not satisfactory as differences of density (bundles) already exist in the powder which conducted to irregularities. This setup was also quite heavy to use and processing time considerably increased.
- Magnesium stearate was evaluated as a powder lubricant which is commonplace in pharmaceutical tablet production, but this trial conducted to the destruction of the first 1A dog-bone mold, with a lot of material flowing between the punches and die which conducted to the blockade of the mold and seizing while opening.

In order to compensate with inevitable heterogeneities, at least 7 repetitions were performed in tensile and bending in order to compensate with uncertain reproducibility and obtain a more reliable evaluation of the mechanical properties. As can be seen on Figure II - 10, homogeneous filling was even more difficult to obtain when molding parts of larger surface area. When specimens presented exterior signs of heterogeneity, they were excluded from the tests.



Figure II - 10: 2D 5x5 plates made from α-cellulose, heterogeneities can be observed even though great attention was paid while filling

II.3.D Mold filling and flow behavior

In 3D, it becomes quite hard to spread the material with a pattern corresponding to the future part. For example, to mold a bowl with its foot, the center of the molded part were the foot is located contains more material therefore it can be assumed that more material has to be loaded in the center of the mold prior to molding. These ideal patterns of filling are impossible to achieve, first because any manual manipulation of the starting material tend to increase apparent density when grabbing it, shoveling, leveling etc. but also due to the free flowing of powders or particles. Hopefully, molded parts were successfully molded without

matching the ideal patterns because some flow (extrusion) does occur under pressure to correct heterogeneous filling. The flowability of the material during compaction molding is very important and depending on pressure, temperature, material, extrusion occurs (Miki et al. 2003; Takahashi et al. 2009). This allows for instance to mold the edge of the "candle holder" (Figure II - 11).

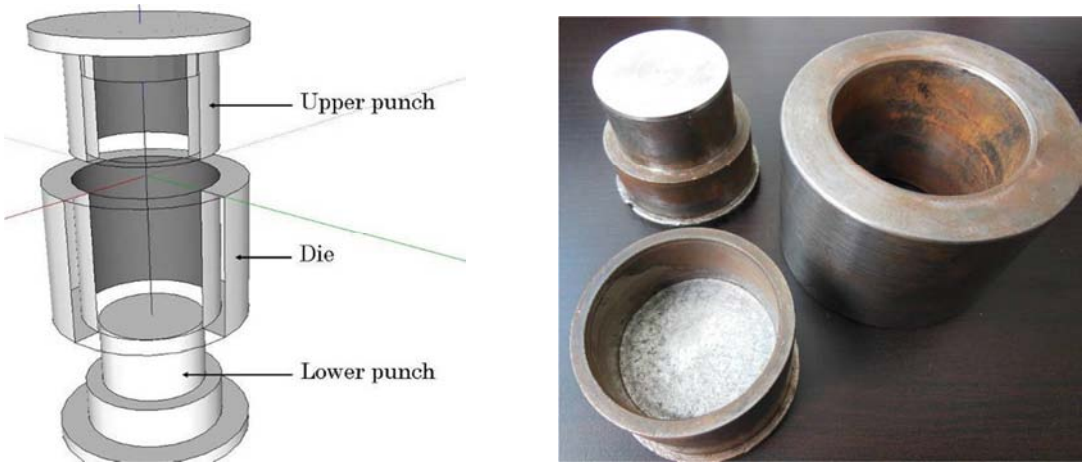

Figure II - 11: Candle holder mold (3 parts)

Molded parts were produced, but heterogeneity was observed, on the edges of the candle holder, like if components of the fibers were separated by compression during flow. The top of the edge of the candle holder (on the bottom of Figure II - 12) is much thicker and darker than the rest of the part, showing that first densification occurred first in this part and secondly flow occurred which formed the edges and bottom of the part (Figure II - 13). A close experiment called "backward extrusion" was reported in the literature in order to evaluate the flowability of wood powders (Miki et al. 2003).



Figure II - 12: Candle holder where lines materializes the flow on the edge of the part

This flow behavior during compaction is complicated to describe, it depends on mold shape, starting materials parameters, molding conditions etc. Here appears another limit of this molding technic: the shape of the molded part is a very important parameter to consider because of flowability in one hand, and possibility of homogeneous filling of starting material in the mold.

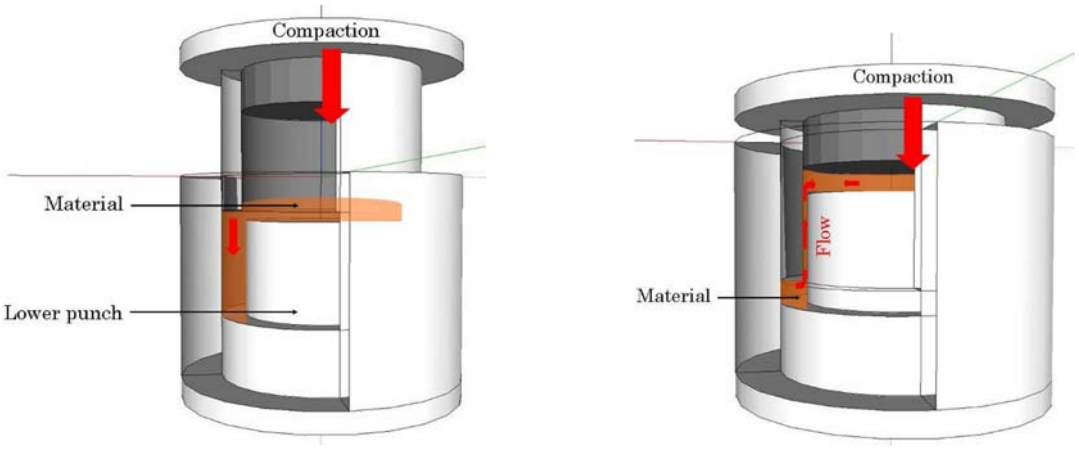

Figure II - 13: Hypothesis of flow behaviour in 3D molding

For instance, when material with poor flow properties are used like α-cellulose, limits of molding are rapidly reached. As seen on Figure II - 14 a color limit could be observed which was concluded to be the sign of not enough compaction on the lighter part due to insufficient flow.

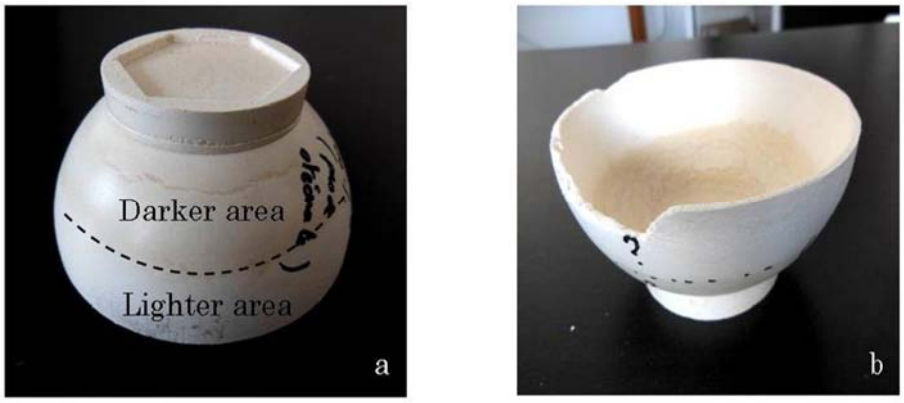

Figure II - 14: Flowability limitation observed on α-cellulose bowl

In fact, in order to mold the 90° part (parallel to compaction force), flow is necessary to transmit the efforts of compaction from the bottom (full compaction – perpendicular to compaction force) to the edges. Depending on materials and conditions the results were different. These observations conducted to the conclusion that a study on the flow behavior of materials was necessary.

II.3.E Steam explosion, delamination

Another very limiting phenomenon during this work was steam delamination: under pressure, water is set free from the plant material because of cells destructuration, densification, hydrogen bonding etc. and remains on the liquid state (subcritical state) under high pressure and temperature. But, at the end of the molding step the pressure is decreased and the free water turns to vapor state and expands, creating pressure and escaping the mold, sometimes causing only minor defects on molded parts, but on extreme conditions the parts can explode when the mold is opened. There is a temperature gradient in the molded

parts (Bouajila et al. 2005). On the surface of the molded part is the highest temperature (mold temperature) and in the inner parts is a lower temperature zone thus water content will be higher inside the material as can be seen on Figure II - 15, and vapor pressure upon demolding will be maximum in the inner layers of the molded material.



Figure II - 15: The two parts of a compaction-molded miscanthus specimen, violent delamination occurred, the centre of the material was observed to be darker due to moisture accumulation

Of course, depending on composition, material condition (moisture, granulometry etc.), molding parameters, shape of the mold, the delamination was different, occurred under different conditions, on different places of a molded part outside from the same mold etc. In the first time, trials were performed in order to minimize steam delamination which did not give satisfactory results, mostly because mechanical properties and/or flowability were also affected.



Figure II - 16: Different plant materials compacted in the same conditions, only some suffered from delamination (175°C – eq. 60% RH – 200 MPa – 30 seconds)

Everything was occurring as if the steam delamination was a compulsory drawback resulting of the expression of flowability and mechanical properties. Whatever the material, satisfactory 3D shapes were obtained in the conditions that heavy steam was generated in

the mold conducted to cracks in the part, and poor flowability and fragile edge were obtained in conditions designed to prevent steam delamination.

When conditions are optimal for strength and flowability, a good surface effect is obtained (plastic-like, shiny and smooth) that vapor cannot penetrate easily. Thus, best conditions of molding are precisely those for which molded parts experience delamination. Once broken due to pressure, and because of compaction, the material acts as a gasket and the punch part of molds are pushed by the steam pressure when the press is opened. In extreme cases, the punch can be ejected from the mold by the steam pressure (Figure II - 17).

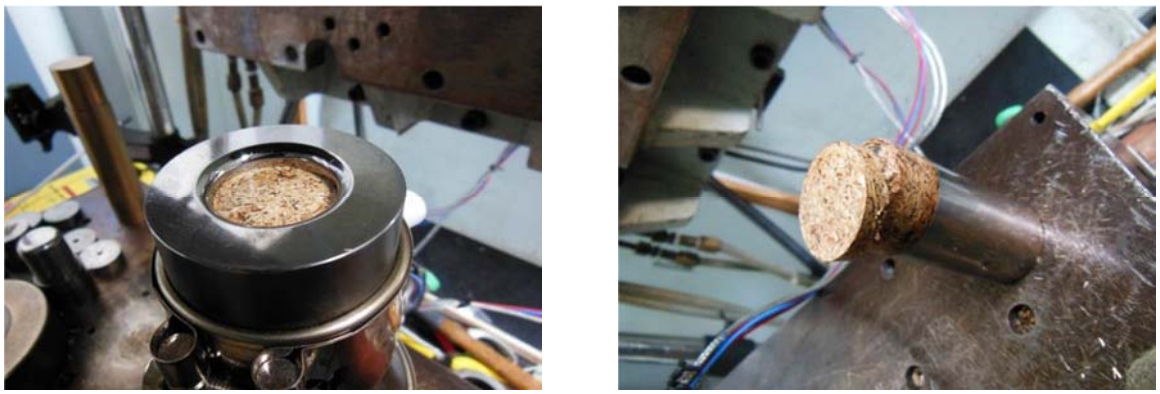

Figure II - 17: Steam delamination phenomenon and gasket effect - pictures

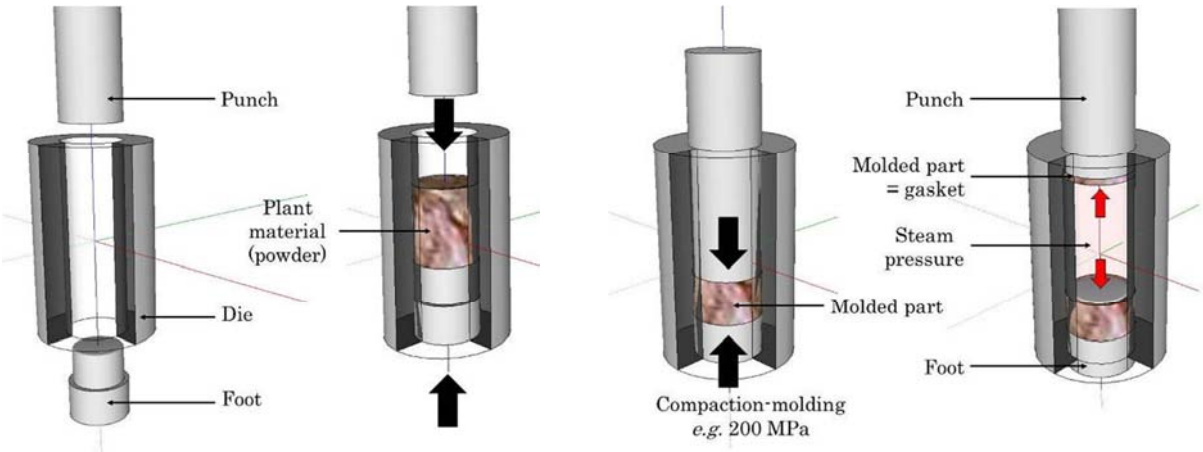

Figure II - 18: Steam delamination phenomenon and gasket effect – interpretation

On Figure II - 17, on the left is the upper part of the molded object that has been pushed by steam pressure all on top of the die (about 8 cm), on the right, the result of the molding: the part is broken in two in the transition zone between the bottom of the small pot and its edges.

In some cases, it is possible of course to release the pressure very slowly, which reduces the damages on the molded parts, but a crack is observed, where in normal condition, a crack would have opened as a result of delamination. The same result was obtained if the mold is let to cool down completely under pressure before releasing it: a weak line remains on the delamination point. Besides, for industrial application, such a cooling step would be so energy and time consuming that this option was excluded from the study.

II.3.F Shear and steam explosion

The molded pieces area where steam delamination occurred is a quite interesting point to mention: it was observed that delamination always occurred in shear transition zones. For instance, on the bowl shape (Figure II - 19), steam explosion occurred on the transition from the foot to the bowl. Also on these points, constituents' separation was observed, darker color, very shiny surfaces showing that some constituents (lignin?) were extracted and concentrated on these high shear points. Probably, water also accumulates were shear is maximum, as a result of cell destructuration. Thereafter, trials were performed in order to find a compromise between flow which produced strong and completely molded parts (hard conditions) and the avoidance of delamination (gentle conditions). It seems a compromise is hard to find, depends on the starting material, operating conditions, but most of all, if steam delamination is avoided, the edges of the bowl are less shiny, weaker which showed that flow was insufficient for the pressure to be transmitted to the edges. The shape of the mold probably also plays an important role.

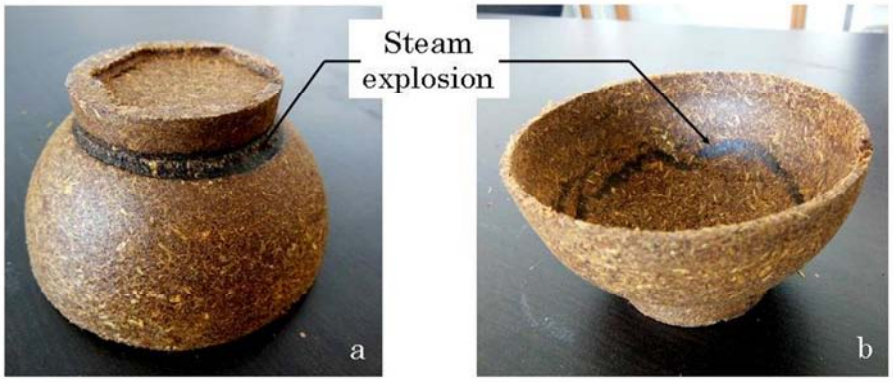

Figure II - 19: Slight steam delamination occurring on bowl (pressure was released slowly)

II.4 Transfer molding

II.4.A Principle

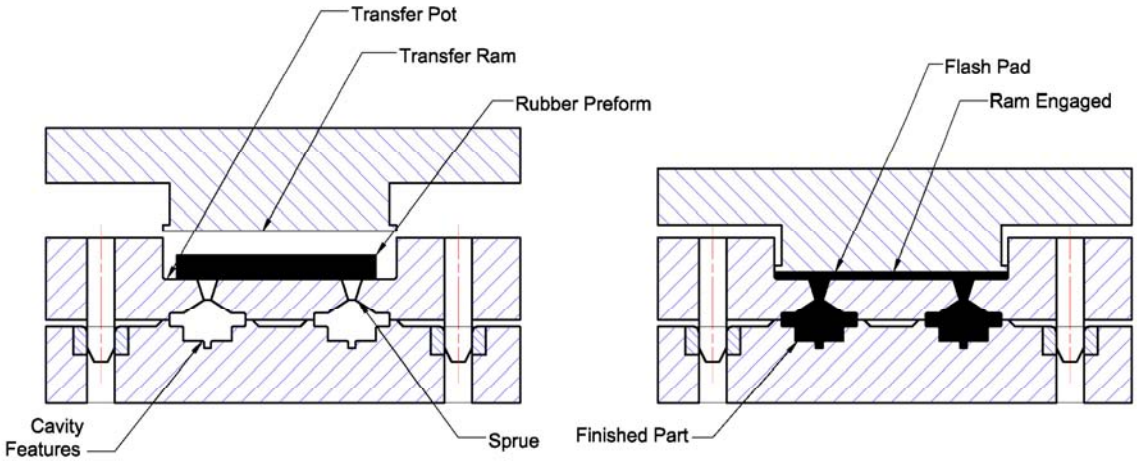

Figure II - 20: Transfer molding for rubber molded objects production (reproduced from twistertechnology.com/)

Transfer molding is industrially used for processing non melting polymers like rubber, PTFE etc. The principle is to force the starting material in a chamber that flows out on exits (dies or sprue) to fill a mold cavity (Figure II - 20).

This technique relies on a certain ability of the material to flow through the die to fill a cavity which relies on the same principle that a capillary rheometer to evaluate the flowability of materials under pressure (Takahashi et al. 2009). Concerning plant fibers molding, the group of Kanayama et al. in Nagoya has been pioneer in designing an apparatus to process bamboo and wood powders using transfer molding (Yamashita et al. 2007).

II.4.B Advantages over compaction molding and drawbacks

Transfer molding has no shape limitation due to its design like compaction molding and thus can produce much more complicated shapes (Figure II - 21). Transfer molds can be designed like injection molds for which there is much more knowledge; the industrialization also would probably be much easier. As the material is preloaded in the compression chamber there is less concern in filling the mold homogeneously. Also, the same compression chamber can be used with different molds, which means that only this part will suffer from friction and damages.



Figure II - 21: Examples of complicated shapes obtained by transfer molding

II.5 Other technical locks

II.5.A Moisture adjustment

The effect of moisture is quite important, thus, moisture adjustment is necessary and uncertainties on moisture content are rapidly occurring. A precise control of moisture is quite difficult, as it requires climatic chambers to adjust moisture, or a precisely controlled partial drying of one material, but most of the difficulty came from the processing steps which obligatorily takes place in room conditions: the starting materials was charged in a hot mold and leveling could take a few seconds, and not always the exact same time which will undoubtedly modify the moisture content and generate some heterogeneity in the results.

II.5.B Particle size

Due to the size of molded objects studied in this work, both techniques required grinding steps which is energy consuming, and raises problems about particle size and distribution and their effects on the molding. Within one batch, heterogeneity was also possible from a specimen to another even though mixing was performed at regular intervals.

II.5.C Machining, thermal dilatation and seizing of molds

Compaction molding and transfer molding both require a lot of pressure for the material to be molded or flow correctly. As temperature was a crucial parameter to evaluate, molding tests were performed from room temperature to 250°C. One very difficult part was the design of the molds. They should be as tight as possible in order to prevent the material from being extruded between the punch and die, but due to metal dilatation with heat, a minimum of slack is needed. When the slack is not enough, seizing occurs, as can be seen e.g. on Figure II - 22. The 2ROP mold was designed with columns and metal was 40CMD8 which is a pre-treated alloy steel capable of 110 - 120 kg/mm². This mold was designed like an injection mold for which the manufacturer is an expert, but too little slack rapidly conducted to seizing on the punch and die. The lack of guiding was not involved because of the presence of 4 guiding columns on this mold. Later trials were made on the 1A dog-bone specimen mold machined by CEE (Grisolles, France) on a stronger alloy (55NCDV7 – 140 to 150 kg/mm²). Mechanical slacks from 3 to 6 µm face to face were tested. 3 µm slack conducted to a very tight mold, but seizing occurred after about 100 cycles. 6 µm slack permitted to mold many more specimens, but when testing material with better flowability, 2 molds were broken by extrusion of the material between punch and die, which, during the removal of the punch from the die conducted to seizing. When seizing initiation was detected, sanding paper was used to smoothen the surface, but then inevitably the slack was increased and soon or later, the mold will tend to be blocked by extruded material.



Figure II - 22: Seizing marks on 2ROP mold (columns guided mold)

The use of alloys with different strength was also tested on the 4th version of the 1A dog-bone specimen mold, which, associated with a treatment on the punch conducted to good results. To date, the understanding of these phenomena remains quite unclear and much work is still needed on the technological part.

III Study on a model polymer: α-cellulose

The processing of cellulose into solid materials have been of raising interest these last decades, generating a lot of scientific papers and ending up with a wide variety of processing routes. This chapter will begin by a quick review over the different techniques. This thesis focused on thermo-compression molding, which have been less studied, for its simplicity and assumed eco-compatibility.

As seen in the literature on binderless thermo-compressed plant materials (Chapter I), cohesion is often associated with hemicelluloses and lignin, or free sugars, starch and proteins if present in the starting plant materials. Binderless molding of pure cellulose have been very rarely reported; and one of the first formulated hypothesis was that cellulose could not pretend to any self-bonding ability without being modified, solubilized or processed in the wet state. At first, cellulose was chosen as a "negative control" model polymer, i.e. with the idea that low mechanical properties would probably be obtained, and that using materials with hemicelluloses and lignin will conduct to higher properties. As will be seen in this chapter, there was much more to study about the thermo-compression molding of cellulose than expected. Surprising features of the compressed cellulose specimens were discovered all along the thesis, and what was expected to be a 3 months short study with lot of negative results ended up to take most of the experiment time in this thesis.

The first available mold at the beginning of this work was the 50 x 50 mm square. First results were obtained by cutting the squares in 5 small test specimens of roughly 10 x 50 mm. High scattering was observed, but some specimens were incredibly strong. In order to avoid the cutting step and to reduce the dispersion of the values, it was decided to design a mold that will allow the molding of 1 specimen per cycle. As the tensile properties were never reported on compression-molded cellulose samples, a dog-bone mold was machined which will allow both tensile and bending tests.

A first step was to validate the method: it was rapidly observed that the filling of the mold was an important parameter that will generate a bit of dispersion on the values (see Chapter II). But there was no comparison with what was obtained from cutting samples out of a 50x50 square. In order to evaluate correctly the mechanical properties, 7 repetitions were performed on each modality, and the effect of the different molding parameters could begin. The first results concerned a first evaluation of the parameters and were published (Pintiaux et al. 2013).

Additional data were produced later, when studying the effect of lower pressure and the conjugated effect of reduced moisture and increased temperature on delamination phenomenon and on the mechanical properties of the specimens.

In parallel to this, some data were collected towards the understanding of the physico-chemical phenomena occurring during the consolidation process. Also, because the interest of 3D molding was high, flow tests were performed thanks to a JSPS internship in Nagoya Japan.

III.1 The different ways to process cellulose into solid material

III.1.A Native cellulose structure

Cellulose is a linear polymer of ß1-4 ether linked glucose. The DP can be as high as 10000 units in common plants, and more in micro-organisms. Molecular chains are assembled in parallel held by a complex hydrogen bonding network which forms crystalline structures. Two crystals allomorphs I_α and $I_ß$ exist in the native cellulose and coexists with some paracrystalline and amorphous cellulose (Nishiyama et al. 2003).

Cellulose in plants has a fractal-type organization. The assembly of several side chains builds up nano-fibrils of a few nm wide. There are evidences of the existence of an elementary unit (CEF: cellulose elementary fiber) of 3.5 nm of diameter which would

integrate 36 adjacent cellulose chains in a diamond like cross sectional organization (Somerville 2006). The CEF are auto-assembled in higher scale structures of approximately 20 to 35 nm wide, which are called micro-fibrils. The distinction between the nano-fibrils and micro-fibrils is quite recent (Chinga-Carrasco 2011) and nano-fibril has more a technological meaning (Figure III - 1). The term micro-fibrils used to described the two of them in the past, with typical sizes reported in a quite large range from 1 to 50 nm which has been a source of debate (Ohad and Danon 1964) that is still not completely elucidated.

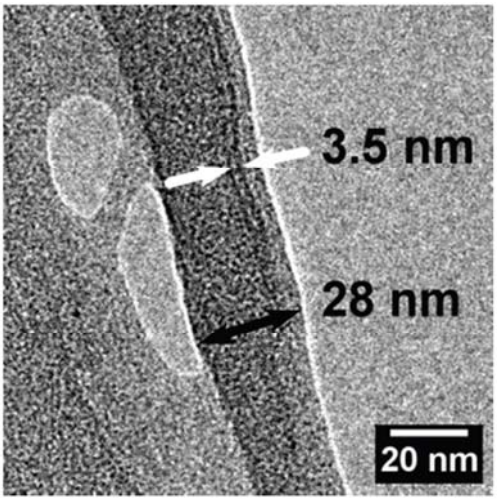

Figure III - 1: TEM picture of a nano-fibril cellulose micro (white arrow) composing a micro-fibril (black arrow), (reproduced from Chinga-Carrasco 2011)

The micro-fibrils together with other components such as hemicelluloses, lignin, pectins, proteins etc. are sometimes reported to be assembled in higher structures called fibrils (or macro-fibrils). The size of the macro-fibrils (20 to 100 nm wide) varies upon species and cell-types (Donaldson 2007) and it remains a rather vague notion that is sometimes mistaken, because the elementary fiber (CEF) is sometimes called micro-fibril and thus micro-fibrils called macro-fibrils (Mellerowicz et al. 2008). The micro-fibrils, these elements composed of several CEF are the "frame" part of a nano-composite material of extreme complexity and performance: the plant cell wall (Figure III - 2).

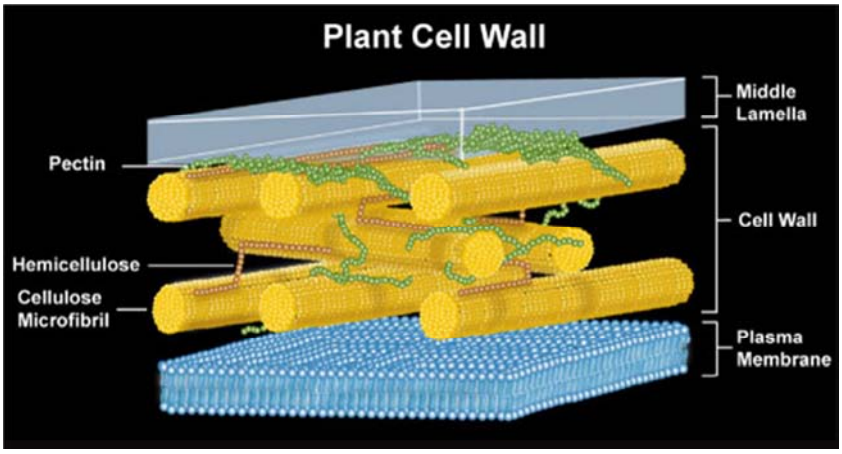

Figure III - 2: Plant cell wall constituents' super organization, reproduced from sigmaaldrich.com

The cell wall is specific to the plant kingdom, and it lies against (or around) the plasma membrane, that is the main cell's barrier of any living organism. The plant cell wall is described as a layered structure, comprising, from the inside to the outside, first the S3, S2, S1 layers of the secondary wall, the primary wall, and finally the middle lamella which is a matrix-like component that forms the "cement" between adjacent cell walls (Figure III - 3). During the cell's growth, the primary wall is the only present, it is soft and grows, deforms, with the cell, but when the rigid secondary wall is synthetized, the cell's growth stops.

These layers also have different constitution, for instance, in wood, the primary cell wall is mostly constituted of cellulose pectin and hemicelluloses while the secondary wall is made of cellulose hemicelluloses and lignin like the middle lamella that rich in lignin, pectin and proteins. Depending on plant origin, the organization can differ a little (Ding et al. 2014). The S1, S2, S3 distinction also takes place in the different orientations of the cellulose fibrils (Figure III - 4), which gives to the plant cell wall a particular strength, necessary to handle the turgor pressure (turgidity).

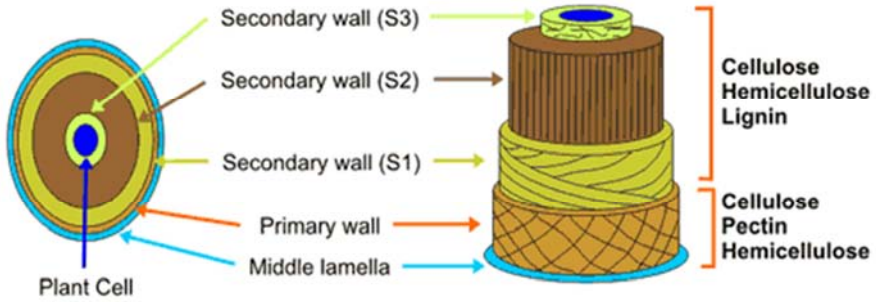

Figure III - 3: Plant cell-wall super-organization, reproduced from bioenergy.ccrc.uga.edu

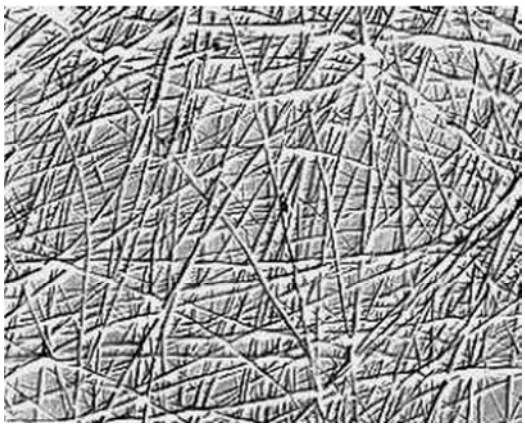

Figure III - 4: Differently oriented cellulose microfibrils in the cell wall (TEM picture, X 30000) reproduced from acces.ens-lyon.fr

The cell wall forms a rigid 3D structure that is called "fiber". In the living plant, the fibers in fact refer to individual cells, which, once they have been extracted are hollow structures of about 20-50 µm wide and about 1 mm long. "Cellulose fibers" can be produced by removal of other components than cellulose (like removing the "cement" and keeping the "frame" intact). This is what can be observed under a SEM of holocellulose, the most basic cellulose extraction out of plant fibers. Holocellulose is prepared from ground plant materials by sodium chloride treatment and filtration which removes lignin and extractives and leaves cellulose and hemicelluloses (Sjöström and Alen 1998). From holocellulose, a 17.5% NaOH

treatment dissolves most of the hemicelluloses (and some of the cellulose) which produces α-cellulose after filtration (α by opposition to ß which was the dissolved part that could precipitate upon acidification and γ the part that is lost and does not precipitate). Today, α-cellulose has the signification of its processing route and the original meaning of the "α" is quite out-dated.

A mild acidic treatment run on α-cellulose will hydrolyze the rest of the pentosans from hemicelluloses and part of the cellulose, beginning with the less stable and most accessible parts of cellulose: the amorphous phase. This will produce micro crystalline cellulose, a pure cellulose material with significantly lower DP than α-cellulose, with increased crystallinity index and wherein the fiber's shape is partially lost due to hydrolysis.

III.1.B Cellulose polymer basic properties

Paracrystalline organization

Cellulose is considered a semi-crystalline polymer, i.e. it comprises crystallites and amorphous phase. Yet, the classic semi-crystalline model originated from synthetic polymers does not fit very well to cellulose. For instance the amorphous phase of cellulose has very vague properties and it is more adequate to consider a crystalline, paracrystalline and amorphous phase, i.e. a paracrystalline model. The paracrystalline phase is reported as a thin mono-molecular layer on the surface of crystals (Ioelovich et al. 2010). The amorphous phase would then be surrounding the paracrystalline phase but its characteristics are still unclear. The natural cellulose crystal are under the I form. Cellulose Iα is majorly found in bacteria and algae while Iß is majorly occurring in plants. Cellulose Iα crystals have a parallel single chain triclinic organization although Iß is two chains monoclinic. Cellulose II which is the form obtained upon mercerization or regeneration of cellulose (Viscose, Lyocell etc.) has an antiparallel two chains monoclinic organization. Cellulose II is thermodynamically more stable than the Cellulose I allomorphs. These are the most current allomorphs, but others can be obtained by chemical treatments (Figure III - 5).

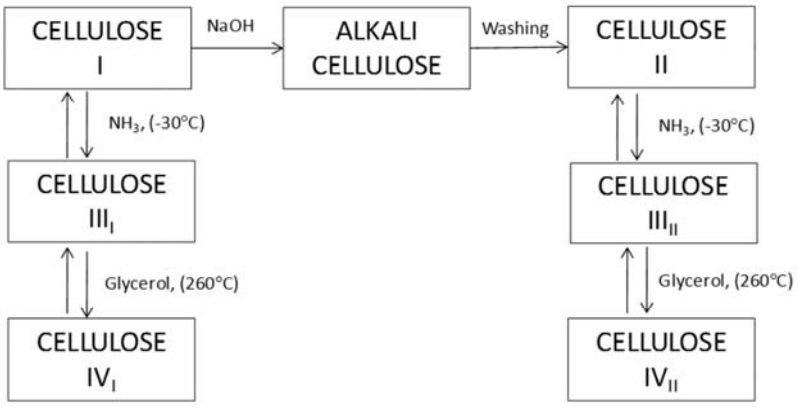

Figure III - 5: The different cellulose allomorphs

Fusion temperature

There is no fusion temperature (Tf) of cellulose, since the energy needed for freeing the polymers is too high and lead to the degradation of the polymer before it melts. However, in very particular conditions (i.e. uniaxial pressure, mechanical shear and short high energy laser beam exposures), the melting of cellulose has been reported (Schroeter and Felix 2005).

Glass transition temperature

The existence of the amorphous phase in cellulose is long time considered, and thus the research of a glass transition temperature has been for a long time under discussion. The glass transition temperature is a feature of a semi crystalline polymer that concerns the amorphous phase. At temperatures under the Tg, the amorphous phase is under the glassy state which confers low or no molecular motion ability. At and after the Tg, some molecular motion is obtained, and the amorphous phase switches to the rubbery state with higher molecular motion and deformability.

In the field of paper processing, the Tg of cellulose seems almost "classical": the Tg of paper is announced at 47 to 67 °C in modern technical books (Ashby 2012) which refers to mechanical properties of paper and a particular interpretation. More generally, the Tg of cellulose has been constantly discussed by chemist among the decades. It was measured around 220°C in the dry state (Back 1987). Values of 230 – 250°C have been found by RMN measurements based on bound water evaluation (Ogiwara et al. 1970). More recently, studies appeared with very low values of Tg reported (Szcześniak et al. 2008). These measurements using DSC are not very reliable and the peak can hardly been observed. Measurements base on DMA of powder have concluded to more reasonable values (Paes et al. 2010).

Thermal decomposition

Thermo-gravimetric analysis of α-cellulose showed that the degradation of cellulose starts around 230 – 240°C in both air and nitrogen conditions.

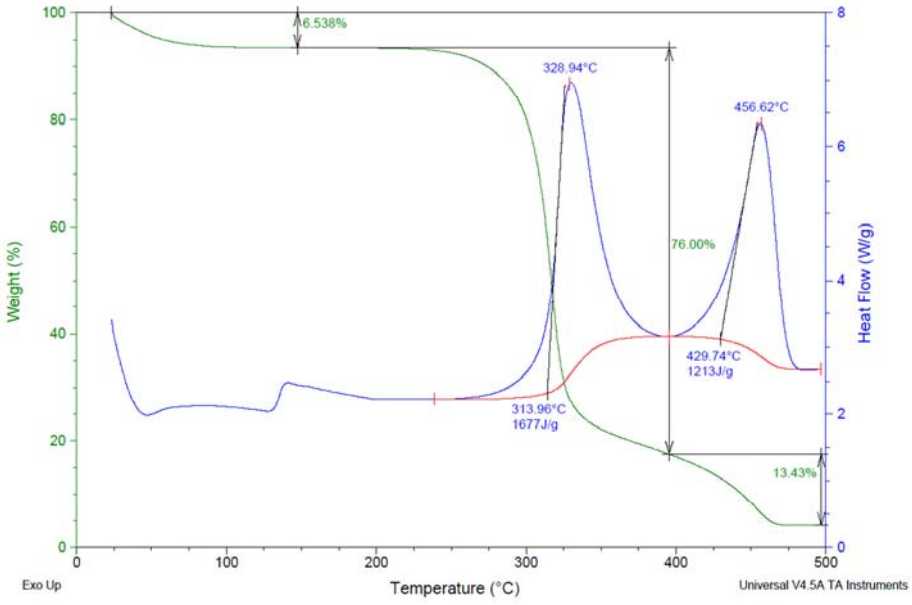

Figure III - 6: DSC-TGA of α-cellulose under air condition

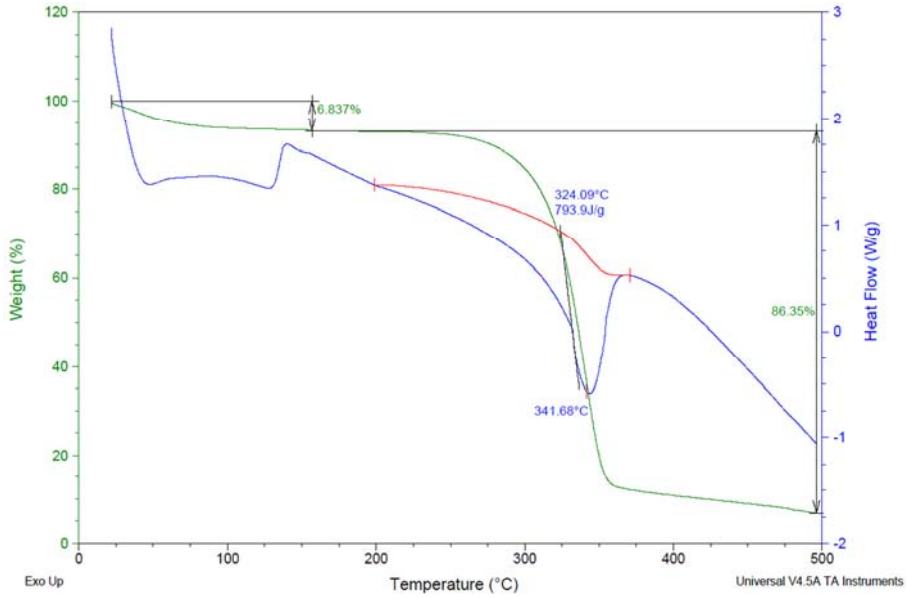

Figure III - 7: DSC-TGA of α-cellulose under inert (nitrogen) condition

These analyses that are run under atmospheric pressure does not inform about the degradation of temperature of cellulose under pressure, for what very few reports have been published. The possible hydrolysis of cellulose in sub-critical water under a pressure of 25 MPa and temperature range from 290 to 400°C has been mentioned (Sasaki et al. 1998) which is probably compatible with the molding conditions used in this thesis work.

III.1.C Cellulose to solid materials processing routes

Paper and other water suspension processes

The first historic example was invented in China short before J.C. The modern paper area started around 1825 with the widened use of paper machines. Paper is based on the transformation of plant materials into "paper pulp". Chemo-mechanical processes are used to break down the plant-cell wall assembly, make the fibers (plant cells) swell in a water suspension, separate from each other and intertwine. Although many plant materials can be used, the properties of paper are highly impacted by the length and strength of the fibers. Hemp or linen can be used, but wood is nowadays the preferred starting material for pulping. Softwood and other low density woods which have longer fibers are preferred to produce paper which will require a certain strength like newspaper that are printed in high speed rolling printing presses.

The pulping process aims at separating the fibers one from the others and hydrate the fibers by felting their surface (fibrillation) in order to increase the surface area for better water access. The link between a type of pulp and a type of paper is tight. Several processes of pulping co-exist, depending on the desired pulp and paper. Chemical pulping and mechanical pulping are the two main processes which for many variants actually exist:

* Chemical pulps are the most produced pulp worldwide, chemical dissolution of the middle lamella (lignin) is performed using either an acidic treatment (bisulfite) or alkali (soda, sodium sulfur) for which the Kraft process is a well-known example. These types of pulp achieve the best cellulose purity (and lowest yield) and produce the less damaged fibers.
* Mechanical pulps using either defibering techniques (abrasion of the debarked wood logs) to strip fibers off which produce a type of pulp known as SGW (Stone Ground Wood) or refining of pre-ground wood chips using disks or cones refiners which produce RMP (Refined

Mechanical Pulp). The refining produces higher quality pulp with longer fibers than the defibering techniques. Mechanical pulping has a high yield over 90%. Thermomechanical pulp is a variant which is characterized by an extra steam pretreatment of the wood chips before being refined.

Most of today's pulping processes combine mechanical and chemical processes. These processes starts with wood chips being treated with chemicals (alkali and sodium sulfite), possibly under steam pressure and proceed further to mechanical refining. The color of the pulp (thus of the paper) is adjusted by a final bleaching step which deals with the removal of the colored lignin elements using oxidizing (hydrogen peroxide) or reducing agents (sodium hydrosulfite). The adjustment of the different parameters on these different steps allows to produce a high variety of pulps, with various cellulose content, strength, optical properties, etc. For instance, highly chemically treated pulps are used to produce newsprint and glossy papers while more mechanically treated pulps will give printing / writing papers.

Related products based on the same phenomena (water suspension process) are numerous: cardboard, papier mâché, egg boxes-type products and more recently materials based on fibrillated cellulose. The fibrillated celluloses are a quite recent development of the paper process, which relies on the refining performed on a higher extent by the separation of smaller elements at a scale between the fiber and the elementary fiber. High pressure homogenizer treatment has been a preferred route for producing micro-fibrillated cellulose (Turbak et al. 1983). MFC is not a very strict denomination, as commercial MFC contains a range of cellulose elements size from the fibers to the nanofibril (Chinga-Carrasco 2011). Zelfo is an example of MFC that is produced using processing tools which are used in the paper industry and under development for producing solid material by spraying or press-wringing processes. Zelfo technology (the company that now possesses the Zelfo patents) recently found applications in the reinforcement of cardboards (Lavoine et al. 2014).

The bonding ability of MFC depends directly on the degree of refining, i.e. the separation of the fibers into thinner elements. The group of Yano et al. produced a micro fibrillated cellulose with nanometer web like network using a repeated (up to 30 times) high pressure homogenizer treatment to produce a hot pressed material with 16 GPa of bending modulus and 250 MPa of bending strength at break (Yano and Nakahara 2004). Another technique based on a water grinding treatment was designed by this research group and hot-pressed into solid material with a reported Young's modulus of 8 GPa and 90 MPa of ultimate stress at break. The process was reported to produce nanofibers with uniform width of 15 nm (Abe et al. 2007). The fundamental difference between these works and Zelfo / MFC is the degree of refining, which came from micro to nano scale.

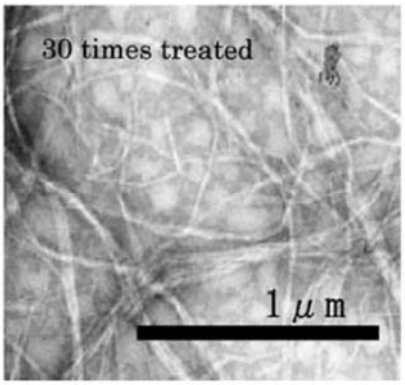

Figure III - 8: "Cellulose microfibers with nanometer unit web like network" also called "microfibrillated cellulose" in the pioneer work of Yano, before the first usage of nanofibrillated cellulose (Yano and Nakahara 2004)

The modern science infatuation for nano objects rapidly led to name "nano-fibrillated cellulose" (NFC) the slurry obtained by cellulose refined to a higher degree than MFC. However, the definition of nano-fibrillated cellulose remains vague, most of all because if confuses with the definition of nanofibrils (the elementary fibrils of 3.5 nm). A pragmatic (technological) characteristic of the elements' size reduction was to obtain so called "nanopapers" with much higher mechanical strength (214 MPa according to Henriksson et al. 2008) and optical transparency. The group of Yano which were pioneers in this way presented a transparent NFC sheet with a Young's modulus 13 GPa and a tensile strength of 223 MPa claiming an enormous potential for industrial applications (Nogi et al. 2009).

Another approach that is based on the same concept for material's cohesion but on a different way for obtaining the nano fibrillated cellulose was found with bacterial cellulose: when microorganisms (for instance Acetobacter aceti) are grown in water adding nutrients, a network of cellulose nanofibers is grown, which gives a slurry wherein solid if 97% α-cellulose after purification (Yamanaka et al. 1989). Films were obtained by casting, and DMA analysis conducted to a Young's modulus of 18.8 GPa and a tensile strength of 260 MPa.

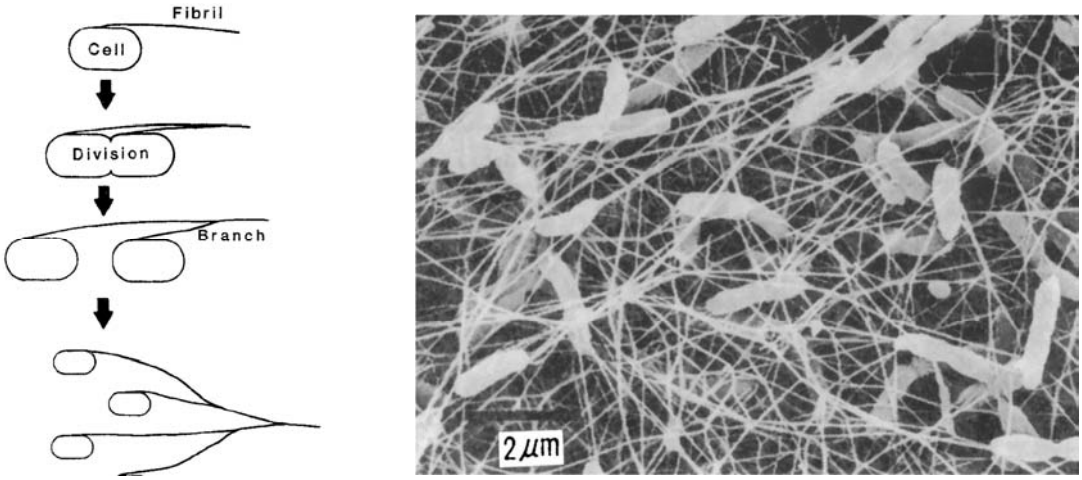

Figure III - 9: Bacterial cellulose (wires) and bacteria, synthesis scheme on the left reproduced from (Yamanaka et al. 1989) and SEM picture on the right reproduced from (Iguchi et al. 2000)

Solubilization process

Nitrocellulose (1855) was the first semi-synthetic polymer produced from cellulose. It was highly flammable which rapidly restricted its use (only Ping-Pong balls are today still made of nitrocellulose because of its unique characteristics). The basic idea was to modify the native cellulose polymer to make it soluble. Shortly after nitrocellulose, cellulose acetate was invented which is still used today. Viscose followed up (1884) and was produced worldwide from 1920 to 1950 when the first synthetic polymers were discovered. The interesting feature of viscose is the fact it is woven from regenerated cellulose, i.e. cellulose that has been dissolved (thanks to modifications involving sodium hydroxide and carbon disulfide) and precipitated. Viscose was a widespread polymer used for textile mainly, and even though the concurrence of synthetic polymers was high, remained under production. This industry produced massive amounts of polluting wastes and was terrible for the workers' health mostly because of carbon disulfite exposure. Health problems led to measures for protecting workers with a 10 ppm maximal exposure limit to CS_2 that is still judged insufficient (Gelbke et al. 2009). Modern alternative solution to viscose appeared in the 1980's (Carbamate cellulose, similar to viscose but CS_2 being replaced by urea) and the 1990's with the

application of NMMO (N-methylmorpholine oxide) as a solvent for cellulose which produced a regenerated cellulose materials without derivatization called Lyocell (Fink et al. 2014).

The question of cellulose's solubilization has been a constant concern of researchers for about hundred years. The newest methods now use the DMAc / LiCl (Dimethylacetamide / lithium chloride) for what recent applications was found for high performances films according to the concepts of "all cellulose composite". The technique relies on a sequential exchange of solvent from water to DMAc through ethanol and acetone and the final addition of LiCl to solubilize cellulose. Depending on the time of contact between cellulose and the solvent system, the extent of the dissolution can be controlled (so-called selective cellulose dissolution). This allows dissolving of only the fibers' surface for obtaining strength but without total solubilization which lowers DP and destroys the advantages of the fibers native structure. The removal of the solvent by rinsing and casting produces very high performance sheets: e.g., Nishino et al. (2004) processed a composite made from pre-oriented ramie fibers and Kraft pulp solubilized cellulose matrix which obtained a dynamic storage modulus of 45 GPa and an amazing tensile strength of 480 MPa. Gindl and Keckes (2005) processed micro-crystalline cellulose the same way and obtained an anisotropic all cellulose film which had 13 GPa of Young's modulus and 243 MPa of tensile strength.

Compaction molding

Cellulose has been used as excipient in the production of pharmaceutical tablets for decades since the discovery of microcrystalline cellulose (Thoorens et al. 2014). The compaction process uses pressure in the same range as employed in this thesis, generally from 100 to 200 MPa. Pressurization speed is however much higher and is in the range of hundreds of mm/s. The process does not really consider a molding time separately from the ram speed, but can imply pre and post compression which acts like an increase of compaction time. An equivalent holding time would be less than a second. The moisture content of the powder is generally low (bellow 3% MC) because water would interfere with the active principle.

The mechanical properties are one of the main concerns of this science; the Young's modulus in elastic uniaxial deformation can be about 10 GPa. Relative porosity is the main parameter that is used to describe the features of the tablets and for the modeling of the compaction process:

$$Relative\ porosity = \frac{Apparent\ tablet\ density}{Absolute\ powder\ density}$$

The apparent tablet density is on the macroscopic point of view. The powder density is measured using an helium picnometer, which for α-cellulose usually gives a value of 1.57 g/cm^3. Jallabert worked on the modeling of the densification process observed in the PVT measurements made at the LCA during his thesis, and it was concluded than the classical pharmaceutical models could not explain the densification observed at elevated temperatures under the conditions of the PVT apparatus (Jallabert et al. 2013).

Other research works have been published recently around the use of compression molding to produce cellulose solid materials:

Nilsson et al. (2010) reported the production of compression molded material from wet cellulose disintegrated pulps using a two-stage (Cold, 7 min, 0.6 MPa/Hot, 20 min,−45 MPa) pressing step, their material reached 11 GPa of Young's modulus and 76 MPa of tensile strength. Also, Rampinelli et al. (2010) studied the mechanical properties of compression molded highly refined micro-fibrillated cellulose. They produced a material with 180 MPa of tensile strength, 165 MPa of bending strength and a bending modulus of 9.4 GPa with an optimized process using 120 MPa of pressure, for 6 min at 160 °C. Also, Zhang et al. (2012) produced ball-milled cellulose material from non-treated cotton linters micro-crystalline

cellulose using a high shear device usually dedicated to the sintering of metals and reported a bending modulus of 1.84 GPa using DMA measurements. Finally, pressures from 700 MPa to 2.5 GPa were used for the compression of cotton linters which led to the destructuration of the original fibers shape to a network of reassembled nanosized elements (Privas et al. 2013).

Table III - 1: Summary of the main processing routes from cellulose to solid materials,

	Product	Product. start	Concept, forming method	Tensile properties*	Energy consum--ption	Pollution	Proces--sing time
Water suspension	Paper	1820	Cellulose pulp press-rolled, dried into sheets of 20 - 120 g/m²	~ 10 - 50 MPa	+	-	-
	Cardboard, paperboard	1850	Less refined, cellulose pulp, much heavier 120 - 300+ g/m²	~30 MPa	+	-	-
	Eggboxes - molded pulp	1900	Pressure-wringing/vacuum forming of papier mache for 3D shape	-	+	-	-
	Zelfo	1997	Fibrillated pulp pressed or molded	6.5 GPa - 55 MPa	+	-	+
	Nanopaper Yano 2004- Nogi 2009	-	Nanofibrillated cellulose casted into transparent films	13 GPa - 223 MPa	++	-	+
	Nanopaper Berglund 2008	-	High strength Nanopaper	214 MPa	++	-	+
	Bacterial cellulose sheets Yamanaka 1989	-	High strength nano cellulose film	18.8 GPa - 260 MPa	-	-	++
Solubilization	Viscose	1920	Regenerated cellulose (NaOH, CS_2)	300 MPa	+	++	-
	Lyocell	1992	Regenerated cellulose (NMMO)		+	+	-
	All-cellulose composite Nishino 2004 (oriented)	-	Partially regenerated cellulose (DMAc LiCl)	45 GPa - 480 MPa	-	+	+
	All-cellulose composite Gindle 2005 (anisotropic)	-	Partially regenerated cellulose (DMAc LiCl)	13 GPa - 243 MPa	-	+	+
Compression molding	Pharmaceutical tablets	1964	Ram direction compression (cold)	10 Gpa	+	-	---
	Nilsson 2010	-	Disintegreated cellulose pulp (cold - hot pressing)	11 GPa - 76 MPa	+	-	-
	Rampinelli 2010	-	Refined micro-fibrillated cellulose (hot pressing)	180 MPa	+	-	-

*Note: in the tensile properties column, values expressed in MPa correspond to the tensile strength at break, values in GPa correspond to the modulus

III.2 Behavior of compressed cellulose under various operating condition

III.2.A Methodology and control conditions

This study basically relies on an attempt to investigate on the relationship between the molding parameters and the properties of the molded specimens. Compaction-molding parameters were defined as follow: moisture content of the α-cellulose powder introduced in the mold, quantity of powder (initial mass), pressing time, pressing temperature, molding pressure and pressurization speed (Figure III - 10). Dog-bone specimens were produced in a specially designed mold which permitted to evaluate the mechanical properties under conditions matching ISO standards for plastic materials (Chapter VI, Materials and Methods). Additionally, equilibrium moisture content and specific gravity were measured.

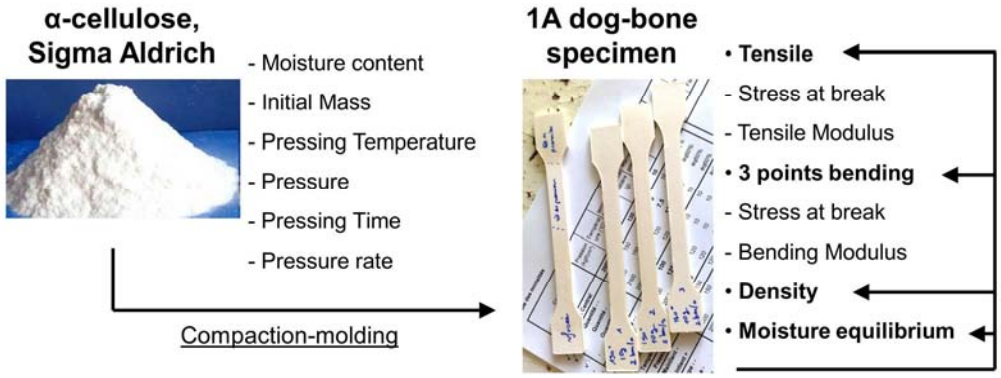

Figure III - 10: Methodology scheme for the evaluations of process's parameters effect

Control conditions of molding were chosen based on preliminary results, 60% and 25°C were common climatic conditions available in the laboratory, therefore, control moisture content for cellulose was selected as the equilibrium reached in these conditions. As the study deals with high pressure molding, control conditions have been set to the maximum pressure available in the 50 tons press (Chapter VI). 10 grams loaded in the mold, a temperature of 150°C and a time of 2 minutes were producing satisfactory results, they have been chosen as control. The pressure rate was another secondary parameter that was set to 10 bar/s as control. Table III - 2 summarizes these control conditions.

Table III - 2: Summary of control conditions for exploration study of the effect of operating conditions on the mechanical properties of compressed α-cellulose

	Pressure (MPa)	Temperature (°C)	Time (s)	Initial Mass (g)	Pressurization (bar/s)	RH (%)
Control conditions	264	150	120	10	10	60

From this starting point, parameters were changed one by one to evaluate their effect on the mechanical properties, specific gravity and equilibrium moisture content of compressed specimens. Complete results have been summarized in Table III - 3.

Table III - 3: Summary of results on compacted α-cellulose physical properties

Data / Modality		Molding parameters						Properties									
		Mass	Time	MC	Press. speed	Temperature	Pressure	Eq. MC		Specific gravity		Bending stress at break		Bending modulus		Tensile stress at break		Tensile modulus	
		g	s	%	bar/s	°C	MPa	Mean (%)	St. dev. (%)	Mean ($g.cm^{-3}$)	St. dev. ($g.cm^{-3}$)	Mean (MPa)	St. dev. (MPa)	Mean (MPa)	St. dev. (MPa)	Mean (MPa)	St. dev. (MPa)	Mean (MPa)	St. dev. (MPa)
Control		**10**	**120**	**8**	**10**	**150**	**264**	**7.02**	**0.04**	**1.503**	**0.008**	**40.2**	**3.4**	**6.18**	**0.31**	**21.2**	**1.3**	**1.60**	**0.04**
Mass	m1	**5**	control					7.02	0.07	1.502	0.008	39.7	1.7	6.50	0.24	20.7	2.1	2.61	0.22
	m2	**7.5**						6.99	0.06	1.503	0.008	38.1	2.9	6.28	0.40	21.7	1.6	1.98	0.20
	m3	**12.5**						7.11	0.04	1.503	0.008	42.4	3.0	6.78	0.32	19.3	2.1	1.37	0.05
Temperature	T4	control				**200**	control	6.86	0.16	1.513	0.008	43.2	3.4	7.17	0.35	22.4	1.5	1.73	0.11
	T3					**175**		6.87	0.02	1.510	0.003	39.9	2.4	6.19	0.18	21.1	1.0	1.59	0.05
	T2					**125**		7.22	0.02	1.505	0.004	37.3	2.7	5.62	0.23	20.0	1.2	1.55	0.09
	T1					**100**		7.56	0.06	1.490	0.007	34.7	2.9	5.39	0.22	20.1	1.8	1.55	0.05
	T0					**25**		8.57	0.03	1.481	0.002	24.5	2.4	4.43	0.43	12.0	0.5	1.27	0.04
Time	t1	control	**3**	control				7.51	0.04	1.494	0.005	35.5	1.0	6.38	0.09	18.4	0.6	1.60	0.00
	t2		**30**					7.02	0.03	1.506	0.003	39.8	1.7	5.80	0.25	20.0	1.3	1.65	0.08
	t3		**300**					6.90	0.02	1.508	0.005	36.4	2.6	5.97	0.35	20.7	1.5	1.59	0.09
Pressurization speed	R1	control			**1**	control		6.93	0.04	1.507	0.005	31.5	2.6	4.93	0.55	18.0	1.5	1.56	0.05
	R2				**2**			6.95	0.01	1.506	0.002	35.0	1.6	5.56	0.31	19.5	1.2	1.60	0.07
	R3				**50**			7.08	0.04	1.499	0.009	41.3	2.7	6.03	0.51	21.9	1.0	1.61	0.08
MC	M1	control		**0**	control			7.62	0.02	1.489	0.004	15.7	2.1	4.02	0.85	8.8	0.5	1.30	0.06
	M2			**6.1**				7.17	0.07	1.497	0.005	36.8	3.6	5.61	0.55	20.0	1.3	1.60	0.06
	M3			**10.8**				7.14	0.04	1.506	0.004	32.4	1.3	5.30	0.25	17.0	0.6	1.57	0.06
Pressure	P1	7.5	30	control	50	control	**264.3**	7.01	0.05	1.500	0.005	28.9	5.7	5.31	0.76	12.5	1.0	1.67	0.04
	P2						**132.1**	7.00	0.05	1.497	0.005	26.8	4.0	4.85	0.60	10.2	1.0	1.60	0.07
	P3						**66.1**	6.95	0.06	1.484	0.014	24.7	1.9	4.45	0.35	7.6	1.3	1.31	0.12
	P4						**44.0**	6.97	0.03	1.469	0.007	16.7	3.9	3.29	0.58	6.5	1.0	1.29	0.04
	P5						**30.8**	6.95	0.05	1.459	0.009	14.0	2.6	2.88	0.36	4.7	1.0	1.17	0.10
	P6						**17.6**	7.11	0.04	1.425	0.011	6.2	1.4	1.49	0.21	3.3	0.3	0.92	0.09
	P7						**8.8**	7.07	0.07	1.392	0.007	3.0	0.3	0.74	0.08	1.0	0.1	0.57	0.03

III.2.B Effect of mass loaded in the mold

Control conditions (10 g of cellulose loaded in the mold) produced specimens with a thickness of 3.61 ± 0.10 mm. 12.5, 7.5 and 5 grams were tested in order to evaluate changes on the molded specimens. Lower mass than 5 g could not be tested because low quantity of material could not be filled homogeneously in the mold which conducted to white spots, locally weaker materials, high scattering thus unreliable data. First of all, thickness was measured and mean and standard deviations calculated on 14 specimens (Table III - 4).

Table III - 4: Thickness-mass relationship upon mass variation

Mass	Thickness	
	Mean	St dev.
5	1.9	0.10
7.5	2.8	0.10
10	3.6	0.13
12.5	4.5	0.14

The change of mass loaded in the mold followed a linear law with a non-null constant coefficient (Figure III - 11). There is a certain deviation from the expected origin (zero) which would indicate that materials produced from a higher mass would have a lower thickness than expected. Probably, the better homogeneity while filling the mold with larger quantity of cellulose explains this.

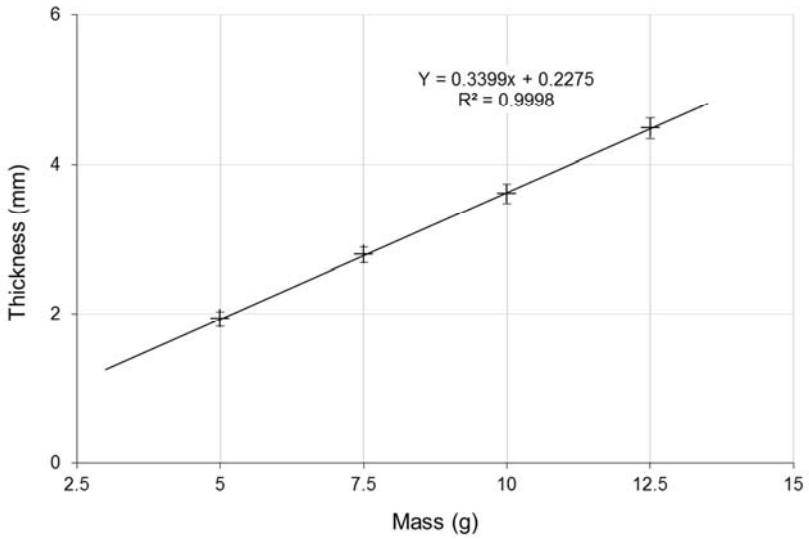

Figure III - 11: Thickness-mass relationship and linear regression upon mass change

Secondly, mechanical properties tests indicated that all parameters were kept approximately constant upon variation of mass except for the tensile modulus which was drastically increased with the decrease of mass loaded in the mold (Figure III - 12).

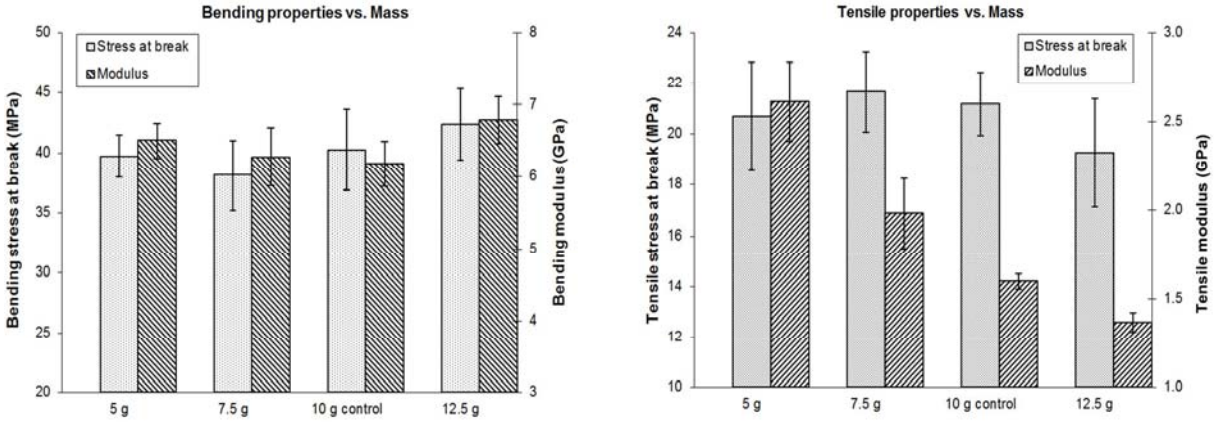

Figure III - 12: Effect of mass on the mechanical properties of compressed α-cellulose samples

Bending properties are much affected by the surfaces of the specimen, because during the bending, the upper surface is compressed and lower surface stretched. With a drastic increase of the tensile modulus it was concluded that certain heterogeneity existed within the material: as the molding conditions were identical, the surfaces (later called skin) must have been kept the same. Increasing thickness, let to specimens with identical skin thickness but a thicker core which decreased the skin / core ratio. The surface of the material expressed a higher modulus than the core, but a comparable strength. This characteristic of brittle materials accommodates very well with optical observations made on the surface that appears true, shiny and plastic-like. As for the specific gravity, it wasn't measured to be different between the core and the skin and so was equilibrium moisture content (Table III - 3). For later experiments, because of these results obtained on the effect of mass loaded in the mold, 7.5 g will be selected as a new reference for saving material consumption when preparing specimens.

III.2.C Effect of processing time

Classical molding time of 10 and 20 minutes are found in the literature in binderless boards pressing, very few data are available on high pressure molding (6 minutes has been mentioned by Rampinelli et al. 2010) yet, preliminary results showed that shorter times produced satisfactory results. From the control 2 minutes, 3 and 30 seconds were tested as trials of shortened operating time, 5 minutes was chosen to evaluate the effect of increased molding time.

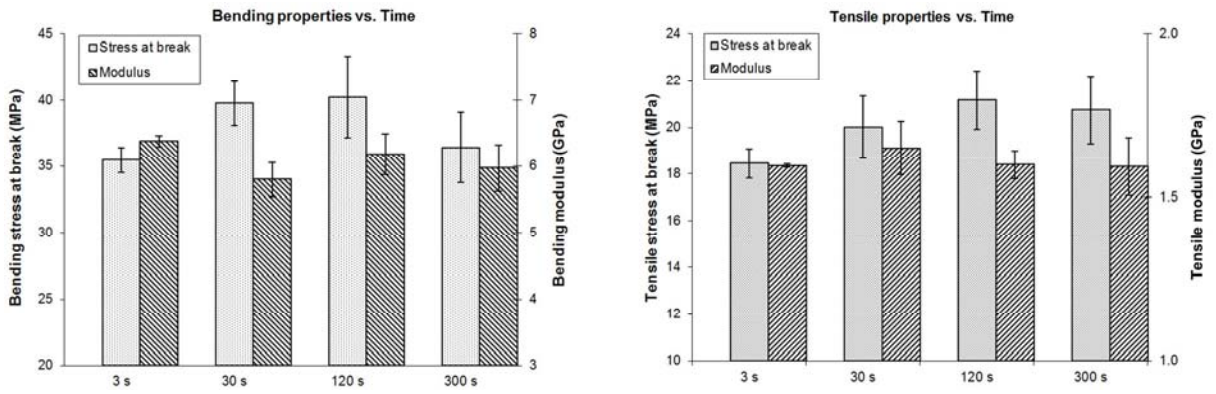

Figure III - 13: Effect of time on the mechanical properties of compressed α-cellulose samples

Surprisingly, time did not produce much effect (Figure III - 13). Statistical tests were performed and the difference were concluded to be non-significant according to Scheffé test, data available in the first published paper (Pintiaux et al. 2013). The independence of the mechanical properties and molding time was an encouraging result, showing that low times of molding could be operated which would save time, energy and facilitate industrialization. The average strengths of 3 seconds however appeared slightly lower than the others (Table III - 3), these specimens also had a slightly higher equilibrium moisture content (MC) and lower specific gravity (SG) which would indicate a lower cohesion. Therefore, for later experiments, and also for saving time on the experiments 30 seconds have been considered as reference.

III.2.D Effect of cellulose moisture content

From the control MC of 8% (equilibrium 60% RH 25°C), variations were investigated, α-cellulose was dried in an oven at 103°C at least for 48 hours to produce dry α-cellulose. Climatic chambers at 45% RH 25°C and 75% RH 25°C respectively produced α-cellulose at 6.1 and 10.8 % MC (Table III - 5).

Table III - 5: Moisture content conditions for the evaluation of the effect of moisture content on the mechanical properties of compressed α-cellulose samples

Temperature (°C)	Relative Humidity (%)	Measured Moisture Content (%)
103	0	0
25	45	6.1 ± 0.1
25	60	8.0 ± 0.0
25	75	10.8 ± 0.1

Drastically lower mechanical properties, higher specific gravity, and higher equilibrium moisture content were observed on specimens molded from dry powder. A lighter color and a rougher surface aspect were observed. Equilibrium MC of these specimens was also higher and SG lower suggesting self-bonding to a lower extent (Table III - 3). Moisture was thus concluded to be necessary to achieve satisfactory molding in these conditions. This apart, not much effect could be observed upon moisture content variation in the range 6 – 11% (Figure III - 14). High moisture produced slightly lower strengths.

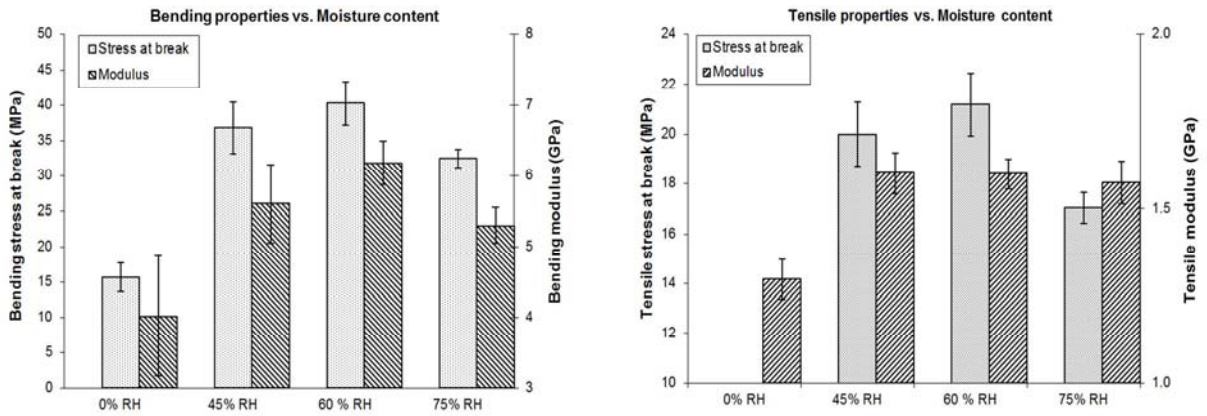

Figure III - 14: Effect of moisture content on the mechanical properties of compressed α-cellulose samples

Because highest mechanical properties were obtained on control conditions of molding, this condition was kept as a reference. The effect of moisture, however remained of primary interest, as the removal of water from the powder produced drastically different results. Moisture content remained one of the primary parameter to study, and was later further investigated.

III.2.E Effect of pressurization speed

Parallel could be made between this work and the production of pharmaceutical tablets. In this industry, α-cellulose can be used as excipient, i.e. as an inert substance for the active drugs to be dispersed in and that can form the tablet for ingestion. Even though compaction speed are much higher than those that can be applied in the laboratory press (Akande et al. 1997), its effect was investigated. Of course, in this experiment, a choice had to be made because pressurization speed, time and pressure are not independent. The integral time.pressure was chosen to be maintained constant, thus when pressurization rate was decreased total molding time increased to maintain an equal time.pressure integral. Explanations can be found in the materials and methods part (Chapter VI).

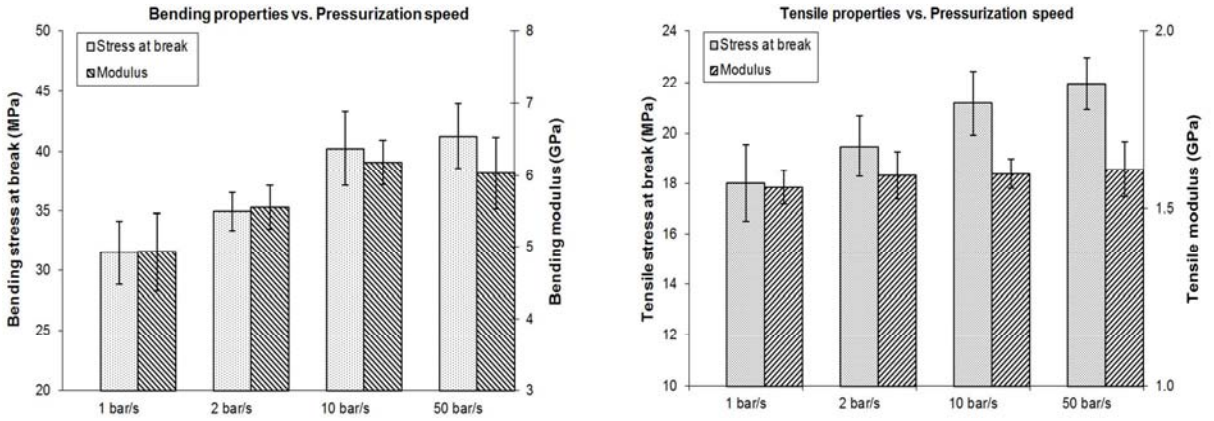

Figure III - 15: Effect of pressurization speed on the mechanical properties of compressed α-cellulose samples

The properties were seen to be slightly degraded when decreasing pressurization speed (Figure III - 15) which could also be an effect of higher time due to thermal degradation (Figure III - 13), lower pressure, or a combination of both. Anyway, higher pressurization speed produced specimens with slightly higher mechanical properties. Also, increasing pressurization speed allowed to slightly lower operating time. 3D molding also had benefits from increasing pressurization speed. Thus, next experiments would have preferentially highest pressurization speeds as a new reference.

III.2.F Effect of temperature

During the first set of experiments, the mechanical properties increased linearly with processing temperature (Figure III - 16). In the same time, specific gravity was increased and equilibrium moisture content was decreased, showing reorganization and less availability on the hydroxyl groups. At 200°C, about 1/3 of the specimens were delaminated (thus discarded from the results), thus more specimens were produced to calculate mean and standard deviation. 200°C appeared to be a limit, which was a classical result in the literature (Chapter I).

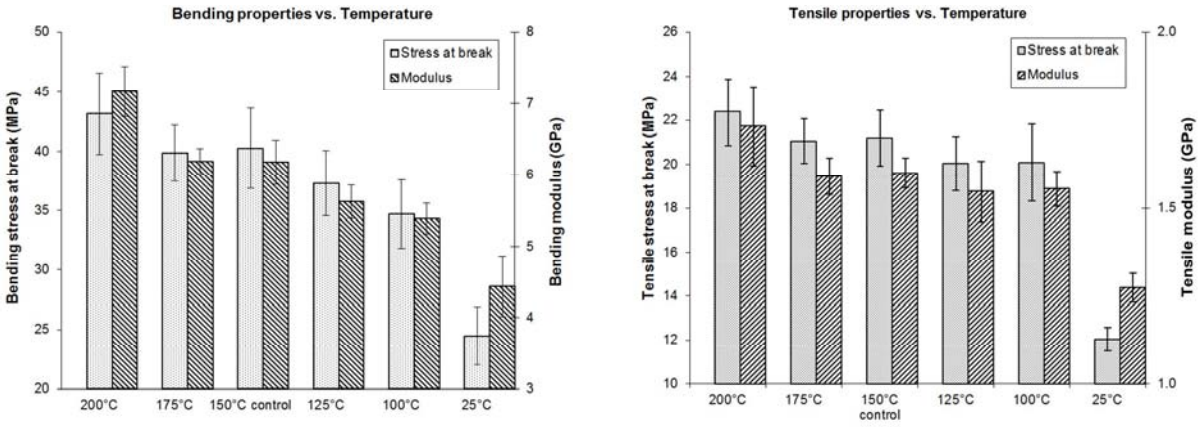

Figure III - 16: Effect of temperature on the mechanical properties of compressed α-cellulose samples

Yet, the understanding of this phenomenon was limited because delamination occurred only "sometimes". One possible explanation would be the time needed to load the powder in the hot mold, a slightly longer time to load the mold would lead to a much higher moisture loss from the powder. More experiments were later performed to understand the moisture / temperature effect on delamination (see III.3).

As can be observed on the SEM pictures taken in Nagoya (Figure III - 17), the inter-particle voids are decreasing from 30 to 200°C, showing a higher deformability of the particles with increased temperatures, which explains the increased density and could be an explanation for the better mechanical properties observed upon increasing molding temperature (Table III - 3).

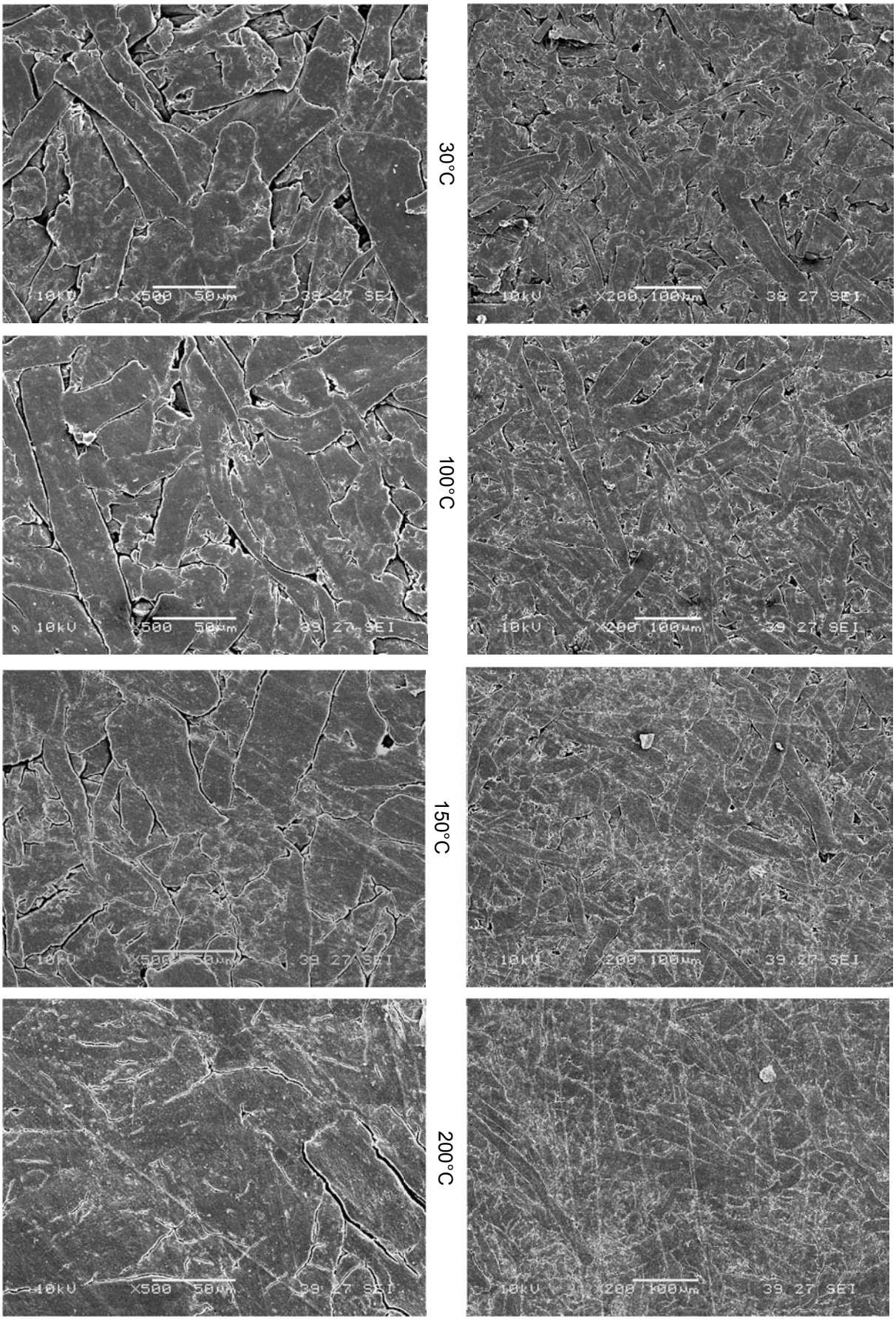

Figure III - 17: SEM pictures of specimens' surface produced at different temperatures

III.2.G Effect of pressure

In the industrial processing of wood-based panels, cellulose is considered a passive polymer, i.e. does not participate actively to the cohesion although lignin and hemicelluloses do. Products of degradation, however could participate to cohesion through the hydroxymethylfurfural route (Chapter I). Anyway, without pressure, no cohesion was expected on pure cellulose, and as this work deals with high pressure molding, low pressure molding was not considered in the first times. A first conclusion was that no significant difference could be observed between specimens compacted at 133 or 265 MPa (Pintiaux et al. 2013). Later, complementary experiments were performed: new control conditions were a pressing temperature of 150°C (average), 8% (control moisture content), 30 seconds (low molding time), 50 bar/s (highest pressurization speed), 7.5 g (reduced mass) and pressure was varied from 8.8 to 264 MPa (Table III - 3).

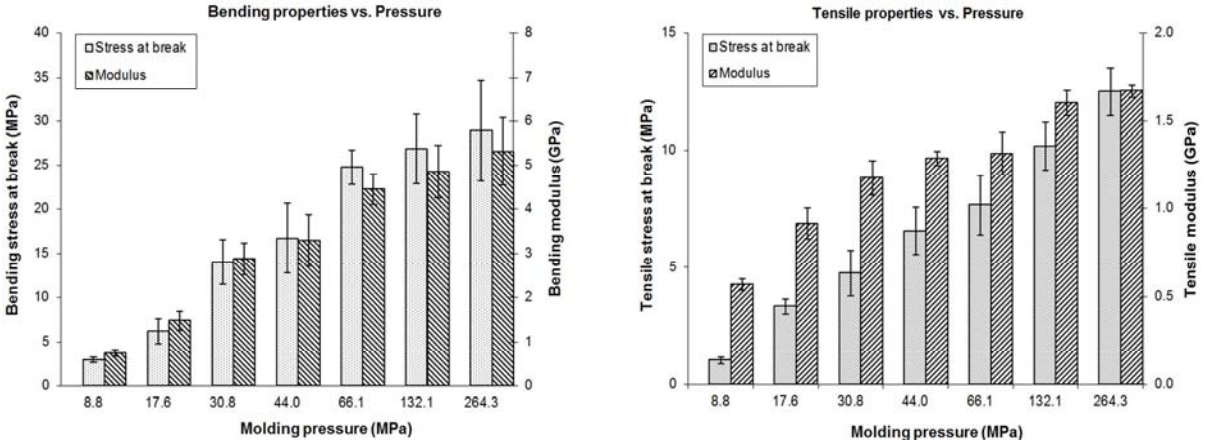

Figure III - 18: Effect of pressure on the mechanical properties of compressed α-cellulose samples

As expected, the mechanical properties increased with pressure (Figure III - 18). The increase rate of the mechanical properties is decreasing with pressure which means that the effect of pressure was less and less important, therefore, it is possible to consider that sufficient properties could be obtained (depending on the requirements) with much lower pressure than 264 MPa. In the meantime, specific gravity was increased and thickness decreased, the specific mechanical properties (i.e. mechanical properties divided by the specific gravity of specimens) were then calculated (Table III - 6) and drawn in (Figure III - 19).

Table III - 6: Specific and standard mechanical properties of compressed α-cellulose samples under various conditions of pressure

Hydraulic pressure	Molding pressure	Thickness		Specific gravity		Bending stress at break			Bending modulus			Tensile stress at break			Tensile modulus		
						Specific	Standard		Specific	Standard		Specific	Standard		Specific	Standard	
		Mean	St. dev.	Mean	St. dev.	Mean	Mean	St. dev.	Mean	Mean	St. dev.	Mean	Mean	St. dev.	Mean	Mean	St. dev.
bar	MPa	mm		g/cm³		MPa.cm³/g	MPa		GPa.cm³/g	GPa		MPa.cm³/g	MPa		GPa.cm³/g	GPa	
300	264.3	2.60	0.04	1.500	0.005	19.3	28.9	5.7	3.5	5.31	0.76	8.3	12.5	1.0	1.1	1.67	0.04
150	132.1	2.75	0.05	1.497	0.005	17.9	26.8	4.0	3.2	4.85	0.60	6.8	10.2	1.0	1.1	1.60	0.07
75	66.1	2.90	0.06	1.484	0.014	16.7	24.7	1.9	3.0	4.45	0.35	5.2	7.6	1.3	0.9	1.31	0.12
50	44.0	3.03	0.05	1.469	0.007	11.4	16.7	3.9	2.2	3.29	0.58	4.5	6.5	1.0	0.9	1.29	0.04
35	30.8	3.13	0.06	1.459	0.009	9.6	14.0	2.6	2.0	2.88	0.36	3.3	4.7	1.0	0.8	1.17	0.10
20	17.6	3.46	0.04	1.425	0.011	4.4	6.2	1.4	1.0	1.49	0.21	2.3	3.3	0.3	0.6	0.92	0.09
10	8.8	4.14	0.07	1.392	0.007	2.1	3.0	0.3	0.5	0.74	0.08	0.7	1.0	0.1	0.4	0.57	0.03

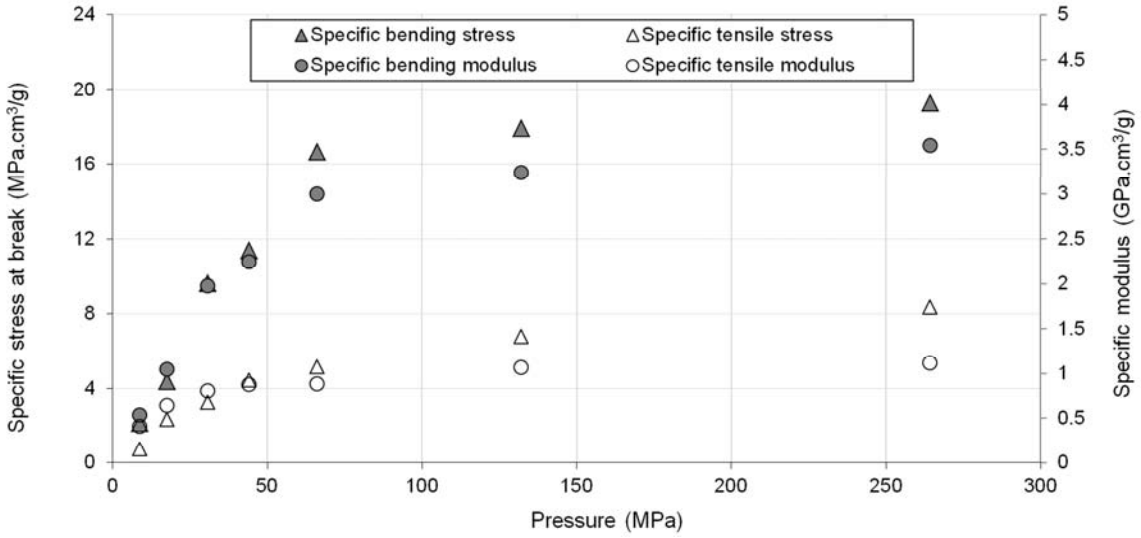

Figure III - 19: Effect of pressure on the specific mechanical properties

The specific mechanical properties were seen to increase following a logarithmic law which would show that not only densification governs the mechanical properties, but also some cohesion mechanism that does not involve densification (but reorganization) could occur.

III.3 The cliff behind the hill: investigating the interdependency of temperature and moisture content on the mechanical properties and delamination

III.3.A Delamination mapping

The temperature of molding is generally reported to be the most important parameter of improvement for the properties of binderless boards. Delamination is often reported as a physical limit to the increase of temperature way before thermal decomposition (as it could be expected). It is also reported as a technological limit in the pharmaceutical tablets production. Delamination also causes troubles in the industry of wood-based panels with adhesives (Chapter I): moisture is needed because it facilitates the heat transfer from the heated press plates through the surfaces of the mat to the inner layers of the pressed material in order to cure the resin. Yet, an excess of moisture is known to let steam accumulate in the inner layers and trigger delamination. Also because free water reacts with the resin, moisture content is commonly reduced to about 3% prior to molding.

Surprisingly, reduced moisture content has been rarely reported in the experiments about binderless boards pressing although results were very encouraging (Nonaka et al. 2013). First results obtained during the present work concluded that moisture content had a limited impact on the mechanical properties in control conditions as defined in Table 2. At 8% MC and 200°C, delamination was observed for about 1/3 of the molded specimens. Only the 2/3 left was tested and exhibited the best mechanical results so far. There is thus a discontinuous behavior of the effect of temperature on the mechanical properties: there is a regular increase of the properties upon increase of temperature until a certain temperature that triggers delamination. Moisture reduction was expected to allow an increase of the molding temperature, but the effect of the moisture decrease / temperature increase on the mechanical properties has to be evaluated.

Thus, in a second time, the effect of moisture and temperature were deeper investigated, high temperature range from 175°C to 250°C (laboratory press maximum temperature) and low moisture range (0 to 8%) were selected. 14 dog-bone specimens were compression-molded for each of the 20 conditions (175 – 200 – 225 – 250°C crossed with 0 – 2 – 4 – 6 – 8 % MC). For these experiments, the control conditions were 7.5g of α-cellulose introduced in the mold, a molding time of 30 seconds and a pressure rate increase of 50 bar/s. Results on delamination, based on the simple observation of the specimens were sum up in Table III - 7.

Table III - 7: Molding results on the moisture / temperature experiments

		Temperature			
		175°C	200°C	225°C	250°C
Moisture content	8	ok	delaminated	slightly delaminated	ok
	6	ok	slightly delaminated	ok	ok
	4	ok	ok	ok	ok
	2	ok	ok	ok	ok
	0	ok	ok	ok	ok

At 175°C, no delamination was observed whatever the moisture content. At 8%, delamination was confirmed for 200°C, about half of the specimens were separated in two, the other half seemed to remain sound but a crack actually existed along the edge of the dog-bone (Figure III - 20). These specimens were not mechanically tested.

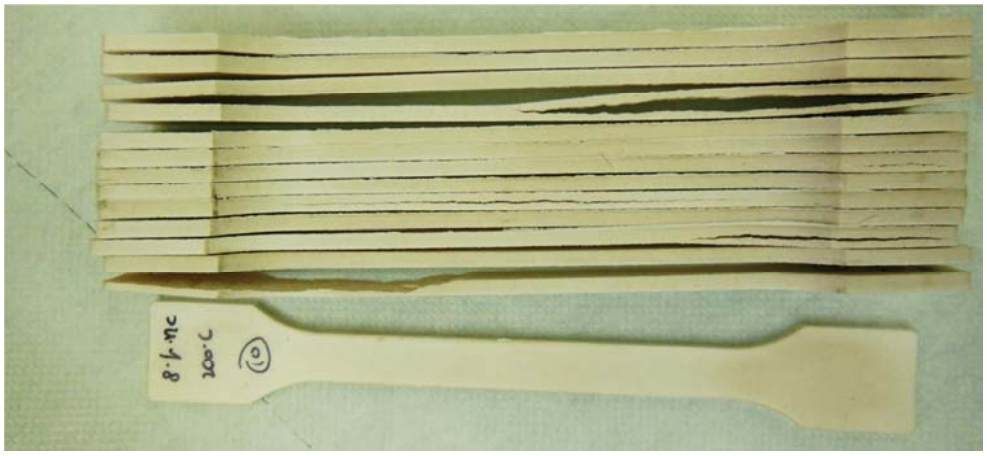

Figure III - 20: compressed α-cellulose samples at 200°C and 8% showing important delamination

Surprisingly, increasing the temperature decreased the effect of delamination and only some of the specimens exhibited slight cracks at 225°C, none of the specimens were truly delaminated and, at 250°C all the specimens were perfectly sound. At 0, 2 and 4 %, none of the temperatures were causing troubles of delamination. Finally, for 6% of moisture content, 200°C of molding temperature made slight cracks appear on the edge of some specimens but later on, at 225 and 250°C the specimens showed no defects.

This mapping of the conditions that triggers delamination was thus successfully obtained. It was confirmed that 200°C and 8% MC were the worst conditions of molding because heavy delamination occurred. Increasing temperature made the delamination phenomena decrease at 225°C and disappear at 250°C. Decreasing moisture to 6% decreased the delamination phenomenon, and a further decrease of the MC to 4 – 2 and 0 % made it disappear. It was concluded that delamination could be avoided if the conditions were kept far from the 200°C – 8% point.

III.3.B Color scale

As can be seen on Figure III - 21, the color of the compressed specimens is gradually darkening with the temperature which is really obvious, but within a temperature, the moisture content had much less effect; there might be a slight correlation between lower moisture and darker color. The 2% series might also appear slightly less dark than the others, they also presented the highest mechanical properties. The color of the specimens seems to be influenced by their density (and possibly heterogeneity) and the temperature of molding. The link between color of the specimens and the mechanical properties was not further studied, but it may be valuable in the future.

III.3.C Mechanical properties mapping

Except for the 200°C – 8% specimens, the 15 remaining conditions were tested in tensile and bending tests. The results are gathered in Table III - 8. It can be observed that the specimens processed at 2% moisture content, whatever the temperature had much higher mechanical properties than the others.

Table III - 8: Summary of the mechanical properties of moisture content / temperature effect experiment, the 2 % experiments appear in bold letters

		Temperature								
		175°C		200°C		225°C		250°C		
		Mean	St. dev.	Mean	St. dev.	Mean	St. dev.	Mean	St. dev.	
Moisture content (%)	8	34.75	3.92	ND		30.24	5.38	37.02	2.04	Bending strength (MPa)
	6	35.65	2.64	39.93	4.27	40.23	2.96	44.485	1.46	
	4	35.21	2.59	34.92	5.02	41.73	1.79	44.84	3.15	
	2	**43.17**	**6.29**	**45.30**	**7.78**	**55.09**	**4.70**	**70.10**	**4.14**	
	0	35.00	1.79	41.13	2.03	39.62	3.38	51.73	5.74	
	8	5.94	0.59	ND		6.23	0.44	7.11	0.33	Bending modulus (GPa)
	6	5.62	0.30	6.16	0.58	6.30	0.40	7.04	0.45	
	4	6.13	0.38	6.03	0.66	6.94	0.24	7.40	0.46	
	2	**6.10**	**0.44**	**6.20**	**0.70**	**7.24**	**0.34**	**8.09**	**0.67**	
	0	5.67	0.32	0.04	0.63	6.71	0.33	7.72	0.26	
	8	17.19	1.24	ND		16.17	3.03	19.16	1.00	Tensile strength (MPa)
	6	22.30	1.85	15.29	8.77	25.09	3.20	27.55	1.92	
	4	18.39	2.47	20.37	1.87	20.59	1.55	22.80	3.93	
	2	**19.15**	**1.70**	**23.35**	**1.45**	**24.27**	**3.13**	**31.13**	**5.91**	
	0	18.14	1.28	16.45	3.42	20.62	1.11	25.22	1.33	
	8	1.88	0.10	ND		1.96	0.03	1.99	0.07	Tensile modulus (GPa)
	6	1.91	0.11	1.75	0.06	2.03	0.14	2.02	0.11	
	4	1.99	0.04	2.00	0.07	2.05	0.11	2.13	0.11	
	2	**1.78**	**0.08**	**1.84**	**0.05**	**1.87**	**0.08**	**1.94**	**0.15**	
	0	1.83	0.10	1.82	0.07	1.94	0.09	2.00	0.08	
		Mean	St. dev.	Mean	St. dev.	Mean	St. dev.	Mean	St. dev.	
		175°C		200°C		225°C		250°C		

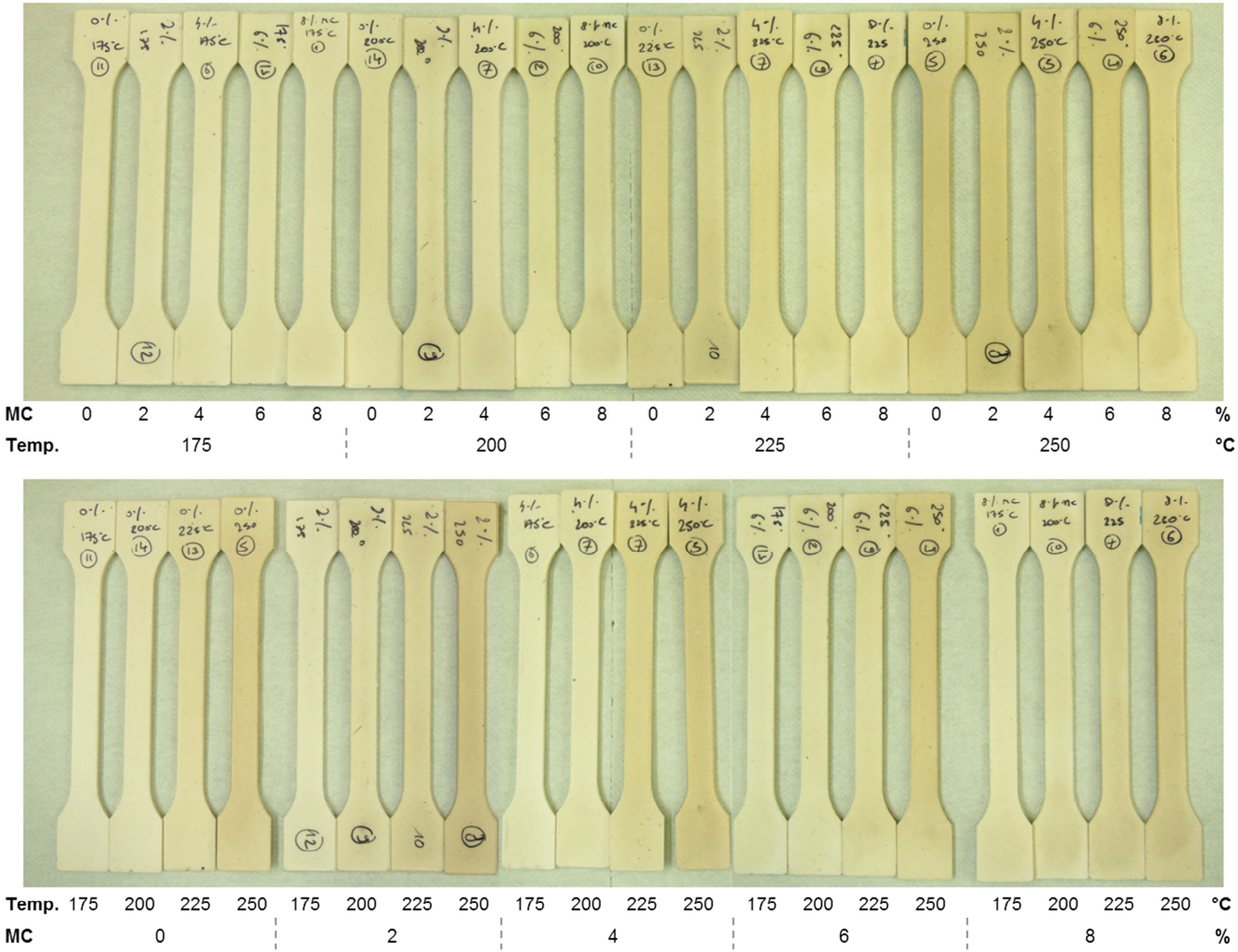

Figure III - 21: Pictures of moisture/temperature mapping samples and differences of colour sorted by moisture – temperature (first picture) and temperature – moisture (second picture)

The mechanical properties of 8%-225°C samples were the lowest within the whole set of conditions, which is a direct effect of the slight delamination experienced during these conditions. The 6%-200°C which also produced a slight delamination had the lowest tensile strength but the bending strength was in the average. Except for these two points, increasing temperature at constant MC generally led to an increase of the mechanical properties. The tensile modulus shows very little variation within the experiments range.

Table III - 9: Bending strength (MPa) on the left and Tensile strength (MPa) on the right, mean values for the MC / Temperature with a colour scale blue – red

Moisture content (%)	Temperature 175°C	200°C	225°C	250°C
8	34.75	ND	30.24	37.02
6	35.65	39.93	40.23	44.5
4	35.21	34.92	41.73	44.84
2	43.17	45.30	55.09	70.10
0	35.00	41.13	39.62	51.73

Moisture content (%)	Temperature 175°C	200°C	225°C	250°C
8	17.19	ND	16.17	19.16
6	22.30	15.29	25.09	27.55
4	18.39	20.37	20.59	22.80
2	19.15	23.35	24.27	31.13
0	18.14	16.45	20.62	25.22

Table III - 10: Bending Modulus (GPa) on the left and Tensile modulus (GPa) on the right, mean values for the MC / Temperature with a colour scale blue – red

Moisture content (%)	Temperature 175°C	200°C	225°C	250°C
8	5.94	ND	6.23	7.11
6	5.62	6.16	6.30	7.04
4	6.13	6.03	6.94	7.40
2	6.10	6.20	7.24	8.09
0	5.67	6.37	6.71	7.72

Moisture content (%)	Temperature 175°C	200°C	225°C	250°C
8	1.88	ND	1.96	1.99
6	1.91	1.75	2.03	2.02
4	1.99	2.00	2.05	2.13
2	1.78	1.84	1.87	1.94
0	1.83	1.82	1.94	2.00

At 175°C, except for the 2% MC, the mechanical properties were about the same all within the moisture range. At 200 and 225°C, the behavior of moisture is quite difficult to analyze especially for the stresses. The bending modulus has a quite smooth response (Table III - 10) the highest value is for 2% - 250°C and lowering temperature or increasing / decreasing moisture lead to a gradual decrease of the bending modulus. The tensile modulus showed a lower response to the variations of temperature than the other parameters.

Specimens produced at 2% - 250°C had remarkable properties and were the best specimens ever produced during this research work. The difference between 2 % and the other values of moisture was so drastic that the experiments were doubled as verification. However, compared to the other solid materials (Table III - 1), the mechanical properties obtained are quite low, and comparable to paper.

The slope of increase of the mechanical properties is high from 200 to 250°C, and the properties of specimens obtained at higher temperature is a burning question ! Unfortunately these experiments could not be performed because 250°C was the temperature limit on the laboratory press. Cellulose starts to degrade around 220-230°C, but the effect of degradation on the mechanical properties is uncertain (Figure III - 7). A lower DP would probably affect negatively the strengths, but the "sugar" chemistry could have a bonding effect through the hydroxymethyl furfural route (see Chapter I).

III.4 Correlation of equilibrium moisture content and density of the compressed specimens

From the first set of experiments (Pintiaux et al. 2013), the equilibrium moisture content and specific gravity of the compressed specimens were plotted and it was observed that within this first set of data the equilibrium moisture content was quite correlated to density (Figure III - 22).

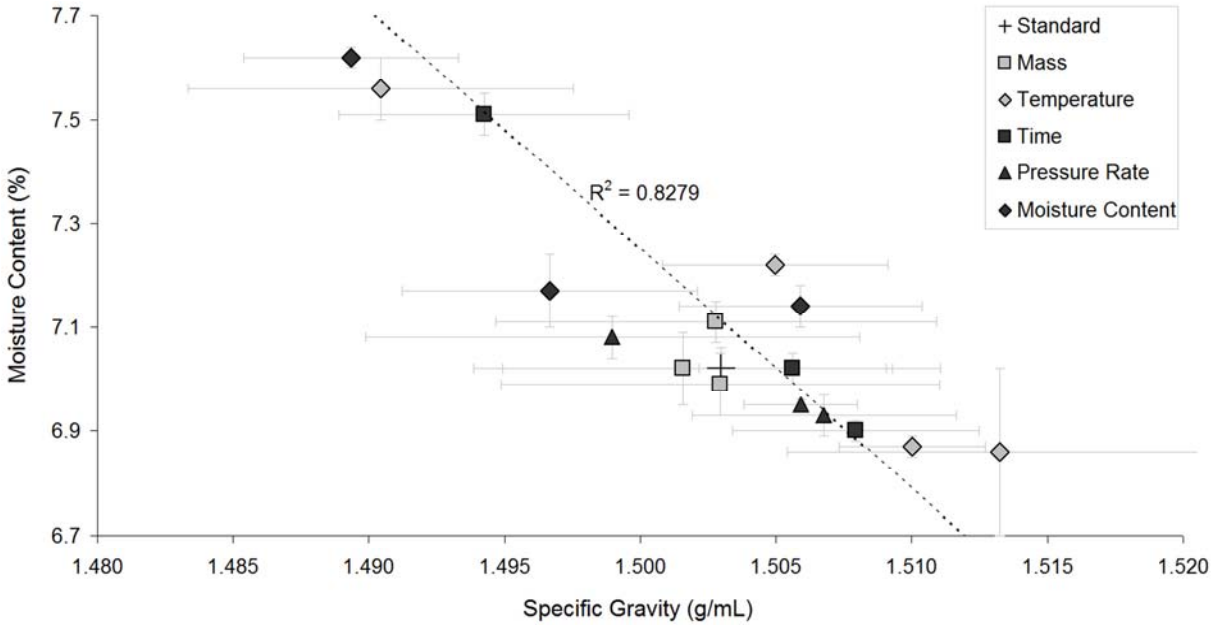

Figure III - 22: MC correlated to specific gravity (first set of experiments, evaluation of different parameters)

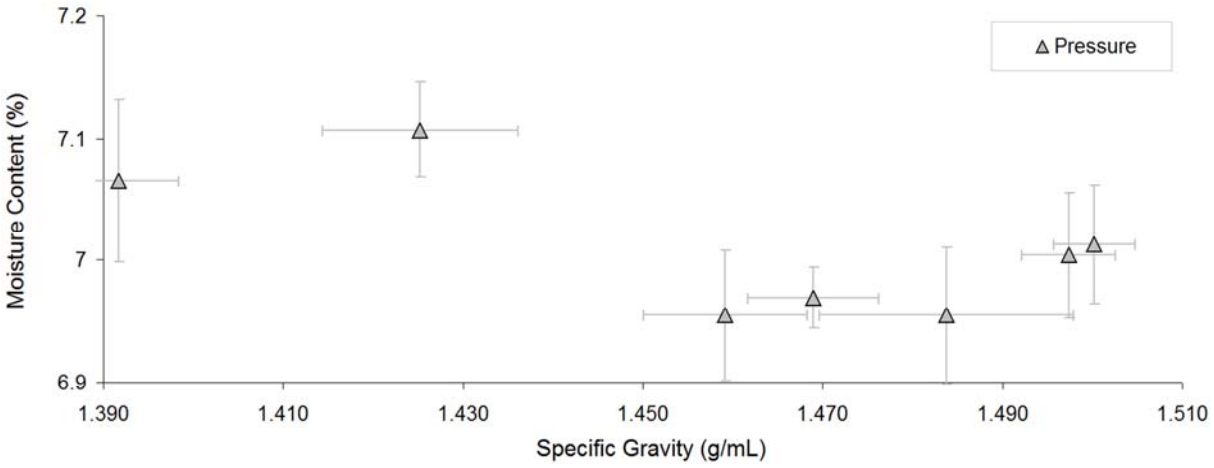

Figure III - 23: MC correlated to specific gravity (second set of experiments, evaluation of pressure)

The reliability of the data being what it is (high standard deviation of the specific gravity measurements) the later interpretation has to be considered with care: Most of the parameters tested in the published paper except mass (i.e. III.2.A to III.2.F), contributed to

draw a correlation between MC and density. In other terms, in this first set of experiment, the loss of accessibility of free hydroxyl groups appeared correlated to the loss of porosity, i.e. increased density (Figure III - 22). But in the "molding pressure" set of experiment (Figure III - 23), when the pressure was evaluated alone (and control conditions slightly changed i.e. mass changed from 10 to 7.5g, time from 2 minutes to 30 seconds, pressure rate from 10 to 50 bar/s, temperature from 150 to 175°C) there was no correlation between MC and density.

This would show that all parameters except pressure induced changes in the compressed specimens what were observable on changes of density and MC in a correlated way that suggest a loss of accessibility of the free hydroxyl groups; possibly due to a higher level of organization (higher crystallinity) thus the hypothesis can be made that pressure only acts as a catalyst when the other parameters (temperature, time and moisture) triggers changes in MC and density. This hypothesis could be verified by producing specimens while varying pressure, temperature, time and moisture simultaneously for instance using an efficient experimental design.

III.5 Humid atmosphere, water and time properties of compaction molded α-cellulose specimens

III.5.A Humid atmosphere behavior

28 control specimens (175°C – 7.5g – 30 s – 264 MPa – 50 bar/s) - that were equilibrated for about 1 month - were separated in 2 lots, the first was pre-weighted, their thickness measured and taken for 15 days in a climatic box at 85% RH and 25°C while the others stayed at 60%RH. The samples were all re-weighted and measured prior to being tested in bending.

The water uptake, from 60 to 85 % RH at 25°C (15 days) was measured to be 2.35 ± 0.04 %. In the same time, the thickness of the specimens was increased by 6.2 % which confirms the poor stability of the compressed cellulose specimens under moist atmosphere at control conditions of molding. The mechanical properties were significantly reduced as seen on Table III - 11. It was also noticed that the specimens had mechanical properties lower than the usual controls. Probably because of the time taken between the molding time and testing time after what it was decided to measure the aging of the specimens (see below, Time stability experiment).

Table III - 11: Mechanical properties of specimens submitted to 15 days under 85% RH 25°C atmosphere

	Thickness (mm)		Bending stress at break (MPa)		Bending modulus (GPa)		Tensile strength at break (MPa)		Tensile modulus (GPa)	
	Mean	St. dev.	Mean	St. dev.	Mean	St. dev.	Mean	St. dev.	Mean	St. dev.
Control	2.73	0.10	35.9	3.6	5.25	0.41	15.5	2.2	1.45	0.12
85% RH	2.90	0.10	22.0	1.1	3.14	0.29	10.3	0.8	1.35	0.02

III.5.B Water resistance measurements

The water resistances were measured on 2 different molding conditions in order to serve as comparison for later work extended to lignocellulosic materials. The water absorption (WA) and thickness swelling (TS) of control conditions i.e. 175°C – 8% MC and 250°C – oven-dried 0% MC were evaluated.

Results are available in Table III - 12. High water sensitivity was expected from the cellulose samples, but the values collected during the WA/TS tests were surprising:

Table III - 12: Water absorption and thickness swelling of compressed cellulose samples

175°C - 8%				250°C - 0%			
WA		TS		WA		TS	
mean	st. dev.	mean	st. dev.	mean	st. dev.	mean	st. dev.
75%	2%	96%	3%	65%	4%	79%	2%

The water properties of the cellulose specimens was later seen to be better than any other plan materials tested in the same conditions (Chapter V). An interesting fact is that they were all cracked from the middle, precisely where, if delamination had occurred, the specimen would have been opened (Figure III - 24)

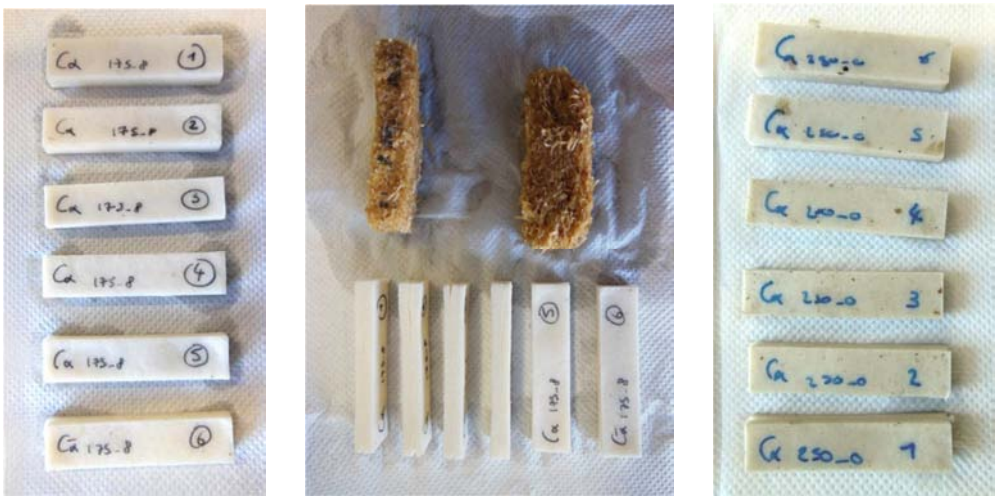

Figure III - 24: Cellulose water properties specimens, from the left to the right: 175°C-8% specimens, compared to WS1 specimens, 250 – 0% specimens.

III.6 Time stability of compressed specimens

In the early stages of this work, the mass of the specimens was observed to be constant after about 4 days to 1 week. Later an experiment was performed in order to evaluate the evolution of the mechanical properties during the equilibrium time and after. 35 specimens of the control conditions (175°C – 7.5g – 30 s – 264 MPa – 50 bar/s) were produced in a row, weighted and their thickness measured precisely 1 minute and again 1 hour after their molding

Between the moment of demolding (1 minute after demolding) and 1 hour under room conditions (20°C ~50% RH) the weight of the 16 first specimens increased by 0.52 ± 0.16 % while the thickness was increased by 0.84 ± 0.85% (i.e. a mean mass gain of 0.037 ± 0.011 g per specimen). The variation of thickness were not reliable because of the precision of the digital caliper used (0.01 mm) but the mass increase during this first hour was significant and about twice higher than the change of mass that occurred during the next 2 months of kinetic measurements.

Table III - 13: Aging tests results

Days	Δ mass		Δ thickness		Bending strength (MPa)		Bending modulus (GPa)	
	mean	st. dev.	mean	st. dev.	mean	st. dev.	mean	st. dev.
0	0		0		51.4	3.0	6.34	0.03
2	0.14	0.02	0.01	0.02	50.8	2.3	6.67	0.03
4	0.19	0.02	0.05	0.09	45.0	4.9	6.47	0.04
8	0.21	0.02	0.08	0.04	42.9	3.5	5.90	0.02
15	0.20	0.01	0.06	0.03	43.3	4.5	6.31	0.05
30	0.22	0.01	0.10	0.04	43.1	2.3	6.70	0.03
60	0.20	0.10	0.11	0.08	44.4	2.1	6.40	0.02

This 1 hour measurement was used to set the initial time of the aging experiment. The first 5 specimens were tested in bending right away. Then, 5 specimens were weighted and tested again after equilibrium of 2, 4, 8, 15, 30 and 60 days. The results were gathered in Table III - 13. It was noticed a negative correlation between the mass gain and the bending strength (Figure III - 25). The modulus showed less variation and no correlation.

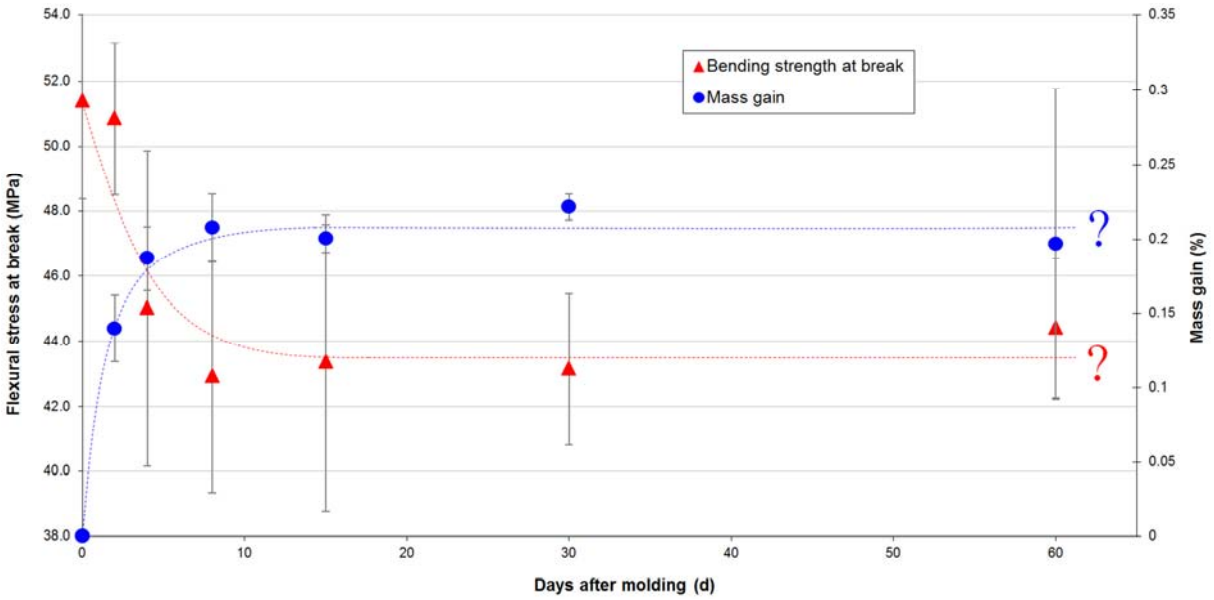

Figure III - 25: Bending strength at break correlated to the weight variation of control specimens, standard deviation calculated from 5 repetitions

This experiment did not permitted to detect an ageing of the specimens although specimens tested at different times of equilibrium all along the project showed some variation of mechanical properties: under the same control conditions (i.e. 8% - 175 °C - 30 seconds - 264 MPa - 50 bar/s), the average bending strength of specimens tested 2 weeks after production were 28.9 MPa in Table III – 6 during the pressure effect evaluation (III.2.G), 34.8 MPa in Table III – 9 during the moisture / temperature effect evaluation (III.3.C) consistent with the value of 35.9 MPa presented in Table II – 1 (2 months old specimens), and 43.3 MPa in Table III – 13 during this last ageing experiment. It is highly possible that the operator effect could explain this variability, and that is why a new reference was produced each time for comparison. The ageing of the specimens should also be run on a longer time period.

III.7 Discussion: about the structure / property relationship of compacted cellulose specimens

III.7.A The specimens' structure as a result of the compaction process

A laminated structure

Commercial α-cellulose is composed of cellulose fibers, which are hollow cylindroids of 10-30 µm of external diameter and a wall thickness of 3 – 5 µm. The length differs from one lot to another; the α-cellulose lot used in this thesis had particles with length from 100µm to 500 µm, and sometimes more, up to 1 mm (Figure III - 26).



Figure III - 26: SEM picture of α-cellulose powder

On the fracture of specimens after bending tests, a laminated structure was observed: sheets of about 300-500 µm wide are aligned perpendicular to the molding pressure, their thickness was evaluated using a digital caliper.



Figure III - 27: Piles of 6 halves of broken specimens in bending (left) and tensile (right)

The tensile specimens also showed a layered organization, but the sheets were a bit less obvious than those resulting from a bending failure (Figure III - 27). On the SEM pictures, without preparation of the samples, the laminated structure and the sheet-orientation of the fibers were confirmed (Figure III - 28).

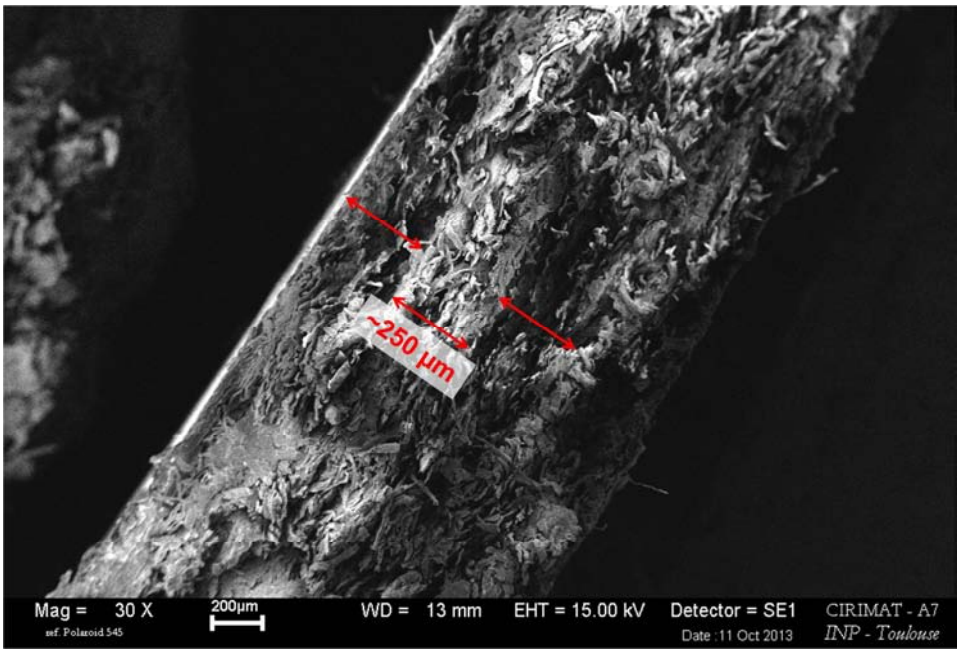

Figure III - 28: Cross sectional SEM picture of a broken control α-cellulose sample (in bending)

At first, it was not certain whether the sheets already exist in the material or were created as a result of the mechanical tests. Yet, the laminated structure appeared in tensile, in bending, and in bending performed in the other direction (with the small side up – Table III - 14). In the field of intertwined materials, the orthotropy resulting from the molding of fibers is a classic. It is also very unlikely that the same structural effect would be resulting from breakage of the material in the two directions of tensile / bending, the laminated structure thus results from the organization of the material itself which can be said orthotropic.

However, every attempt to perform observations on clean cross sections failed in retrieving the laminated structure. Upon sanding paper grinding, stone abrasion, microtone cutting, liquid nitrogen breaking, the inner structure of the specimens always appeared continuous, composed of particles (cross sections of compacted fibers - Figure III - 29) but the 300 microns sheets that should appear as a repeated pattern was never observed. A procedure for what was thought to be the best sample preparation is described in Figure III - 30. The wedge-shape was first given with grinding on 180 grit sandpaper (P180 ISO standards), and successfully passed on 360, 600 and finally 1200 grit sandpaper for a fine finish.

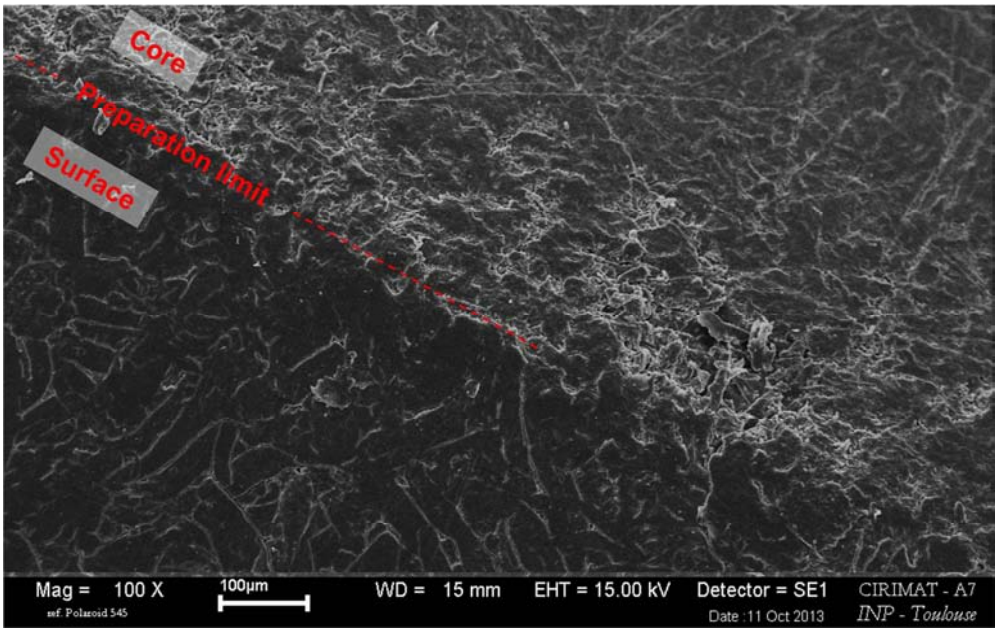

Figure III - 29: SEM picture of a surface and cross section of a sample after sandpaper preparation (180 – 360 – 600 – 1200 ISO grit)

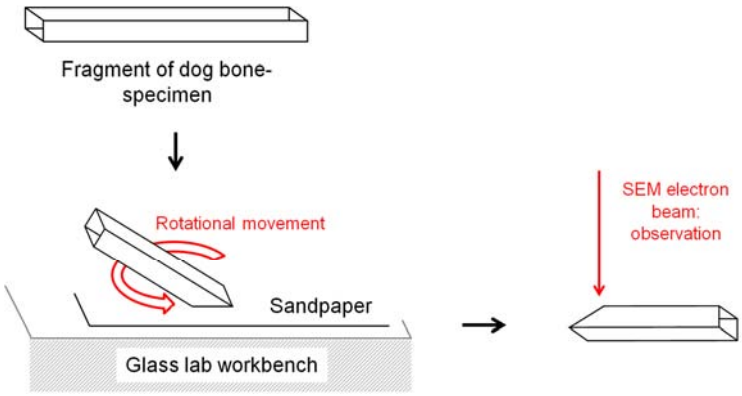

Figure III - 30: Sandpaper preparation for cross section observations

A marked surface effect

All along this work, bending properties have always been higher than tensile properties (Table III - 10 for instance). Normally, homogeneous materials should have tensile properties higher than bending properties, but, in the case of compacted cellulose, the orthotropic character (i.e. layered structure in the direction of bending) partially explains this behavior.

It was rapidly stated that the smoothness of the surface differed totally from the roughness of the inside of a specimen. After a breakage, the grinding and polishing of the inner structure did not produce anything comparable to the surface. Also, during the evaluation of the effect of specimens' thickness on the mechanical properties (III.2.B), it was detected (statistically significant, Pintiaux et al. 2013) that the tensile modulus was increased upon increase of the skin/core ratio (Figure III - 12). 3-points-bending is very impacted by the surface of a specimen because of the deformation pattern occurring during bending, whereas tensile deformation tests the specimen quite homogeneously among its cross-section (Figure III - 31).

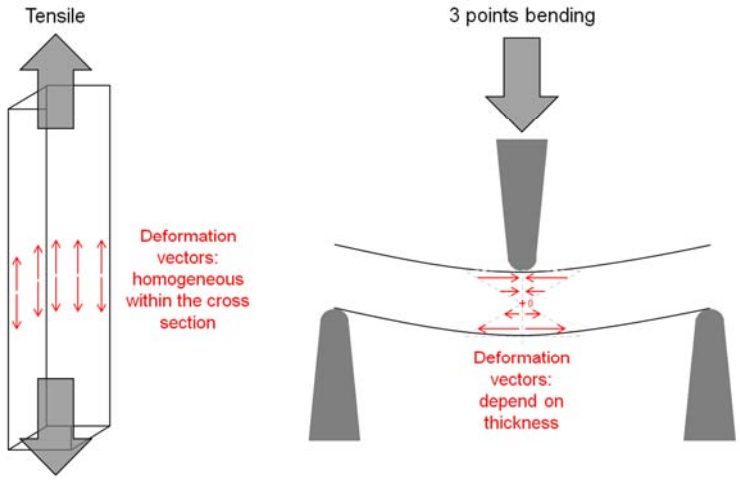

Figure III - 31: Deformation vectors in the case of tensile and 3 points bending

The compacted cellulose material was thus being considered, as a first simple approach, like a "sandwich structure", consisting of 3 layers (skin – core – skin). In this model, the tensile modulus of the skin was confirmed to be higher than the core, although the skin's density was equivalent to that of the core (Table III - 3). Later, it appeared that the lateral sides of the molded object were much more dense and thick than the up and down sides (in contact to the mold), which would complicate the model.

Nevertheless, the "sandwich model" with a stronger skin explains the higher bending properties observed all along this work. It also provides explanations about the higher response in bending to the variations of operating conditions: the skin, in contact of the mold is more rapidly at the mold temperature, moisture changes can occur more rapidly, and in contact of the mold, the pressure is more directly applied than in the core.

Manuel Marcus from the IMFT (Fluids Mechanics Institute of Toulouse) offered the opportunity to perform X-ray 3D tomography on some materials in order to evaluate structural differences at the skin. After scanning the specimens on the sides, the 3D image was reconstructed which permitted to visualize the porosity in the direction of the fibers. Generally, a higher porosity was detected in the core of the specimens. The pattern of porosity distribution showed that the faces in contact of the punches (perpendicular to the pressure) were only a few µm thick. The opposite surfaces in contact of the die were much thicker at about 300 µm thick which was quite surprising. On the following pictures, a color scale was applied to the porosity, high porosity appeared in deep blue medium porosity in light blue / grey, and orange – red was used for lower porosity zones. The same absolute scale was applied on all 4 specimens tested, in order to allow significant comparisons.

On the cross section of 8% cellulose pressed at room temperature (25°C – line T0 in Table III - 3), a large zone of high porosity (deep blue) can be observed in the core of the specimen compared to the other (Figure III - 32). The specific gravity of the specimen was measured at 1.481 g/cm^3 and was the lowest of Table III - 3. These specimens also had an equilibrium moisture content of 8.57 % which was even higher than the original powder (8.0 %).

In comparison, the specimen molded at 150°C from dry cellulose (0% MC powder – line M1 in Table III - 3) had a reduced low density zone, and a wider high density zones on the sides of the specimen (Figure III - 33). Extreme densities (red) were even observed on the lateral sides, and the up and down sides had a thicker high density area. The specific gravity measured on these specimens was consistently higher (1.489 g/cm^3) than the cold pressed specimens and their equilibrium moisture content also lower (7.62 %). However, the comparison of the mechanical properties of these specimens is surprising: the cold pressed, lower density, higher equilibrium MC specimens (8% – 25 °C) had better properties than the

specimens pressed at 0% 150°C (Table III – 3) which confirmed that density / porosity is not sufficient to explain the mechanical properties of the specimens (Cf III.2.G Effect of pressure).

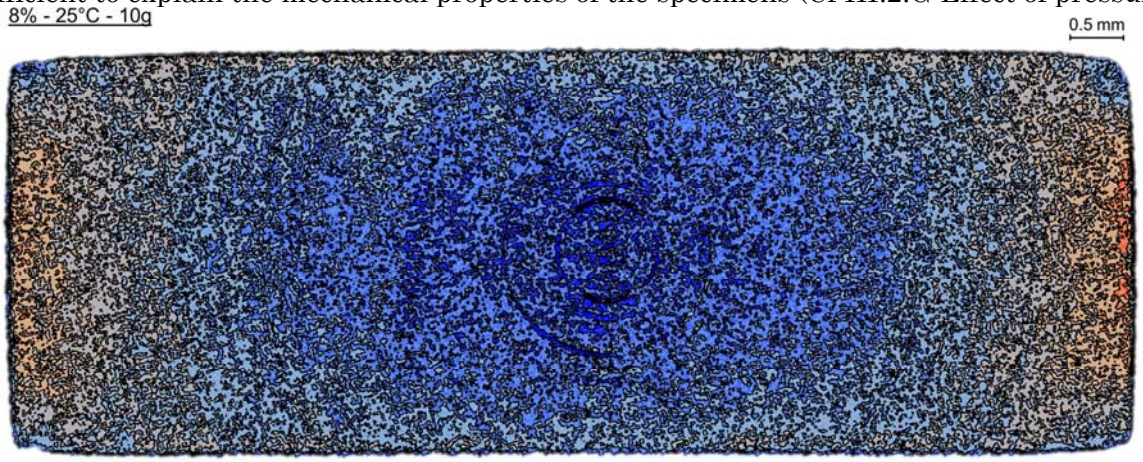

Figure III - 32: Cross section of compacted cellulose specimen at 8% - 25°C obtained in X ray tomography with a coloured blue – red porosity scale

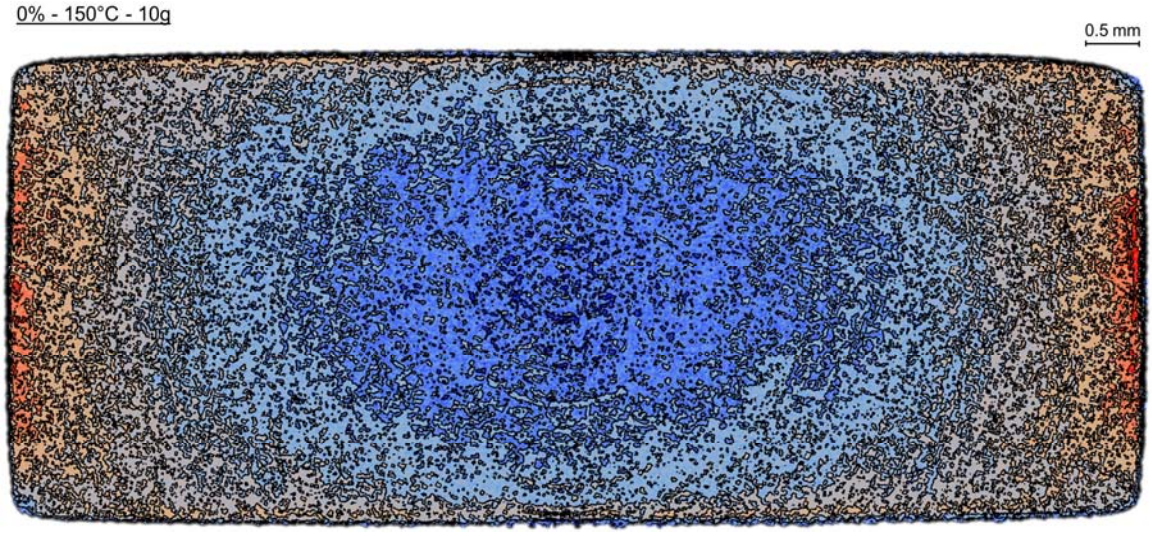

Figure III - 33: Cross section of compacted cellulose specimen at 0% - 150°C obtained in X ray tomography with a coloured blue – red porosity scale

Consistently strange results were obtained on X-ray tomography cross sections of 8% - 175°C and 2% - 250°C specimens: although the later had much higher mechanical properties than the former. The comparison of the porosity pattern showed that the low density zone in the core of 8% - 175°C (Figure III - 35) was smaller than 2% - 250°C (Figure III - 34). The 8% - 175°C (reference specimens) had an average density zone (grey / light blue) that appeared larger and much more continuous than the 2% - 250°C. The sides, however were about the same proportion between the two conditions, but significantly higher density was observed on the 2% - 250°C specimen.

Despite its extraordinary mechanical performances, the porosity pattern of the 2% - 250°C specimen was very similar to the 0% - 150°C (Figure III - 33) which had the lowest mechanical properties ever obtained during this PhD work.

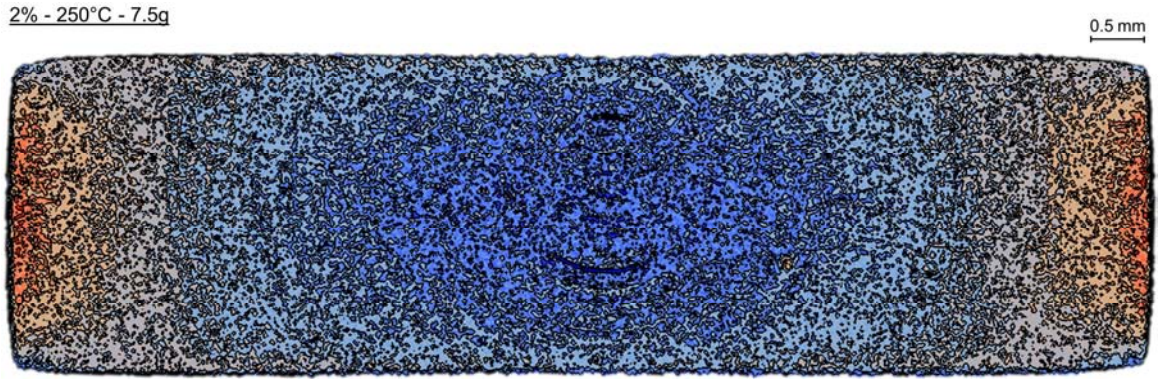

Figure III - 34: Cross section of compacted cellulose specimen at 2% - 250°C obtained in X ray tomography with a coloured blue – red porosity scale

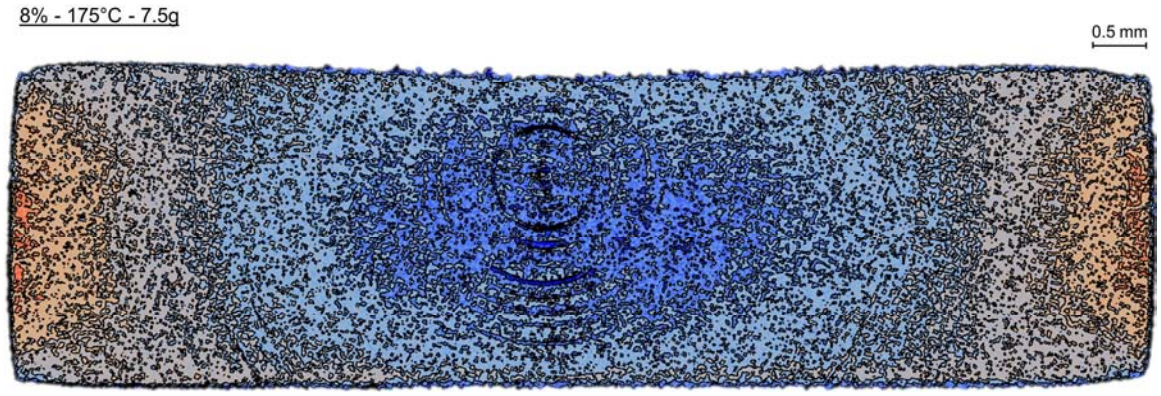

Figure III - 35: Cross section of compacted cellulose specimen at 8% - 175 °C obtained in X ray tomography with a coloured blue – red porosity scale

Following the discovery of the much higher thickness of the high density skin zone on the lateral (short) sides of the specimens compared to the up and down sides, bending tests were performed in the direction of the short side i.e. the specimen lying on its side on the 3 points bending setup. The bending properties were thus calculated, considering a thickness of 10 mm (long side) and a width of about 2.7 mm while testing the material on the short side.

Table III - 14: Bending tests performed in the two directions of the long side (classic) and short side

	Bending strength at break		Bending modulus	
	MPa		GPa	
	Mean	St dev	Mean	St dev
Long side (reference)	45.3	1.2	6.9	0.3
Short side	51.8	2.8	6.7	0.2

As seen on Table III - 14, a higher bending strength at break was obtained while testing the material in bending on the short side compared to the long side reference. On the other hand, the bending moduli were similar under the two conditions. This confirms the skin effect and its important role in the mechanical properties of the specimens and the fact it has to be considered in the explanation of the mechanisms of cohesion.

III.7.B Mechanisms of cohesion

The structural changes during compaction molding

The first step of compaction molding is the pre-compression of the powder, which consumes most of the porosity by expelling the air between the particles. This step requires very low pressure and does not produce any mechanical properties; pre-compressed powder does not possess sufficient cohesion to be held by hand.

During the second step, the particles get closer one to the others and friction occurs, which locally increases temperature, increases further the density but the deformation of the particles is not complete as the surface area (Table III - 15) is not much affected (Vaca-Medina et al. 2013). Studies performed by Laurent HEUX at the CERMAV in Grenoble showed that the material resulting from cold compression was much more amorphous than the original powder which precises the effect of pressure on the breaking and disordering of the crystallites. Consistently, cold pressed specimens had an equilibrium moisture content higher than the original powder (Table III – 3 and previous part III.7.1) which could be a result of its amorphization. The data provided by Vaca-medina did not observe this decrease of crystallinity which would much likely be due to the effect of crystal orientation on the X-ray diffraction measurements between the powder and a compacted sample (Figure III - 14).

Table III - 15: Properties of compressed cellulose samples (from Vaca-medina et al. 2013)

Cellulose sample	Crystallinity index[a]	BET		
		Surface area (m^2/g)	Sorption constant	R^2
Vitacel L600/30				
Powder	48 (4.2)	169	8.006	0.997
25 °C	59 (1.9)	163	7.159	0.999
160 °C	64 (2.5)	122	6.953	0.998
α-Cellulose				
Powder	62 (3.0)	136	9.136	0.998
25 °C	66 (3.1)	135	6.617	0.997
160 °C	73 (3.6)	124	7.639	0.998

The third step is characterized by the action of temperature, which begins, and takes place to a higher extent at the surface of the material, where the temperature is first increased and higher in the process. Jallabert (PhD thesis 2014) showed that during the compaction process, a transition temperature is crossed for what hypothesis was that it could be the glass transition temperature of cellulose (Figure III - 36). The decrease of surface area on the resulting material compared to the original powder and to the cold-compressed material (Table III - 15) supports this hypothesis: under the effect of temperature, the Tg is crossed and the fibers can be deformed and remain in this deformed state which facilitates the establishment of the hydrogen bonding network. In parallel, crystallinity studies made at the CERMAV have shown a much higher crystallinity at the skin than in the core of the hot-pressed samples which was consistent with the data of Vaca-medina et al. (Table III - 15).

The temperature effect is well described in this chapter as a drastic increase of the mechanical properties, which are directly impacted by the establishment of a hydrogen bonding network to a higher extent. Data available in this chapter (Table III - 3) have also shown an increase of density with molding temperature which can be explained by the higher deformability of the fibers because higher temperature allowed more material (not only the surface) to cross the Tg. An hypothesis was thus formulated: The effect of pressure

would be the amorphization of the cellulose, but then temperature allows to recrystallize some of this amorphized cellulose (co-crystallize), which brings higher mechanical properties, lower porosity, lower BET surface area. The recrystallization step could either take place during the molding, or during the cooldown of the sample.

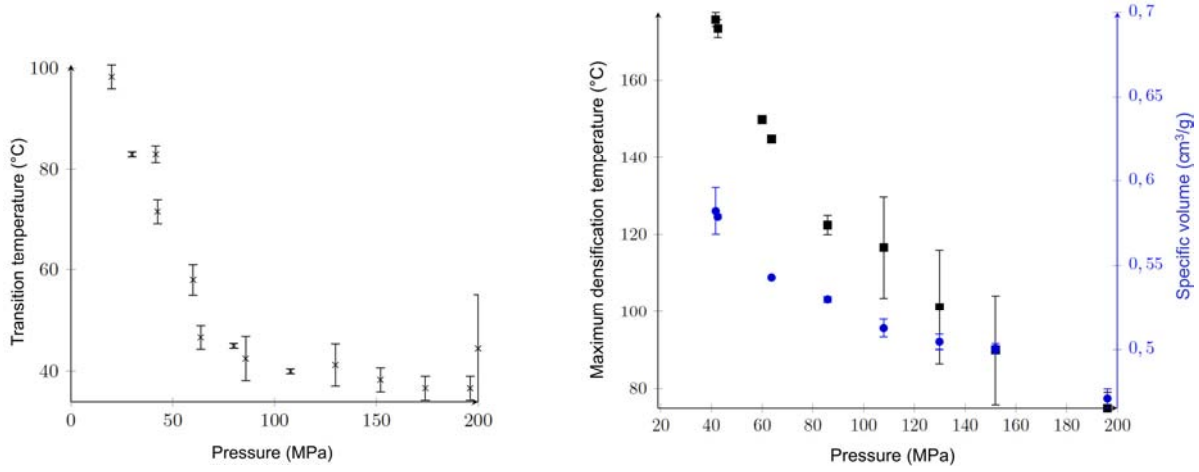

Figure III - 36: Transition temperature, maximum densification temperature and specific volume plotted against molding pressure (from Jallabert 2014 PhD thesis)

Surprisingly, the increase of the molding time was not observed to increase the mechanical properties (Table III – 3), although it should help to conduct the temperature inside the material and cross the Tg in the whole specimen. The X-ray tomography analysis in the previous part are consistent with this observation, as the porosity pattern are not directly correlated to the in a specimen does not change as much as its mechanical properties. Further anlysis would be needed to fully elucidate these statements.

The central role of water

The presence of some moisture was concluded to be necessary in the research of increased mechanical properties. Jallabert also confirmed that the densification step did not occur on dry compacted powder from 0 to 160°C (Figure III - 37).

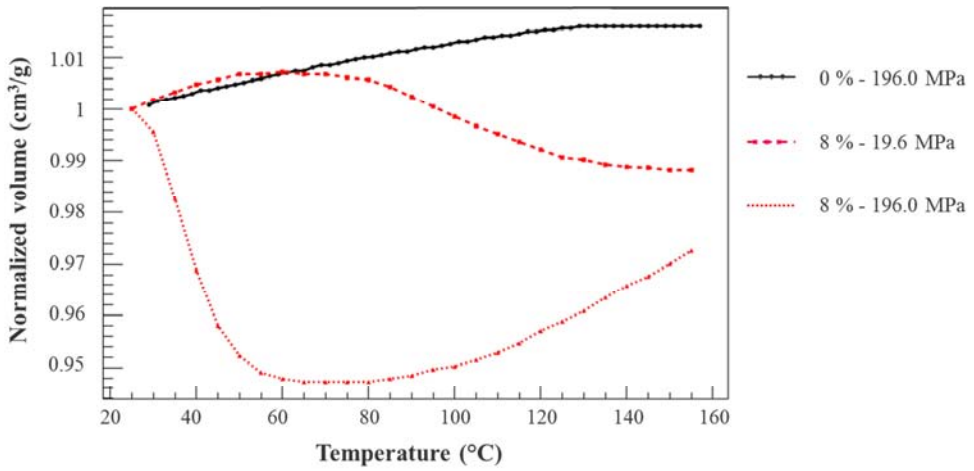

Figure III - 37: PVT diagrams for compacted α-cellulose (Jallabert PhD thesis 2014)

Plant lignocellulosic constituents' Tg depends on moisture (Chapter I). It is possible that Jallabert did not observe a densification because the Tg of dry cellulose (220°C) was not crossed in these conditions of temperature (i.e. up to 160°C). Consistently, the mechanical properties of dry cellulose brutally increased from 225°C (mold temperature) to 250°C (Table III - 9 and Table III - 10). More data would be needed to verify these statements.

The concomitant effect of temperature and moisture had been studied in regard to the mechanical properties in this chapter (III.3) and it was found that the best properties were obtained at 2% moisture which is below the monolayer of sorbed water for cellulose (5% see materials and methods VI.2.C). Jallabert during his PhD work also obtained the best specimens with gelatinized starch at 4% of MC, below the monolayer calculated at 9.7% (Jallabert, PhD thesis 2014).

The moisture / temperature effect is also responsible for a major drawback of compaction molding: delamination. When moisture is high (i.e. 8%) the increase of the temperature from 175 to 200°C leads to delamination. Upon increase of the temperature to 225 and 250 °C the delamination decreases. Yet, at 250°C and 8% MC, the mechanical properties are only slightly increased compared to the other moistures. Two main hypotheses can be formulated to explain the reduction of the delamination at increased temperature:

* Water could be consumed in hydrolysis reactions (Sasaki et al. 1998), which would reduce the steam pressure in the inner structure and explain the darkening of the specimens at higher temperatures.
* Water is not consumed and steam pressure increases but the strengthening of the skin due to high temperature permit to counteract the delamination effect and the higher strength of the specimens allows to prevent it from bursting. This hypothesis explains why the properties are only slightly increased at 250°C and 8% MC because the more water is in the material, the higher the steam pressure is, and thus the lower the core properties are.

About the steam pressure: most of these molding conditions put water into a subcritical state, which means that during the establishment of the hydrogen bonding, liquid (actually subcritical) water is accumulated in the inner part of the material and remains there which probably prevents the core's fibers from establishing hydrogen bonding because of this excess of water. It can be imagined that, in the inside of the material, liquid water is pushed by the pressure and temperature from the sides (because hydrogen bonding on the sides frees up water that follows the temperature gradient) and thus cellulose particles are "floating" in water which totally prevents contact and chances of hydrogen bonding. The group of Navard et al. studied the effect of pressure molding from 700 MPa to 2.5 GPa on the destructuration of cotton linters. One of their conclusions was that moist cotton linters were torn apart into 15 to 150 nm nanoelements at the surface only whereas dry cotton linters underwent this transformation in the whole specimens (Privas et al. 2013). In this case, moisture prevented the destructuration of the cotton linters in the core of the samples and the establishment of a hydrogen bonding network was thus hindered which is compatible with the hypothesis formulated here.

Thus, upon reduction of moisture, high temperature is necessary to remain over the Tg, which guarantees a strong skin capable of resisting to the steam pressure inside the material, but the reduction of moisture also reduces the steam pressure and lowers the overall quantity of water in the material which gives more chances to cellulose fibers to create cohesion. Moisture is reduced and the strength of the specimens is increasing until 2% (monolayer) which provides a strong skin and the least steam pressure (or no pressure?) which participate in higher cohesion in the core of the material. If more water is removed, the thermal conductivity is lowered, and even though at 250°C the Tg is crossed, the resulting skin is probably thinner or weaker as the temperature dependent cohesion mechanisms cannot take place in the inner part.

The double role of water can be summarized this way: water reduces the Tg which is crucial for deforming particles and thus creating a hydrogen bonding network, and it

increases the thermal conductivity which permits to build up stronger cohesion at the surface and deeper in the core of the material.

However, the X-ray tomography did not support these hypotheses, the skin of the strongest materials did not appear much thicker or with much higher density, at least not in the proportion of the properties' increase and the core of these specimens exhibited as much porosity as the others. From the data collected on the structure / property relationship during this thesis work, it can be concluded that the densification process is not sufficient in order to explain the mechanical properties. These explanations were not the primary objective of this thesis, thus only hypothesis have been formulated on incomplete data which nevertheless conducted to a solid basis for future research.

III.8 α-cellulose flowability investigation trials (Nagoya)

While trying to mold cellulose in 3D, certain flowability was observed (Figure II - 14). The idea of trying to measure to flow properties of cellulose arose with the internship in Nagoya, in the research team of Miki et al. that have already been working on measuring the flow properties of highly charged WPC composites (Imanishi et al. 2005a; Imanishi et al. 2005b).

The setup used in Nagoya was capable of 285 MPa in the chamber. Several dies were available, the first one to be tested was a 4 mm diameter and 10 mm length die. The abbreviation (4,10) is used in this part for dies' diameter and length. An average extrusion speed was set up for the first tests (10 mm/min). As the extrusion is working, the pressing machine automatically adapt the force needed to maintain the flow rate, this force is recorded. If the force exceeds the capacity of the press, the experiment stops.

Cellulose equilibrated with reference climatic conditions (25°C – 60% RH) did not flow at 150°C. The temperature was increased to 200°C, and it did not flow either. In order to increase the flowability, cellulose was let to equilibrate in a high moisture environment (50°C – 100% RH) which produced a MC of 13.66 ± 0.43 %. Another trial was made, and it did not flow. At this time, the powder was charged directly in the hot chamber, with possibility of losing moisture during the charging time thus it was decided to pre-mold cylinders (28 mm diameter) in a cold chamber, letting the pre-compressed plots a few days more to equilibrate, and another trial was performed using these pre-compressed plots as starting material which permitted to charge the mold and start the experiment in only a few seconds. This last trial was a success, a flow occurred and a force - displacement curve was recorded. The experiments were pursued using dies (4,20), (3,10), (2,10) and (5,10). Force displacement curves for these experiments were drawn together in Figure III - 38.

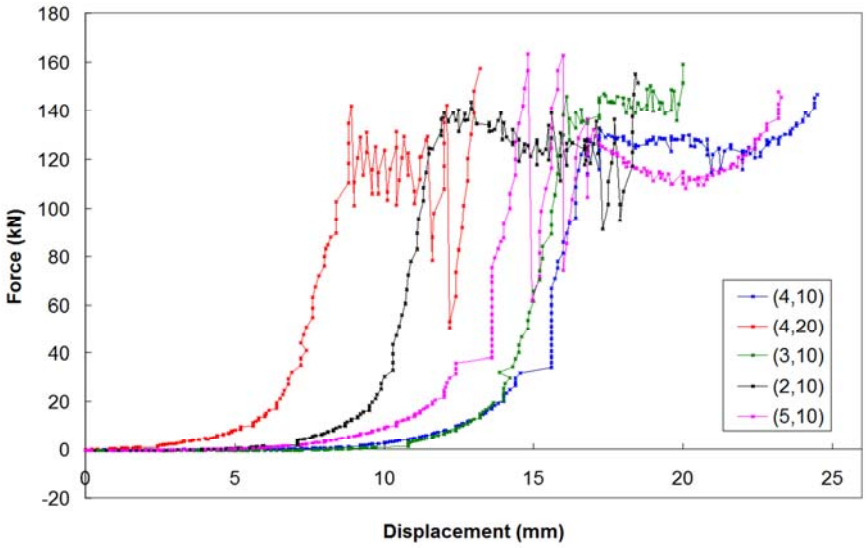

Figure III - 38: Force-displacement curves for moistened cellulose flow tests at 200°C in Nagoya

The (2,10) and the (4,20) had an extremely erratic behavior, with no stabilization of the extrusion force. During the experiment, the material was ejected through the die with violent vibration and sound of explosion and spread all around the press. The hypothesis was formulated that steam accumulation could have produced this explosive extrusion. The (4,10) and the (3,10) curves were almost usable as a plateau was present at the end of the experiment for which a relatively stable extrusion force of 128 and 142 kN were recorded. The (5,10) experiment started with explosions and finally extrusion begun but the flow did not reach a stabilized state.

The results of the flow experiment were collected and are presented in Figure III - 39. Even if most of the extrusion took place at a relatively stable force, the extrudate formed small pellets of cellulose that reminds the shark-skin aspect of highly charged extruded WPC composites.



Figure III - 39: Extruded moistened cellulose off the (4,10) at 200°C (on the left), 100°C on the right

The explosive extrusion on dies (2,10) and (4,20) occurred because of the stick slip phenomenon. The possibility of having steam accumulating, suddenly released at the exit of the die and pushing the material out was formulated. It was thus decided to perform the tests at 100°C (Figure III - 40).

The stick slip phenomenon did not occur at 100°C as much as it did at 200°C but the extrusion force was still unstable and the desired values were not obtained. The extruded product had a quite different aspect compared to the previous tests at 200°C (Figure III - 39).

Because of the impossibility of measuring a stabilized force during extrusion on several dies, another possibility was to study a fewer number of dies but different extrusion speeds. First trials were made on the (4,10) die, and extrusion speeds of 1.5, 10, 20 and 50 mm/min were tested (Figure III - 41) but again, the data were not usable.

Magnesium stearate (10%) which is a classic powder lubricant for the pharmaceutical industry, was evaluated in order to correct the poor flowability of cellulose. The magnesium stearate addition produced even worse curves than pure cellulose (data not shown), these measurements were finally abandoned.

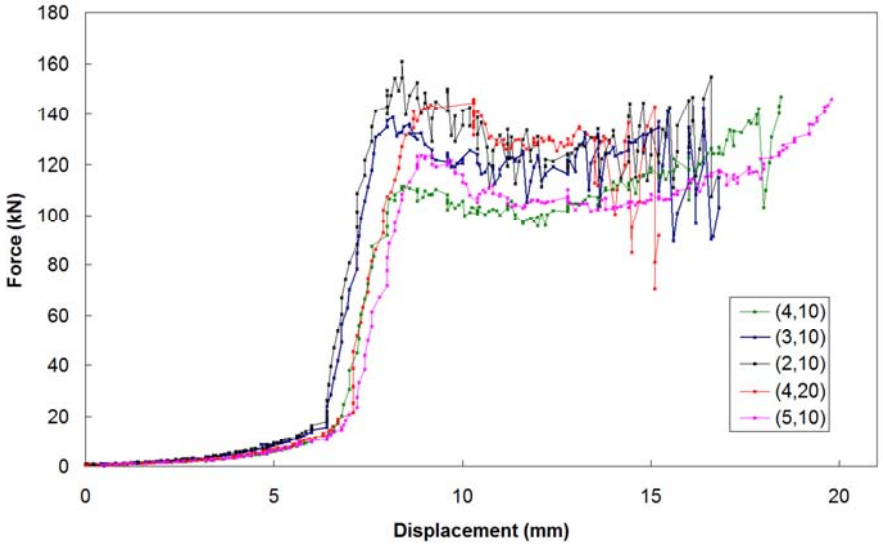

Figure III - 40: Force-displacement curves for moistened cellulose flow tests at 100°C in Nagoya

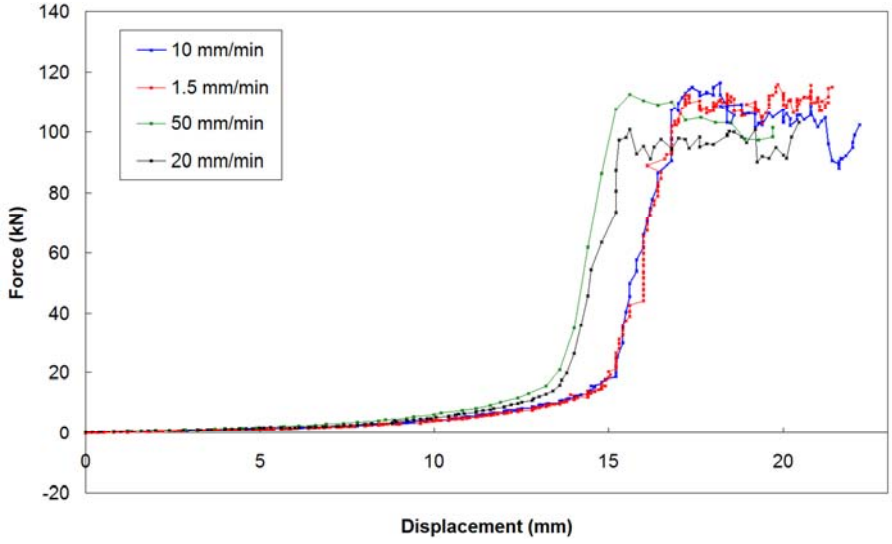

Figure III - 41: Force-displacement curves for moistened cellulose flow tests at 100°C through a (4,10) die in Nagoya

Conclusions

1. The effect of the molding parameters was first studied independently one from the others. The molding time (studied from 3 to 300 seconds) was seen to have no effect on the mechanical properties but specimens molded for a longer time tended to have a lower equilibrium moisture content and a higher density. The increase of pressurization speed was observed to produce higher mechanical properties. These two parameters were not further examined and had the least effect of all. Thus, their values were set to respectively 30 seconds and 50 bar/s (maximum) for the rest of the chapter. The effect of mass variation was studied, and although the bending properties and the tensile strength were not affected, the tensile modulus was drastically increased upon mass reduction. This revealed the existence of different layers in the material, a weaker core and a skin with a higher modulus i.e. less deformability. The density and equilibrium moisture content measurements performed did not permit to detect structural differences between the core and the skin. A reference was established at 7.5 g (i.e. specimens of ~2.7 mm thick). The effect of moisture was first studied at 0 - 6 - 8 and 10%, by drying and equilibrating cellulose to relative humidities of 45, 60 and 75 %. Dry specimens had the lowest mechanical properties, low density and high equilibrium moisture content. Slightly lower mechanical properties were obtained for the highest moisture but less difference was observed between the two other conditions. The effect of pressure was studied although this work was based on high pressure molding and less effect was observed after 100 MPa. It appeared that the specific mechanical properties followed a logarithmic curve, which concluded that higher mechanical properties were not only an effect of higher density. The effect of temperature was first studied at 25°C, and from 100 to 200°C. Temperature increased all the mechanical properties, the specimens' density and reduced the equilibrium moisture content and the interparticular voids, linearly until 200°C, temperature which triggered the delamination of the samples. Temperature was definitely the most impacting parameter.

2. Some additional data related to the properties of compacted cellulose samples were also provided: water tests were conducted on reference samples which showed that the swelling and adsorption were important, but less than expected. The mechanical properties of moist specimens were also performed which confirmed the water sensitivity of the cellulose specimens. All along this thesis work, reference samples have been produced and although being produced in the same operating conditions, exhibited slightly different mechanical results. The ageing of the specimens was performed and did not provide a satisfactory explanation to the observed variation, which thus resulted from other poorly controlled parameters (for instance operator effects like manual filling of the mold).

3. As delamination resulted from steam pressure in the inner layers of the material, built up at high temperature, these two parameters (moisture and temperature) were deeper investigated. The effect of moisture reduction (8 to 0 %) and increase of temperature (175 to 250 °C) were studied together, in order to understand the conditions that triggered delamination and measure the evolution of the mechanical properties. Delamination occurred around the 8% - 200°C point but only slightly at 6% - 200°C and 8% -225°C. 2% of moisture produced specimens with by far the best mechanical properties. The further increase of the temperature consistently increased the mechanical properties, as well as initiated a colour change on the specimens. 250°C specimens were by far the strongest specimens produced within this thesis work. When moisture was further reduced (0%) the mechanical properties were decreased but not as much as previously stated because mostly of the higher temperature employed.

4. These results, together with those obtained by Jallabert during his PhD thesis and the works of Vaca-medina et al. permitted to formulate hypotheses concerning the structure / property relationship. The compacted cellulose material was heterogeneous orthotropic because of the orientation of the fibers perpendicular to the molding pressure. The skin effect

detected while evaluating the effect of mass changes together with the orthotropy of the material provided an explanation for the higher properties measured in bending than in tensile and the hypothesis of a "sandwich model" was proposed. X ray tomography analyses permitted to visualize the porosity distribution along the cross section of some samples. It was revealed that the long side faces (orthogonal to the pressure axis) in contact to the punches were much less dense and thick than the short sides (parallel to the pressure axis) in contact to the die of the mold. The difference of density / thickness of the skin on parallel / orthogonal sides was only slightly correlated to higher properties when testing the material in bending on the parallel sides. Also, poor correlation was established between the specimens' mechanical performances and the porosity distribution within their cross section. This, together with the results obtained upon the evaluation of the effect of pressure led to the conclusion that density / porosity patterns were not sufficient to explain the mechanical properties and the mechanisms of cohesion. Additional data were provided by crystallinity changes: the skin and core of cold-pressed and the core of hot-pressed specimens were more amorphous than the original cellulose powder and the skin of hot-pressed specimens had a crystallinity index comparable to that of the powder. All these elements permitted to formulate hypotheses concerning the mechanisms of cohesion: The high pressure constraint has a destructuring effect on cellulose which reduces crystallinity, increases the equilibrium moisture content of the samples compared to the powder and does not affect the BET surface area. Temperature and moisture are important to give molecular motion to the cellulose chains (glass transition) which provides better particles deformation, thus better contact between the particles, and, at a molecular scale the establishment of a solid hydrogen bonding network, followed by possible recrystallization / co-crystallisation phenomenon. Higher temperature and a minimum moisture are necessary to cross the Tg but also to develop the hydrogen bonding network between adjacent particles. The temperature / moisture couple also has a negative effect called delamination. There are thus two contradictory effects of moisture: a beneficial effect that is conducting heat from the skin to the core of the material and bringing additional molecular motion (lower Tg), and a negative effect that is the accumulation of free water in the core layers which prevents the establishment of the hydrogen bonding network and builds up steam pressure which leads to the delamination of the samples. The mechanical properties observed would thus be the results of the balance between cohesion at the skin and steam pressure in the core layers for which an optimum probably exist around 2% moisture.

5. Finally, the flowability of α-cellulose was studied during an internship in Japan in a research team who specialized in the study of flowability of bulk wood and resin-impregnated wood, and there was no way to make the cellulose flow under the reference conditions of moisture (equilibrium with 60% RH). The increase of MC allowed to obtain data but they were not exploitable for calculation. These experiments confirmed that the problem of the flowability of such non melting polymers is a difficult issue that would require much more investment and high technology and thus no data concerning 3D-molding were presented in this thesis work.

IV Pressure and heat catalyzed esterification for the hydrophobation of compressed cellulose materials

Early in the research progress of project HYPMOBB was born the wish of working on increasing the water resistance of the specimens with the idea of grafting fatty side chains on the cellulose backbone (Peydecastaing et al. 2011) during the molding process, using heat and pressure as reaction catalysts. Preliminary results were performed on a bowl produced from miscanthus, which was re-processed after having coated the inside of the bowl with oleic acid. Steam was generated after this second processing and a quick water test was conducted, comparing one bowl that received oleic acid with another treated in the same conditions but without the fatty acid. The treated bowl did retain water for a few hours although the control swelled and let water leak after about one minute.

From this experiment, it was not clear what was responsible for the waterproofing because the basic adsorption of any fatty compounds on the surface of the object and in the porosity of the material would have been a satisfactory explanation. Nevertheless, a first set of trials were performed in order to test different fatty materials on cellulose, and the water drop angle was measured over time (kinetically).

Secondly, the grafting was more precisely studied on a case study and investigated with use of the analytics skills available in the LCA. This second part IV.2 was submitted for publication in Bioresources.

IV.1 Preliminary results, mapping of fatty compounds

Control conditions were defined for the evaluation of fatty compounds for hydrophobating cellulose samples, a control mass of 10 g was selected for a 50x50 mm plate shape; fatty compounds were added in proportions of 2, 5 and 10 %. Stearic acid, linoleic acid, sebacic acid, magnesium stearate, sodium stearate, highly oleic sunflower oil, and 95/5 mixtures of stearic acid and magnesium/sodium stearates were evaluated (Table IV - 1).

Table IV - 1: Summary of experimental conditions for fatty compounds evaluation for the hydrophobation of cellulose samples

Cellulose (g)	Additive	Additive addition (g)	Additive content (%)
10	none	0	0%
9.8	Stearic acid	0.2	2%
9.5	Stearic acid	0.5	5%
9	Stearic acid	1	10%
"	Mg stearate	"	"
"	Na stearate	"	"
"	Stear. ac./Mg - 95/5	"	"
"	Stear. ac./Na - 95/5	"	"
"	Sebacic acid	"	"
"	Linoleic acid	"	"
"	Sunflower oil	"	"

The 25 modalities (8 fatty compounds . 3 percentages + 1 control) were prepared, molded in 50x50mm squares in duplicate at 200 MPa, 150°C for 2 minutes, and equilibrated 2 weeks at 60% RH 25°C before testing. For each of the 2 plates per modality, 5

measurements were performed according to Figure IV - 1 in order to obtain satisfactory representativeness of the whole surface and counter heterogeneity. The 10 curves of the water drop penetration on the surface were not repeatable, but the representation of the 10 curves together allows comparison. The complete results are presented in Figure IV - 2, Figure IV - 3 and Figure IV - 4.



Figure IV - 1: 50x50 mm cellulose samples with fatty compound after 5 drop angle measurements

An adequate way of proceeding is to compare each modality of additivation with the control condition. There are three factors to consider in the analysis of the penetration curves:

- Initial drop angle
- Absorption length
- Curve's shape

The addition of stearic acid produced materials with initial angle significantly over the control and begun with a small slope indicating that after sitting the drop on the surface of the materials it stayed quite stable whatever the additive content. This last point was comparable to the control. The absorption length was about 50% higher for 2% stearic acid, about 100% higher for 5 % but about 50% lower for 10% showing a limit of the fatty compounds addition. It seemed that too much additive produced excessive porosity that made the drop penetrate the material quicker than the control, even if initial drop angle was higher.

The addition of magnesium stearate produced materials with a higher initial drop angle compared to the control (and comparable to stearic acid) but the shape of the curve was quite different as, during the first seconds of the test, the drop angle decreases brutally to retrieve values comparable with the control (especially 2 and 5%). The adsorption length was about 50% higher for 2% addition but comparable to the control for 5 and 10%.

The addition of sodium stearate was very different: the initial drop angle was comparable to the control but the penetration curve showed the same trend than magnesium stearate with a brutal decrease of the drop angle during the first seconds of the test. Consequently, the drop angle was rapidly lower and absorption time lower than the control. Possibly, the addition of sodium stearate was hindering the cohesion mechanism and generated porosity which provoked higher water sensitivity than without the additive. The effect of the counterion Mg or Na was very drastic. Some differences exist between these two, Mg is divalent although Na is monovalent, which modifies the counterion / sterate ratio, and the ionic strength. Mg is also known to have a more diffuse charge than Na which creates reactivity differences.

The addition of the 95/5 mixture of stearic acid and magnesium stearate had a behavior comparable to pure stearic acid modality at 2% but 5 and 10% additions were

producing very water sensitive materials with shorter absorption length and a brutal drop of the drop angle at the beginning of the curve. Quite consistent results were observed on the 95/5 mixture of stearic acid / sodium stearate with a rapid decrease of the drop angle at the beginning of the curve and much quicker penetration of the drop into the material.

The addition of sebacic, linoleic acid and sunflower oil produced materials with much higher water sensitivity, with initial drop angle comparable or higher than the control condition, but a very quick penetration of the drop in the material, which could be explained by a higher porosity of the material and which gave much lower absorption lengths. The stearic / linoleic acid showed drastic difference which could be explained by the U and linear conformation of these acids.

These experiments showed the possible interest of stearic acid (short and linear fatty acid) and magnesium stearate for hydrophobation of cellulose samples but the behavior of the different fatty compounds rose issues about whether the increased water resistance was produced by an effective grafting or a simple surface adsorption. Water properties were also sometimes decreased with the addition of several compounds which was concluded to be because of a lack of cohesion of the samples. Possibly the addition of these compounds prevented the establishment of the hydrogen bonding network but the reason for this and why these compounds remained unanswered.

In order to investigate about the possibility of having an esterification reaction occurring during the molding, a short fatty acid was selected (octanoïc acid) and a analytical protocol was set up.

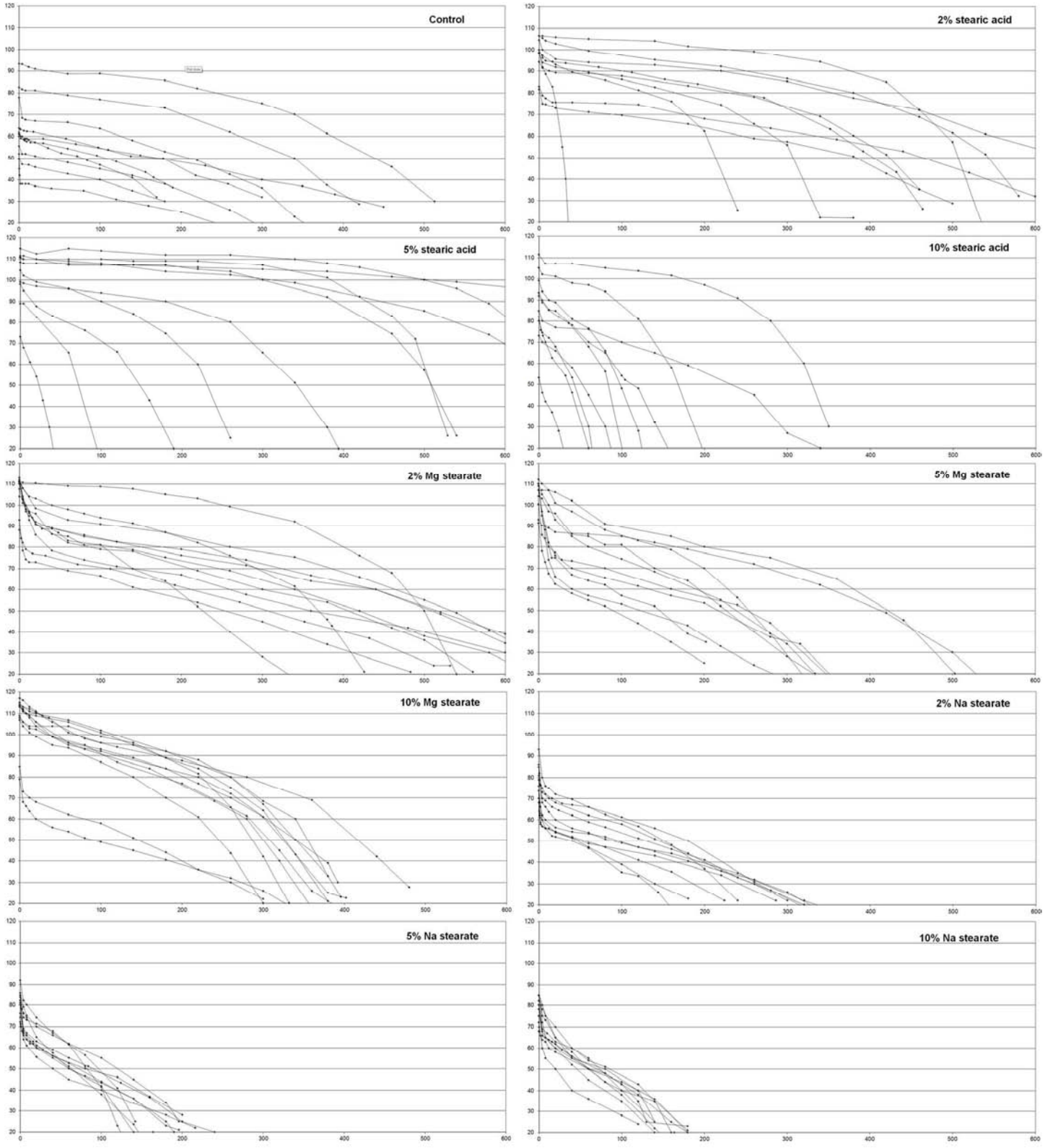

Figure IV - 2: (1/3)Evaluation of fatty compounds for hydrophobation, water drop penetration, x axis time (s), y axis drop angle (°)

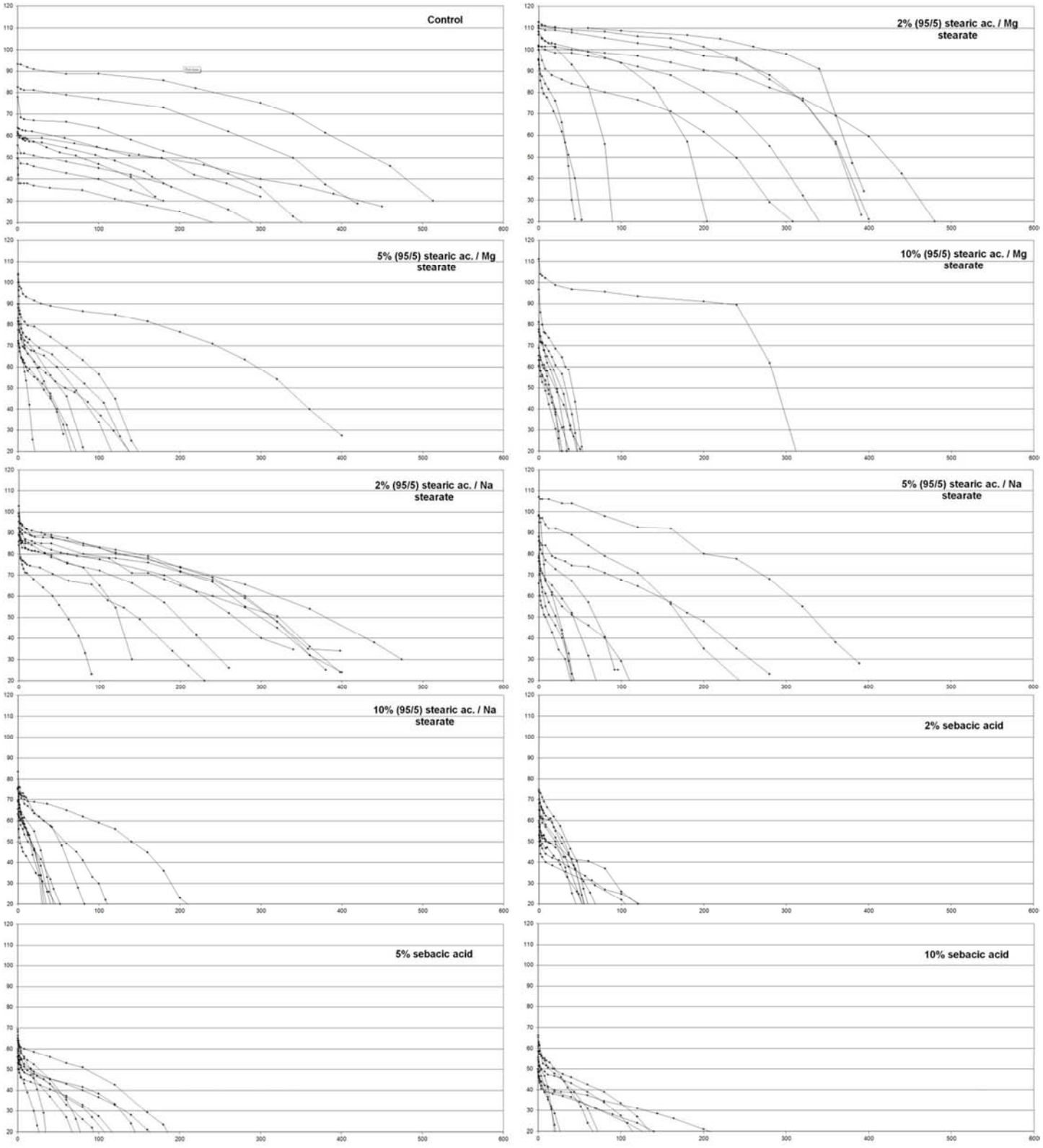

Figure IV - 3: (2/3)Evaluation of fatty compounds for hydrophobation, water drop penetration, x axis time (s), y axis drop angle (°)

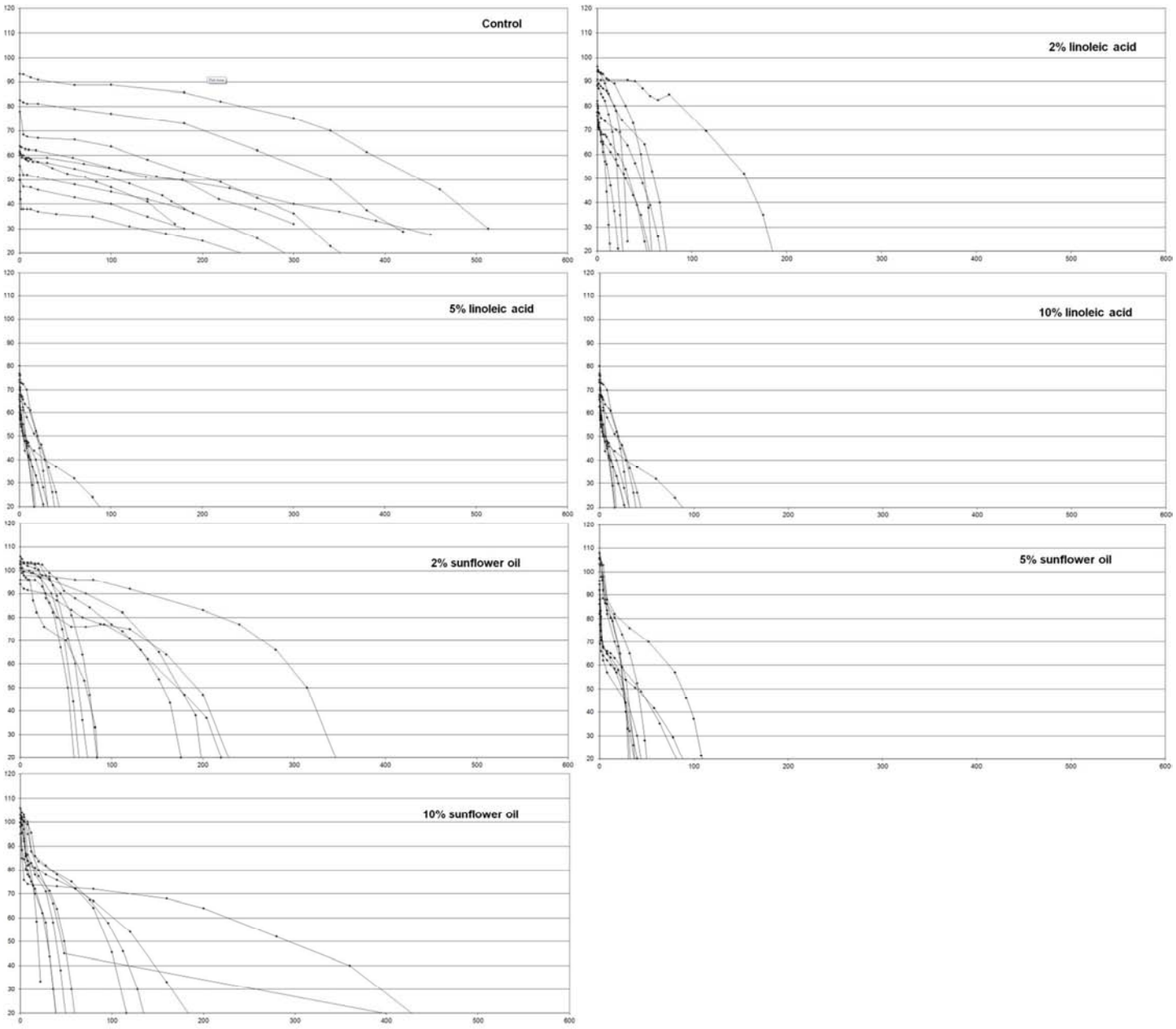

Figure IV - 4: (3/3) Evaluation of fatty compounds for hydrophobation, water drop penetration, x axis time (s), y axis drop angle (°)

IV.2 High-pressure driven solvent-free heterogeneous phase esterification of cellulose

Classically, the esterification of cellulose required solvents, involving reactors, solvent recycling, and phase separation, all of which are material- and time-consuming processes. A different approach was studied in this part: the use of high pressure at elevated temperatures as the contact method and energy supply to initiate the reaction.

IV.2.A List of Experiments

Eleven different experimental conditions were tested to evaluate the possibility of grafting octanoïc acid (OA) and anhydride octanoïc (OAn) onto cellulose and miscanthus under heterogeneous phase conditions at high pressure.

The first experiment involved standard compressed alpha cellulose, without additives, and was coded "Alpha_c." The second made use of standard compressed miscanthus powder, without additives, and was coded "Mis."

Six pretreatment conditions were used to test the efficacy of grafting OA onto cellulose. An emulsion pretreatment using OA, water, and cellulose, as described in the Experimental section, was coded "Emul." Three different solvent exchange pretreatments were implemented. The first solvent exchange, as described in the Experimental section, involved washing with OA and was coded "OA_exch." A variant of this procedure, in which the pH of the water exchange was adjusted to 2 (Pantze et al. 2007) was coded "OA_exch_pH." A second variant was coded "OA_exch_pH_6," in which cellulose was left to stir in OA for 6 h at the end of the contact step.

A high-pressure homogenizer pretreatment in water, followed by a solvent exchange step, was coded "OA_homo_exch." Another high-pressure homogenizer pretreatment, in which water was replaced by OA in the apparatus, was coded "OA_homo." The material did not show the same gel-like appearance in OA as it did in water. To graft OAn onto cellulose, a solvent exchange pretreatment was conducted with water, solvent, and OA, then one additional rinsing with OAn; this method was coded "OAn_exch." Grafting of OA onto miscanthus was performed using a high-pressure homogenizer pretreatment; 20 g of miscanthus powder was introduced into the high-pressure homogenizer, along with 2 L of OA, and this procedure was coded "Mis_OA_homo." Grafting of OAn onto miscanthus involved a high-pressure homogenizer pretreatment, in the same way as that of the "Mis_OA_homo" experiment, with an additional filtering and suspension in OAn; this experiment was coded "Mis_OAn_homo."

Table IV - 2: Summary of results, investigation of the esterification reaction during molding

Experiment						Results									
				Molding		Drop angle		IR peak 1724 cm^{-1}	GR		DS	Bending properties			
												Modulus		Strength	
Experiment code	Material	Pretreatment	Graft	Temp	Time	Drop angle	Absorb. time (s)		Mean	St. dev.	Mean	Mean	St. dev.	Mean	St. dev.
				°C	h	°	s		($mEq_{OA}.kg^{-1}$)			MPa			
Alpha_c	α Cellulose	none	none	none		N/A		-	0.03	0.05	5.3E-06	N/A			
				165	2	49	7	-	0.02	0.02	2.7E-06	4387	539	35.3	3.8
				190	1	49	5	-	0.03	0.04	5.1E-06	4757	1484	33.1	11.3
Emul	α Cellulose	OA-water emulsion	OA	none		N/A		-	2.7	0.2	4.3E-04	N/A			
				165	2	57	12	-	5.1	0.4	8.3E-04	1489	320	6.7	1.2
				190	1	52	79	-	12.3	0.7	2.0E-03	677	436	3.1	1.6
OA_exch	α Cellulose	Solvent exchange	OA	none		N/A		-	4.2	0.1	6.8E-04	N/A			
				165	2	50	16	+	48	3	7.8E-03	3742	600	17.6	0.4
				190	1	50	18	+	34	2	5.5E-03	3033	605	11.7	0.5
OA_exch_pH	α Cellulose	Solvent exchange at pH2 (water step)	OA	none		N/A		-	5.0	0.3	8.1E-04	N/A			
				165	2	54	74	+	125	36	2.0E-02	3025	112	19.8	4.1
				190	1	48	5	+	78	3	1.3E-02	3448	86	22.7	1.0
OA_exch_pH_6	α Cellulose	Solvent exchange at pH2 (water) + 6h in OA	OA	none		N/A		-	3.0	0.2	4.9E-04	N/A			
				165	2	64	12	+	170	10	2.8E-02	2707	854	19.2	2.3
				190	1	67	39	+	171	13	2.8E-02	2781	863	21.5	6.3
OAn_exch	α Cellulose	Solvent exchange	OAn	none		N/A		+	274	11	4.4E-02	N/A			
				165	2	77	208	+	266	5	4.3E-02	2724	118	16.7	1.7
				190	1	77	492	+	297	26	4.8E-02	1918	100	11.5	1.4
OA_homo	α Cellulose	HP-Homogeneizer (in OA)	OA	none		N/A		-	1.0	0.5	1.6E-04	N/A			
				165	2	58	65	-	16.0	0.4	2.6E-03	3510	1182	22.2	4.0
				190	1	41	17	-	12.8	0.7	2.1E-03	3108	395	20.5	6.2
OA_homo_exch	α Cellulose	HP-Homogen. (in water) + Solvent exchange	OA	none		N/A		-	7.2	0.2	1.2E-03	N/A			
				165	2	63	102	+	207	10	3.4E-02	2622	255	12.5	1.2
				190	1	73	88	+	241	13	3.9E-02	2259	519	10.8	2.8
Mis	Miscanthus	none	none	none		N/A		+	3.9	0.4	N/A	N/A			
				165	2	81	5	ND	2.18	0.03	N/A	4287	449	28.6	1.8
				190	1	78	17	ND	4.41	0.07	N/A	3537	370	26.1	2.6
Mis_OA_homo	Miscanthus	HP-Homogen. (in OA)	OA	none		N/A		ND	1.6	0.1	N/A	N/A			
				165	2	70	11	ND	16	6	N/A	4678	493	27.5	5.0
				190	1	72	2	ND	24	3	N/A	4516	385	29.0	6.0
Mis_OAn_homo	Miscanthus	HP-Homogen. (in OA) + OAn suspension	OAn	none		N/A		ND	21.9	0.3	N/A	N/A			
				165	2	83	153	ND	31.6	0.6	N/A	3736	339	20.4	2.5
				190	1	81	106	ND	39	3	N/A	3978	1106	15.0	1.5

ND: non determined, N/A: Not applicable

IV.2.B Results

Table IV - 2 summarizes the results of all the experiments. Each line in the first column contains three lines as sub-elements; the first line corresponds to the pretreated material without the molding step, while the second and third lines describe the compression molding experiments at 165 °C for 2 h and 190 °C for 1 h, respectively.

The IR peaks of ester bands were detected, and the DS was measured according to the technique of Peydecastaing et al. (2009). This technique confirmed the esterification reaction with the unique conditions of an unstirred, solvent-free solid-liquid heterogeneous phase medium at high pressure and elevated temperature.

A GR value greater than 60 mEq kg^{-1} (i.e., a DS value greater than 0.01) was measured for a group of cellulose experiments, including OAn_exch, OA_homo_exch, OA_exch_pH_6, and OA_exch_pH, in decreasing GR order. The other experiments, including every experiment performed on miscanthus, obtained a lower GR value. The GR results obtained in OA_homo and Mis_OA_homo were quite low and comparable.

The detection limit of the IR setup was between GR values of 16 and 34 mEq kg^{-1} (i.e., a DS value between $2.6 * 10^{-3}$ and $5.5 * 10^{-3}$), as seen in the results of OA_homo_165_2h (GR= 16 mEq kg^{-1} with no ester peak) and OA_exch_190_1h (GR= 34 mEq kg^{-1} with an ester peak detected).

The two pressing conditions, 190 °C for 1h or 165 °C for 2 h, did not influence the results, and no significant difference was observed between these two conditions.

Solvent exchange was the key pretreatment that affected the performance of the reaction. Without it, no reaction was significantly observed (based on preliminary experiments; unreported data).

The use of OAn in "OAn_exch" produced the best GR values (266 and 297 mEq kg^{-1} under the two different pressing conditions), which were tremendously higher than the GR values of 48 and 34 mEq kg^{-1} obtained with OA under the same conditions (OA_exch). With OA, only the combination of the high-pressure homogenizer and solvent exchange pretreatments permitted a GR value close to those obtained with OAn (GR values of 207 and 241 mEq kg^{-1} were obtained in the OA_homo_exch experiment).

On the contrary, the high-pressure homogenizer by itself did not make much difference, considering the low GR value obtained in the OA_homo experiment. The emulsion pretreatment was very unsuccessful and produced a low GR value and poor mechanical properties. The adjustment of pH to 2 during the water step of the solvent exchange was beneficial and facilitated a higher GR value (OA_exch_pH), as did the 6-h stirring step with OA in a similar experiment (OA_exch_pH_6); the explanation for this phenomenon would require further investigation, as these conditions were quite different from those of the work reported by Pantze et al. (2007).

Every pretreated powder that was not compression-molded (deemed the "standards") had a very low GR value, which confirmed that the reaction occurred during the molding step. The use of OAn was the only exception (producing a GR value of 274 mEq kg^{-1}), which showed that the reaction did not need the molding step to occur and confirmed the much higher reactivity of OAn over OA. The standard samples were stored for about 1 week before analysis in a closed container (at room temperature), which, in the case of the OAn_exch experiment, allowed the reaction to occur.

Mechanical results showed that all experiments on cellulose produced lower bending moduli and strength than the non-grafted standard (Alpha_c). For miscanthus, the mechanical properties of the compressed specimens were comparable between the standards and the Mis_OA_homo results, but lower properties were measured in the Mis_OAn_homo experiment.

IV.2.C Discussion

A satisfactory correlation ($R^2 = 0.92$) was observed between the water drop angle and the GR value for cellulose experiments with a GR value greater than 60 mEq kg^{-1} (i.e., a DS value greater than 0.01), as seen in Figure IV - 5. The extrapolation of the linear regression curve indicated that hydrophobicity (evidenced by an angle > 90°) would have been obtained at a GR value of 370 mEq kg^{-1} (DS value of $6 * 10^{-2}$).

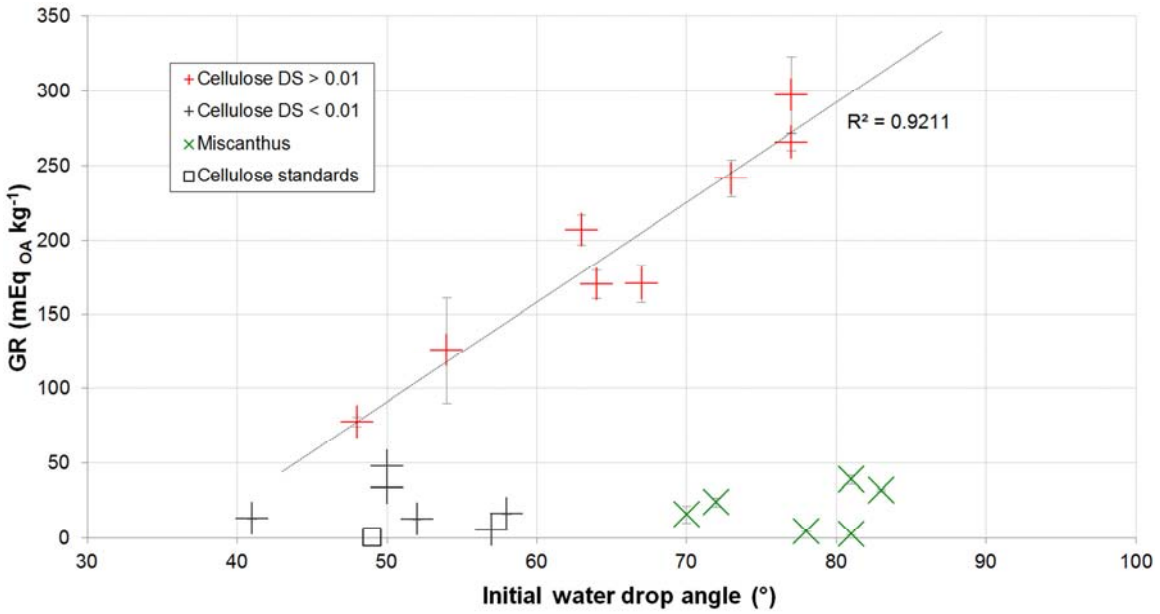

Figure IV - 5: Correlation between GR value and initial water drop angle of recompressed specimens

For comparison, Peydecastaing et al. (2011) performed the esterification of C18 and C2 fatty acids in a reactor with a solvent medium and observed that a DS value of $5 * 10^{-3}$ (C18 basis) was sufficient to induce hydrophobicity (after 60 s). A difference in chain length, the presence of two types of grafts on the chain, the time of measurements, and the porosity of the recompressed specimens for the water drop experiments are some possible explanations as to the differences observed compared to the results of Peydecastaing et al. (2011). Also, changes in the DP of cellulose after pretreatment and molding would have been an interesting parameter to study for a better understanding of the relationship between macroscopic water properties and the GR value of the specimens.

In the miscanthus experiments, quite low GR values were observed, and the cellulose-miscanthus equivalent experiments produced comparable results (OA_homo: 16 and 13 mEq kg^{-1}; Mis_OA_homo: 16 and 24 mEq kg^{-1}), which was surprising considering the higher reactivity of lignin and hemicellulose than cellulose (Hon 1995). The other experiment on miscanthus added an OAn suspension step, which did improve the grafting yield significantly (GR values of 32 and 39 mEq kg^{-1}), but the reaction also occurred on the standard (non-compressed) specimen just as it did on cellulose. Due to the quite drastic conditions of pressing, the probability of degrading hemicellulose and lignin was high (Takahashi et al. 2010). There was thus a possibility of consuming OA and OAn in the esterification reaction of hemicellulose and lignin before these parts were further degraded, made soluble, and rinsed out during the washing step. The only experiments under the same conditions with cellulose and miscanthus are OA_homo and Mis_OA_homo, which obtained comparable but low GR values. The water-ethanol-OA-OAn solvent exchange (tested on cellulose OAn_exch) was not tested on Miscanthus, thus the comparison between cellulose and miscanthus in terms of reactivity cannot be established. Also an experiment comparable

to Mis_OAn_homo on cellulose would have permitted to impute more certainly to the solvent exchange the majority of the effect on increasing the grafting.

A comparison of the absorption times was made in Figure IV - 6, confirming that higher GR values were correlated with a longer absorption time.

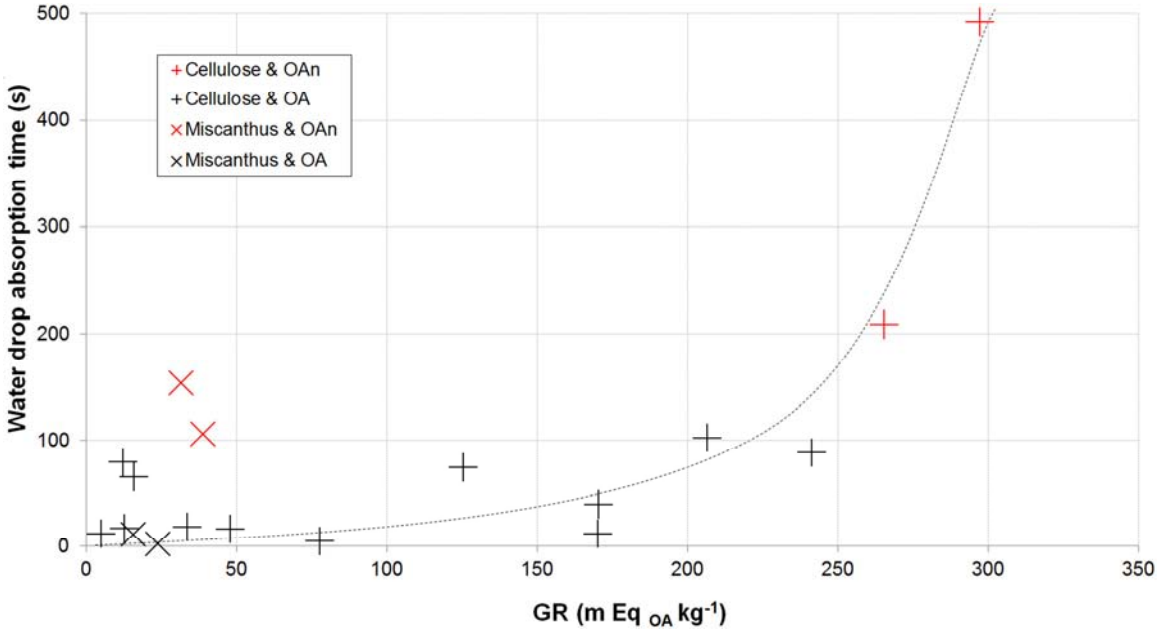

Figure IV - 6: Starting material, grafted material, and comparison of the water drop absorption time on recompressed specimens.

However, there was no correlation between the initial drop angle and absorption time (Table IV - 2) although these two parameters are supposed to describe the hydrophobicity of the material. In other words, specimens with long absorption times could nevertheless have quite low initial drop angle values associated with low GR values. Thus, it seems that the nature of the reactant actually had a high impact; the four experiments conducted with OAn on cellulose and miscanthus (the red points in Figure IV - 6) produced longer absorption times than any other OA experiment.

From extrapolation of the data in Figure IV - 6, a limit would appear (infinite absorption time, or hydrophobicity) for GR values around 350 mEq kg^{-1}, which would be consistent with the value obtained upon extrapolation in Figure IV - 5 (370 mEq kg^{-1}). A trend is observable from the same group of data on the mechanical properties with DS values greater than 0.01 displayed in Figure IV - 7 (correlation between the bending modulus and the GR value).

Through this correlation, it was concluded that the more the material is grafted, the lower the modulus. A similar trend existed for the bending strength at break (Table IV - 2); an explanation for this phenomenon probably lies in the consideration that the side chains grafted on the cellulose backbone prevented the establishment of a strong hydrogen bond network (Pintiaux et al. 2013). Therefore, it was concluded that bulk esterification under high-pressure conditions required a compromise between water properties and mechanical properties. A better approach and a better use of this technique would consist of producing specimens with two layers, a core of pure α-cellulose powder (or other plant material) covered by a layer of pretreated powder compressed together. Such a biocomposite should be capable of high mechanical properties, with a hydrophobic skin to protect it against water.

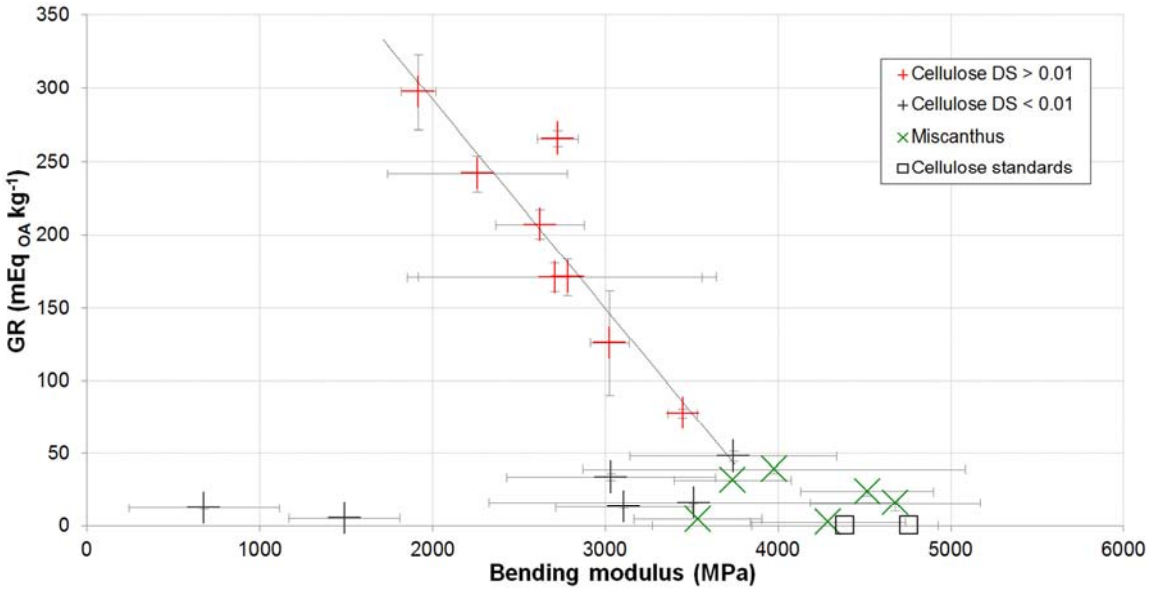

Figure IV - 7: The correlation between GR value and the bending modulus of compressed specimens.

Conclusions

1. High-pressure compression molding was successfully used to perform the esterification of octanoïc acid on commercial α-cellulose powder. However, pretreatment of the powder was necessary to improve its reactivity and obtain a significant grafting yield.

2. The use of octanoïc anhydride instead of octanoïc acid produced higher grafting yields. A direct prospect of this study would be the combination of the high-pressure homogenizer and solvent exchange pretreatments applied to the reaction with octanoïc anhydride, which should provide higher grafting yields.

3. Water properties were measured on ground and recompressed specimens in order to eliminate the possible effect of adsorbed but non grafted fatty compounds on cellulose. The water resistance should be tested directly on the washed compressed specimens first, then again without the washing step. The good surface effect that would be imparted by the thermo-compressed specimens combined with fatty acids adsorbed onto the α-cellulose powder would probably increase the water resistance. Investigations are also needed in order to explain the low grafting yields obtained with miscanthus.

4. The decrease of the mechanical properties was undoubtedly correlated to the grafting yield, which implied that prospective water-resistant, compression-molded α-cellulose specimens would necessarily have weak mechanical properties. Considering a "sandwich" structure, with a skin of pretreated materials covering a core of non-treated powder, would be a natural continuation of this present work.

5. Further study would be needed to understand the water properties of the specimens. For instance, investigation into the dynamic vapor sorption properties of the materials, the measurements of the degree of polymerization and its influence on the water properties, and establishment of the recovery yield would be interesting. The influence of the thermo-compression parameters would also need to be investigated.

V The processing of native plant materials

One of the primary objectives of this thesis was to evaluate the possibility for compaction molding to produce objects from raw plant materials as opposed to refined materials like cellulose. Following the surprising results obtained on cellulose, many experiments were performed around the understanding of the parameters effect and mechanisms of cohesion. The best properties obtained were a bending strength of 70 MPa and a tensile strength of 31 MPa, associated to moduli of 8 and 2 GPa in bending and tensile respectively.

After these quite high mechanical properties, the burning question was about the influence of the chemical composition and physical properties of the starting materials on the properties of the molded specimens. According to the literature (Chapter I) the presence of lignin, hemicelluloses, proteins and polyphenols in the starting material had a great chance to impact the bonding ability and flowability.

23 different materials were thus collected from different other projects of the laboratory and kindly provided by colleagues. The 23 plant materials were first ground to smaller particles (2 mm screen) because some materials' particle size would not be compatible with the molds. It also permitted to obtain materials of comparable particle size and not generate too much effect from this parameter. Physical characteristics and chemical composition were measured on the starting plant materials (results available in Table V - 1), and specimens were processed in the same conditions in order to evaluate the properties of the corresponding materials. At first, flow tests were performed, and compaction molding was performed on 50 x 50 mm squares, and finally dog-bone specimens and 45 x 10 mm DMA specimens.

V.1 Physico-chemical analyses of the native plant materials

At first, the physical analyses were run on the 23 plant materials. The apparent (tapped) density, the particle size distribution (in mm, < 0.12, [0.12 – 0.25[, [0.25 – 0.5[, [0.5 – 0.8[, [0.8 – 1[, [1 – 1.25[, [1.25 – 1.6[, [1.6 – 2[, > 2 mm), and the form factor distribution (=1,]1 – 2],]2 – 3],]3 – 5],]5 – 10], >10) were analyzed.

The apparent density of two materials (Carded hemp and Cellulose wadding) was very different from the rest of the specimens. Carded hemp already had a density lower than average but the grinding treatment produced an even more fluffy material as well as upon the grinding of cellulose wadding. As a consequence, the particle size analysis of these two specimens was biased because the particles could not be separated one from the others and the form factor distribution could not be measured for the same reason.

Olive kernels flour is an industrial micronized flour which thus had a very marginal particle size distribution. For this reason, the form factor distribution could not be measured because of the small size of the particles.

As far as cellulose is concerned, the form factor distribution could be analyzed for the same reason as Olive kernels flour and the particle size was set to 100% < 0.12 mm because of the SEM pictures of the powder (Chapter III, Figure III - 26).

Secondly, the chemical composition of these plant materials was studied: moisture, ashes, lipids, hemicelluloses, cellulose, lignin, proteins and polyphenols contents were measured. The complete results are available in Table V - 1. Some remarkable elements have been highlighted thereafter:

The ashes content of cellulose wadding was the highest (16%) probably because of the additives and inks used onto paper. High values were also obtained for wheat straws (7 to 10%) probably because of the silica content. The value of the extruded wheat with NaOH was also marked by this treatment and a high value of 11 % was measured.

Table V - 1: Physico-chemical analyses of the native plant materials

		Moisture content		Ashes content		Tapped density		Particle size distribution (%)									Form factor distribution %												Lipid content		ADF NDF - Fiber content analysis (%)								Protein content		Total polyphenols	
		(%)		(%)		(g/cm^3)		>2	1.6 - 2	1.25 - 1.6	1 - 1.25	0.8 - 1	0.5 - 0.8	0.25 - 0.5	0.12 - 0.25	<0.12	=1		1-2		2-3		3-5		5-10		>10		(%)		Cellulose		Hemi celluloses		Lignin		NDF		(%)		(mg_{eqGA}/g)	
		Mean	St. dev.	Mean	St. dev.	Mean	St. dev.	Mean									Mean	St. dev.	Mean	St. dev.	Mean	St. dev.	Mean	St. dev.	Mean	St. dev.	Mean	St. dev.	Mean	St. dev.	Mean	St. dev.	Mean	St. dev.	Mean	St. dev.	Mean	St. dev.	Mean	St. dev.	Mean	St. dev.
Compaction-molding set	AC	8	0.01	0	0	0.30	0.003	0	0	0	0	0	0	0	0	100	-	-	-	-	-	-	-	-	-	-	-	-	0	0	96	0	4	0	0	0	0	0	0	0	0	0
	WS2	8.7	0.043	7.1	0.135	0.16	0.002	0	0.1	0.1	20	7.9	31	29	8.8	2.5	30	5.115	23	0.693	24	2.514	18	1.89	4.7	0.233	0.1	0.135	0.2	0.06	41	0.1	29	0.9	11	0.2	19	2.3	0.05	3.4	0.128
	WS3	8	0.011	8.4	0.124	0.16	0.002	0	0.2	1	18	8	18	26	20	9.6	45	2.157	23	1.072	19	2.127	10	1.285	2.9	0.169	0.1	0.068	0.3	0.07	43	0.2	29	0.1	11	0.3	17	2.3	0.05	3.4	0.04
	WE1	10	1.215	11	0.07	0.16	0.007	0.1	0.4	1.4	19	9	19	30	14	7.1	41	0.587	23	0.612	23	0.72	11	1.06	2.8	0.243	0	0.075	0.3	0.04	41	0.1	24	0.6	7.9	0.2	28	3.4	0.06	8.1	0.303
	WE2	8.7	0.045	8.1	0.099	0.18	0.005	0.1	0.2	1.1	14	5.7	14	22	14	29	52	1.525	25	0.718	18	0.601	4.9	0.682	0.6	0.11	0	0	0.3	0.03	40	0.3	34	0.5	7.1	0.2	20	3.6	0.04	4.6	0.248
	WE3	8.9	0.044	8	0.173	0.13	0.005	0.4	0.2	0.7	21	6.3	13	23	18	17	50	2.21	21	1.735	19	0.879	7.8	2.213	1.8	0.57	0	0.036	0.3	0.06	41	0.4	32	0.5	8.5	0.2	19	2.5	0.06	4.7	0.258
	Mis	8	0.047	1.8	0.022	0.20	0.001	0.9	1.1	2.3	15	6.6	20	37	11	5.9	50	6.023	18	1.726	16	0.746	11	4.296	4.6	2.595	0.1	0.1	0.1	0.006	52	0.8	25	1	15	1.1	7.7	0.2	0.01	3.1	0.175
	Che	8.5	0.134	2.1	0.022	0.19	0.004	0.2	0.7	4.3	29	14	21	18	7.4	6.7	54	2.93	24	2.605	17	1.039	4.6	1.014	0.4	0.143	0	0.012	0	0.01	51	3.14	18	0.49	18	2.79	13	0.3	0.01	3.2	0.196
	BCa	8	0.665	1.7	0.256	0.16	0.005	0.1	0.3	1	2.1	6.2	24	37	14	16	50	3.354	30	1.872	14	0.978	4.4	0.819	1	0.351	0	0.015	4.9	0.79	47	1.5	29	0.4	13	1.9	10	1.3	0.06	3.8	0.161
	Bagv	9	0.073	8.1	0.516	0.28	0.001	0.1	0.2	0.5	9.9	2.6	9.1	43	26	9.5	28	3.521	21	2.442	22	1.796	19	0.858	9.9	2.671	0.5	0.226	0.5	0.01	41	-	24	-	11	-	24	2.1	0.44	2.8	0.084
	Pin	7.1	0.153	3.3	0.278	0.27	0.008	0.3	0.4	0.7	15	3.7	9.7	37	19	14	54	1.533	18	1.199	17	0.269	8	0.473	2.6	0.538	0.1	0.015	0.2	0.01	44	-	27	-	17	-	12	2.7	0.11	2.5	0.104
	FNO	7.5	0.028	1.7	0.003	0.63	0.002	0.7	1.5	1.7	8.1	1	1	4	6.1	76	-	-	-	-	-	-	-	-	-	-	-	-	3.5	0.38	51	0.7	22	0.6	17	0.7	9.6	1.2	0.01	7.7	0.363
	Bee	9.5	0.031	0.5	0.023	0.30	0.006	0.2	1.5	6.7	21	14	22	20	9.1	5.6	36	9.351	14	2.581	21	3.769	21	4.769	7.3	1.875	0	0.052	0.4	-	57	-	22	-	20	-	2	1	-	1.4	0.078
	Euc	9.3	0.06	0.5	0.042	0.13	0.002	0	0.2	1	25	10	24	24	8.9	6.4	50	2.48	21	0.504	19	0.734	8.6	1.728	1.2	0.24	0	0.017	0.5	0.31	60	-	11	-	25	-	4	0.6	0.01	12	0.097
	Vin	9.8	0.047	2.9	0.077	0.35	0.007	0.3	1.9	5.6	6.5	10	20	31	12	12	46	2.039	26	2.645	17	1.094	8.6	0.656	2.6	0.808	0.1	0.04	0.7	0.23	43	-	26	-	17	-	14	3.6	0.06	12	0.358
	Pop	10	0.06	6.7	1.671	0.28	0.022	0.2	0.4	2.1	18	5	13	33	16	13	55	0.308	24	1.782	15	0.57	5.2	1.14	1.4	0.731	0	0.01	2.6	0.2	55	0.7	13	0.9	13	0.3	20	2.7	0.13	9.7	0.438
	CWa	5	0.318	16	0.81	0.03	0.001	74	26	0	0	0	0	0	0	0	-	-	-	-	-	-	-	-	-	-	-	-	0.3	0.09	53	0.2	15	0.3	11	0.3	22	0.1	0	1.4	0.338
	Car	7.1	0.053	2.9	0.052	0.05	0.002	79	21	0	0	0	0	0	0	0	-	-	-	-	-	-	-	-	-	-	-	-	0.3	0.02	76	0.3	9.4	0.5	3.1	0.1	11	0.3	0	1.4	0.196
	WS1	8.7	0.014	9.9	0.089	0.17	0.002	0	0.2	0.5	19	0.6	0.4	23	33	23	65	1.292	19	1.161	13	0.823	3.1	0.683	0.5	0.05	0	0	0.5	0.037	38	0.1	27	0.74	10	0.4	25	2.5	0.05	5.3	0.492
	BS	9.3	0.034	5	0.146	0.12	0.001	0	0.5	2.5	28	16	17	23	8.9	3.7	37	2.593	25	0.777	23	1.593	13	0.699	3.4	0.517	0.1	0.046	0.2	0.06	40	-	26	-	18	-	16	3.2	0.09	3.8	0.026
	SBP	9.7	0.028	7.1	0.314	0.73	0.004	0.1	0.5	6.9	19	15	23	19	8.2	7.7	54	6.783	37	5.641	8.3	1.149	0.6	0.072	0.1	0.081	0	0	0.5	-	21	-	23	-	4.8	-	51	7.9	-	1.3	0.125
	SCR	9	0.039	3.7	0.1	0.09	0.001	0.5	2.1	3.6	15	5.1	17	34	14	9.8	51	1.18	32	1.034	14	0.715	2.2	0.15	0.3	0.11	0	0	0.1	0.02	39	-	36	-	4	-	21	3.3	-	4.9	0.113
	SSC	9.2	0.022	6.1	0.048	0.63	0.002	0.2	0.3	0.9	8.1	5.6	23	33	16	13	58	5.052	26	3.084	14	1.483	2.4	0.677	0.1	0.038	0	0	2.6	0.23	28	1.5	11	3.8	7.4	0.4	54	34	0.18	17	0.719
	Cof	10	0.047	1.3	0.025	0.45	0.002	0.1	0.1	0.2	8.6	0.4	7.8	72	7	4.1	39	1.868	49	1.09	11	0.769	0.5	0.058	0	0.012	0	0	19	1.81	25	0.5	33	0.4	16	0.6	26	14	0.07	5.6	0.106

The lipid content was somehow binary: Most of the materials had very low lipid content, inferior to 0.5 %. Then, poplar bark and Sunflower seed cake had a value of 2.6 %, Olive kernels flour had a value of 3.5 %, Sugarcane bagasse 4.9 % and the maximum value was reached with Coffee waste (19 %).

The protein content was overall low, except for Sugar beet pulp (7.9 %), Coffee waste (14 %) and Sunflower seed cake (34 %).

V.2 Evaluation of the flowability of the different materials

The idea of trying to improve the flowability of cellulose appeared early in the project, and tests were performed with addition of magnesium stearate in cellulose (2%) which conducted to the destruction of a dog-bone mold. After the experiments in Nagoya, where it was impossible to run flow tests correctly on cellulose (Chapter III part 8), it seemed too much investment (on time and equipment) to try to run true viscosity tests. Nevertheless an empiric scale was desirable (and necessary) to evaluate the flowability and at least obtain a comparison of the different materials between them in order to predict and avoid the damages to the molds. Every 23 plant materials and cellulose were extruded through a (4,10) die at 175°C and 3 bar/s of pressure increase using the transfer molding equipment designed in Toulouse.

The value at which the material started to flow was retrieved from these experiments that were run in triplicates. The experiment was stopped at 140 bar of hydraulic pressure which corresponded to 500 MPa in the compression chamber for minimizing damages on the equipment. Results are presented in Table V - 2, sorted by decreasing flowability.

Table V - 2: Flow tests results for the 24 tested materials at 175°C through a (4,10) die

Plant material	Code	Hydraulic pressure at flow		Chamber pressure (MPa)
		mean (bar)	st. dev (bar)	
Coffee waste	Cof	26	0.7	94
Beet pulp	SBP	45	0.7	162
Sunflower seed cake	SSC	51	14.1	184
Barley straw	BS	54	5.5	194
Sweet maize residue	SCR	57	15.7	205
Extruded wheat straw	WE1	65	0	234
Poplar bark	Pop	64	0	230
Wheat straw <0.5 mm	WS1	70	3.1	252
Vine prunnings	Vin	72	0.7	259
Wheat straw [0.5,1[mm	WS2	73	0.6	263
Extruded wheat straw H_20 100	WE3	78	4.2	281
Wheat straw >1 mm	WS3	86	3.5	310
Eucalyptus wood	Euc	88	3.5	317
Extruded wheat straw H_20 70	WE2	90	2.8	324
Sugarcane bagasse	Bca	101	0.7	364
Chenevotte	Che	105	20.5	378
Pinsotte	Pin	109	1.4	393
Olive kernels flour	FNO	110	8.7	396
Agave bagasse	Bag	110	6.4	396
Miscanthus	Mis	120	n/a	432
Beech wood	Bee	123	0	443
Carded hemp	Car	130	6.6	468
Cellulose wadding	CWa	no	n/a	no
α-Cellulose	AC	no	n/a	no

The pressure needed to make the material flow permitted to initiate a ranking of flowability between the different materials, the lower the pressure of extrusion (flow) the higher the flowability. Thus, during the molding of dog-bone specimens, in order to prevent damages to the mold, the materials will be tested by increased flowability order starting with

the material with the poorest flowability and so on. For the realization of 3D molding, this flowability ranking is of high interest because it indicates what materials will preferrably flow and permit to mold 3D shapes, or can orientate towards mixing a poor flowing material with another easy flowing one. Some tests were performed following this idea and are presented in the perspectives of this work.

α-cellulose and cellulose wadding were the only two that did not flow at all. This confirmed the poor flowability of cellulose and the benefits of other components in increasing the flowability, at least in these conditions of moisture and temperature. The correlation between the cellulose content and extrusion pressure was drawn (Figure V - 1) which shows that a link exist between these two parameters but also that the correlation is not perfect and could be further refined by adding other composition factors. For instance, SBP and SSC are the two matters with the highest NDF extractives value, Euc has the highest lignin content and Car was defibrated which could lower its flowability.

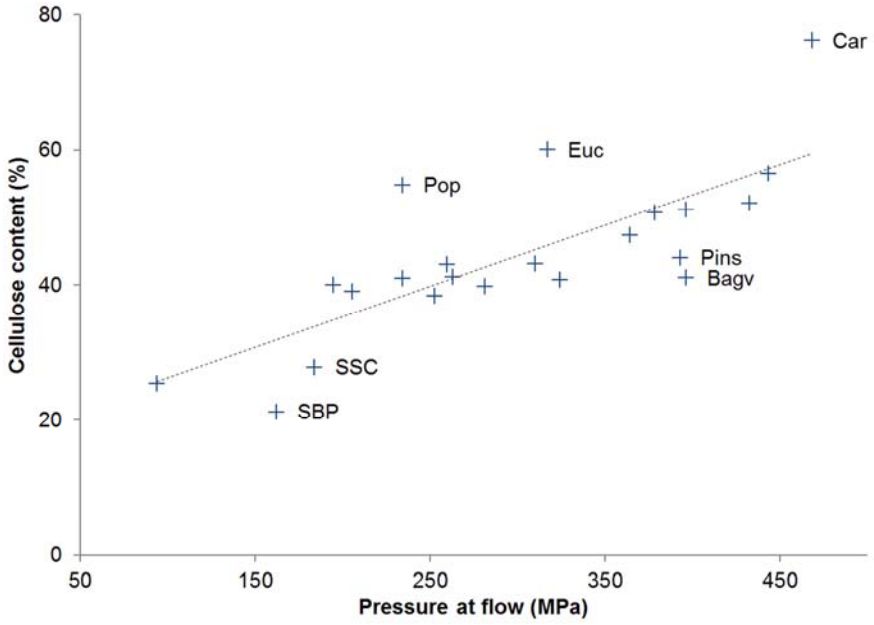

Figure V - 1: Correlation between cellulose content and extrusion pressure

The extrudates were very much influenced by the material's origin. Most of them were not continuous, and very fragile. It seems the easy flowing materials had extrudates with better cohesion and continuity. The extrudate continuity was much influenced by the pressurization speed during the flow test. This parameter was unfortunately not further studied.

Nice patterns of orientated fibers following the material's flow could be observed on materials left in the compression chamber at the end of a test (Figure V - 2). A close look at the extrusion sprue left in the die indicated that the discontinuity observed on the extrudates was initiated right at the beginning of the die when materials was leaving the compression chamber to enter the die. The high shear taking place in this area probably induces the discontinuous extrusion, what could be a subject of further studies.

At the end of these tests, the punch and dies of the equipment were severely damaged and had to be replaced which shows how much work is still needed on the technological part…



Figure V - 2: Orientation of fibers in the direction of flow upon entering the die during flow test

V.3 The influence of the volume/surface ratio

V.3.A 50 x 50 mm square molding as a preliminary study

At first, the square mold was used because it is the most versatile tool, which suffers less from blockades than the highly justified and thus fragile dog-bone mold. The 23 materials and cellulose were first tested in the reference conditions for cellulose, i.e. at 175°C and moisture equilibrated to 60% RH. Other parameters were: 200 MPa of molding pressure (maximum), 50 bar/s of pressure increase, 30 seconds of molding time. Three 50 x 50 mm squares were first molded.

Surprisingly, although these conditions produced sound dog-bone specimens, i.e. without cracks or being delaminated, as well as perfect 50 x 50 mm squares for cellulose, the molding of a many other materials led to delamination. Only Poplar bark, Vine prunings, Beech wood, Pinsotte and Agave bagasse produced satisfactory specimens. All the others were more or less delaminated. The molding results were collected in Table V - 3. It was difficult to quantify delamination, even though it was certain that different degree of damages existed, from slight and discrete cracks to the complete opening of the specimen which usually let steam audibly escape from the mold upon releasing pressure: levels of delamination were reported in table V - 2 from very slightly delaminated "cracks", mildly delaminated samples "delam.", and highly delaminated samples, that led to the splitting of the specimen, noted "delam. +".

Following these deceiving results, another condition that was producing sound dog-bone specimens on cellulose (Chapter III) was tested on the 50 x 50 mm square mold: 250°C and equilibrium to 60% RH. Cellulose was successfully molded into squares without delamination. On the other native plant materials, consistent results were obtained compared to the previous condition: a majority of the square specimens were delaminated, and most of the time, the delamination was even worse at 250 than 175°C. Also, extrusion occurred which was noted "extr." in Table V - 3 when a significant part of the material was lost by extrusion.

Because dog-bone specimens and squares could be produced at 60% RH and 175 and 250°C and because the same conditions applied on native plant materials let to the delamination of most of the samples, it was concluded that native plant materials could not be molded in the same conditions than cellulose and that delamination was also affected by the chemical composition and probably other physical parameters (e.g. particle size).

Table V - 3: Compaction molding results comparing 50 x 50 mm squares and dog-bone shape

	Code	Shape	50 x 50 mm		dog-bone	
		Time - Pressure	30 s - 200 Mpa		30 s - 264 MPa	
		Temperature - RH	175°C - 60%	250°C - 60%	175°C - 60%	250°C - 0%
Material	AC	α-Cellulose	ok	ok	ok	ok
	CWa	Cellulose wadding	delam. +	delam. +	n/a	n/a
	WS1	Wheat straw <0,5 mm	delam. +	delam. +	delam.	delam.
	WS2	Wheat straw [0,5;1[mm	delam. +	delam. +	ok but cracks	ok
	WS3	Wheat straw > 1 mm	delam. +	delam. +	ok	ok but cracks
	WE1	Extruded wheat straw NaOH	delam.	delam. +	ok	ok but cracks
	WE2	Extruded wheat straw H_2O	delam.	delam. +	ok	ok
	WE3	Extruded wheat straw H_2O	delam. +	delam.	delam.	ok
	BS	Barley straw	delam. +	delam. +	sticking effect	sticking effect
	Mis	Miscanthus	delam.	delam.	ok	ok
	Car	Carded hemp	delam.	delam.	n/a	n/a
	Che	Chenevotte	delam.	delam. +	ok	ok
	SBP	Sugar beet pulp	delam.	extr.	n/a	n/a
	SCR	Sweet maize residue	delam.	extr.	extr.	extr.
	BCa	Sugarcane bagasse	delam. +	delam. +	delam.	ok but cracks
	BAg	Agave bagasse	ok	ok	ok	ok
	Pin	Pinsotte	ok	ok	ok	ok
	SSC	Sunflower seed cake	delam.	extr.	n/a	n/a
	FNO	Olive kernels flour	delam.	delam.	delam.	ok
	Cof	Coffee waste	delam.	extr.	n/a	n/a
	Bee	Beech wood	ok	ok	ok	ok
	Euc	Eucalyptus wood	delam.	delam. +	ok	ok
	Vin	Vine prunnings	ok	extr.	ok	ok
	Pop	Poplar bark	ok	delam. & extr.	ok	ok

V.3.B Dog-bones specimen molding from the native plant materials

Molding in reference conditions (175°C – 60 % RH equilibrium)

Dog-bones specimens were even produced in the control conditions (175°C equilibrium 60 % RH, 264 MPa of molding pressure, 50 bar/s pressurization and 30 seconds holding time), beginning with the materials which did not experience delamination in the 50 x 50 mm square mold. Then, materials with the lowest delamination damages were tested, which suprisingly produced sound specimens. It was decided to try to mold dog-bone specimens from all materials, from the lowest flowability to the highest and significant differences were observed between results obtained on squares and on dog-bones. The results have been assembled in Table V - 3: many specimens that produced delaminated 50 x 50 mm squares ended-up producing sound dog-bones specimens, showing the important effect of the molded shape, and more precisely, the surface volume ratio, which is much higher in the dog-bone than on the square shape.

Additional troubles were encountered upon the molding of Carded hemp and Cellulose wadding : because having much too low apparent density, the volume of 7.5 g of these two materials was much too high for the mold, and filling had to be done in several steps, required to pre-compress the material between two steps, and ended up having very poor homogeneity (Figure V - 3) and potential danger for the mold as it was not possible to guarantee a sufficient homogeneous filling of the mold in the longitudinal. These two materials were abandoned and noted “n/a” in Table V - 3.

Extrusion burr started to appear on the sides of the molded specimens. The extruded wheat straw with NaOH (WE1) was the first to exhibit significant burr and demolding started to be difficult (Figure V - 4).



Figure V - 3: Heterogeneity upon filling cellulose wadding because of its very low apparent density, the specimen is presented next to the 7.5g of origin material



Figure V - 4: WE1 sample with significant burr on the side



Figure V - 5: Barley straw specimens exhibited burr and a surprising sticking effect

WE1 specimens were successfully molded, but it seems this material had a limit flowability for the molding of dog bone specimens because the next one on the flowability list (Table V - 2) which was sweet maize residue was extruded between the punches and die of the dog-bone mold, after what the experiments had to be stopped. Barley straw was also tested, which also produced burrs on the sides of the specimens, in addition to a surprising

sticking effect: the removal of the punches from the die was difficult and the molded specimen stuck to both punches (Figure V - 5). While demolding some materials remained on the surfaces of the molds and some specimens were damaged upon demolding. Barley straw was the only material with such a behaviour, it was also abandoned ("sticking effect" is noted in the BS line of Table V - 3).

The mold was not too damaged by these experiments, but none of the materials with higher flowability were tested (i.e. coffee waste, sugarbeet pulp and sunflower seed cake were not tested). The reduction of molding pressure would probably have solved the problem of burr / extrusion, but then the comparison between the different samples would be impossible. Compaction molding can be concluded a not suitable technique for molding highly flowing materials and probably transfer molding would be more appropriate.

Inspired by the work of Jallabert with the PVT apparatus, a test was performed by the introduction of perfectly adjusted dog-bone teflon gaskets, which led to the extrusion of the gaskets and the blockage of the mold.

As a summary, the materials with a too low apparent density were discarded (Cellulose wadding and Carded hemp) as well as specimens with too much flowability (Coffee, Sugar beet pulp, Sunflower seed cakes, Sweet maize residues) and Barley straw which produced a sticky effect on the metal of the mold. The remaining plant materials after removal of the later cited ones was defined as the "compaction molding set". The complete results are presented in Table V - 4. Following the dog-bone specimens production, the materials of the "compaction molding set" were molded into 6 DMA specimens in order to perform the water resistance tests. Consistent results were obtained upon molding DMA specimens compared to dog-bones.

Molding in alternative conditions (250°C – 0% MC)

Considering the lack of results under the first condition, another condition was desirable to increase que volume of data for interpretation and also start the investigation of the influence of molding conditions on these materials processed from native plant materials, similarly to what was done with cellulose in Chapter III. Because of the number of specimens to test which was taking a considerable time to process, the other condition had to be chosen carefully. Because of the results obtained on squares at 250°C and equilibirum with 60% RH (Table V - 3), a reduced moisture content was preferrable. A condition giving increased properties to cellulose samples was also of high interest. 250°C and 2% was giving the best results on cellulose samples, but the reduction of moisture to 2% for each plant sample was quite difficult to manage and would have taken much time. On cellulose, a surprising conclusion appeared in the molding of dry material (103°C dried), this condition was thus selected (250°C – 103°C dried) as the second molding condition on the 23 native plant materials. Other parameters were the same than the reference condition. These experiments were performed on the possible-to-mold materials as defined with the first condition, i.e. the "compaction molding set".

Table V - 4: Properties of compaction-molded specimens from native plant materials

		Bending test 175°C 60% RH				Tensile test 175°C 60% RH				Water immersion test 175°C 60% RH				Bending test 250°C 0% MC				Tensile test 250°C 0% MC				Water immersion test 250°C 0% MC			
		Bending strength (MPa)		Bending modulus (GPa)		Tensile strength (MPa)		Tensile modulus (GPa)		WA (%)		TS (%)		Bending strength (MPa)		Bending modulus (GPa)		Tensile strength (MPa)		Tensile modulus (GPa)		WA (%)		TS (%)	
		Mean	St. dev.	Mean	St. dev.	Mean	St. dev.	Mean	St. dev.	Mean	St. dev.	Mean	St. dev.	Mean	St. dev.	Mean	St. dev.	Mean	St. dev.	Mean	St. dev.	Mean	St. dev.	Mean	St. dev.
Compaction-molding set	AC	34.8	3.9	5.9	0.6	17.2	1.2	1.9	0.1	75	2	96	3	51.7	5.7	7.7	2.0	25.2	1.3	2.0	0.1	65	4	79	2
	WS2	4.4	0.6	1.2	0.1	1.8	0.3	0.6	0.1	-	-	-	-	7.5	0.7	2.1	0.3	5.7	0.4	1.2	0.1	225	15	248	20
	WS3	6.6	1.0	2.4	0.3	3.1	0.6	1.1	0.1	379	41	366	26	9.8	1.2	2.9	0.5	6.5	0.4	1.3	0.0	227	6	234	8
	WE1	15.7	2.1	2.5	0.4	5.8	1.2	1.2	0.2	391	13	420	15	16.1	1.6	2.6	0.3	7.9	0.9	1.3	0.1	228	14	224	8
	WE2	11.2	3.6	2.4	0.5	3.8	0.6	1.2	0.1	-	-	-	-	13.3	2.3	2.9	0.5	8.7	0.7	1.3	0.1	218	72	221	19
	WE3	-	-	-	-	-	-	-	-	-	-	-	-	16.8	4.1	3.6	0.8	9.2	1.1	1.4	0.1	208	31	213	34
	Mis	13.1	2.6	4.0	0.7	6.0	0.5	1.3	0.1	284	4	267	3	18.0	1.7	5.8	0.5	8.7	0.7	1.4	0.1	83	6	95	10
	Che	12.6	2.7	4.2	0.5	4.6	0.5	1.4	0.1	366	9	396	12	14.4	2.0	5.2	0.6	7.1	0.9	1.4	0.0	175	13	186	12
	BCa	-	-	-	-	-	-	-	-	-	-	-	-	15.4	1.2	4.5	0.3	10.6	0.7	1.5	0.1	125	9	148	12
	Bagv	9.9	5.2	2.0	0.8	4.0	0.0	1.1	0.1	266	2	277	46	13.5	4.8	2.1	0.6	4.6	1.7	1.2	0.1	153	7	192	22
	Pin	13.0	3.1	2.6	0.3	4.2	0.6	1.1	0.1	258	64	309	18	14.2	2.4	2.7	0.5	6.0	1.3	1.2	0.1	149	15	179	27
	FNO	-	-	-	-	-	-	-	-	-	-	-	-	8.3	2.6	4.0	1.3	2.8	0.7	1.2	0.2	57	5	33	8
	Bee	8.2	2.5	2.4	0.8	3.4	0.8	1.3	0.6	-	-	-	-	15.9	3.6	4.5	0.8	5.1	1.4	1.4	0.1	207	37	125	9
	Euc	17.0	2.2	4.4	0.6	7.4	1.1	1.4	0.1	323	2	299	22	24.2	1.5	5.7	0.3	12.5	1.1	1.4	0.1	73	7	87	9
	Vin	5.7	1.5	1.6	0.5	3.2	0.6	1.2	0.1	211	25	172	30	11.7	1.8	2.8	0.5	4.2	1.0	1.2	0.1	109	4	122	8
	Pop	9.2	1.9	2.4	0.4	3.5	0.3	1.0	0.0	173	6	120	10	11.4	1.3	3.0	0.2	4.7	0.7	1.2	0.1	149	15	179	27
	CWa	-	-	-	-	-	-	-	-	-	-	-	-	-	-	-	-	-	-	-	-	-	-	-	-
	Car	-	-	-	-	-	-	-	-	-	-	-	-	-	-	-	-	-	-	-	-	-	-	-	-
	WS1	-	-	-	-	-	-	-	-	-	-	-	-	-	-	-	-	-	-	-	-	-	-	-	-
	BS	-	-	-	-	-	-	-	-	-	-	-	-	-	-	-	-	-	-	-	-	-	-	-	-
	SBP	-	-	-	-	-	-	-	-	-	-	-	-	-	-	-	-	-	-	-	-	-	-	-	-
	SCR	-	-	-	-	-	-	-	-	-	-	-	-	-	-	-	-	-	-	-	-	-	-	-	-
	SSC	-	-	-	-	-	-	-	-	-	-	-	-	-	-	-	-	-	-	-	-	-	-	-	-
	Cof	-	-	-	-	-	-	-	-	-	-	-	-	-	-	-	-	-	-	-	-	-	-	-	-

The first effect of this alternative condition was a higher number of valid specimens, i.e. not delaminated. In fact, Olive kernels flour, Extruded wheat straw 3 and Sugarcane bagasse, which produced delaminated samples under the first condition, produced sound specimens despite the small cracks on the sides of Sugarcane bagasse specimens. These specimens were tested under the second conditions which was not possible under the first condition. The quantity of information was then increased from the first to the second condition. 6 DMA specimens (water resistance evaluation) for each condition were also molded, and consistent results obtained (Table V - 4).

V.4 Analysis of "compaction molding set" results

V.4.A Summary of results

Missing values

In this part, only the plant materials that gave successful results in compaction molding i.e. which was defined as the "compaction molding set" are considered.

A first look at the mechanical properties results showed that none of the native plant materials was able to produce values close to cellulose which remained way over. Under the two conditions of molding, cellulose specimens had strengths at break in bending and tensile about two folds higher than the best native plant specimens (Eucalyptus). As for the moduli, the gap was much less than two folds but cellulose still had the maximum values.

Under the first molding condition, Extruded wheat straw 3, Sugarcane bagasse and Olive kernels flour produced delaminated specimens which were not tested mechanically.

The consideration of the water resistance values led to consistent conclusions: cellulose had by far the best water resistance under the first molding condition with about twice lower swelling (TS) and water absorption (WA) than the more water resistant specimen from the other plant materials (Poplar bark). The specimens molded under the first condition were overall very sensitive to water, none of them could have been tested mechanically except cellulose and several specimens (WS2, WE2 and Bee) were not tested because they could not be taken out of the frame used for the 24 hours of swelling (Figure V - 6).



Figure V - 6: Example of results of the swelling tests under the first condition

Yet, under the second condition of molding (250°C – 0% MC), the results were overall improved: all the specimens were successfully produced and none of them was delaminated. It was thus possible to perform mechanical tests and obtain values in the whole "compaction-molding set" without any missing values. The mechanical properties were overall improved under the second molding condition but not as much as the water resistance which was drastically increased: no specimens returned to its original powder shape like it did for some specimens under the first condition (Figure V - 6).

The complete results are presented in Table V - 4 for the mechanical and water properties, and the physicochemical analysis in Table V - 1.

Inspection of variable ranges

A summary of the results is presented in Table V - 5, Table V - 6 and Table V - 7 which also present the coding of the variables that was used on the graphs and tables for the statistical analysis part.

Table V - 5: Summary of results for the chemical composition of the "compaction molding set" plant materials

Plant material composition	Min	Max	Mean	Median	Unit	Code
Moisture content	7.1	10.4	8.69	8.68	%	Moist
Ashes content	0	10.8	4.48	3.1		Ash
Lipid content	0	4.89	0.93	0.34		Lip
Cellulose content	39.8	96	50.1	45.7		Cell
Hemicelluose content	4	33.5	23	24.4		hemi
Lignin content	0	25	13.2	12.9		Lig
NDF extractives	0	27.5	13.7	13.6		NDF
Protein content	0	3.62	1.86	2.21		Prot
Polyphenol content	0	12	5.16	3.64	mg_{GAEeq}/g	Pphe

Table V - 6: Summary of results for the physical characteristics of the "compaction molding set" plant materials

Plant material physical characteristic	Min	Max	Mean	Median	Unit	Code
Tapped density	0.13	0.63	0.24	0.19	g/cm^3	Dens
Particle size > 2 mm	0	0.88	0.23	0.16	%	P>2
Particle size [1.6mm-2mm[	0	1.9	0.57	0.32		P1.6
Particle size [1.25mm-1.6mm[	0	6.66	1.89	1.05		P1.25
Particle size [1mm-1.25mm[	0	18.5	15.1	16.5		P1
Particle size [0.8mm-1mm[	0	14	6.88	6.44		P0.8
Particle size [0.5mm-0.8mm[	0	31.1	16.1	18.4		P0.5
Particle size [0.25mm-0.5mm[	0	42.5	25.9	27.7		P0.25
Particle size [0.12mm-0.25mm[	0	25.6	12.7	13.1		P0.12
Particle size ≤ 0.12	2.5	100	20.7	10.9		P<0.12
Form factor =1	28	54.6	45.8	50.2		F1
Form factor]1-2]	14.3	30	22.3	22.9		F1-2
Form factor]2-3]	14.4	24	18.6	18.4		F2-3
Form factor]3-5]	4.44	21.5	10.2	8.57		F3-5
Form factor]5-10]	0.41	9.88	3.13	2.61		F5-10
Form factor >10	0	0.45	0.08	0.04		F>10

Table V - 7: Summary of results for the molded specimens properties of the "compaction molding set"

Specimen parameter	Min	Max	Mean	Median	Unit	Molding condition	Code
Bending strength	4.36	34.8	12.4	11.2	MPa	60% RH 175°C	BS_1
Bending modulus	1209	5940	2921	2438	GPa		BM_1
Tensile strength	1.85	17.2	5.24	3.99	MPa		TS_1
Young's modulus	616	1880	1220	1171	GPa		TM_1
Water absorption	74.8	391	273	275	%		WA_1
Thickness swelling	96.5	420	272	288	%		SWE_1
Bending strength	7.48	51.7	16.4	14.3	MPa	0% MC 250°C	BS_2
Bending modulus	2102	7720	3875	3296	GPa		BM_2
Tensile strength	2.85	25.2	8.09	6.8	MPa		TS_2
Young's modulus	1164	2000	1353	1318	GPa		TM_2
Water absorption	57.2	228	153	151	%		WA_2
Thickness swelling	33.2	248	160	179	%		SWE_2

The restriction to the "compaction molding set" led to the reduction of the diversity in the chemical composition especially for the lipids and protein contents that were in narrow ranges (0 – 4.89 % and 0 – 3.62 % respectively). These parameters that have a low variability are probably to consider with care in the analysis, because enlarging the range could led to drastic changes on the conclusions. The mean and median values for the chemical composition appearing in Table V - 5 provides the portrait of the typical "compaction-moldable" materials, with high cellulose content, low extractives ashes protein and polyphenol contents.

When looking at the summary of physical characteristics results (Table V - 6), some variables also appear very centered, for instance the particles with size over 1.6 mm are very rare (max value for P>2 and P1.6 are 0.88% and 1.9% respectively), which is consistent with the values on F>10 (=0.45%). Such particles are not well represented, thus the analysis should not consider these results with too much weight.

As far as the compacted specimens are concerned (Table V - 7), the first observation was the quite low values observed for the mechanical properties and quite high WA and TS on the native plant materials compared to cellulose. The median was also systematically lower than the mean for mechanical properties and higher for water resistance which means a disbalance within the specimens. All the maximum values of the mechanical properties and minimum values for the water resistance belonged to the cellulose samples. Considering that the conditions defined here are based on cellulose study (Chapter III), this result is not so surprising. The second condition, however appears to significantly improves all the specimens properties as it did for cellulose.

V.4.B Statistical analysis

The main objective of this chapter was to establish links between the characteristics of plant materials and the parameters of the resulting compaction molding parameters. Due to the number of variables, statistical analysis (linear cross correlation and PCA, see Materials and Methods VI.3.D) was used in order to summarize the information.

First considering the whole "compaction molding set", the cross correlation table was established between the starting plant material's variables (columns) in one hand and the compressed specimen properties (lines) in the other hand (Table V - 8). The figures in the table indicates the correlation between the variables, values close to -1 means a negative correlation (and +1, positive), values close to 0 means the independency of the two variables.

A color scale was used in order to graphically observe the significant correlations either positive (red) or negative (blue).

Table V - 8: Cross correlation table "compaction molding set"

	Moist	Ash	dens	P>2	P1.6	P1.25	P1	P0.8	P0.5	P0.25	P0.12	P<0.12	F1	F1-2	F2-3	F3-5	F5-10	F>10	Lip	Cell	hemi	Lig	NDF	Prot	Pphe
BS_1	-0.24	-0.41	0.07	-0.15	-0.36	-0.35	-0.42	-0.48	-0.63	-0.66	-0.55	0.85	0.44	-0.24	-0.12	-0.37	-0.30	-0.25	-0.25	0.85	-0.72	-0.44	-0.48	-0.51	-0.25
BM_1	-0.33	-0.62	-0.08	0.07	-0.23	-0.15	-0.11	-0.20	-0.41	-0.65	-0.63	0.64	0.59	-0.24	-0.42	-0.42	-0.37	-0.38	-0.27	0.83	-0.74	-0.12	-0.65	-0.78	-0.23
TS_1	-0.22	-0.46	0.14	-0.13	-0.29	-0.31	-0.51	-0.47	-0.60	-0.70	-0.60	0.88	0.39	-0.22	-0.17	-0.30	-0.24	-0.20	-0.25	0.91	-0.74	-0.45	-0.55	-0.55	-0.24
TM_1	-0.21	-0.62	0.16	0.06	0.04	0.11	-0.28	-0.11	-0.53	-0.71	-0.56	0.68	0.52	-0.24	-0.44	-0.35	-0.27	-0.36	-0.30	0.78	-0.62	-0.15	-0.66	-0.61	-0.21
WA_1	0.09	0.44	-0.79	0.01	-0.04	0.12	0.77	0.70	0.74	0.33	0.35	-0.74	-0.15	-0.07	0.58	0.07	-0.14	-0.17	-0.30	-0.69	0.57	0.43	0.44	0.12	0.13
SWE_1	-0.06	0.40	-0.74	-0.05	-0.15	0.00	0.69	0.57	0.55	0.24	0.31	-0.60	-0.15	-0.22	0.62	0.11	-0.07	-0.09	-0.47	-0.60	0.54	0.30	0.40	0.07	-0.08
BS_2	-0.11	-0.43	-0.07	-0.23	-0.29	-0.22	-0.35	-0.31	-0.39	-0.50	-0.52	0.62	0.32	-0.31	-0.14	-0.15	-0.14	-0.24	-0.23	0.90	-0.69	-0.42	-0.56	-0.51	-0.29
BM_2	-0.27	-0.75	0.03	0.13	0.01	0.06	-0.16	-0.05	-0.20	-0.56	-0.72	0.51	0.44	-0.17	-0.44	-0.23	-0.25	-0.44	-0.02	0.84	-0.65	0.00	-0.81	-0.86	-0.23
TS_2	-0.18	-0.33	-0.25	-0.32	-0.47	-0.38	-0.34	-0.30	-0.26	-0.46	-0.50	0.57	0.42	0.18	-0.18	-0.44	-0.50	-0.44	-0.17	0.81	-0.55	-0.50	-0.49	-0.47	-0.31
TM_2	-0.22	-0.46	-0.13	-0.19	-0.28	-0.19	-0.35	-0.20	-0.26	-0.58	-0.62	0.62	0.31	0.06	-0.22	-0.24	-0.33	-0.48	-0.11	0.85	-0.54	-0.43	-0.61	-0.61	-0.38
WA_2	0.32	0.73	-0.51	-0.41	-0.29	0.03	0.49	0.42	0.40	0.26	0.44	-0.53	-0.35	-0.04	0.57	0.25	0.07	-0.04	-0.33	-0.57	0.56	-0.25	0.62	0.55	-0.24
SWE_2	0.24	0.83	-0.63	-0.47	-0.52	-0.24	0.40	0.23	0.38	0.45	0.59	-0.55	-0.25	0.24	0.46	0.02	-0.04	0.15	-0.31	-0.60	0.54	-0.35	0.77	0.62	-0.18

This first analysis showed that some parameters were remarkably correlated: the 8 mechanical properties appeared correlated positively with the cellulose content, in the same time water properties were negatively correlated. The particle size < 0.12 followed a similar trend, and on the opposite, the other particle sizes parameters, the hemicelluloses content, the NDF extractives content, protein content and ashes content were correlated positively with the water properties and negatively with the mechanical properties. These parameters are precisely those for which cellulose has the min / max values of the set, far from the average, i.e. the highest mechanical properties and cellulose content by far, the highest proportion of particles < 0.12, the lowest WA, TS, the lowest proportion of the other particle sizes, lowest hemicelluloses, NDF extractives, protein, and ashes contents (Table V - 1). The values of the cellulose sample are too different from the rest of the materials and also have properties that are much better than the plant materials, which influences a lot the correlation.

When performing the PCA analysis of this set of experiments, the first principal component had 41% of the explained value, which went down to 16% for PC2. 9 principle components would have been needed to explain 95 % of the variance, which is a lot compared to the number of variables and the last PCs contained a very low proportion of the information.

The analysis was performed on the 2 first principal components (PC1 and PC2, 57 % of the variance: Figure V - 7) and results were not much different from the cross correlation table: there is a first group on that has high correlation loading along the PC1 which includes the 8 mechanical properties (BM, BS, TM, TS for the 2 molding conditions), Cell (cellulose content), P<0.12 (% of particle < 0.12 mm) and F1 (% of spherical particles). AC has a very high score on PC1 and is the only one in this case which confirms the particular behaviour of this material.

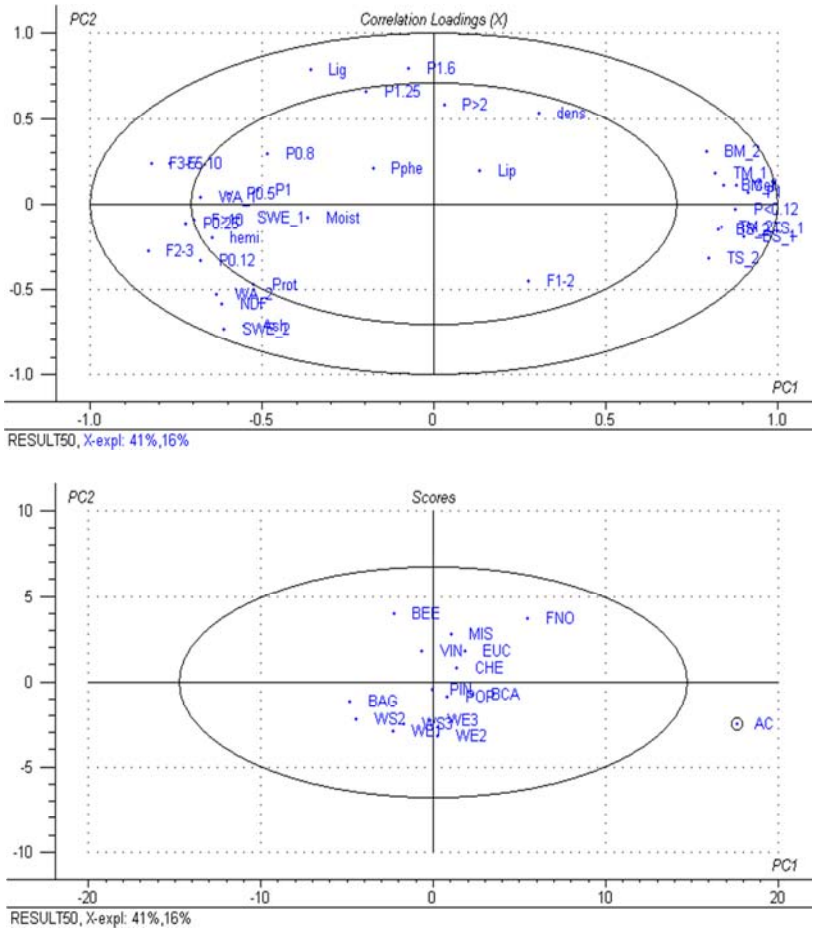

Figure V - 7: PCA1, "compaction molding set", standardized values, results for PC1, PC2

On the opposite on the PC1 axe, WA_1 and SWE_1 form a group with hemi, P0.12, P0.25, P0.5, P0.8, P1 (part of particles size between 0.12 and 1 mm), and F2-3, F3-5, F5-10, F>10 (part of particles with form factor between 2 and 10 and over). No specimens presented low scores on the PC1 axe, so this group is likely to be much influenced by the cellulose results which had the lowest values in this group within the whole set of samples. With high scores on PC1 and PC2, another group is formed by SWE_2, WA_2 and Prot (protein content), Ash (Ashes content) and NDF (NDF extractives) but no specimens was related to this group. On the opposite of the PC1/PC2 diagonal is the specimen FNO which had particularly low values on these variables.

On the score plot, cellulose appeared circled which meant it is considered as an outlier for this set of experiments and except cellulose, none of the other materials had significant scores to join one or the other group of variable. Cellulose was seen to influence too much the results which led to biased conclusions of this PCA about the influence of the chemical composition / physical parameters of the native plant materials; thus the analysis was run again without the cellulose sample in the calculation (Figure V - 8).

It can be observed on PCA2 that upon the removal of cellulose, the variables are much more separated, with an appreciable amount of variable being significant (outer ellipse). The 2 first PCs contained 52 % of the variance which is again low. Again, many PCs were necessary to explain 90% of the variance and PC3 and next had a very low proportion of the variance explained; the analysis was thus made on PC1/PC2 only. FNO was detected as an outlier which can be explained by its very particular particle size and missing results on form factor.

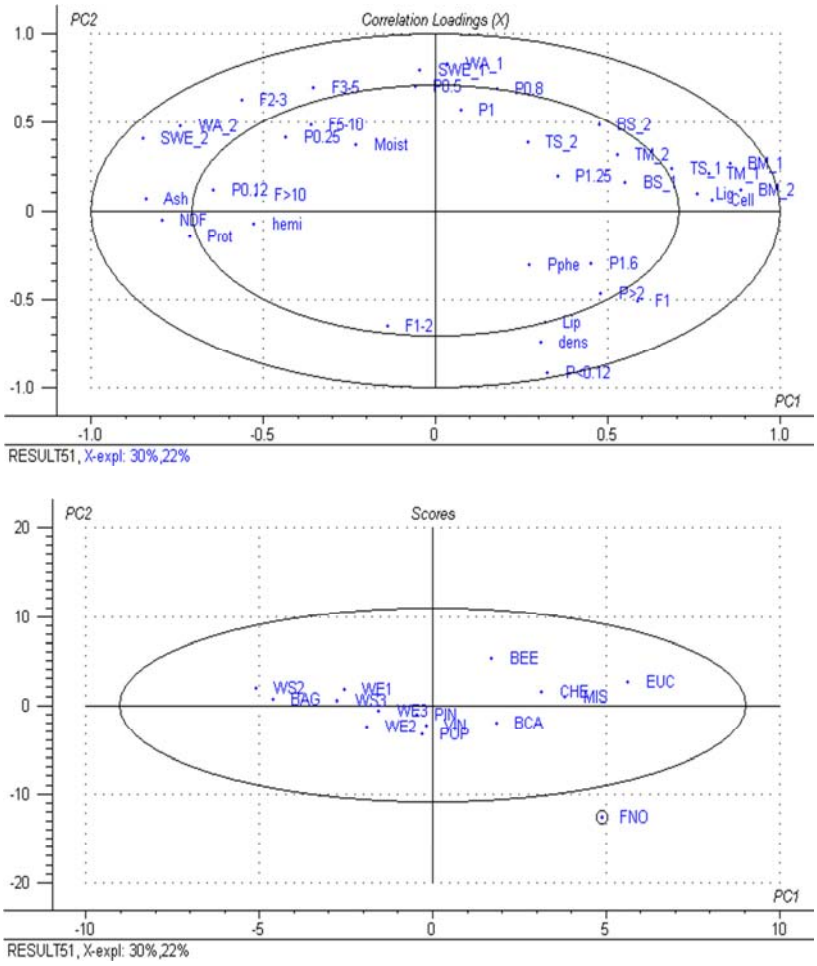

Figure V - 8: PCA2, "compaction molding set" except cellulose, standardized values, results for PC1, PC2

Results were analyzed whatsoever: there are variables forming two groups on the PC1 axe, and specimens are disposed along the PC1 axe which is a good conformation for the analysis of the results. At the positive correlation loadings on PC1, a first group is formed by the bending moduli BM_1 and BM_2, the tensile modulus TM_1, the tensile strength TS_1 and the lignin and cellulose contents (Lig, Cell). On a lower extent, along to the PC1 axe but inside the first ellipse (50% variance), a group is formed by the rest of the mechanical properties BS_1, TM_2, BS_2 TS_2 (and P 1.25). On the opposite (on PC1), another group is formed with WA_2, SWE_2, and Ash, NDF, Prot, P0.12, F>10 and hemi. The conclusion is that plant materials with high cellulose content (even without the cellulose samples in the calculation), high lignin content, low ashes, NDF, proteins, hemicelluloses contents will produce compressed materials with the highest mechanical properties and best water resistance (under the second molding condition). Eucalyptus wood, Miscanthus and Chenevotte are examples of plants fitting these requirements and which produced specimens with improved properties. Wheat straw, Sugarcane bagasse are examples of plants which had the wrong characteristics, and thus produced compressed materials with lower properties.

The water properties under the first condition (i.e. SWE_1 and WA_1) were highly correlated with the PC2 axe, forming a group together with P0.5, P0.8, P1, and opposed to F1-2, P<0.12Pphe (polyphenols content), Lipids content, apparent density, P<0.12. This opposition on PC2 tend to show a correlation between water resistance under the first condition and a high lipids and polyphenols content, a high proportion of the smallest (and spherical) particles (P<0.12, F1, F1-2) and a higher apparent density. On the PC2, FNO had

particularly low scores and precisely had the best water properties SWE_1 and WA_1 and high values of lipid and polyphenols contents, smaller particles etc. As FNO is considered an outlier in this PCA, and that few specimens had particularly high or low scores on PC2, this result is to consider with a lot of precaution.

Table V - 9: Cross correlation table "compaction molding set" except cellulose

	Moist	Ash	dens	P>2	P1.6	P1.25	P1	P0.8	P0.5	P0.25	P0.12	P<0.12	F1	F1-2	F2-3	F3-5	F5-10	F>10	Lip	Cell	hemi	Lig	NDF	Prot	Pphe
BS_1	-0.02	-0.17	-0.41	0.14	-0.25	-0.21	0.37	-0.02	-0.18	-0.02	-0.09	0.03	0.44	-0.24	-0.12	-0.37	-0.30	-0.25	-0.15	0.34	-0.42	0.26	-0.13	-0.32	0.18
BM_1	-0.21	-0.53	-0.42	0.34	-0.05	0.07	0.60	0.29	0.07	-0.28	-0.38	-0.16	0.59	-0.24	-0.42	-0.42	-0.37	-0.38	-0.17	0.65	-0.54	0.54	-0.50	-0.75	0.06
TS_1	0.07	-0.32	-0.38	0.26	-0.09	-0.10	0.31	0.09	-0.01	0.01	-0.18	-0.14	0.39	-0.22	-0.17	-0.30	-0.24	-0.20	-0.14	0.47	-0.51	0.42	-0.28	-0.45	0.34
TM_1	-0.03	-0.53	-0.06	0.32	0.33	0.44	0.29	0.43	-0.15	-0.40	-0.26	0.11	0.52	-0.24	-0.44	-0.35	-0.27	-0.36	-0.22	0.50	-0.32	0.48	-0.51	-0.49	0.08
WA_1	-0.14	0.22	-0.83	-0.29	-0.40	-0.21	0.57	0.50	0.46	-0.55	-0.18	-0.70	-0.15	-0.07	0.58	0.07	-0.14	-0.17	-0.67	-0.16	0.18	-0.12	0.07	-0.30	-0.31
SWE_1	-0.26	0.22	-0.72	-0.27	-0.43	-0.27	0.53	0.37	0.25	-0.42	-0.07	-0.58	-0.15	-0.22	0.62	0.11	-0.07	-0.09	-0.75	-0.29	0.27	-0.14	0.13	-0.24	-0.46
BS_2	0.20	-0.32	-0.46	-0.01	-0.15	0.05	0.33	0.32	0.24	0.17	-0.05	-0.37	0.32	-0.31	-0.14	-0.15	-0.14	-0.24	-0.20	0.44	-0.35	0.41	-0.38	-0.39	0.16
BM_2	-0.19	-0.74	-0.07	0.40	0.24	0.31	0.27	0.37	0.22	-0.28	-0.57	0.01	0.44	-0.17	-0.44	-0.23	-0.25	-0.44	0.12	0.75	-0.41	0.63	-0.76	-0.85	0.03
TS_2	0.00	-0.09	-0.74	-0.22	-0.52	-0.32	0.24	0.22	0.45	0.16	-0.06	-0.34	0.42	0.18	-0.18	-0.44	-0.50	-0.44	-0.04	0.14	0.01	0.06	-0.18	-0.25	0.05
TM_2	-0.09	-0.37	-0.47	0.06	-0.11	0.07	0.22	0.43	0.44	-0.16	-0.35	-0.17	0.31	0.06	-0.22	-0.24	-0.33	-0.48	0.09	0.33	0.01	0.22	-0.46	-0.58	-0.11
WA_2	0.27	0.69	-0.51	-0.56	-0.43	-0.08	0.38	0.30	0.26	0.05	0.30	-0.40	-0.35	-0.04	0.57	0.25	0.07	-0.04	-0.44	-0.55	0.45	-0.64	0.54	0.47	-0.44
SWE_2	0.19	0.81	-0.63	-0.60	-0.67	-0.36	0.27	0.08	0.25	0.33	0.51	-0.49	-0.25	0.24	0.46	0.02	-0.04	0.15	-0.40	-0.69	0.45	-0.73	0.74	0.56	-0.35

The cross correlation analysis was run again without the cellulose sample in order to visualize and confirm some of the results from PCA2 (Table V - 9): compared to the previous cross correlation table (Table V - 8), much more values are close to zero (and coloured in white) which means no linear correlation between the two variables in the table. Some results in accordance with previous results can yet be retrieved, for instance, a significant correlation exists between the water resistance under the second molding condition (WA_2 and SWE_2) and the apparent density, high particle sizes, lipids, cellulose, lignin and polyphenols contents and negatively with the ashes, NDF extractives, protein and hemicelluloses contents. The particular behaviour of the water resistance under condition 1 is also marked with a negative correlation with the apparent density, proportion of smallest particles and lipids content. Finally, the mechanical properties consistently appeared correlated to the cellulose and lignin content, and negatively with protein hemicelluloses and protein contents.

Considering the very low part of variance explained by the PCA plots, these results have to be carefully considered: there is a lot of variance which is not explained by the statistical tests and for which no explanation was found. This variance could be either a mis-evaluation of the true properties of the compressed samples (reliability and regularity of the molding process, especially the mold-filling step), experimental error during the evaluation of these properties (measurements during the water resistance tests for instance), experimental error during the measurements of the plant material chemical composition and properties (sampling, analytical methods not always perfectly adapted, limited repetitions) or noise generated by other parameters that were not taken into account. All these reasons probably participate together in lowering the reliability of these analyses which can be considered as first steps toward the explanation of the correlation between the plant materials properties and the performances of the resulting compressed specimens.

V.5 Transfer molding or compaction molding: The perspectives of a promising processing route ?

V.5.A The limitations of compaction molding

The conclusions drawn upon the analysis of the performances of materials molded from the different biomass in the last part are also specific to the 2 molding conditions that were tested. It is probable that the composition and physical properties of the starting material also influences the reaction of the material to variations of the molding conditions (pressure, temperature, moisture, time). Probably a huge experimental design would be needed in order to satisfactorily analyze the link between the plant material's parameters, the operating conditions and the resulting performances of the compressed specimen. A supermodel could be created to make all these variables interact in order to deliver the desired plant properties and processing conditions to achieve the best possible material, or match certain industrial specifications, or predict the potential applications of any kind of plant materials based on its physic-chemical properties. That was an idea of this thesis at the beginning but the objectives had to be trimmed down.

The main reasons behind the complexity of this work are related to the technological limits of compaction molding:

- the achievement of the equal distribution of material in the mold remained random due to manual operations
- low density material would require pre-compression to avoid an over-sizing of the molds
- delamination is always a limit that is to be considered carefully when working on the effect of temperature and moisture
- last but not least, as soon as one plant material exhibits significant flowability (which should be desirable for molding), extrusion occurs which either blocks the molds or destroys it.

Compaction molding can be then considered a fragile technique, dependent on many parameters that bring limitations. A lot of conditions (plant's or processing conditions) can lead to a lack of values because specimens cannot be molded or tested which is highly problematic for the construction of a model.

One potential alternative is the use of transfer molding which should allow to mold a higher diversity of materials (with higher flowability), would solve the problem of homogeneous filling, thus improving reproducibility and measurements reliability and could possibly partly solve the problem of delamination. Of course more parameters would be entering the model, with the effect of shear being another constraint that would complicate a bit the experiments, but also bring new possibilities.

Most of all, the difference of properties between specimens processed by compaction molding and transfer molding should be carefully compared, which could lead to materials being more suitable for compaction, and others more suitable for transfer. With this comparison in mind, a prototype was designed (materials and methods, Figure VI - 12and Figure VI - 13) during this thesis in order to mold tensile and bending tests specimens using the technique of transfer molding. Due to technical troubles, only a few experiments could be run (WS1, 2 and 3).

V.5.B Exploratory results on the mechanical properties evaluation of extruded materials

Principle

The idea here was to use the transfer molding apparatus to produce dog-bones specimen and bending specimens. Due to the size of the apparatus, only the 5B dog-bone described in EN ISO 527-2 was suitable. This transfer molding module was designed with aim to produce at the same time (i.e. in one press cycle) 2 bending tests specimens of 34.5 x 5 mm and 2 tensile tests specimens of matching ISO 527-2 (see Materials and Methods Figure VI - 12).



Figure V - 9: WS1 injected in the mechanical properties specimens' module



Figure V - 10: Demolding of the transferred specimens using an aluminum punch

The procedure is the same as for flowability evaluation, plant materials is precompressed, loaded in the chamber and the cycle is run from 0 to 140 bar with a 3bar/s increase of pressure. One some point, the pressure brutally drops a few bars, and comes back to normal, i.e. the material has been injected. The pressure is let to increase to the max in order to apply the same final force on material's which would have different flowability (thus different values of injection pressure). The apparatus is put apart and the material is molded (Figure V - 9). A tool was machined in order to remove the specimen from the module which is performed by pushing gently the module on the tool which pushes the specimen out of the die (Figure V - 10). The molded specimens are retrieved with the transfer sprue still on, they exhibited a smooth and shiny surface, the molded shape is very precise does not look like the

original material (Figure V - 11). Each experiment was run in triplicate in order to obtain 6 specimens for the tensile and bending tests. They can be separated one from the others using a cutting wrench, and after 2 weeks of equilibrium at 60% RH and 25°C, the mechanical tests were performed.

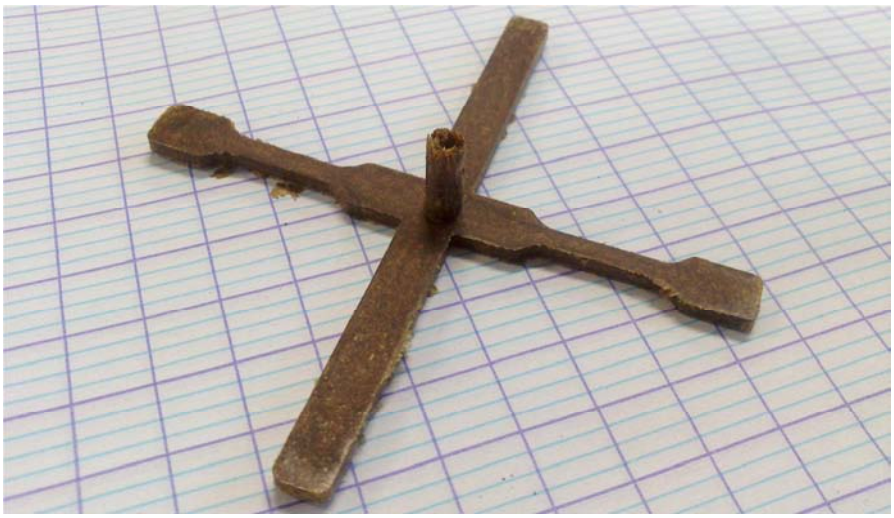

Figure V - 11: Demolded specimen, burr has been partially removed

Results

The results are presented in Table V - 10: the first element is that delamination which was occurring during compaction-molding of WS1 did not occur in transfer molding. The high shear during transfer test probably explains a better homogeneity and water diffusion thorough the material in transfer although in compaction, it was shown that water was accumulated and imprisoned in the core layer of the material.

Table V - 10: Mechanical properties of transfer molded wheat straw specimens compared to compaction -molded

	Transfer molding								Compaction molding							
	Tensile test (20,5mm)				Bending test (22 mm)				Tensile test (80 mm)				Bending test (80 mm)			
	5B dog-bone				34x5mm				1A dog-bone				1A dog-bone			
	Modulus (GPa)		Strength (MPa)		Modulus (GPa)		Strength (MPa)		Modulus (GPa)		Strength (MPa)		Modulus (GPa)		Strength (MPa)	
	Mean	St. dev	Mean	St. dev	Mean	St. dev	Mean	St. dev	Mean	St. dev	Mean	St. dev	Mean	St. dev	Mean	St. dev
WS1	0.24	0.02	4.4	1.0	2.1	0.1	12.0	1.8	-	-	-	-	-	-	-	-
WS2	0.28	0.03	3.5	0.9	1.9	0.5	11.9	3.4	0.6	0.1	1.8	0.3	1.2	0.1	4.4	0.6
WS3	0.28	0.01	6.6	1.1	2.0	0.2	11.0	1.0	1.1	0.1	3.1	0.6	2.4	0.3	6.6	1.0

The strengths at break in bending and tensile were approximately doubled comparing transfer to compaction. The bending moduli were comparable but the tensile moduli were drastically reduced in transfer compared to compaction molding. The orientation of the fibers was not observable on the transferred specimens although it was obviously on the compacted ones. But, due to the design of the apparatus, flow occurs in the direction of the specimens which should orientate the fibers about the same way than in compaction. The destructuration of the fibers due to high shear in transfer molding may be part of the explanation. However, these results have to be considered with care because of the difference

of sizes between the specimens used in transfer / compaction, especially in tensile for which the results on 1A and 5B dog-bones cannot be compared directly.

In compaction, WS3 had higher properties than WS2 which was also the case in transfer molding. In transfer WS1 had higher properties (in tensile) than WS2 which again should be considered with care due to the low number of replicates and considering that the apparatus was in testing phase. An hypothesis can anyway be formulated to explain the better properties obtained for WS3: the higher shear undergone by particles of higher size when going through the die in transfer could lead to more destructuration and matrix effect as reported in the literature (Chapter I).

Even though the mechanical properties were increased by the use of transfer, they remained low compared to what was observed on cellulose in compaction molding. A direct perspective of this work would be to continue in this direction and perform the same analysis of the links between the results of the transfer molded materials and the composition of the plant materials they are made of.

Conclusions

1. Compaction molding is not suitable for producing specimens from materials that would express too much flowability. A too low apparent density also made it impossible to mold the specimens. This conducted a major reduction of the number of plant materials successfully processed, which a consequence on the diversity in the plant characteristics which was reduced, reducing the significance of the analysis.

2. Many troubles were encountered with delamination, which was already the case with cellulose in Chapter III. The surface/volume parameter was revealed to impact the delamination. The design of the experiments was to process a high number of specimens in the reference conditions determined for cellulose. The main parameters of this study were based on results from Chapter III. None of the specimens reached half of the mechanical strengths obtained on cellulose, which remained by far the best specimen. Probably the molding parameters that were optimized on cellulose were not optimal for the other plant materials, and the study of the impact of the parameters should be done on some typical materials which could probably lead to much better properties (like reported in the literature).

3. The properties of the cellulose samples were so high that the analyses were distorted. The analyses were run again without the cellulose sample which permitted to obtain some interesting conclusions: The cellulose and lignin contents were the two variables that significantly influenced the mechanical properties positively. On the opposite, the protein, ashes, NDF extractives, hemicellulose contents and the fine particles were negatively correlated with the mechanical properties. The water properties were also well correlated to the mechanical properties.

4. These results provide the portrait of the materials that would provide the best possible properties in compaction-molding under these conditions. But, these results are probably very impacted by the molding conditions that were optimized on cellulose, thus, the fact that high cellulose content was desirable for better mechanical properties was actually quite obvious. The impact study of the operating conditions should thus be performed on the raw plant materials, which would require a lot of work due to the immense number of experiments needed. Experimental designs could be used, but as they rely on models, missing values (extrusion, delamination or other incapacity to mold) can seriously hinder the reliability of the analyses.

5. The technological part also had a high impact on the results, due to the experimental conditions, some specimens were not molded, which reduced the field of investigation. It is highly probable that with a better control on the technological part, the results could have been different. Much work is needed on reducing the results' dependency on the technology.

6. Transfer molding was considered a potential alternative to avoid the technological difficulties encountered with compaction molding. The objective of this chapter was to evaluate the difference between compaction and transfer on the properties of the molded specimens, and find the correlation to the plant compositions in both cases. This objective was not completed again because of technological failures.

General conclusion

In the context of worldwide plastic pollution and fossil resources depletion, this thesis provides an exploratory work towards the evaluation of a one-step thermo-compressive process for the production of bio-based (and hopefully biodegradable and eco-compatible) objects from lignocellulosic materials without pretreatment nor binders. It is included in a longer ANR (French National Research Agency) project of the laboratory (HYPMOBB) which purpose is to investigate thermo-compressive molding of renewable resources for producing agromaterials. The project has been organized in two workpackages, a first one dedicated to the study of the pressure-volume-temperature relationships and the associated microstructural changes of model carbohydrates, and a second one dedicated to the technical application, and study of the properties of the processed materials. The first workpackage was completed during a first thesis defended by Bastien Jallabert at the end of 2014. The second workpackage which comprised a lot more technological investigations was completed through the present thesis work: a CIFRE thesis with the young company The Green Factory, partially supported by the ANRT (French National Agency for promoting Research and Technology). Although during the first workpackage different model polymer were studied (i.e. cellulose, native starch, gelatinized starch) the present work focused on lignocellulosic materials and took cellulose as a model polymer.

At first the available literature in the field of self-bonded lignocellulosic materials was closely examined. The majority of the reports concerned the molding of lignocellulosic materials (crop residues and wood) into binderless boards, i.e. at low pressure (a few MPa) for a long time (5 to 20 minutes). The optimal conditions were collected and temperature was already considered the most important parameter. The problem of delamination was also a concern in binderless particle boards pressing. One of the major differences between the available literature and the present thesis was the molding pressure which was a hundred times higher. The difference of pressure control was also major, as boards pressing has thickness (and thus density) control and pressing pressure adjusted to match the requirements of thickness in the case of boards. During this thesis, the pressing machine was pressure controlled and density could not be adjusted, it was a consequence of operating conditions. A tight link was actually reported between density and the mechanical properties of binderless boards.

Much data were available with pretreatments involving steam. The chemical changes occurring during these pretreatements were examined and compared to those reported to occur during hot-pressing and many common elements were found. Additional data from other fields of research were collected (wood welding, polymer science) in order to gather the knowledge about the mechanisms of cohesion of self-bonded materials. It appeared that the majority of the reports did not concern much about the mechanisms of cohesion. Some elements were still available which permitted to formulate hypotheses of two different mechanisms: a “thermoplastic mechanism” which would take place bellow 200°C, and which would rely on crossing the Tg of the lignocellulosic polymers in order to produce sufficient deformability of the polymers and provide a matrix effect. Above 200°C, another mechanism would start and it was called “thermoset mechanism”. This second mechanism would rely on heavier degradation of polymers, autohydrolysis and the formation of reactive compounds and new complexes.

Naturally, these two mechanisms were addressed to polymers which exhibited a true Tg, lignin and hemicelluloses mostly, and proteins, starch secondly. However, some reports were available about the molding of pure cellulose, and it was decided to start the experimental work of the present thesis by this model polymer.

The properties of compacted cellulose were surprising, and a method was designed to mold dog-bone specimens for measuring properly the mechanical properties in tensile and

bending, and the influence of the parameters was investigated. Some parameters with low influence were concluded to be secondary: the molding time, and the pressurization speed. The most important parameter was temperature, which was consistent with the literature. A minimum of moisture was observed to be necessary for the self-bonding, which made it an important parameter. The temperature / moisture couple was then identified as a priority for the study of the delamination phenomena and the research of improved mechanical properties. The reduction of moisture and increase of temperature were successful in avoiding delamination and increasing the mechanical properties which reached 31 and 70 MPa of stress at break in tensile and bending, with moduli values of 2 and 8 GPa, in tensile and bending, for 2% moisture and 250°C.

Thanks to the data produced in this thesis and within the whole project HYPMOBB, a discussion was proposed about the structure / property relationship of the compacted cellulose materials. Hypotheses are made about the effect of uniaxial high-pressure thermocompression on cellulose and the mechanical properties of the compacted specimens: Most of the strength of the material comes from the skin, and most of all from the Tg of cellulose in the conditions of molding, i.e. in regard to the moisture of the sample and molding temperature. The higher above the Tg, the higher the deformability and possibilities for the hydrogen bonding network to be established. In this model, pressure acts as a catalyst and provides a destructuring effect, breaking the fibers original structure and with an effect on the amorphization of cellulose. Temperature and moisture are responsible for the self-bonding effect and the mechanical properties obtained through hydrogen bonding and possibly co-crystallization at different particles interface.

Yet, the role of water is contradictory, a minimum of moisture is necessary in order to lower the Tg of cellulose, but free water also seemed to accumulate in the inner layers of the material, hindering the establishment of fiber-fiber hydrogen bonding, and building up steam pressure, which in case provoked the delamination of the samples.

Some additional data were collected to complete to evaluation of the compacted cellulose materials, ageing tests were performed for 2 months without modification of the mechanical properties after 10 days, the water resistance properties were measured and the sensitivity of the material to moisture and water was confirmed.

Experiments were thus run in order to investigate to possibility of adding fatty compounds to cellulose prior to molding which would provide a hydrophobating effect. After a quick mapping of the potential usable fatty compounds, a deeper study was run on the grafting of octanoïc acid (using the acid and the anhydride) on cellulose during the molding process. Pretreatments (high pressure homogenizer and solvent exchange) were necessary to improve the contact between the grafts and cellulose, and the grafting was finally confirmed by CPG analysis. Degree of substitution of $4.8\ 10^{-2}$ and $3.9\ 10^{-2}$ were obtained under the best conditions with respectively the anhydride and the fatty acid. The grafted cellulose powder exhibited a more hydrophobic character which hopefully could widen the application field for this kind of materials.

A good correlation was obtained between the grafting yield and the decrease of the mechanical properties. An hypothesis for this was that the grafting of side chains on the cellulose backbone provoked distortions in the establishment of a hydrogen bonding network, which consequently lowered the mechanical properties.

Based on the cellulose results, a panel of raw lignocellulosic materials (crop residues and by products of crop agroprocessing) were processed into test specimens and the influence of the plant composition and physical properties (particle size, form factor, apparent density) on the mechanical properties and water resistance was investigated using cross correlation and principle component analyses. In addition, flow tests were conducted in order to start the investigation about the rheological behavior of the raw plant materials. The equipment used in this thesis that were validated for cellulose molding showed limits in processing raw plant materials: too much flowability conducted to extrusion of materials between the punches and die, which conducted to the blockage of the mold. Materials with a too low apparent density

were also not possible to mold because of impossible charging and heterogeneity. About 1/3 of the desired plant materials were discarded which drastically reduced the diversity of compositions and physical properties. Besides, none of the specimen was able to exhibit mechanical properties close to what was obtained on cellulose.

Nevertheless, the statistical analysis was computed on the moldable materials, and the significance was not very high i.e. a lot of variance was not explained. Some correlations were detected between cellulose and lignin contents, water resistance and mechanical properties positively, and extractives, ashes, proteins and hemicelluloses negatively. This draws the profile of the desirable plant materials candidate for obtaining improved results in compaction molding.

In order to cover the limits of compaction molding, an alternative process was proposed based on the flow test apparatus: transfer molding. Some 3D parts were successfully produced, and a tool was designed in order to mold tensile and bending specimen but unfortunately too much technical troubles arose and these experiments could only be started.

Technological mastery was confirmed to be a key point all along this work. Despite all the trials, which led to significant improvements on the molding equipment, a lot of work would still be required: on a scientific point of view because the technique should not impact the results as it did in this work, on an industrial point of view, because major improvement are required before considering industrial applications.

The major part of this thesis was dedicated to cellulose, which provided mind-blowing results and conducted to significant scientific research and discussions on the mechanisms of cohesion at stake during compaction under high temperature.

In a second time, it was highly desirable to study the influence of the chemical composition of the plant materials and other physical properties on the molded specimens. The choice about the molding parameters was made when it came to switching from the cellulose to the native plant materials and it naturally was based on cellulose results. These conditions, as well as the technological limits majorly influenced the conclusion which provided mixed results.

3D molding were performed in the early stages of this work, flowability was rapidly noticed to influence the possibility of molding, and mixing plants with high flowability (like sunflower seed cake) with low flowability plants (like miscanthus or wheat straw for instance) improved the results. The use of coffee waste in small proportion was observed to provide a desirable lubricant effect. The improvement of the overall flowability was also made with temperature, which was concluded to majorly influence the molding results and strength of the 3D specimens. Unfortunately, steam delamination came in, and was observed to be a result of material composition and molding parameters. The concomitant influence of all these parameters is at the heart of the problematic of this whole project, which could occupy the work of a whole thesis. Hopefully, this thesis work provides a strong basis for the future developments of these innovative molding technique and materials.

Prospects

Despite the high volume of data generated during this thesis, a lot of grey zones still remained, which on investigations would make an obvious continuum to this thesis work. The prospects can be sorted in 3 ordered levels: at first, (1) technological improvements can be made for the high-pressure molding process to become more reliable and versatile, which will permit to improve the (2) quality of the scientific data and increase the knowledge about the physico-chemical phenomena involved in the consolidation process. Technological

mastery and knowledge about the material could then be used towards (3) the improvement of the material properties, aiming at an industrialization.

Technical prospects needed to improve the process of uniaxial high-pressure thermocompression molding:

* Much troubles were encountered because of heterogeneity in the samples while charging the material in the mold (Figure II - 9). Most of the scattering probably came from this manual step that was highly operator dependent and not very reproducible. The possibility of performing reproducible and reliable homogeneity of the specimens would be a major improvement of the technique. In the field of board processing, automatic processes exist that spread the material evenly in the frame / mold. This problem of homogeneous filling was also encountered some time ago in the processing of pharmaceutical tablets: automatic feed hopper were used for even repartition, but then the flowing properties of the powder was problematic, partially solved with the employment of lubricants like stearate magnesium, or by precompacting the excipient to pellets which increased drastically the hopper flow but caused additional troubles in tablets cohesion.

* There could be a possibility of precompressing the material before entering the mold (especially useful for the low density materials like Carded hemp or Cellulose wadding).

* The extrusion occurring between the punches and dies of the molds was a serious limit to the technique. Reducing the mechanical slack in order to prevent extrusion conducted to another limit: the seizing of the molds (Figure II - 22). Some work was made on the mechanical slack needed and different alloys tested, the employment of gaskets was tested but none of these investigations allowed to mold materials with high flowability (Chapter II).

* Delamination was another important limit of the technique, which was partially solved upon moisture reduction (Table III - 7). Yet, the density patterns acquired in X-ray tomography (e.g. Figure III - 34) suggested the existence of a porous core (assumed containing more water, Figure II - 15). An apparatus could be designed in order to proceed to the degasing of the interior of the material during the molding using microperforation for instance. Such a capacity would be particulary useful in 3D molding where water would probably be needed to guarantee flow ability and steam thus being highly problematic.

* These technological improvements (and others) should be directed towards the capacity of producing results independently from the technique. In other words, being able to form test specimens under uniaxial high pressure thermo compression from whatever starting materials.

Scientific prospects for the increase of knowledge about the physico-chemical phenomena occurring during molding and explaining the consolidation process:

* The better qualification of the delamination process is desirable. A quantitative scale should be found in order to study the correlations between materials parameters and operating conditions. The water sorption isotherms could be used to quantify the water / polymer interactions according to the temperature, using for example the parameters of Guggenheim–Andersen–de Boer (GAB) like presented in the materials and methods VI.2.C. An interesting experiment would be using materials (e.g. cellulose) of different moisture contents and spread them in layers along the thickness of the specimen, for instance, dry material in the core layer, and moist materials on the outside.

* The delamination could be linked with the thickness of the material and also the volume / surface ratio of the molded parts in order to better understand this phenomenon. These results would participate in validating the hypothesis formulated in Chapter III concerning the strength of the material being mostly coming from the skin and the disappearing of delamination under 8% and 250°C conditions.

* The second hypothesis formulated concerned the mechanisms of cohesion, being based on the establishment of hydrogen bonding, which to a high extent would be responsible for crystallization of the cellulose samples at the surface preferably. A method for systematic analyses of the samples crystallinity should be used and the crystallinity changes within the thickness of the samples measured under different operating conditions and compared to X-ray tomography porosity patterns. There is a high possibility that these two parameters would not be directly correlated (III.7).

* There is still a research quest for measuring the Tg of cellulose, because the whole concept of amorphous phase for cellulose remains quite uncertain. The influence of pressure on the Tg was thought to be explaining the densification process in the work of Jallabert (PhD thesis, 2014) and gave satisfactory explanations for the mechanisms of cohesion and the mechanical properties obtained in this thesis. Yet, many experiments could be run in order to validate the hypotheses formulated in these two thesis. For instance, experiments close to those found in the literature (applied to board molding and concerning the Tg of lignin) for measuring the local temperature within the compacted material during the molding and correlation of the T-Tg gradient to the local strength of the material would be major.

* Data collected by the CERMAV showed the destructuring effect of high pressure molding of cellulose crystallinity, for which some reports were consistent in the literature. The DP might also probably be alterated and could be an interesting parameter to measure, and to put in relation to the mechanical properties (even though the evaluation of the molecular mass distribution of cellulose is already is challenge by itself).

* In the context of the hydrophobation studies, much work is needed in explaining the effect of the different fatty compounds added to cellulose (IV.1). In IV.2, the grafting was confirmed but on drastic conditions of molding, which needs to be varied again, it is probable that such long processing time is not needed to perform the reaction. The influence of the molding time (i.e. reaction time) would be interesting to study.

* The functional properties of hydrophobated materials observed in some experiments could be further studied in order to evaluate the part of responsibility of adsorbed fatty compounds and grafting respectively. For instance, in IV.2, the hydrophobation effect was measured on the powder but not on the material itself which needs to be done. The water properties of modified compacted specimens could be tested right out of the pressing machine, then washed for rinsing unreacted materials, tested again etc.

* There is much hope in working on layered material (grafted materials on the outside and non-grafted in the inside) for solving the problem of the loss of the mechanical properties due to the grafting. Such a method could be problematic as we demonstrated that most of the strength comes from the skin of the material, and that grafted materials had mechanical properties lowered in the proportion of the grafting yield. To avoid this problem, there could be a possibility of molding specimen and further coat it either with modified powder, or make the reaction on the surface of a premolded specimen.

* Transfer molding was supposed to be a promising technique, prototyping made in this thesis were almost successful in providing tools for studying the flow ability and transfer molding of raw plant materials. These analyses should be carried on, studying the influence of extrusion dies length and diameters, angles, and establishing the link between extrusion

conditions, the other parameters (temperature, moisture) and the composition / morphology of the raw plant materials processed.

Prospects directed towards the improvement of the bio-based, simple and elegant material obtained:

With improved technological mastery and knowledge about the cohesion mechanisms and impact of the composition and morphology of the plant materials used, an enormous model could be designed. The entry variables would be the plant materials composition, morphology, operating conditions (extrusion or compaction) and output variables would be the properties of the molded materials (mechanical, morphology, water resistance, ageing behavior etc.). Actually two models could be established, one for compaction and one of transfer. This model would be able to predict and optimize the properties of materials obtained from a known biomass, but also using the opposite approach, based on industrial specifications (in terms of strength, water resistance, colour, etc.) the model could predict what materials and conditions should be used to fulfill the requirements.

The collaboration of scientists and industrials from different fields (ceramic, pharmacy, board processing, metal sheets stamping etc.) would probably be a necessary condition to the future development and hope for industrialization.

Scientific contributions

Open access publications

* High Pressure Compression-Molding of α-Cellulose and Effects of Operating Conditions
Thibaud Pintiaux, David Viet, Virginie Vandenbossche, Luc Rigal and Antoine Rouilly
In: Materials 2013, 6(6), 2240-2261.
Submitted: 22 January 2013 / Revised 12 March 2013 / Accepted 21 May 2013 / Published 30 May 2013.

* Binderless Materials Obtained by Thermo-Compressive Processing of Lignocellulosic Fibers: A Comprehensive Review.
Thibaud Pintiaux, David Viet, Virginie Vandenbossche, Luc Rigal and Antoine Rouilly
In: Bioresources 2015, 10 (1)
Submitted: August 4, 2014 / Revised September 4, 2014 / Accepted December 11, 2014 / Published: January 16, 2015.

* High-Pressure Driven Solvent-Free Heterogeneous Phase Esterification of Cellulose
Thibaud Pintiaux, Feriel Laourine, Guadalupe Vaca-medina, Antoine Rouilly and Jerome Peydecastaing
In: Bioresources.
Submitted: November 17, 2014, under review.

International conferences

* High pressure compression molding of pure cellulose as a potential way towards the production of biomaterials: pressure-volume-temperature behavior, mechanical properties, microstructure changes and operating conditions study.
Thibaud Pintiaux, Antoine Rouilly, Bastien Jallabert, Guadalupe Vaca-medina
3rd European Polysaccharide Network of Excellence (EPNOE 2013): "Polysaccharides and polysaccharide-derived products, from basic science to applications", October 21 – 26, 2013 Nice (France).

Posters

* Effects of a high pressure compression-molding process and its parameters on the mechanical properties of compressed α-cellulose
Thibaud Pintiaux, Guadalupe Vaca-medina, David Viet, Luc Rigal, Antoine Rouilly
3rd International Cellulose Conference (ICC 2012), October 10 – 12, 2012, Sapporo (Japan).

* Effect of pre-treatment in thermo-mechanico-chemical reactor on self-bonding capacity of lignocellulosic materials.
Assad Mogni, Thibaud Pintiaux, Joël Albet, Antoine Rouilly, Pierre-Yves Pontalier
9th International Conference on Renewable Resources & Biorefineries (RRB9), June 5 – 7, 2013, Antwerp (Belgium).

* Valorization of palm date by-products as self-bonded materials
Nabila Saadaoui, Antoine Rouilly, K. Fares, Thibaud Pintiaux, Luc Rigal
8th International Conference on Renewable Resources and Biorefineries (RRB8), June 8 – 10, 2011, Bruges (Belgium).

Acknowledgments

I would like to sincerely thank the jury's members for their participation in judging my work and make it improve, especially the referees for their meticulous examination. The ANRT and The Green Factory (Grégoire, Martin, David) who made this work possible with the financial support and collaboration. For the warm welcome, professional skills, confortable everyday work experience and cheerfulness, I would like to thank all the LCA staff members that I have been seeing during these 4 years. Thanks to the HYPOMOBB team, Bastien, Lupita, Jerome, Virginie. Particular thanks to Carlos, for the sympathy, contact easiness and freedom of speech, support and wise advises. I could not have produced all that scrap metal during this thesis without the help of the INP mechanic workshop: I would like to express my sincere thanks to all the staff there, Gilles, Alain, Rafik, Vincent and the others. Thanks for all the advices, good and funny times and of course tools and molds machining. This was such a great opportunity to work with you as we did, and be sure that you put on some serious bricks to assemble this work. For the work that was not possible at the INP workshop especially when electro erosion was needed, I have found awesome skills and professionalism from CEE and its CEO Christian who greatly contributed to the comprehension on the seizing that we were facing. For their hard work and adaptability, Mathieu, Feriel and Floréal, the three interns I have had under supervision. Thanks to Manuel from IMFT for the X-ray tomography, Laurent from the CERMAV for the RMN crystallinity measurements. Many thanks to the JSPS (Japan Society for the Promotion of Science), Miki-san, Kanayama-sensei and all the AIST staff members (Aishi Institute of Science and Technology – host laboratory in summer 2013 in Japan) for their unbelievable kindness, the inspiration and this great opportunity of discovering this awesome country. Thanks to Luc for his precious advice all along the thesis. Last but not least Antoine, thank you so much for the continuous support, ideas, freedom in my research, for the trust that you put in me since the first day.

Remerciements

Je souhaite sincèrement remercier les membres du jury pour leur participation à juger mon travail et contribuer à le faire grandir, et particulièrement les rapporteurs pour leur travail minutieux. Merci à The Green Factory (Grégoire, Martin, David) et à l'ANRT pour le soutien financier indispensable à tout travail de recherche. Merci à toute l'équipe du LCA pour l'accueil chaleureux, les compétences et leur contribution à maintenir un environnement de travail confortable dans la bonne humeur durant ces 4 ans. Merci à toute l'équipe HYPMOBB, Bastien, Lupita, Jérome, Virginie. Merci particulièrement à Carlos, pour la sympathie, la facilité de contact, le franc-parler, le soutien et les bons conseils. Merci au personnel de l'atelier de l'INP sans qui il m'aurait été impossible de réaliser autant de « presse-papiers », Gilles, Alain, Rafik, Vincent, merci pour les bons moments et pour tout le soutien « technologique » sur la création des outils et moules. Mes travaux de thèse ont en partie été possibles grâce à vous, et ça a été une véritable aubaine de pouvoir travailler avec vous comme nous l'avons fait. Pour tout ce qui n'était pas possible de réaliser à l'atelier (notamment l'électro-érosion) j'ai trouvé auprès de CEE un complément idéal, merci également au directeur de CEE Christian qui a contribué à la compréhension sur les problèmes de grippage rencontrés tout au long de la thèse. Merci aux stagiaires, Mathieu, Fériel et Floréal pour leur travail acharné et leurs facultés d'adaptations. Merci à Manuel de l'IMFT pour la tomographie rayon X, et Laurent du CERMAV pour les données de cristallinité en RMN. Merci à la JSPS (Japan Society for the Promotion of Science), Miki-san, Kanayama-sensei, et les autres membres de l'AIST (Aishi Institute of Science and Technology - laboratoire d'accueil lors du stage doctoral effectué au Japon à l'été 2013) pour la gentillesse, l'inspiration et cette immense opportunité de découvrir ce merveilleux pays. Merci à Luc pour les précieux conseils tout au long de la thèse. Et enfin, merci à Antoine, pour le soutien que tu m'as apporté tout au long de ce travail, les idées, la liberté que tu m'as laissé, pour avoir cru en moi dès le début.

References cited

Abe, Kentaro, Shinichiro Iwamoto, and Hiroyuki Yano. 2007. Obtaining cellulose nanofibers with a uniform width of 15 nm from wood. *Biomacromolecules* 8: 3276–3278.

Akande, O. F., M. H. Rubinstein, P. H. Rowe, and J. L. Ford. 1997. Effect of compression speeds on the compaction properties of a 1:1 paracetamol-microcrystalline cellulose mixture prepared by single compression and by combinations of pre-compression and main-compression. *International Journal of Pharmaceutics* 157: 127–136.

Álvarez, Catalina, Benjamín Rojano, Ovidio Almaza, Orlando J. Rojas, and Piedad Gañán. 2011. Self-bonding boards from plantain fiber bundles after enzymatic treatment: adhesion improvement of lignocellulosic products by enzymatic pre-treatment. *Journal of Polymers and the Environment* 19: 182–188.

Ando, Motoe, and Masatoshi Sato. 2009. Manufacture of plywood bonded with kenaf core powder. *Journal of Wood Science* 55: 283–288.

Ando, Motoe, and Masatoshi Sato. 2010. Evaluation of the self-bonding ability of sugi and application of sugi powder as a binder for plywood. *Journal of Wood Science* 56: 194–200.

Anglès, M. N., F Ferrando, X Farriol, and J Salvadó. 2001. Suitability of steam exploded residual softwood for the production of binderless panels. Effect of the pre-treatment severity and lignin addition. *Biomass and Bioenergy* 21: 211–224.

Anglès, M. N., J. Reguant, D. Montané, F. Ferrando, X. Farriol, and J. Salvadó. 1999. Binderless composites from pretreated residual softwood. *J. Appl. Polym. Sci.* 73: 2485–2491.

Ashby, Michael F. 2012. *Materials and the Environment: Eco-informed Material Choice*. Elsevier.

Back, Ernst L. 1987. The Bonding Mechanism in Hardboard Manufacture. *Holzforschung - International Journal of the Biology, Chemistry, Physics and Technology of Wood* 41: 247–258.

Björkman, Anders. 1956. Studies on finely divided wood. Part 1. Extraction of lignin with neutral solvents. *Svensk papperstidning* 59: 477–485.

Boon, Jia Geng, Rokiah Hashim, Othman Sulaiman, Salim Hiziroglu, Tomoko Sugimoto, and Masatoshi Sato. 2013. Influence of processing parameters on some properties of oil palm trunk binderless particleboard. *European Journal of Wood and Wood Products* 71: 583–589.

Boonstra, Michiel J., and Bôke Tjeerdsma. 2006. Chemical analysis of heat treated softwoods. *Holz als Roh- und Werkstoff* 64: 204–211.

Bouajila, J., A. Limare, C. Joly, and P. Dole. 2005. Lignin plasticization to improve binderless fiberboard mechanical properties. *Polymer Engineering & Science* 45: 809–816.

Bundhoo, Zumar M. A., Ackmez Mudhoo, and Romeela Mohee. 2013. Promising Unconventional Pretreatments for Lignocellulosic Biomass. *Critical Reviews in Environmental Science and Technology* 43: 2140–2211.

Célino, Amandine, Sylvain Freour, Frederic Jacquemin, and Pascal Casari. 2014. The hygroscopic behavior of plant fibers: a review. *Polymer Chemistry* 1: 43.

Chinga-Carrasco, Gary. 2011. Cellulose fibres, nanofibrils and microfibrils: The morphological sequence of MFC components from a plant physiology and fibre technology point of view. *Nanoscale Research Letters* 6: 417.

Chow, Poo. 1975. WO 3927235. Reconstituted Board Products from Plant-Fiber Residues.

Cristescu, Carmen, and Olov Karlsson. 2013. Changes in Content of Furfurals and Phenols in Self-Bonded Laminated Boards. *BioResources* 8: 4056–4071.

Van Dam, Jan E.G., Martien J.A. van den Oever, and Edwin R.P. Keijsers. 2004. Production process for high density high performance binderless boards from whole coconut husk. *Industrial Crops and Products* 20: 97–101.

Van Dam, Jan E.G., Martien J.A. van den Oever, Wouter Teunissen, Edwin R.P. Keijsers, and Aurora G. Peralta. 2004. Process for production of high density/high performance binderless boards from whole coconut husk: Part 1: Lignin as intrinsic thermosetting binder resin. *Industrial Crops and Products* 19: 207–216.

Ding, Shi-You, Shuai Zhao, and Yining Zeng. 2014. Size, shape, and arrangement of native cellulose fibrils in maize cell walls. *Cellulose* 21: 863–871.

Donaldson, Lloyd. 2007. Cellulose microfibril aggregates and their size variation with cell wall type. *Wood Science and Technology* 41: 443–460.

Döpfner, Horst, Martin Ernegg, and Robert Bramsteidl. 1997. Process for producing workpieces and molded pieces out of cellulose and/or cellulose-containing fiber material.

Eichhorn, S. J., C. A. Baillie, N. Zafeiropoulos, L. Y. Mwaikambo, M. P. Ansell, A. Dufresne, K. M. Entwistle, et al. 2001. Review: Current international research into cellulosic fibres and composites. *Journal of Materials Science* 36: 2107–2131.

Euring, Markus, Martin Rühl, Nina Ritter, Ursula Kües, and Alireza Kharazipour. 2011. Laccase mediator systems for eco-friendly production of medium-density fiberboard (MDF) on a pilot scale: Physicochemical analysis of the reaction mechanism. *Biotechnology Journal* 6: 1253–1261.

Evon, Philippe, Virginie VanDenBossche, Pierre-Yves Pontalier, and Luc Rigal. 2010. Thermo-mechanical behaviour of the raffinate resulting from the aqueous extraction of sunflower whole plant in twin-screw extruder: manufacturing of biodegradable agromaterials by thermo-pressing. *Advanced Materials Research* 112: 63–72.

Evon, Philippe, Virginie Vandenbossche, and Luc Rigal. 2012. Manufacturing of renewable and biodegradable fiberboards from cake generated during biorefinery of sunflower whole plant in twin-screw extruder: Influence of thermo-pressing conditions. *Polymer Degradation and Stability* 97. 3rd International Conference on Biodegradable and Biobased Polymers (BIOPOL-2011) - Strasbourg 2011: 1940–1947.

Faruk, Omar, Andrzej K. Bledzki, Hans-Peter Fink, and Mohini Sain. 2012. Biocomposites reinforced with natural fibers: 2000–2010. *Progress in Polymer Science* 37. Topical Issue on Polymeric Biomaterials: 1552–1596.

Fink, Hans Peter, Johannes Ganster, and André Lehmann. 2014. Progress in cellulose shaping: 20 years industrial case studies at Fraunhofer IAP. *Cellulose* 21: 31–51.

French, Alfred D., Noelie R. Bertoniere, R. Malcolm Brown, Henri Chanzy, Derek Gray, Kazuyuki Hattori, and Wolfgang Glasser. 2000. Cellulose. In *Kirk-Othmer Encyclopedia of Chemical Technology*. John Wiley & Sons, Inc.

Gao, Zhenhua, Xiang Ming Wang, Hui Wan, and Gilles Brunette. 2011. Binderless panels made with black spruce bark. *BioResources* 6: 3960–3972.

Gaudin, S., D. Lourdin, D. Le Botlan, J.L. Ilari, and P. Colonna. 1999. Plasticisation and mobility in starch-sorbitol films. *Journal of Cereal Science* 29: 273–284.

Gelbke, Heinz-Peter, Thomas Göen, Mathias Mäurer, and Sandra I. Sulsky. 2009. A review of health effects of carbon disulfide in viscose industry and a proposal for an occupational exposure limit. *Critical Reviews in Toxicology* 39 Suppl 2: 1–126.

Gfeller, B., M. Zanetti, M. Properzi, A. Pizzi, F. Pichelin, M. Lehmann, and L. Delmotte. 2003. Wood bonding by vibrational welding. *Journal of Adhesion Science and Technology* 17: 1573–1589.

Gindl, W., and J. Keckes. 2005. All-cellulose nanocomposite. *Polymer* 46: 10221–10225.

Glasser, Wolfgang G., Rajai H. Atalla, John Blackwell, R. Malcolm Brown, Walther Burchard, Alfred D. French, Dieter O. Klemm, and Yoshiharu Nishiyama. 2012. About the structure of cellulose: debating the Lindman hypothesis. *Cellulose* 19: 589–598.

Golon, Agnieszka, and Nikolai Kuhnert. 2012. Unraveling the Chemical Composition of Caramel. *Journal of Agricultural and Food Chemistry* 60: 3266–3274.

Gosselink, Richard J.A., Dam Jan E.G. van, Jong Ed de, Göran Gellerstedt, Elinor L. Scott, and Johan P.M. Sanders. 2011. Effect of periodate on lignin for wood adhesive application. *Holzforschung* 65: 155–162.

Hashim, Rokiah, Wan Noor Aidawati Wan Nadhari, Othman Sulaiman, Fumio Kawamura, Salim Hiziroglu, Masatoshi Sato, Tomoko Sugimoto, Tay Guan Seng, and Ryohei Tanaka. 2011. Characterization of raw materials and manufactured binderless particleboard from oil palm biomass. *Materials & Design* 32: 246–254.

Hashim, Rokiah, Norhafizah Saari, Othman Sulaiman, Tomoko Sugimoto, Salim Hiziroglu, Masatoshi Sato, and Ryohei Tanaka. 2010. Effect of particle geometry on the

properties of binderless particleboard manufactured from oil palm trunk. *Materials & Design* 31: 4251–4257.

Hashim, Rokiah, Norafizah Said, Junidah Lamaming, Mohana Baskaran, Othman Sulaiman, Masatoshi Sato, Salim Hiziroglu, and Tomoko Sugimoto. 2011. Influence of press temperature on the properties of binderless particleboard made from oil palm trunk. *Materials & Design* 32: 2520–2525.

Henriksson, Marielle, Lars A. Berglund, Per Isaksson, Tom Lindström, and Takashi Nishino. 2008. Cellulose Nanopaper Structures of High Toughness. *Biomacromolecules* 9: 1579–1585.

Hidayat, H., E. R. P. Keijsers, U. Prijanto, J. E. G. van Dam, and H. J. Heeres. 2014. Preparation and properties of binderless boards from Jatropha curcas L. seed cake. *Industrial Crops and Products* 52: 245–254.

Hiller, Alma, John Plazin, and Donald D. Van Slyke. 1948. A Study of Conditions for Kjeldahl Determination of Nitrogen in Proteins Description of Methods with Mercury as Catalyst, and Titrimetric and Gasometric Measurements of the Ammonia Formed. *Journal of Biological Chemistry* 176: 1401–1420.

Hon, David N.-S. 1995. *Chemical Modification of Lignocellulosic Materials*. CRC Press.

Howard, Guy C., and Lloyd T. Sandborn. 1937. US2080077. Molded products and process of making same.

Hsu, W. E., Dr W. Schwald, Mrs J. Schwald, and Mr J. A. Shields. 1988. Chemical and physical changes required for producing dimensionally stable wood-based composites. *Wood Science and Technology* 22: 281–289.

Iguchi, M., S. Yamanaka, and A. Budhiono. 2000. Bacterial cellulose—a masterpiece of nature's arts. *Journal of Materials Science* 35: 261–270.

Imanishi, Hiroshi, Naho Soma, Kazutoshi Takeuchi, Hideaki Sugino, and Kozo Kanayama. 2005a. Flow Properties of Wood Powder-Plastic Mixture II. *Mokuzai Gakkaishi* 51: 172–179.

Imanishi, Hiroshi, Naho Soma, Osamu Yamashita, Tsunehisa Miki, and Kozo Kanamaya. 2005. Effect of production conditions of wood powder on bending properties of wood powder molding material without adhesive. *JSME International Journal Series A Solid Mechanics and Material Engineering* 48: 432–436.

Imanishi, Soma, Takeuchi, Sugino, and Kanayama. 2005b. Flow Properties of Wood Powder-Plastic Mixture I. *Mokuzai Gakkaishi* 51: 166–171.

Ioelovich, Michael, Alex Leykin, and Oleg Figovsky. 2010. Study of cellulose paracristallinity. *BioResources* 5: 1393–1407.

Irvine, G. M. 1985. The significance of the glass transition of lignin in thermomechanical pulping. *Wood Science and Technology* 19: 139–149.

ISO 178. 2010. Plastics: Determination of flexural properties.

ISO 527-2. 1993. Plastics: Determination of tensile properties -- Part 2: Test conditions for moulding and extrusion plastics.

ISO 3167. 2002. Plastics: Multipurpose test specimens.

Ito, Youichi, Mitsuhiko Tanahashi, Mikiji Shigematsu, and Yoshihiko Shinoda. 1998. Compressive-molding of wood by figh-pressure steam-treatment: part 2. mechanism of permanent fixation. *Holzforschung* 52: 217–221.

Ito, Y., M. Tanahashi, M. Shigematsu, T. Shinoda, and C. Ohta. 1998. Compressive-molding of wood by high-pressure steam-treatment: Part 1. Development of compressively molded squares from thinnings. *Holzforschung* 52: 211–216.

Jallabert, Bastien, Guadalupe Vaca-Medina, Sophie Cazalbou, and Antoine Rouilly. 2013. The pressure–volume–temperature relationship of cellulose. *Cellulose* 20: 2279–2289.

JIS A 5908,. 2003: Particleboards. Japanese Standard Association, 1–24 Akasaka, 4 Minato–ku, Tokyo 107, Japan.

Kelly, M. W. 1977. Critical literature review of relationships between processing parameters and physical properties of particleboard. *USDA Forest Service General Technical Report FPL (USA)*.

Kim, Jae-Young, Hyewon Hwang, Shinyoung Oh, Yong-Sik Kim, Ung-Jin Kim, and Joon Weon Choi. 2014. Investigation of structural modification and thermal characteristics of lignin after heat treatment. *International Journal of Biological Macromolecules* 66: 57–65.

Kjeldahl, J. 1883. A new method for the estimation of nitrogen in organic compounds. *Z. Anal. Chem.* 22: 366–382.

Laemsak, Nikhom, and Motoaki Okuma. 2000. Development of boards made from oil palm frond II: properties of binderless boards from steam-exploded fibers of oil palm frond. *Journal of Wood Science* 46: 322–326.

Lamaming, Junidah, Othman Sulaiman, Tomoko Sugimoto, Rokiah Hashim, Norafizah Said, and Masatoshi Sato. 2013. Influence of chemical components of oil palm on properties of binderless particleboard. *BioResources* 8: 3358–3371.

Lavoine, Nathalie, Julien Bras, and Isabelle Desloges. 2014. Mechanical and barrier properties of cardboard and 3D packaging coated with microfibrillated cellulose. *Journal of Applied Polymer Science* 131: unavailable pages.

Lebreton, L. C. -M., S. D. Greer, and J. C. Borrero. 2012. Numerical modelling of floating debris in the world's oceans. *Marine Pollution Bulletin* 64: 653–661.

Li, J, G Henriksson, and G Gellerstedt. 2007. Lignin depolymerization/repolymerization and its critical role for delignification of aspen wood by steam explosion. *Bioresource technology* 98: 3061–3068.

Liu, Hongling, Jin Shang, Xianqing Chen, Frederick A. Kamke, and Kangquan Guo. 2014. The influence of thermal-hydro-mechanical processing on chemical characterization of Tsuga heterophylla. *Wood Science and Technology* 48: 373–392.

Lo, J., and S. V. Hoa. 2006. *Design, Manufacturing and Applications of Composites: Proceedings of the Sixth Joint Canada-Japan Workshop on Composites*. DEStech Publications, Inc.

Marchessault, R. H., Suzanne Coulombe, Hiromichi Morikawa, and Danielle Robert. 1982. Characterization of aspen exploded wood lignin. *Canadian Journal of Chemistry* 60: 2372–2382.

Mason, William H. 1926a. US 157860. Process and apparatus for disintegration of wood and the like.

Mason, William H. 1926b. US 1586159. Low-temperature explosion process of disintegrating wood and the like.

Mason, William H. 1928. US 1663504. Press-dried structural insulating board and process of making same.

Mason, William H., Robert M. Boehm, and Koonce Wilbur Euclid. 1937. US 2080078. Molding composition and process of making same.

Matsuura, Norio, Masashi Narita, Tsunehisa Miki, Kozo Kanayama, and Norio Takakura. 2012. Attempt on improving property of highly-densified biomass resources for renewable energy. *Int. J. Comput. Appl. Technol.* 45: 93–97.

Mellerowicz, Ewa J., Peter Immerzeel, and Takahisa Hayashi. 2008. Xyloglucan: The Molecular Muscle of Trees. *Annals of Botany* 102: 659–665.

Micard, V., R. Belamri, M.H. Morel, and S. Guilbert. 2000. Properties of chemically and physically treated wheat gluten. *J. Agric. Food Chem.* 48: 2948–2953.

Miki, Tsunehisa, Hiroyuki Sugimoto, and Kozo Kanayama. 2007. Thermoplastic behavior of wood powder compacted materials. *Journal of Materials Science* 42: 7913–7919.

Miki, Tsunehisa, Norio Takakura, Takashi Iizuka, Katsuhiko Yamaguchi, and Kouzou Kanamaya. 2003. Possibility of extrusion of wood powders. *JSME International Journal Series A Solid Mechanics and Material Engineering* 46: 371–377.

Miki, Tsunehisa, Kazutoshi Takeuchi, Hiroyuki Sugimoto, and Kozo Kanayama. 2008. Material development from wood powder without adhesive by vapor steaming compaction process. *Journal of Materials Processing Technology* 199: 396–401.

Miki, T., K. Takeuchi, H. Sugimoto, and K. Kanayama. 2007. Performance Study of compact wood powder material processing for improved impact characteristics aiming at substitute for plastics. *Journal of Materials Processing Technology* 192–193: 422–427.

Mobarak, Fardous, Yehia Fahmy, and Hans Augustin. 1982. Binderless lignocellulose composite from bagasse and mechanism of self-bonding. *Holzforschung - International Journal of the Biology, Chemistry, Physics and Technology of Wood* 36: 131.

Murugan, Pulikesi, Nader Mahinpey, Keith E. Johnson, and Malcolm Wilson. 2008. Kinetics of the Pyrolysis of Lignin Using Thermogravimetric and Differential Scanning Calorimetry Methods. *Energy & Fuels* 22.

Nadhari, Wan Noor Aidawati Wan, Rokiah Hashim, Othman Sulaiman, Masatoshi Sato, Tomoko Sugimoto, and Mohd Ezwan Selamat. 2013. Utilization of oil palm trunk waste for manufacturing of binderless particleboard: optimization study. *BioResources* 8: 1675–1696.

Newman, Roger H. 2004. Carbon-13 NMR evidence for cocrystallization of cellulose as a mechanism for hornification of bleached kraft pulp. *Cellulose* 11: 45–52.

Niklas, Karl J., Hanns-Christof Spatz, and Julian Vincent. 2006. Plant biomechanics: an overview and prospectus. *American Journal of Botany* 93: 1369–1378.

Nilsson, Helena, Sylvain Galland, Per Tomas Larsson, E. Kristofer Gamstedt, Takashi Nishino, Lars A. Berglund, and Tommy Iversen. 2010. A non-solvent approach for high-stiffness all-cellulose biocomposites based on pure wood cellulose. *Composites Science and Technology* 70: 1704–1712.

Nishino, Takashi, Ikuyo Matsuda, and Koichi Hirao. 2004. All-Cellulose Composite. *Macromolecules* 37: 7683–7687.

Nishiyama, Yoshiharu, Junji Sugiyama, Henri Chanzy, and Paul Langan. 2003. Crystal structure and hydrogen bonding system in cellulose I(alpha) from synchrotron X-ray and neutron fiber diffraction. *Journal of the American Chemical Society* 125: 14300–14306.

Nogi, Masaya, Shinichiro Iwamoto, Antonio Norio Nakagaito, and Hiroyuki Yano. 2009. Optically Transparent Nanofiber Paper. *Advanced Materials* 21: 1595–1598.

Nonaka, Sho, Kenji Umemura, and Shuichi Kawai. 2013. Characterization of bagasse binderless particleboard manufactured in high-temperature range. *Journal of Wood Science* 59: 50–56.

Ogiwara, Yoshitaka, Hitoshi Kubota, Shoichi Hayashi, and Noriko Mitomo. 1970. Temperature dependency of bound water of cellulose studied by a high-resolution NMR spectrometer. *Journal of Applied Polymer Science* 14: 303–309.

Ohad, I., and D. Danon. 1964. On the dimensions of cellulose microfibrils. *The Journal of Cell Biology* 22: 302–305.

Okuda, Nobuhisa, Keko Hori, and Masatoshi Sato. 2006a. Chemical changes of kenaf core binderless boards during hot pressing (II): effects on the binderless board properties. *Journal of Wood Science* 52: 249–254.

Okuda, Nobuhisa, Keko Hori, and Masatoshi Sato. 2006b. Chemical changes of kenaf core binderless boards during hot pressing (I): influence of the pressing temperature condition. *Journal of Wood Science* 52: 244–248.

Okuda, Nobuhisa, and Masatoshi Sato. 2004. Manufacture and mechanical properties of binderless boards from kenaf core. *Journal of Wood Science* 50: 53–61.

Okuda, Nobuhisa, and Masatoshi Sato. 2006. Water resistance properties of kenaf core binderless boards. *Journal of Wood Science* 52: 422–428.

Overend, R. P., E. Chornet, and J. A. Gascoigne. 1987. Fractionation of Lignocellulosics by Steam-Aqueous Pretreatments [and Discussion]. *Philosophical Transactions of the Royal Society of London. Series A, Mathematical and Physical Sciences* 321: 523–536.

Paes, Sabrina S., Shaomin Sun, William MacNaughtan, Roger Ibbett, Johannes Ganster, Timothy J. Foster, and John R. Mitchell. 2010. The glass transition and crystallization of ball milled. *Cellulose* 17: 693–709.

Page, D. H., F. El-Hosseiny, and K. Winkler. 1971. Behaviour of single wood fibres under axial tensile strain. *Nature* 229: 252–253.

Pantze, Anna, Olov Karlsson, and Ulla Westermark. 2007. Esterification of carboxylic acids on cellulosic material: Solid state reactions. *Holzforschung* 62: 136–141.

Park, Junyeong, Jiajia Meng, Kwang Hun Lim, Orlando J. Rojas, and Sunkyu Park. 2013. Transformation of lignocellulosic biomass during torrefaction. *Journal of Analytical and Applied Pyrolysis* 100: 199–206.

Pelaez-Samaniego, Manuel Raul, Vikram Yadama, Manuel Garcia-Perez, Eini Lowell, and Armando G. McDonald. 2014. Effect of temperature during wood torrefaction on the formation of lignin liquid intermediates. *Journal of Analytical and Applied Pyrolysis* 109: 222–233.

Pelaez-Samaniego, Manuel Raul, Vikram Yadama, Tsai Garcia-Perez, Eini Lowell, and Thomas Amidon. 2014. Effect of hot water extracted hardwood and softwood chips on particleboard properties. *Holzforschung* 68: 807–815.

Pelaez-Samaniego, Manuel Raul, Vikram Yadama, Eini Lowell, and Raul Espinoza-Herrera. 2013. A review of wood thermal pretreatments to improve wood composite properties. *Wood Science and Technology* 47: 1285–1319.

Peydecastaing, J., S. Girardeau, C. Vaca-Garcia, and M. E. Borredon. 2006. Long chain cellulose esters with very low DS obtained with non-acidic catalysts. *Cellulose* 13: 95–103.

Peydecastaing, J., C. Vaca-Garcia, and E. Borredon. 2009. Accurate determination of the degree of substitution of long chain cellulose esters. *Cellulose* 16: 289–297.

Peydecastaing, J., C. Vaca-Garcia, and E. Borredon. 2011. Bi-acylation of cellulose: determining the relative reactivities of the acetyl and fatty-acyl moieties. *Cellulose* 18: 1015–1021.

Pintiaux, Thibaud, David Viet, Virginie Vandenbossche, Luc Rigal, and Antoine Rouilly. 2013. High pressure compression-molding of α-cellulose and effects of operating conditions. *Materials* 6: 2240–2261.

Pintiaux, Thibaud, David Viet, Virginie Vandenbossche, Luc Rigal, and Antoine Rouilly. 2015. Binderless Materials Obtained by Thermo-Compressive Processing of Lignocellulosic Fibers: A Comprehensive Review. *BioResources* 10.

Privas, Edwige, Eric Felder, and Patrick Navard. 2013. Destructuration of cotton under elevated pressure. *Cellulose* 20: 1001–1011.

Quintana, Germán, Jorge Velásquez, Santiago Betancourt, and Piedad Gañán. 2009. Binderless fiberboard from steam exploded banana bunch. *Industrial Crops and Products* 29: 60–66.

Rampinelli, Gabriele, Luca Di Landro, and Toru Fujii. 2010. Characterization of biomaterials based on microfibrillated cellulose with different modifications. *Journal of Reinforced Plastics and Composites* 29: 1793–1803.

Reddy, Murali M., Singaravelu Vivekanandhan, Manjusri Misra, Sujata K. Bhatia, and Amar K. Mohanty. 2013. Biobased plastics and bionanocomposites: Current status and future opportunities. *Progress in Polymer Science* 38. Progress in Bionanocomposites: From Green Plastics to Biomedical Applications: 1653–1689.

Roffael, E., and H.-G. Hüster. 2012. Complex chemical interactions on thermo hydrolytic degradation of urea formaldehyde resins (UF-resins) in recycling UF-bonded boards. *European Journal of Wood and Wood Products* 70: 401–405.

Rose, Jocelyn K. C. 2003. *The Plant Cell Wall*. CRC Press.

Rouilly, A., and L. Rigal. 2002. Agro-materials: a bibliographic review. *Journal of Macromolecular Science, Part C: Polymer Reviews* 42: 441–479.

Rouilly, A., Rigal, L. and Vandenbossche, V. 2012. Process for manufacturing an eco-compatible solid material and eco-compatible solid material obtained. Patent WO2012069736.

Runkel, Roland, and Joachim Jost. 1956. GB743401. Method for the production of articles by moulding substances of vegetable origin under pressure and at elevated temperatures.

Saadaoui, Nabila, Antoine Rouilly, Khalid Fares, and Luc Rigal. 2013. Characterization of date palm lignocellulosic by-products and self-bonded composite materials obtained thereof. *Materials & Design* 50: 302–308.

Saari, Norhafizah, Rokiah Hashim, Othman Sulaiman, Salim Hiziroglu, Masatoshi Sato, and Tomoko Sugimoto. 2014. Properties of steam treated binderless particleboard made from oil palm trunks. *Composites Part B: Engineering* 56: 344–349.

Saito, Yukie, Miyuki Ishii, and Masatoshi Sato. 2013. The suitable harvesting season and the part of moso bamboo (Phyllostachys pubescens) for producing binderless boards. *Wood Science and Technology* 47: 1071–1081.

Sakurada, Ichiro, Yasuhiko Nukushina, and Taisuke Ito. 1962. Experimental determination of the elastic modulus of crystalline regions in oriented polymers. *Journal of Polymer Science* 57: 651–660.

Salvado, J., J.A. Velasquez, and F. Ferrando. 2003. Binderless fiberboard from steam exploded Miscanthus Sinensis : optimization of pressing and pretreatment conditions. *Wood Science and Technology* 37: 279–286.

Sasaki, Mitsuru, Bernard Kabyemela, Roberto Malaluan, Satoshi Hirose, Naoko Takeda, Tadafumi Adschiri, and Kunio Arai. 1998. Cellulose hydrolysis in subcritical and supercritical water. *The Journal of Supercritical Fluids* 13: 261–268.

Schroeter, Johannes, and Florian Felix. 2005. Melting. *Cellulose* 12: 159–165.

Segal, L., J. J. Creely, A. E. Martin, and C. M. Conrad. 1959. An Empirical Method for Estimating the Degree of Crystallinity of Native Cellulose Using the X-Ray Diffractometer. *Textile Research Journal* 29: 786–794.

Sekino, Noboru, Masafumi Inoue, Mark Irle, and Tim Adcock. 2005. The mechanisms behind the improved dimensional stability of particleboards made from steam-pretreated particles. *Holzforschung* 53: 435–440.

Shen, Kuo C. 1986. WO 4627951. Process for manufacturing composite products from lignocellulosic materials.

Singh, Tripti, Adya P. Singh, Ibrar Hussain, and Peter Hall. 2013. Chemical characterisation and durability assessment of torrefied radiata pine (Pinus radiata) wood chips. *International Biodeterioration & Biodegradation* 85: 347–353.

Sjöström, Eero, and Raimo Alen. 1998. *Analytical Methods in Wood Chemistry, Pulping, and Papermaking*. Springer Science & Business Media.

Slade, L., and H. Levine. 1991. Beyond Water Activity : Recent Advances Based on an Alternative Approach to the Assessment of Food Quality and Safety. *Critical Reviews in Food Science and Nutrition* 30: 115–360.

Van Soest, P. J., and R. H. Wine. 1967. Use of detergents in the analysis of fibrous feeds. IV. Determination of plant cell-wall constituents. *Journal of the association of official agricultural chemists* 50: 50–55.

Somerville, Chris. 2006. Cellulose Synthesis in Higher Plants. *Annual Review of Cell and Developmental Biology* 22: 53–78.

Srinivas, Kavyashree, and Krishna K. Pandey. 2012. Effect of heat treatment on color changes, dimensional stability, and mechanical properties of wood. *Journal of Wood Chemistry and Technology* 32: 304–316.

Stelte, Wolfgang, Craig Clemons, Jens K. Holm, Jesper Ahrenfeldt, Ulrik B. Henriksen, and Anand R. Sanadi. 2011. Thermal transitions of the amorphous polymers in wheat straw. *Industrial Crops and Products* 34: 1053–1056.

Suchsland, Otto, Georges E. Woodson, and Charles W. McMillin. 1987. Effect of cooking conditions on fiber bonding in dry-formed binderless hardboard. *Forest Products Journal* 11/12: 65–69.

Sun, X. F., F. Xu, R. C. Sun, P. Fowler, and M. S. Baird. 2005. Characteristics of degraded cellulose obtained from steam-exploded wheat straw. *Carbohydrate Research* 340: 97–106.

Suzuki, Satoshi, Hiroyuki Shintani, Seung-Young Park, Kyoko Saito, Nikhom Laemsak, Motoaki Okuma, and Kenji Iiyama. 1998. Preparation of binderless boards from steam exploded pulps of oil palm (elaeis guneensis jaxq.) fronds and structural characteristics of lignin and wall polysaccharides in steam exploded pulps to be discussed for self-bindings. *Holzforschung - International Journal of the Biology, Chemistry, Physics and Technology of Wood* 52: 417–426.

Szcześniak, Ludwik, Adam Rachocki, and Jadwiga Tritt-Goc. 2008. Glass transition temperature and thermal decomposition of cellulose powder. *Cellulose* 15: 445–451.

Takahashi, Isoko, Takanori Sugimoto, Yasuo Takasu, Mariko Yamasaki, Yasutoshi Sasaki, and Youji Kikata. 2010. Preparation of thermoplastic molding from steamed Japanese beech flour. *Holzforschung* 64: 229–234.

Takahashi, Isoko, Yasuo Takasu, Takanori Sugimoto, Youji Kikata, and Yasutoshi Sasaki. 2009. Thermoplastic flow behavior of steamed wood flour under heat and compression. *Wood Science and Technology* 44: 607–619.

Tanahashi, M. 1990. Characterization and degradation mechanisms of wood components by steam explosion and utilization of exploded wood. *Wood research* 77: 49–117.

Thoorens, Gregory, Fabrice Krier, Bruno Leclercq, Brian Carlin, and Brigitte Evrard. 2014. Microcrystalline cellulose, a direct compression binder in a quality by design environment—A review. *International Journal of Pharmaceutics* 473: 64–72.

Tjeerdsma, B. F., M. Boonstra, A. Pizzi, P. Tekely, and H. Militz. 1998. Characterisation of thermally modified wood: molecular reasons for wood performance improvement. *Holz als Roh- und Werkstoff* 56: 149–153.

Tunga Salthammer, Sibel Mentese, and Rainer Marutzky. 2010. Formaldehyde in the Indoor Environment. *Chemical Reviews* 110: 2536–2572.

Turbak, A. F., F. W. Snyder, and K. R. Sandberg. 1983. Microfibrillated Cellulose, a New Cellulose Product: Properties, Uses, and Commercial Potential. *J. Appl. Polym. Sci.: Appl. Polym. Symp.; (United States)* 37.

Vaca-Medina, Guadalupe, Bastien Jallabert, David Viet, Jerome Peydecastaing, and Antoine Rouilly. 2013. Effect of temperature on high pressure cellulose compression. *Cellulose* 20: 2311–2319.

Vandenbossche, Virginie, Julien Brault, Gérard Vilarem, Oscar Hernández-Meléndez, Eduardo Vivaldo-Lima, Martín Hernández-Luna, Eduardo Barzana, et al. 2014. A new lignocellulosic biomass deconstruction process combining thermo-mechano chemical action and bio-catalytic enzymatic hydrolysis in a twin-screw extruder. *Industrial Crops and Products* 55: 258–266.

Vandenbossche, Virginie, Catherine Doumeng, and Luc Rigal. 2014. Thermomechanical and Thermo-mechano-chemical Pretreatment of Wheat Straw using a Twin-screw Extruder. *BioResources* 9: 1519–1538.

Velasquez, J. A., F. Ferrando, X. Farriol, and J. Salvado. 2003. Binderless fiberboard from steam exploded Miscanthus sinensis. *Wood Science and Technology* 37: 269–278.

Velasquez, J. A., F. Ferrando, and J. Salvado. 2002. Binderless fiberboard from steam exploded Miscanthus sinensis: The effect of a grinding process. *Holz als Roh- und Werkstoff* 60: 297–302.

Widsten, Petri, Alfred Hummer, Carol Heathcote, and Andreas Kandelbauer. 2009. A preliminary study of green production of fiberboard bonded with tannin and laccase in a wet process. *Holzforschung* 63: 545–550.

Widsten, Petri, and Andreas Kandelbauer. 2014. Industrial scale evaluation of cationic tannin as a binder for hardboard. *Journal of Adhesion Science and Technology* 28: 1256–1263.

Widyorini, Ragil, Takashi Higashihara, Jianying Xu, Takashi Watanabe, and Shuichi Kawai. 2005. Self-bonding characteristics of binderless kenaf core composites. *Wood Science and Technology* 39: 651–662.

Widyorini, Ragil, Jianying Xu, Kenji Umemura, and Shuichi Kawai. 2005. Manufacture and properties of binderless particleboard from bagasse I: effects of raw material type, storage methods, and manufacturing process. *Journal of Wood Science* 51: 648–654.

Widyorini, Ragil, Jianying Xu, Takashi Watanabe, and Shuichi Kawai. 2005. Chemical changes in steam-pressed kenaf core binderless particleboard. *Journal of Wood Science* 51: 26–32.

Xu, Jianying, Guangping Han, E.D. Wong, and Suichi Kawai. 2003. Development of binderless particleboard from kenaf core using steam-injection pressing 49: 327–332.

Xu, Jianying, Ryo Sugawara, Ragil Widyorini, Guangping Han, and Shuichi Kawai. 2004. Manufacture and properties of low-density binderless particleboard from kenaf core. *Journal of Wood Science* 50: 62–67.

Xu, Jianying, Ragil Widyorini, Hidefumi Yamauchi, and Shuichi Kawai. 2006. Development of binderless fiberboard from kenaf core. *Journal of Wood Science* 52: 236–243.

Yamanaka, S., K. Watanabe, N. Kitamura, M. Iguchi, S. Mitsuhashi, Y. Nishi, and M. Uryu. 1989. The structure and mechanical properties of sheets prepared from bacterial cellulose. *Journal of Materials Science* 24: 3141–3145.

Yamashita, Yokochi, Imanishi, and Kanayama. 2007. Transfer molding of bamboo. *Journal of Materials Processing Technology* 192/193: 259–264.

Yamashita, Yokochi, Miki, and Kanayama. 2009. The pliability of wood and its application to molding. *Journal of Materials Processing Technology* 209: 5239–5244.

Yang, Haiping, Rong Yan, Hanping Chen, Dong Ho Lee, and Chuguang Zheng. 2007. Characteristics of hemicellulose, cellulose and lignin pyrolysis. *Fuel* 86: 1781–1788.

Yano, H., and S. Nakahara. 2004. Bio-composites produced from plant microfiber bundles with a nanometer unit web-like network. *Journal of Materials Science* 39: 1635–1638.

Zauer, Mario, Jens Kretzschmar, Livia Großmann, Alexander Pfriem, and André Wagenführ. 2014. Analysis of the pore-size distribution and fiber saturation point of native and thermally modified wood using differential scanning calorimetry. *Wood Science and Technology* 48: 177–193.

Zhang, Xiaoqing, Xiaolin Wu, Dachao Gao, and Kenong Xia. 2012. Bulk cellulose plastic materials from processing cellulose powder using back pressure-equal channel angular pressing. *Carbohydrate Polymers* 87: 2470–2476.

Zhang, Ya Mei, Yang Lun Yu, and Wen Ji Yu. 2013. Effect of thermal treatment on the physical and mechanical properties of phyllostachys pubescen bamboo. *European Journal of Wood and Wood Products* 71: 61–67.

Zheng, Yi, Jia Zhao, Fuqing Xu, and Yebo Li. 2014. Pretreatment of lignocellulosic biomass for enhanced biogas production. *Progress in Energy and Combustion Science* 42: 35–53.

VI Materials and methods

VI.1 Starting materials and chemicals

VI.1.A Cellulose

In chapter III, IV and V, α-cellulose, 96% purity according to the provider, with 4% insoluble hemicelluloses (French et al. 2000) was purchased from Sigma-Aldrich (St Louis, MO, USA) under the reference "bulk cellulose", this product was extracted from aspen trees. The crystallinity index has been measured at 62%. The crystallinity index of starting material was measured using X-ray diffraction. It was performed on a quartz-lead sampler loaded with the α-cellulose powder using a MiniFlex II Desktop X-ray Diffractometer with Cu Kα radiation (Rigaku ,Tokyo, Japan). Scans were obtained from 5 to 50 degrees 2θ in 0.05 degree steps for 15 seconds per step. The crystallinity index was evaluated according to the method of Segal et al.(Segal et al. 1959).

VI.1.B Hydrophobating agents (Chapter IV, part IV.1)

Stearic acid, linoleic acid, sebacic acid, magnesium stearate, sodium stearate were purchased from Sigma Aldrich (St Louis, MO, USA) and highly oleic sunflower oil was provided by La toulousaine des céréales (Toulouse, France).

Stearic acid was melted, stirred and 5% of sodium and magnesium stearate were added in order to generate 95/5 mixtures of the acid and corresponding salts (Mg and Na). These two mixtures were cooled down and added to the cellulose under their solid state.

A ceramic mortar bowl and pestle were used in order to mix the additives to cellulose powder in proportions of 2, 5 and 10 % and used the day of preparation for molding. The mixing of solid material was quite easy and uniform (magnesium stearate, sodium stearate, stearic acid, mixtures of those and sebacic acid) whereas for sunflower oil and linoleic acid (liquids at room temperature) the homogeneity has been difficult to obtain especially for low additive contents.

VI.1.C Esterification reagents (Chapter IV, part IV.2)

Octanoïc acid (OA) with purity over 98% was purchased from Alfa Aesar (Schiltigheim, France). Anhydride octanoïc (OAn) with purity over 95% was purchased from TCI (Zwijndrecht, Belgium). Potassium laurate was produced from mixing of lauric acid heated to 80 °C with a $1.59.10^{-2}$ M potassium hydroxide aqueous solution, and successive vacuum drying at 50°C. Potassium laurate is described as a catalyst for the esterification of cellulose (Peydecastaing et al. 2006). 2 % of potassium laurate was added to the OA, consequently, for the purpose of this work OA will refer to the 98% OA / 2% potassium laurate mixture.

VI.1.D Native plant materials

In chapter IV, miscanthus (Miscanthus sinensis, purchased from Burlerrow Farm, Bodmin, UK) was ground on a 250 µm screen in a Pulverisette 15 grinder from Fritsch (Idar-Oberstein, Germany) and manually sieved at 150 µm to obtain a fine and homogeneous powder.

In chapter V, diverse raw plant materials were processed, most of them were collected in the laboratory from other research projects:

- Wheat (Triticum sp.) straw was obtained from Arterris (Castelnaudary, France) and ground with a VS1 hammer mill from Electra (Podenas, France) with 2 mm grid and separated in 3 fractions, >0.5 mm - [0.5,1] mm - <1 mm using an automatic industrial sieving machine from RITEC (Toulon, France). The three fractions were coded **WS1**, **WS2** and **WS3** respectively.

- Olive (olea europaea) kernels flour was given by Bardon Ets (Le Muy, France) and was coded **FNO**.

- Cellulose wadding (**CWa**) (Univercell®) was collected from SOPREMA (Strasbourg, France).

- Sweet corn (**SCR**) (Zea mays saccharata) co-products came from industrial corn grain canneries and were provided, dehydrated, by SARL Soupro+ (Castelmoron sur Lot, France).

- Agave (Agave tequilana) bagasse is the fiber residue from the manufacture of Tequila. It was air dried, and kindly provided by the PATRON Spirits Company in Mexico (Atotonilco, State of Jalisco). Agave bagasse was coded **Bag**.

- Oil palm (Elaeis guineensis) empty fruit bunch (pinsotte) is the residue after separation of the fruits in the production of palm oil. It was air dried before being sent from Costa Rica (Palma Tica grupo NUMAR). Pinsotte was coded **Pin**.

- Barley (hordeum vulgare) straw (**BS**) came from Spain and was provided by the Centre for the Development of Renewable Energy Sources (CEDER – Soria, Spain).

- Sugarcane bagasse (saccharum) came from Brasil and was coded **BCa**. Eucalyptus wood came from Uruguay and was coded **Euc**. The vine prunings (vitis vinifera) came from Chili and was coded **Vin**. No more information were available about these materials as they were used in a no more active research project. Originally these 7 later materials were studied for their hydrolysis ability and evaluated for the production of 3rd generation ethanol(Vandenbossche, Brault, et al. 2014).

- Miscanthus (miscanthus sinensis) which normal use is animal bedding has been provided by The Green Factory and purchased from Burlerrow Farm (Bodmin, UK). Micanthus was coded **Mis**.

- Chenevotte, coded **Che** is the center part of hemp (cannabis sativa) and is normally used as ecofriendly wall coating (hemp and lime for instance) or hemp concrete construction material. It was collected from Agrofibre SAS (Cazères, France).

- Sunflower (helianthus annuus) seeds cake (**SSC**) pellets and sugarbeet (beta vulgaris) pulp (**SBP**) were obtained from an agricultural cooperative: La toulousaine des céréales (Toulouse, France).

- Carded hemp (cannabis sativa) was collected from AGROMAT (Tarbes, France) and coded **Car**.

- Coffee (coffea) waste (**Cof**) was collected at the laboratory employees cafeteria and air dried.

- Beech wood (fagus sylvatica) and Poplar bark (populus) were obtained from the FCBA (Forêt Cellulose Bois construction Ameublement, Grenoble, France). They were coded **Bee** and **Pop**, respectively.

VI.2 Preparation methods

VI.2.A Thermo-mechanical refining

Even though the thermomechanical refining was not investigated as a priority, some preliminary trials were performed pushed by scientific curiosity, and good results obtained. Thus, the thermomechanical refining of wheat straw was performed in 3 different conditions, in order to evaluate its impact on the molded materials.

The thermo-mechanical refining was conducted using a Clextral (Firminy, France) BC 45 co-penetrating and co-rotating twin-screw extruder. It comprises 7 modular barrels induction-heated and thermoregulated (The wheat straw is introduced in the extruder using a volumetric hopper screw feeder set to 15 kg/h. A piston pumps with power control (Clextral DKM K202 PP32) was used to inject water at a controlled flow. Water was injected in the extruder as to maintain a liquid solid ratio of 0.7 (L/S = 0.7).

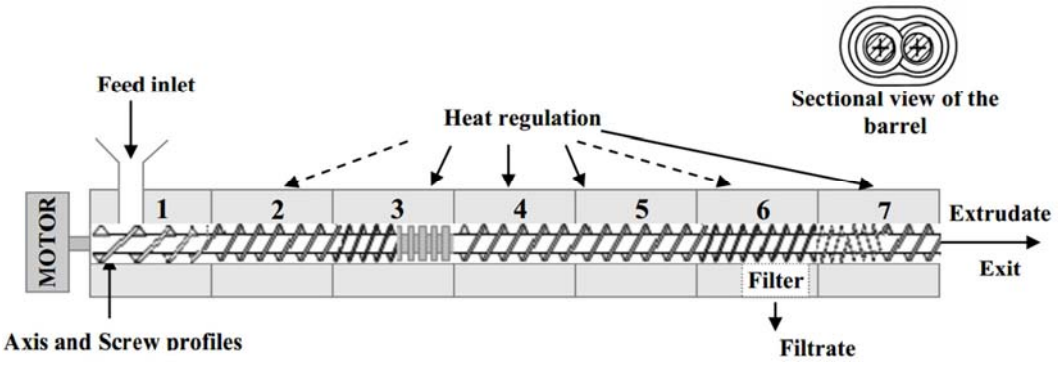

Figure VI - 1: Schematic modular barrels possibilities of the Clextral BC 45 twin screw extruder

The screw profile (Figure VI - 1) is a very important parameter, it was inspired by other works conducted in the laboratory, for which a paper was published recently by Vandenbossche et al. (Vandenbossche, Doumeng, et al. 2014). In Figure VI - 2 each set of screws is indicated by a type (T2F: trapezoidal double-thread, C2F: conveying double-thread, BB: bilobe paddle screw, C1FT: reverse pitch simple-thread screw) followed by a number indicating the pitch except for the BB type for which number indicated the length of the screw module.

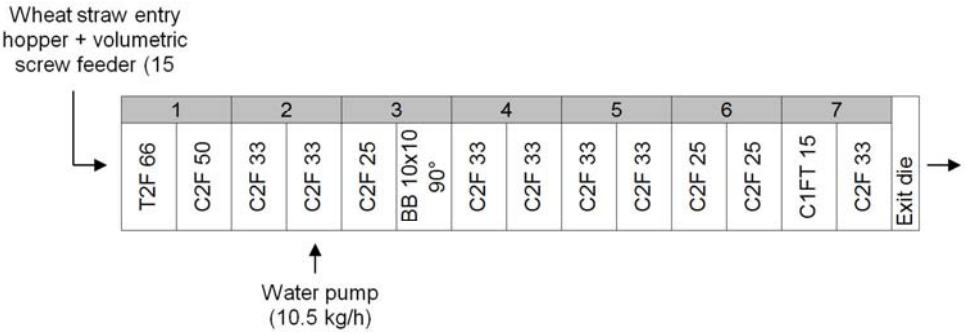

Figure VI - 2: Screw profile for WE1, WE2 and WE3 production

3 different conditions were tested, in the first one, water was added with 3% sodium hydroxide and the pretreatment was conducted at 100°C. This experiment was called **WE1**. In the second and third trial, the extrusion was performed with water only and at 100 and 70 °C which resulted in materials called **WE2** and **WE3** respectively.

VI.2.B Grinding

In Chapter IV, in order to increase the contact surface area, the Miscanthus was ground on a 250 µm screen in a Pulverisette 15 grinder from Fritsch (Idar-Oberstein, Germany) and manually sieved at 150 µm to obtain a fine and homogeneous powder.

In Chapter V, because the 23 materials had very different particle size and some of them not compatible with the size of the molds, they were all ground using a VS1 hammer mill from Electra (Poudenas, France) fitted with a 2 mm grid. No sieving was performed but the particle size distribution and form factor distribution were measured in order to evaluate the influence of these parameters on the molded specimens' properties.

VI.2.C Moisture conditioning and dynamical vapor sorption

Two different methods were used to get starting materials to the desired values of moisture content. First and most used method was the equilibrium of one material to air calibrated to specific RH. For example, in chapter III, celluloses with different moistures were conditioned in a climatic chamber (Fisher Scientific, Bioblock Scientific, Illkirch, France) tuned at 45% - 60 % - 75% RH and 25°C which produced celluloses with 6.1, 8.0, 10.8 % MC respectively. In this case, materials were let to equilibrate in said atmospheres for at least 15 days. The relationship between RH and MC of cellulose samples was verified on the sorption/desorption graph (Figure VI - 3) made on a Dynamic Vapor Sorption (DVS) apparatus from Surface Measurements System Ltd (Alperton London, UK).

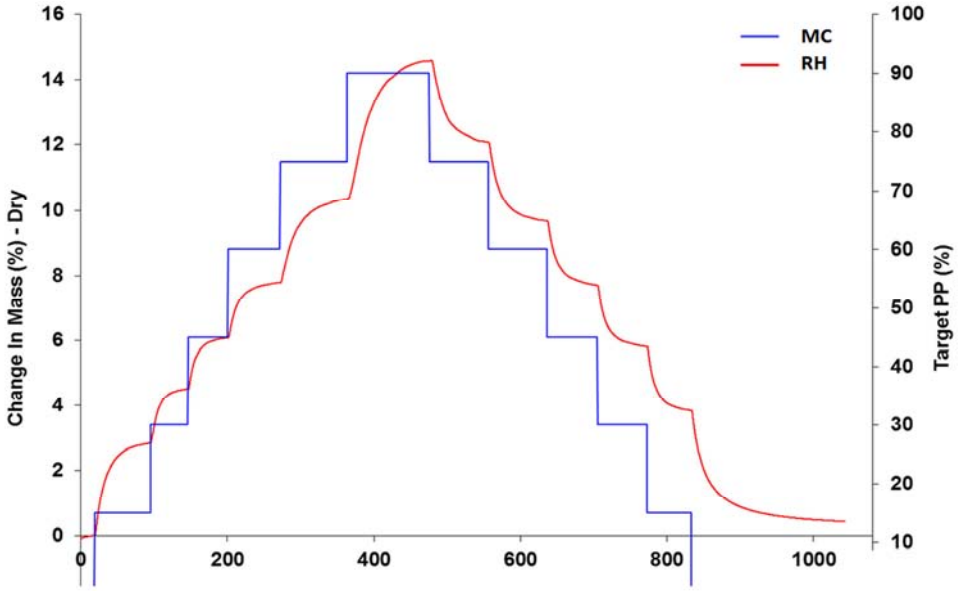

Figure VI - 3: Water uptake against atmosphere Partial Pressure of alpha cellulose

From the water sorption desorption isotherms, the parameters of Guggenheim–Andersen–de Boer (GAB) were calculated which permitted to obtain the mole number of water monomolecular coverage (first GAB parameter) at 2.8 10^{-3} mol/g. The monolayer is thus reached at 5 % moisture content.

As atmosphere below 30% RH are difficult to obtain in climatic chambers, a second method was used to generate lower moisture content cellulose in chapter III: cellulose

equilibrated to control conditions (60% RH 25°C – with known MC) was let to dry in a 70°C vented oven while kinetically measuring the weight loss in order to reach a specific value. For example, for generating 4% MC cellulose, 8.0 % MC cellulose was dried until a 4.0% weight loss weight loss was measured etc. Dry samples were generated by letting them 48 hours in a 103°C oven.

VI.3 Methods of analysis for physic-chemical properties of plant materials

VI.3.A Physical parameters

Apparent density of the powder (tapped density)

In this work, the apparent density (g/cm^3) referred to the tapped density of the one starting material, uncompressed. The tapped density was measured by measuring mass and volume occupied by one analyzed material equilibrated with 60% RH 25°C atmosphere, after 750 hits (tap) using a Densitap apparatus from Granuloshop (Chatou, France). Several runs of 750 hits were performed sequentially until the variation of tapped density from the run n compared to the run n-1 was below 5% (usually 2 or 3 runs are needed).

Particle size distribution

Pre-weighted sieves with different opening (2.0, 1.6, 1.25, 1.0, 0.8, 0.5, 0.25 and 0.12 mm) were used in a Retsch (Düsseldorf, Germany) model AS 200 basic automatic laboratory sieving machine in order to analyze the particle size distribution, as a result of the grinding treatment. About 100 g of the plant materials were put in the first sieve (2.0 mm) and the apparatus was let to vibrate at 75% of its amplitude for 45 minutes. After what the sieves were reweighted and material weight retained in each sieve was obtained. The different particle sizes were expressed in percentage: P>2 represented the percentage of particles retained in the 2.0 mm sieve, P1.6, P1.25, P1, P0.8, P0.5 P0.25 and P0.12 represented the particles retained in the corresponding sieve number. P<0.12 represented the bottom container of the sieves pile, i.e. the particles with size inferior to 0.12 mm. Although the grinding treatment was the same for all materials through a 2 mm screen the particle size distribution was quite different. This analysis being reliable and made on a significant quantity of material (about 100 g), only one measurement was made.

Form factor profile

An EPSON image scanner model G860B was used to obtain pictures of plant materials powder spread on either a mat white or black sheet of paper. An image analyser software (Lucia from Laboratory imaging s.r.o., Prague, Czech Republic) was tuned in order to measure for each particle the minimum and maximum Feret's diameter (respectively minferet and maxferet). The form factor is classically the ratio of the minferet to the maxferet. In this work, in order to work on finite numbers, the term F was used, and defined as the inverse of the aspect ratio. F is thus calculated from the ratio of the maxferet to the minferet.

F1 was defined as the percentage of particles with aspect ratio (or F) equal to 1. Fx-y was defined as the percentage of particles with a ratio strictly superior to x and inferior or equal to y. The distribution was analysed using F1, F1-2, F2-3, F3-5, F5-10 and F10 variables, F10 representing the percentage of particles with F>10.

3 different images were analysed and the F factors were expressed with the mean of the triplicates ± standard deviation.

VI.3.B Chemical composition

Moisture content

Moisture content (MC) evaluation was performed on materials after at least 15 days of equilibrium with atmosphere under known conditions. The MC measurement was performed by difference of weight between an equilibrated sample (m_{moist}) on its dry mass (m_{dry}) obtained with 2 days drying at 103°C, in triplicates.

$$MC = \frac{m_{moist} - m_{dry}}{m_{moist}} \times 100\ (\%)$$

Mineral matter

Ashes content was evaluated after MC evaluation by ashes weight (m_{ashes}) after calcination at 550°C for 3 hours using a Nabertherm Gmbh oven (Lilienthal, Germany). This analysis was performed in triplicate.

$$Ashes\ content = \frac{m_{ashes}}{m_{dry}} \times 100\ (\%)$$

Total lipids

The total lipids content was measured by weighting the result of a Soxlhet extraction using a 125 mL Soxlhet apparatus for 6 hours in cyclohexane on one plant material ($m_{initial}$) powder imprisoned in a paper filter cartridge. At the end of the extraction time and final solvent draining, the content of the balloon was evaporated using a rotative evaporator in order to obtain the extracted mass ($m_{extracted}$). This analysis was performed in triplicate.

$$Total\ lipids = \frac{m_{extracted}}{(1 - MC/100) \times m_{initial}} \times 100\ (\%)$$

Protein content

The protein content was evaluated using the total nitrogen content analysis or Kjeldahl procedure assisted by a Tecator Kjeltec 2000 apparatus from Foss (Nanterre, France). This analysis relies on first the mineralization of the proteins and other sources of nitrogen of the analyzed sample into ammonia by acid hydrolysis (98.5% sulfuric acid) catalyzed by hydrated copper sulfate for 2 hours at 400°C. Secondly sodium hydroxide is added which converts the ammonium ions into ammonia, the solution is distilled and vapor (ammonia gas) trapped in a flask containing a 4% boric acid solution, methyl red and bromocresol indicators. Hydrochloric acid is finally added to the flask until neutralization of the remaining ammonia, and the calculation of the ammonia distilled from the mineralized solution can be made (Kjeldahl 1883). A blank control is made in order to ease the calculation and avoid titration troubles with the boric acid.

The protein content is then evaluated by multiplying the equivalent nitrogen content given by the Kjeldahl procedure by 6.25. The factor of 6.25 for the conversion of N values to protein is known to be varying from one protein source to another, but has been the most widely used since despite its obscure origins (Hiller et al. 1948). In this work, it was sufficient to use the classical protein factor for comparison purpose between the different plant materials.

$$Protein\ content = \frac{\left(V_{hydrochloric\ acid} - V_{standard}\right) \times N_{hydrochloric\ acid} \times 14.007}{m_{plant\ material} \times (1 - MC/100)} \times 6.25\ (\%)$$

Lignocellulosic constituents

The ADF/NDF method of van Soest et al.(van Soest and Wine 1967) was used for determining the cellulose, hemicelluloses and lignin, using a Tecator Fibertec M1017 from Foss (Nanterre, France), in triplicates.

The analysis works with 2 initial sintered glass filters. First takes place the Neutral Detergent Fiber treatment with the first filter, at ebullition temperature and reflux in the NDF solution (sodium laurylsulfate, sodium ethylenediaminetetraacetic, sodium borate decahydrate) for 1 hour. This treatment solubilizes all the non lignocellulosic constituents (metabolites, proteins, fat, ashes etc.) thus after phase separation and rinsing with hot water, the solid remaining in the sintered glass filter would contain only lignin, cellulose and hemicelluloses which can be measured after drying ($m_{NDF\ treatment}$). This first sintered glass filter is calcined and weighted ($m1_{ashes}$).

In parallel, another sintered glass filter is used and the Acid Detergent Fiber treatment takes place, at ebullition temperature using the ADF solution (hexadecyltrimethylammonium bromide 2% in 1N sulphuric acid) for 1 hour. This treatment solubilizes the hemicelluloses thus the remaining solid after rincing with hot water contains only lignin and cellulose. After drying, the lignin and cellulose content can be measured by weight difference ($m_{ADF\ treatment}$).

Successively the oxidant treatment takes place using potassium permanganate at room temperature for 1 hour and a half which solubilizes the lignin. The solid is separated by filtration and a demineralizing solution (dehydrate oxalic acid, ethanol, hydrochloric acid, distilled water) which permits to bleach the fibers by elimination of the remaining permanganate salts ($m_{permanganate\ treatment}$). The sintered glass filter is finally calcined ($m2_{ashes}$).

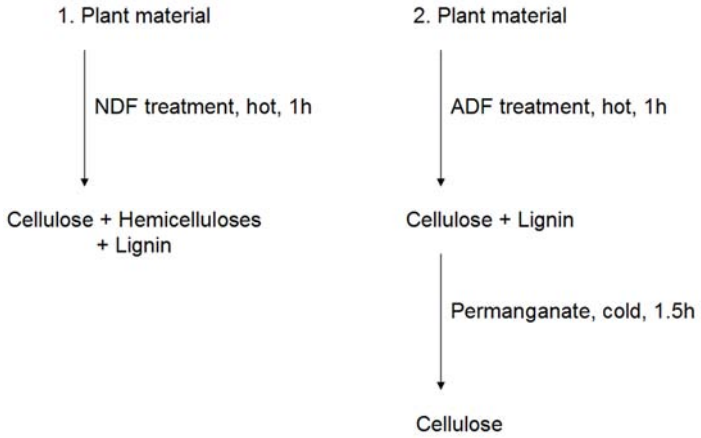

Figure VI - 4: ADF/NDF method scheme

By weight difference of the successive extractions summed up in Figure VI - 4, the cellulose, lignin and hemicelluloses content can be calculated :

$$Cellulose\ cont. = \frac{m_{permanganate\ treatment} - m_{ashes}}{m2_{plant\ material} \times (1 - MC/100)} \times 100\ (\%)$$

$$Lignin\ cont. = \frac{m_{ADF\ treatment} - m_{permanganate\ treatment}}{m2_{plant\ material} \times (1 - MC/100)} \times 100\ (\%)$$

$$Hemicell.cont. = \frac{m_{NDF\ treatment} - m1_{ashes}}{m1_{plant\ material} \times (1 - MC/100)} \times 100 - Lignin\ cont. - Cellulose\ cont.\ (\%)$$

Total polyphenols

The Folin-Ciocalteu method was used to analyze the total polyphenols content in the plant materials. This analysis relies on a reduction reaction of yellow colored ionic polymer complexes formed from phosphotungstic and phosphomolybdic acids into blue molybdo-tungstene complexes by the polyphenols in an alkaline media. First, extracts were made on the different plant materials, a known mass ($m_{plant\ material}$) of each plant material was added to a known volume ($V_{extract}$) of 30% distilled water 70% ethanol and left to stir together for 2 hours at room temperature (19°C) and finally filtered. The extraction was performed in triplicates and each extract was analyzed.

A known volume of extract was collected, diluted (d times) when needed (colour observation) and added to 1 mL of sodium carbonate (20% w/w) and 0.5 mL of the Folin-Ciocalteu reagent, purchased from VWR (Fontenay sous bois, France) in a test tube (of V volume). Controls were prepared for the calibration by adding gallic acid. The test tubes were placed in a stirred water bath at 70°C for 10 minutes followed by the reaction being stopped by ice-quenching for 20 minutes. The absorbance at 700 nm was then measured using a UVS 1800 ultraviolet spectrophotometer from Shimadzu (Noisiel, France). The Beer-Lambert law permitted to retrieve the equivalent gallic acid concentration $C_{eq.\ gallic\ acid}$ (mg / L) in each sample, which was converted in $mg_{eq.\ galic\ acid}$/g of raw plant material using the following equation:

$$Total\ polyphenols: \frac{C_{eq.gallic\ acid} \times V_{extract} \times d}{m_{plant\ materials} \times (1 - MC/100)}\ (mg_{eq\ galic\ acid}/g\ )$$

Thermo-compressive molding

Pressing machines

The major part of the experiment have been performed in a MAPA 50 computer-controlled laboratory-scale hydraulic press (Pinette Emideceau, Chalon-sur-Saône, France), capable of 530 kN of effort (about 50 tons). The metal plates (50cm x 50cm) were thermo-regulated, and used to warm up the mold at least 30 m before each molding attempt.

In chapter IV (and only) a manual hydraulic press was used. It has a capacity of 10 tons and is from the same manufacturer than the MAPA 50 was used, and both plates (25 x 25 cm) are also thermo-regulated.

In chapter III, the pressing machine from AIST in Nagoya was used, it had a capacity of 200 kN and was manufactured by SAGINOMIYA (Tokyo, Japan).

2D molding

All the molds used in this work were custom made to produce different specimens: 1A dog-bone specimens:

50x50 mm square specimens: This first available mold was used to produce squares plates, for numerous preliminary tests and in chapter IV (part IV.1) in order to perform water drop angle measurement tests in the evaluation of fatty compounds as hydrophobation agents. WA/TS experiments were initially designed to be performed on squares (in chapter V) but it had to be abandoned because of inconsistency between the results on 1A dog-bone in one hand, and squares. The difference probably came from a too different surface / volume ratio in 50x50 specimen compared to a 150x10 (dog-bone shape).

A mold (Figure VI - 5) was machined (Cristin Electro Erosion, Grisolles, France) in order to produce 1A dog-bone tensile specimens according to ISO 3167 standard (ISO 3167 2002) . The molds were machined in 55NCDV7 (given to 140-150 kg/mm² of strength) steel allow without further modification except for the 4th version of this mold for which lower and upper punches were hardened by quenching (Figure VI - 6). Such apparatus has never been reported in the literature and tensile strength on compression molding tests is rarely reported. The production of ISO 1A dog-bone also haven't been seen anywhere else.

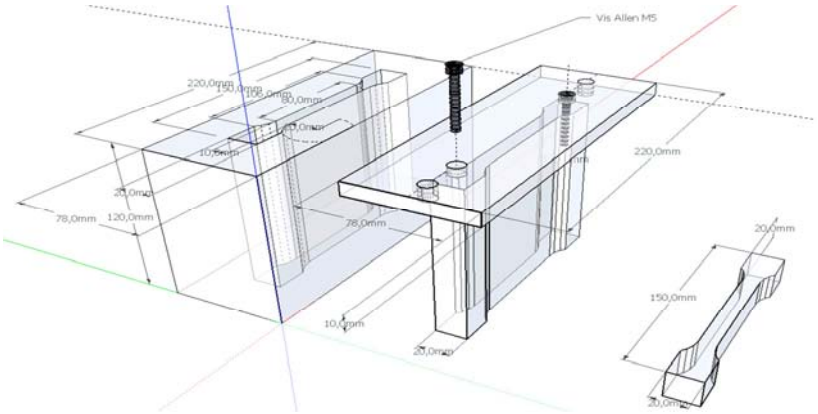

Figure VI - 5: NF EN ISO 3167 1A specimen compression mold: schematics, first version



Figure VI - 6: Picture of the 4th 1A dog-bone specimen compression mold preheating in the MAPA 50 press

45x10 mm DMA specimens: This mold was designed in order to perform DMA analysis, for the other part of project HYPMOBB, and it was used for molding the WA/TS specimens (Chapter III, Chapter V) and also during the esterification study (Chapter IV). A first version was made out of 55 NCDV7 steel, and a second version used the same allow with hardened punches (Figure VI - 7).

In chapter IV, the specimens were pressed in the 10 tons press, at maximum force capacity and the resulting pressure in these conditions was about 220 MPa. For each molded specimen, 1 g of material (cellulose, miscanthus with a certain quantity of OA or OAn in it) was manually charged in the mold in the hot press with preheated mold, after 1 or 2 hours of experiment, the material was manually unloaded without a cooling step. Preliminary results based on IR measurement indicated that no grafting was detected unless quite drastic conditions of molding were used. Two conditions of molding were tested in each experiment for the need of comparison: First condition was a rather low temperature (165°C) and a long time of 2 hours, second condition was a higher temperature (190°C) and shorter time of molding (1 hour).



Figure VI - 7: 45 x 10 mm DMA specimens used for molding water resistance and esterification specimens

3D molding

A bowl-shape and a candle holder shape molds were available to produce 3D moldings. They have been described in Chapter II, in Figure II - 3 and Figure II - 11. Although many tests were performed on these molds, obtaining a perfect shape ended up to be very difficult. 3D molding appeared much more complicated than 2D molding because of the flow parameters playing a role in the resulting specimens. No scientific data were produced thanks to these molds.

Molding cycle

The pressing machine was preheated, and the initialization of the mold is made before each set of experiments so that the pressing machine integrates the position of the mold. The mold is preheated, laying on the hot plates, and at least 30 minutes were waited

between the time at which the plates were at temperature and the beginning of the experiments. The temperature of the mold was regularly verified using an IR temperature sensor, it was between 2 and 5 degrees below the temperature of the plates.

The material to compress is charged in the mold manually, using a laboratory spoon and looking directly in the die from over the mold (in the press). Attention was paid to first charge quickly in order to prevent moisture changes of the sample in contact to the hot mold (evaporation for moist samples, moisture uptake for dry samples) and secondly to fill up the mold as homogeneously as possible.

The mold is then closed (upper piston, or upper shape) put on the material and press cycle launched. Several parameters are programmed in the computer, temperature of the plates (°C), hydraulic pressure (bar), pressure increase slope (i.e. pressurization speed, bar/s), maintaining time (s) and depressurization speed (bar/s).

In chapter III and in the first published paper, the effect of the pressurization speed was investigated, which was performed by calculating an integral I on the control press cycle (Figure VI - 8). Pressure rate was set up at 1 bar/s, 2 bar/s, 50 bar/s (hydraulic pressure) while adjusting time to maintain equal I. Therefore, the time was different for each experiment, but also the maximum pressure of 267 MPa was not obtained for the 1 bar/s experiments (Table VI - 1) because the integral I was reached before.

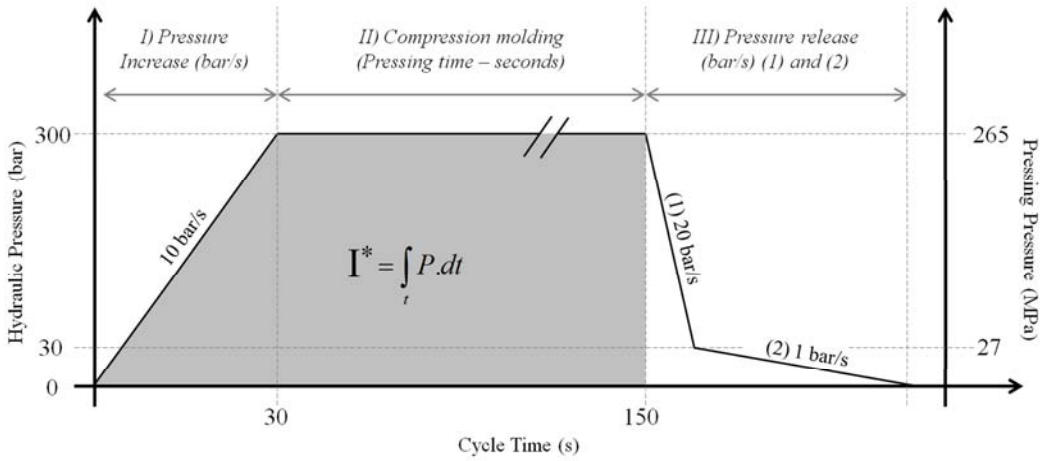

Figure VI - 8: Description of the press cycle (Chapter III)

Table VI - 1: Parameters for pressurization speed evaluation in chapter (Chapter III)

Prate	I pressure incrase phase (bar.s)	I plateau at max pressure (bar.s)	I (bar.s)	Time on pressure increase phase (s)	Time on plateau at max pressure (s)	Max hydraulic pressure reached (bar)	Max process pressure reached (Mpa)
10 bar/s	4500	36000	40500	30	120	300	267
50 bar/s	900	39600		6	132	300	267
2 bar/s	22500	18000		150	60	300	267
1 bar/s	40500	0		285	0	285	254

Molding pressure

The calculation of the molding pressure was made by two different means, first by considering the hydraulic pressure gauge, which the pressing machine uses for controlling the pressure:

$$P_{specimen} = \frac{P_{hydraulic} \times S_{piston}}{S_{mold}}$$

Secondly, a force sensor installed in the MAPA 50 press was used to confirm the calculations on pressure:

$$P_{specimen} = \frac{F_{sensor}}{S_{mold}}$$

For instance, the dog-bone specimen mold has an area of 20.057 cm² (S_{mold}), the pressing machine (MAPA 50) piston has a surface of 176.7 cm² (S_{piston}) and maximum hydraulic pressure ($P_{hydraulic}$) on the pressing machine is 300 bar so the maximum pressure produced by this press on the dog-bone mold was 2643 bar i.e. 264 MPa. With hydraulic pressure set up to 300 bar, the force sensor indicated 530 kN, which confirms a specimen pressure of 2642 bar.

Flow test apparatus (Nagoya) – Chapter III

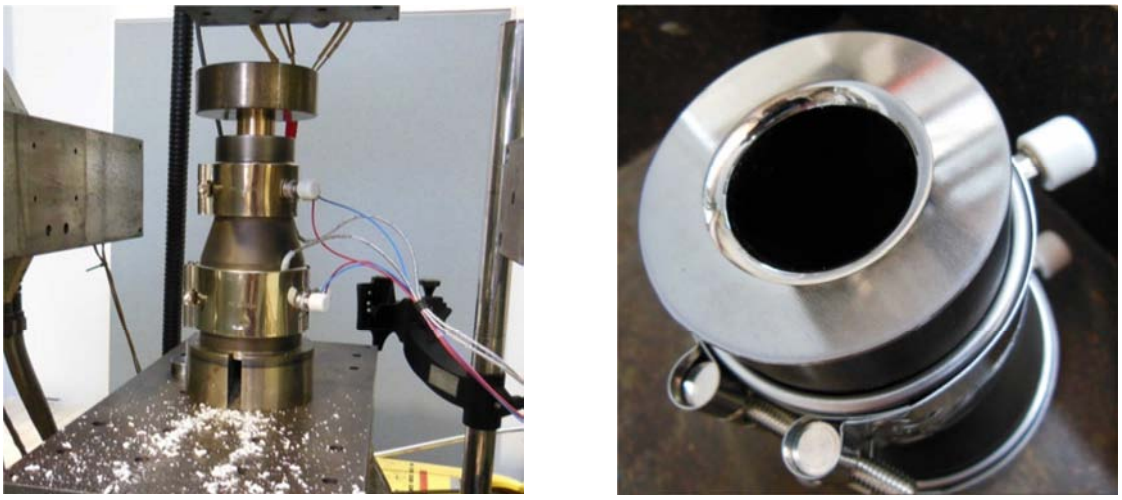

Figure VI - 9: Flow test setup in Nagoya

In Nagoya, the main elements of the molding and flow tests was a rectified and polished, nickel-chrome plated, hardened steel chamber with a 30 mm inner diameter. The very smooth and resistant surface provided a high durability of this equipment. Tungsten carbide dies were available with different diameters and lengths and were entered in the chamber. Several setup were possible, a foot to install bellow the chamber in order to let the material flow out for the extrusion tests, lower punches (flat or small pot shaped) for molding experiments, and a gear shape.

Transfer molding and flow tests (Toulouse) – Chapter V

In Toulouse, a versatile setup was also designed for performing the flow tests experiments and allows molding of several parts. The 2 main elements were the chamber (with inner diameter of 25 mm) and the punch machined directly in pre-hardened steel (55NCDV7). The chamber was equipped with a heating band, a K-type thermocouple and a

PID regulator. Different dies were produced, but finally only one die (diameter 4mm , length 10 mm) was used.

Pre-compression was performed thanks to a manual 10 tons press in a 24 mm chamber which permitted to load the material in the 25 mm compression chamber with ease, and permitted to put on the punch and start the test right away.

A foot was machined for free flowing experiments Figure VI - 11, and several molding modules were machined to produce different objects: a small gear, an M10 bolt, an M10 screw and a 2 tensile 2 bending tests specimens module (Figure VI - 12, Figure VI - 13). These modules were barely used due to a lack of time and technical troubles.



Figure VI - 10: Flow test setup in Toulouse



Figure VI - 11: Example of flow test with the prototype made in Toulouse

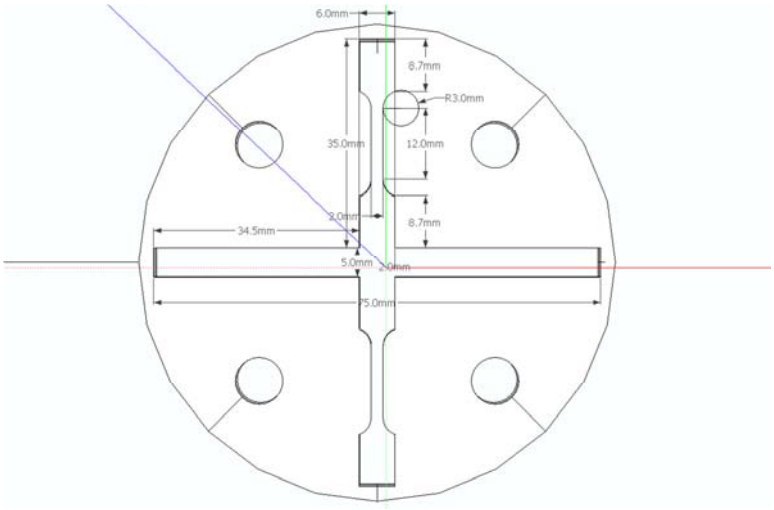

Figure VI - 12: Transfer molding module for producing mechanical tests specimens

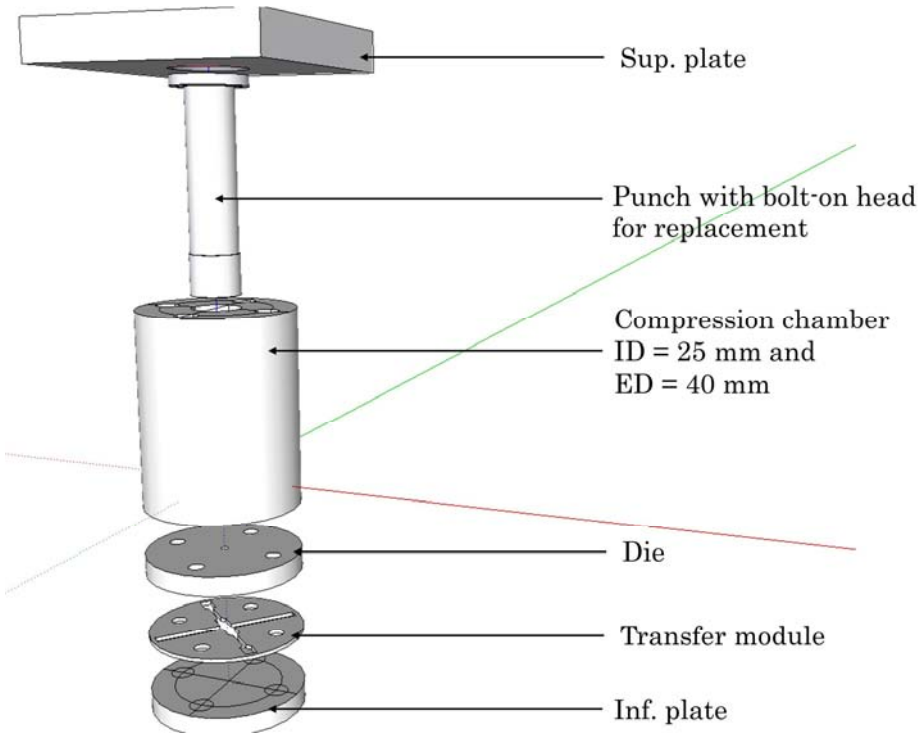

Figure VI - 13: Example of mounting of the transfer prototype / flow test built in Toulouse presented equipped with the transfer module.

VI.3.C Thermo-compressed material specimens evaluation

SEM Observations

SEM pictures were taken using a LEO 435 VP microscope from Leo Electron Microscopy Ltd (Cambridge, UK) and sample silver plating before observation.

Specific Gravity and moisture equilibrium measurements

Six 2 cm long pieces were cut out of six different dog-bone specimens (from the mechanical tests) to measure specific gravity and moisture content of the materials. These six small pieces were first let to equilibrate in a 60% relative humidity 25 °C climatic device, room and moisture content was measured on 103 °C oven-dry basis (24 hours). The dried 6 pieces were then used for evaluation of specific gravity using an YDK01 density determination kit on a Sartorius MC210P precision scale (Sartorius AG, Goettingen, Germany). The specimen were weighted in the air, and then dipped into cyclohexane (Sigma Aldrich, St Louis, MO, USA, Chromsolv for HPLC purity > 99.7%) and the resulting Buoyancy ($W_{air} - W_{fluid}$) was measured. Specific gravity was measured using the following equation:

$$\rho_{sample} = \frac{W_{air} \times (\rho_{cyclohexane} - 0.0012}{0.99983 \times (W_{air} - W_{cyclohexane})} \ (g/cm^3)$$

wherein ρ_{sample} is the specific gravity of the materials tested; Wair and Wcyclohexane the weight of the tested specimen in the air and in the cyclohexane respectively; $\rho_{cyclohexane}$ the specific gravity of cyclohexane at the measured temperature during the experiment; 0.0012 (g/cm3) the specific gravity of air at 20 °C and 101.325 kPa; and 0.99983 a manufacturer's correction factor related to the increase of the fluid level and immersion of the wires in the fluid when the specimen is dipped in the fluid.

Cyclohexane was chosen arbitrary, air bubbles were chased out of the material when immersing it in the solvent, but some of the porosity of the material might remain inaccessible to the solvent, so the specific gravity measured here may differ from real absolute value of density. However, it is thought to be close to the real density and significantly higher than the apparent density.

Measuring dried specimen was thought to prevent misevaluation of specific gravity due to difference of water content between the specimens. On the control specimens (Chapter III), the measured specific gravity of the material equilibrated at 60% relative humidity and 25 °C was 1.485 ± 0.003 g/cm^3, but the measured specific gravity of the dried same specimens was 1.503 ± 0.002 g/cm^3. This analysis was done on the same specimens that were measured, dried and measured again, and confirmed on other specimens that were dried directly and measured. Same results were obtained and no modification was observed due to cyclohexane dump-in.

X-ray tomography

Manuel Marcoux from the IMFT (Fluids Mechanics Institute of Toulouse) offered the possibility to use 3-D X-ray tomography in order to evaluate the porosity distribution within cellulose samples (results presented in III.7). The principle is the scanning of a specimen by X-rays all along the rotation of the sample at 360°. A Skyscan 1174 tomograph model 1174 from Brucker (Kontich, Belgium) was used for acquisition at 0.5° of sampling rate, triplicates image were taken and averaged. 3-D reconstruction was performed using the Avizo software from FEI Visualization Sciences Group (Hillsboro, USA) and an 8 level colour scale of porosity was applied to the group of samples.

Tensile and 3 Points Bending Tests

Prior to testing, the specimens were let to equilibrate 2 weeks in the main climatic chamber available at the laboratory (60% RH, 25°C). The weight variation was seen to be stable after about 10 days of equilibrium. The mechanical properties were later observed to

vary within the first 15 days, and to remain stable thereafter (Figure III - 25). Tensile and 3 point bending tests were conducted according to ISO 527-2 (ISO 527-2 1993) and ISO 178 (ISO 178 2010) using a H5KT Universal testing machine (Tinius Olsen, Horsham, PA, USA) at 1mm/min speed. These standards are related to the evaluation of mechanical properties of plastics which was chosen on purpose. From the stress/strain curves, four variables were collected: The tensile modulus (Et), tensile strength at break (σt), bending modulus (Ef) and bending strength at break (σf).

Because the compacted specimens obtained in this thesis had a heterogeneous laminar structure, the Tensile modulus was calculated (and not the Young's modulus). The basic expression of an elastic modulus E is (with σ the stress and ε the strain):

$$E = \frac{\sigma}{\varepsilon}$$

The extensional strain ε is basically calculated from its derivate, with l the effective tested length of the specimens during the test:

$$d\varepsilon = \frac{dl}{l}$$

Which, upon integration from 0 to i, makes:

$$\varepsilon_i - \varepsilon_0 = ln\left(\frac{l_i}{l_0}\right)$$

With $\varepsilon_0 = 0$ and $\Delta l = l_i - l_0$,

$$\varepsilon_i = ln\left(\frac{l_0 + \Delta l}{l_0}\right) = ln\left(1 + \frac{\Delta l}{l_0}\right)$$

The maximum deformation in tensile was usually less than 2 mm, which makes 2.5% of deformation (ε). Materials with ε < 10 % are in the "small strain" domain which, using the limited development of ln (1+x), permits to simplify the previous equation to:

$$\varepsilon_i = ln\left(1 + \frac{\Delta l}{l_0}\right) \simeq \frac{\Delta l}{l_0}$$

Considering this approximation, and with the introduction of $S_{tensile}$ and $S_{bending}$, the test's span in the apparatus (= l_0) for the tensile and bending test, 80 mm for 1A dog-bone specimens, 38 mm for the smaller DMA-type specimens; $W_{specimen}$ and $T_{specimen}$ the width and thickness of the tested specimen respectively; F_{break} the force (in N) measured when the specimen broke (maximum force of the stress / strain curve); (ΔF/Δl) the slope of the strain/stress curve, taken at the beginning of the deformation; the following equations were used in order to calculate the mechanical properties:

$$Et = \frac{S_{tensile}}{W_{specimen} \times T_{specimen}} \times \frac{\Delta F}{\Delta l}\ (GPa)$$

$$\sigma t = \frac{F_{break}}{W_{specimen} \times T_{specimen}}\ (MPa)$$

$$Ef = \frac{S_{bending}^3}{4 \times W_{specimen} \times T_{specimen}^3} \times \frac{\Delta F}{\Delta l}(GPa)$$

$$\sigma f = \frac{3 \times F_{break} \times S_{bending}}{2 \times W_{specimen} \times T_{specimen}^2} \ (MPa)$$

Some specimens were presenting defects like cracks when compression molded (e.g. at 200 °C and 8% moisture), or sometimes heterogeneity marked by lighter spots where density seemed lower. These "low density" spots generated when charging the material in the mold inhomogeneously discarded these specimens from the tests.

VI.3.D Statistical analysis (Chapter V)

The statistical analyses (Cross correlation and Principal components analysis - PCA) in chapter V were performed with The Unscrambler 9.5 software from CAMO AS (Oslo, Norway).

The cross correlation ("Statistics" in the software) is a 2 entry table (the plant materials characteristics in columns, the molded materials parameters in line) wherein correlation coefficients between -1 and +1 are presented. These coefficients are computed as the covariance between 2 variables divided by the square root of their variance. If values are close to 1 it means the 2 variables tend to increase simultaneously. If values are close to -1 it means that one of the variable increases when the other decreases. Values close to 0 means the 2 variables vary independently one from each other.

The PCA tool was used as a way to detect groups of variables, group of specimens and correspondences between significant variables and specimens, in a simplified way. Prior to this analysis, because of the differences of units and range of the variables, the data were standardized (i.e. values were divided by the standard deviation of the serie). This gives the variables the same chance to influence the estimation of the components as they get all the same variance.

The principle of the PCA (Principle Components Analysis) is the following: find the directions in space along which the distance between data points is the largest. In other words, find the linear combinations of the initial variables that contribute the most to making the samples different from each other. These directions or combinations are called principal components (PCs) computed iteratively in such way that the first PC (PC1) carries the most explained variance, the second PC carries the maximum share of the residual information, and so on. PCA produces an orthogonal bilinear matrix decomposition where components are obtained in a sequential way explaining the maximum variance.

The results of the PCA model are presented as 2 plots: the variable loadings and specimens scores. The loading plot (also called map of variables) displays information about the variables in the PCA model. A variable that has low loadings is badly accounted in the PC(s), which means it cannot be interpreted using this plot. A positive variable loading means that all samples with positive scores have higher than average values for that variable. When a variable has a negative loading, all samples with positive scores have lower than average value for this variable. The higher the positive scores of a sample, the larger its values for variables with positive loadings and vice versa. From the loadings, "correlation loadings" are computed for each variable for the displayed PCs and drawn in two ellipses: the outer ellipse is indicates 100% explained variance and the inner ellipse indicated 50% of explained variance. Thus, variables close to the outer circle will have most of their variance explained by the two plotted PCs.

VI.3.E Methods for performing and studying the esterification in high pressure molding conditions (Chapter IV part 2)

Liquid solid separation

A 6-16K Centrifuge equipped with a 12500 rotor from SIGMA Laborzentrifugen GmbH (Osterode am Harz, Germany) was used at 18°C, 10000 g for 15 minutes for liquid solid separation. A 100 microns nylon tissue, used as a filter, was wedged between the cap and the centrifugation pot, in order to retain the solid in the filter and collect the liquid in the pot. The state of the material after contact between cellulose/miscanthus and reactants after phase separation was a solid, slightly humid powder, which weight consisted of roughly 30 % of reactants adsorbed on the powder. The precise composition of material entering the mold was not measured due to the number of transfer steps during pretreatments. Also at the beginning of the compression step, liquid was extracted from the solid material and leaked onto the press plates. The liquid solid ratio, during the molding step was thus not determined.

Materials pretreatments for solid-liquid pre-contact

Emulsion: The solid material was emulsified with water and grafts (Peydecastaing et al. 2006) using a high shear mixer, L4RT from Silverson (East Longmeadow, USA) in order to increase water content of cellulose and test the emulsion contact method between cellulose and OA. 200 g of OA and water 5/12 were mixed together and emulsified at 7000 rpm for 15 minutes, then 10 g of cellulose were added.

High pressure homogenizer: 20 grams of cellulose was suspended in 2 L of distilled water and introduced progressively in the APV 1000 high pressure homogenizer from APV (Albertslund, Denmark). The first pass was performed at relatively low pressure (average 40 bar, not constant), on the second pass pressure was increased to 100 bar, the third pass pressure was increased to 400 bar, and then 3 more passes were performed at 800 bar. After the second of these three 800 bar passes, the suspension became stable in water with a gel-like appearance. After the 6 passes, the temperature was measured to be around 70°C.

Solvent exchange: Cellulose was left to swell in a large excess of distilled water for 12 hours, filtered and washed twice with ethanol (2 * 160 mL), stirred in ethanol for 5 minutes, and successively washed twice with the desired reactant (OA or OAn). Cellulose is left to stir in the last reactant bath for 5 minutes. The solvent exchanged cellulose is then filtered on a Buchner set up and centrifuged at 18°C, 10000 g for 15 minutes.

Reactant removal prior to analysis

Powders (generated using a small kitchen grinder) from molded specimens were washed using a Soxlhet for 8 hours in technical ethanol using small filter paper bags in order to get rid of the non-grafted reactants from the solid. After washing, the filter paper bags were left to evaporate for 24 hours at 70°C to remove the solvent and the washed powder recovered.

IR Analysis

A FTIR apparatus from Perkin Elmer (Courtaboeuf, France) was used for obtaining IR spectra, acquisition was performed from 400 to 4000 cm^{-1}. KBr tablets were produced with

a manual screw press. IR analysis has been used to track esters on early preliminary results (data not shown), and also on cellulose grafting experiments shown in this paper. As for miscanthus, the starting material showed ester bands as expected, which would overlap with ester resulting from grafting, thus, IR spectra were not performed on miscanthus grafting experiments (ND appears in corresponding lines in Table 1).

Drop angle determination method

A R&D Digidrop apparatus from GBX (Bourg de Péage, France) was used to perform the drop angle measurements with distilled water (Figure VI - 14). In IV.1, the measurements were performed directly on the compressed specimens and differences were observed within the results of one specimen, which was attributed to different surface porosity due to heterogeneity generated during filling of the mold. Thus, in IV.2, in order to avoid surface effect due to high pressure molding and also because homogeneity in the compressed material could not be guaranteed, the measurements were made on washed and ground powder recompressed in a basic IR tablet press. The analysis was kinetically measured thus initial water drop angle (t_0) and penetration time (t_{final}) were collected from the experiments and reported here.

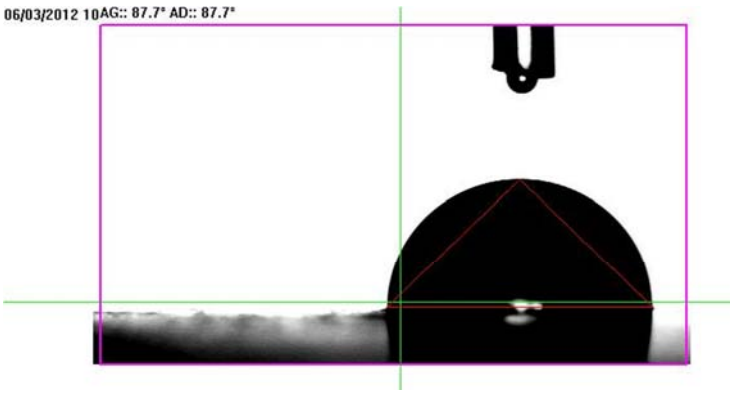

Figure VI - 14: Picture obtained with the Digidrop and used for drop angle measurements in chapter IV

Degree of substitution (cellulose) and grafting rate measurements

The method was derived from Peydecastaing et al. (2009). The methylester transesterification was performed on a precise quantity of solid material (cellulose or miscanthus) by Trimethylsulfonium (TMSH) in Tertbutylmethyl (TBME). The reaction was carried out at 75°C for 1 hour in 2 mL vials stirred at 1200 rpm in a Vortemp 56 incubator from Labnet International (Edison, USA). After cooling and decanting, the supernatant was analyzed in a Varian 3900 gas chromatography from Agilent Technologies (Santa Clara, USA) and its FID detector. The separation is performed thanks to a CP select CB column. Helium as carrier gas had a flow of 1.2 mL/min. Injector temperature and detector were set to 260°C, oven temperature to 110°C stable for 4 minutes and a 15°C/min slope to 230°C and a final plateau at 230°C for 7 minutes. Detector gasses had flow rate of 25, 30 and 300 mL/min for helium, hydrogen and air respectively. 1 µl of supernatant sample is injected. For comparison and for the need of figure's drawing, the grafting yield (GR) was first calculated as the millimole number of OA divided by the mass of tested grafted material (cellulose or miscanthus, in kg) using the following equation:

$$GR = \frac{10^6 \times C_{GC} \times V_{standard}}{m_{specimen} - C_{GC} \times V_{standard} \times (M - 18.02)} (mEq_{octanoïc\ acid}/kg)$$

wherein:
C_{GC} is the concentration of OAME after transesterification determined by GC peak integration in $mol.L^{-1}$, $V_{standard}$ the internal standard volume added to the sample in L, 500 µL were injected in each vial, $m_{specimen}$ the solid test specimen mass in g, M the molar mass of OA in $g.mol^{-1}$and 18.02 the molar mass of H_2O lost during the transesterification reaction.

Secondly, for cellulose samples, the degree of substitution (DS) was calculated using the following equation:

$$DS = \frac{162.14 \times C_{GC} \times V_{standard}}{m_{specimen} - C_{GC} \times V_{standard} \times (M - 18.02)}$$

wherein:
162.14 is the cellulose monomer molar mass.

Duplicate vials were prepared from the same sample and 2 injections were performed for each vial. The mean of 4 obtained values was made and the standard deviation was calculated to evaluate reproducibility.

Table of figures and tables

Chapter I:

Figure I - 1: Comparison between dry and wet mechanical properties (Okuda and Sato 2004, republished with the kind permission of the Japan Wood Research Society) 17
Figure I - 2: Correlation between loss of hemicelluloses and improvement of water resistance in binderless fiberboards, WA on the left (steam exploded miscanthus, adapted from Velasquez et al. 2003), TS on the right (steam exploded banana bunch, adapted from Quintana et al. 2009) 20
Figure I - 3: Example of correlation between MOR / MOE and density on a wide range of density from Xu et al. (2004), where the dotted line is modelling from Xu et al. (2003), all results on steam injected binderless particleboards from 5mm chips of kenaf core. Figures republished with the kind permission of the Japan Wood Research Society 25
Figure I - 4: Example of correlation between mechanical properties and density of boards. Left graph (Okuda and Sato 2004) binderless particleboards from fine powder (53 µm) bagasse with a linear correlation, right graph (Ando and Sato 2010) particleboards from Japanese cedar milled through 1 mm screen with a non-linear correlation, republished with the kind permission of the Japan Wood Research Society 27
Figure I - 5: Correlation between pressure and bending strength (adapted from Mobarak et al. 1982) 28
Figure I - 6: Correlation between extrusion pressure and density at high pressure extrusion of wood powders (reproduced from Miki et al. 2003, with kind permission of the Japan Society of Mechanical Engineers) 28
Figure I - 7: Correlation between pressure and bending strength in dynamic test (gray dots) and static (black squares) (adapted from Miki et al. 2007a and Miki et al. 2008) 29
Figure I - 8: Effect of particle size on mechanical properties in high pressure molding under steam atmosphere (adapted from Miki et al. 2007a) 36
Figure I - 9: Furfural (and derivatives) content changes during steam pretreatment and molding (adapted from Suzuki et al. 1998) 40
Figure I - 10: Link between the increase of lignin content and pretreatment severity (adapted from Quintana et al. 2009) 41
Figure I - 11: Experiment of methanol extractives (lignin components) addition (E-type) and removal (R-type) compared to original kenaf core powder (republished from Okuda et al. 2006a, with kind permission of the Japan Wood Research Society) 42
Figure I - 12: Glass transition temperature of biopolymers according to their water content (adapted from Gaudin et al. 1999; Micard et al. 2000; Slade and Levine 1991) 44

Table I - 1: Properties of different plant fibers and synthetic fibers, adapted from Eichhorn et al. (2001) 9
Table I - 2: Summary table of mechanical performances of binderless boards and compared properties obtained by steam pretreatment, steam injection pressing and without treatment* .. **Error! Bookmark not defined.**
Table I - 3: Summary table of mechanical performances of high pressure molding experiments for producing self-bonded plant materials 15

Table I - 4: Summary table of water resistances of self-bonded thermo-compressed plant materials and comparison between steam pretreatement, steam injection and without steam*.....**Error! Bookmark not defined.**
Table I - 5: First report of a time-temperature equivalence for steam pretreatement adapted from US patent 1,824,221 (Mason et al. 1937)..... 21
Table I - 6: Summary table of pptimal steam pretreatment severity for producing self-bonded materials..... 22
Table I - 7: Examples of conditions and mechanical properties of steam injection pressing experiments for production of self-bonded materials..... 24
Table I - 8: Moisture content and effect on the mechanical properties of molded bagasse products (density 1.34-1.36 g/cm^3) - (adapted from Mobarak et al. 1982)..... 30
Table I - 9: List of optimal temperature as reported in the literature for producing self-bonded plant materials without steam 32
Table I - 10: List of optimal temperature as reported in the literature for producing self-bonded plant materials with Process involving steam 32
Table I - 11: Degradation and weight loss measured upon steam pretreatment severity (adapted from Anglès et al. 2001)..... 38

Chapter II:

Figure II - 1: Remains of wheat straw extrusion blockage 49
Figure II - 2: Drawing of a 2D mold (5x5 square shape) 50
Figure II - 3: Drawing of a 3D mold (bowl shape)..... 50
Figure II - 4: Semi 3D compaction molding, the hourglass example 51
Figure II - 5: Drawing of a hourglass shape mold alongside and punch..... 52
Figure II - 6: 2ROP mechanical ejection system 52
Figure II - 7: 2ROP mechanical ejection system (full setup) 53
Figure II - 8: Forced heterogeneity of filling experiment 54
Figure II - 9: Weak spot (whiter) in the centre of dog-bone compacted in forced heterogeneity experiment 54
Figure II - 10: 2D 5x5 plates made from α-cellulose, heterogeneities can be observed even though great attention was paid while filling..... 55
Figure II - 11: Candle holder mold (3 parts)..... 56
Figure II - 12: Candle holder where lines materializes the flow on the edge of the part..... 56
Figure II - 13: Hypothesis of flow behaviour in 3D molding 57
Figure II - 14: Flowability limitation observed on α-cellulose bowl 57
Figure II - 15: The two parts of a compaction-molded miscanthus specimen, violent delamination occurred, the centre of the material was observed to be darker due to moisture accumulation 58
Figure II - 16: Different plant materials compacted in the same conditions, only some suffered from delamination (175°C – eq. 60% RH – 200 MPa – 30 seconds) 58
Figure II - 17: Steam delamination phenomenon and gasket effect - pictures..... 59
Figure II - 18: Steam delamination phenomenon and gasket effect – interpretation 59
Figure II - 19: Slight steam delamination occurring on bowl (pressure was released slowly) 60
Figure II - 20: Transfer molding for rubber molded objects production (reproduced from twistertechnology.com/)..... 60

Figure II - 21: Examples of complicated shapes obtained by transfer molding 61
Figure II - 22: Seizing marks on 2ROP mold (columns guided mold)..... 62

Table II - 1: Properties of specimens obtained with forced heterogeneity compared to control 54

Chapter III:

Figure III - 1: TEM picture of a nano-fibril cellulose micro (white arrow) composing a micro-fibril (black arrow), (reproduced from Chinga-Carrasco 2011) 64
Figure III - 2: Plant cell wall constituents' super organization, reproduced from sigmaaldrich.com.... 64
Figure III - 3: Plant cell-wall super-organization, reproduced from bioenergy.ccrc.uga.edu..... 65
Figure III - 4: Differently oriented cellulose microfibrils in the cell wall (TEM picture, X 30000) reproduced from acces.ens-lyon.fr 65
Figure III - 5: The different cellulose allomorphs..... 66
Figure III - 6: DSC-TGA of α-cellulose under air condition..... 67
Figure III - 7: DSC-TGA of α-cellulose under inert (nitrogen) condition 68
Figure III - 8: "Cellulose microfibers with nanometer unit web like network" also called "microfibrillated cellulose" in the pioneer work of Yano, before the first usage of nanofibrillated cellulose (Yano and Nakahara 2004) 69
Figure III - 9: Bacterial cellulose (wires) and bacteria, synthesis scheme on the left reproduced from (Yamanaka et al. 1989) and SEM picture on the right reproduced from (Iguchi et al. 2000)..... 70
Figure III - 10: Methodology scheme for the evaluations of process's parameters effect 73
Figure III - 11: Thickness-mass relationship and linear regression upon mass change..... 75
Figure III - 12: Effect of mass on the mechanical properties of compressed α-cellulose samples 76
Figure III - 13: Effect of time on the mechanical properties of compressed α-cellulose samples 76
Figure III - 14: Effect of moisture content on the mechanical properties of compressed α-cellulose samples..... 77
Figure III - 15: Effect of pressurization speed on the mechanical properties of compressed α-cellulose samples..... 78
Figure III - 16: Effect of temperature on the mechanical properties of compressed α-cellulose samples 79
Figure III - 17: SEM pictures of specimens' surface produced at different temperatures..... 80
Figure III - 18: Effect of pressure on the mechanical properties of compressed α-cellulose samples . 81
Figure III - 19: Effect of pressure on the specific mechanical properties..... 82
Figure III - 20: compressed α-cellulose samples at 200°C and 8% showing important delamination .. 83
Figure III - 21: Pictures of moisture/temperature mapping samples and differences of colour sorted by moisture – temperature (first picture) and temperature – moisture (second picture)..... **Error! Bookmark not defined.**
Figure III - 22: MC correlated to specific gravity (first set of experiments, evaluation of different parameters)..... 87
Figure III - 23: MC correlated to specific gravity (second set of experiments, evaluation of pressure) 87
Figure III - 24: Cellulose water properties specimens, from the left to the right: 175°C-8% specimens, compared to WS1 specimens, 250 – 0% specimens. 89

Figure III - 25: Bending strength at break correlated to the weight variation of control specimens, standard deviation calculated from 5 repetitions 90
Figure III - 26: SEM picture of α-cellulose powder 91
Figure III - 27: Piles of 6 halves of broken specimens in bending (left) and tensile (right) 91
Figure III - 28: Cross sectional SEM picture of a broken control α-cellulose sample (in bending) 92
Figure III - 29: SEM picture of a surface and cross section of a sample after sandpaper preparation (180 – 360 – 600 – 1200 ISO grit) 93
Figure III - 30: Sandpaper preparation for cross section observations 93
Figure III - 31: Deformation vectors in the case of tensile and 3 points bending 94
Figure III - 32: Cross section of compacted cellulose specimen at 8% - 25°C obtained in X ray tomography with a coloured blue – red porosity scale 95
Figure III - 33: Cross section of compacted cellulose specimen at 0% - 150°C obtained in X ray tomography with a coloured blue – red porosity scale 95
Figure III - 34: Cross section of compacted cellulose specimen at 2% - 250°C obtained in X ray tomography with a coloured blue – red porosity scale 96
Figure III - 35: Cross section of compacted cellulose specimen at 8% - 175 °C obtained in X ray tomography with a coloured blue – red porosity scale 96
Figure III - 36: Transition temperature, maximum densification temperature and specific volume plotted against molding pressure (from Jallabert 2014 PhD thesis) 98
Figure III - 37: PVT diagrams for compacted α-cellulose (Jallabert PhD thesis 2014) 98
Figure III - 38: Force-displacement curves for moistened cellulose flow tests at 200°C in Nagoya ... 101
Figure III - 39: Extruded moistened cellulose off the (4,10) at 200°C (on the left), 100°C on the right 101
Figure III - 40: Force-displacement curves for moistened cellulose flow tests at 100°C in Nagoya ... 102
Figure III - 41: Force-displacement curves for moistened cellulose flow tests at 100°C through a (4,10) die in Nagoya 102

Table III - 1: Summary of the main processing routes from cellulose to solid materials 72
Table III - 2: Summary of control conditions for exploration study of the effect of operating conditions on the mechanical properties of compressed α-cellulose 73
Table III - 3: Summary of results on compacted α-cellulose physical properties.... **Error! Bookmark not defined.**
Table III - 4: Thickness-mass relationship upon mass variation 75
Table III - 5: Moisture content conditions for the evaluation of the effect of moisture content on the mechanical properties of compressed α-cellulose samples 77
Table III - 6: Specific and standard mechanical properties of compressed α-cellulose samples under various conditions of pressure 81
Table III - 7: Molding results on the moisture / temperature experiments 83
Table III - 8: Summary of the mechanical properties of moisture content / temperature effect experiment, the 2 % experiments appear in bold letters 84
Table III - 9: Bending strength (MPa) on the left and Tensile strength (MPa) on the right, mean values for the MC / Temperature with a colour scale blue – red 86
Table III - 10: Bending Modulus (GPa) on the left and Tensile modulus (GPa) on the right, mean values for the MC / Temperature with a colour scale blue – red 86

Table III - 11: Mechanical properties of specimens submitted to 15 days under 85% RH 25°C atmosphere 88
Table III - 12: Water absorption and thickness swelling of compressed cellulose samples..... 89
Table III - 13: Aging tests results..... 90
Table III - 14: Properties of compressed cellulose samples (from Vaca-medina et al. 2013) 97

Chapter IV:

Figure IV - 1: 50x50 mm cellulose samples with fatty compound after 5 drop angle measurements 106
Figure IV - 2: (1/3)Evaluation of fatty compounds for hydrophobation, water drop penetration, ... 108
Figure IV - 3: (2/3)Evaluation of fatty compounds for hydrophobation, water drop penetration, ... 109
Figure IV - 4: (3/3) Evaluation of fatty compounds for hydrophobation, water drop penetration, ... 110
Figure IV - 5: Correlation between GR value and initial water drop angle of recompressed specimens 114
Figure IV - 6: Starting material, grafted material, and comparison of the water drop absorption time on recompressed specimens. 115
Figure IV - 7: The correlation between GR value and the bending modulus of compressed specimens. 116

Table IV - 1: Summary of experimental conditions for fatty compounds evaluation for the hydrophobation of cellulose samples 105
Table IV - 2: Summary of results, investigation of the esterification reaction during molding .....**Error! Bookmark not defined.**

Chapter V:

Figure V - 1: Correlation between cellulose content and extrusion pressure..... 121
Figure V - 2: Orientation of fibers in the direction of flow upon entering the die during flow test ... 122
Figure V - 3: Heterogeneity upon filling cellulose wadding because of its very low apparent density, the specimen is presented next to the 7.5g of origin material..... 124
Figure V - 4: WE1 sample with significant burr on the side 124
Figure V - 5: Barley straw specimens exhibited burr and a surprising sticking effect..... 124
Figure V - 6: Example of results of the swelling tests under the first condition 127
Figure V - 7: PCA1, “compaction molding set”, standardized values, results for PC1, PC2 131
Figure V - 8: PCA2, “compaction molding set” except cellulose, standardized values, results for PC1, PC2..... 132
Figure V - 9: WS1 injected in the mechanical properties specimens’ module..... 135
Figure V - 10: Demolding of the transferred specimens using an aluminium punch..... 135
Figure V - 11: Demolded specimen, burr has been partially removed 136

Table V - 1: Physico-chemical analyses of the native plant materials.....**Error! Bookmark not defined.**
Table V - 2: Flow tests results for the 24 tested materials at 175°C through a (4,10) die 120
Table V - 2: Compaction molding results comparing 50 x 50 mm squares and dog-bone shape 123
Table V - 4: Properties of compaction-molded specimens from native plant materials**Error! Bookmark not defined.**

Table V - 5: Summary of results for the chemical composition of the “compaction molding set” plant materials 128
Table V - 6: Summary of results for the physical characteristics of the “compaction molding set” plant materials 128
Table V - 7: Summary of results for the molded specimens properties of the “compaction molding set” 129
Table V - 8: Cross correlation table “compaction molding set” 130
Table V - 9: Cross correlation table “compaction molding set” except cellulose 133
Table V - 10: Mechanical properties of transfer molded wheat straw specimens compared to compaction -molded 136

Chapter VI, material and methods:

Figure VI - 1: Schematic modular barrels possibilities of the Clextral BC 45 twin screw extruder 158
Figure VI - 2: Screw profile for WE1, WE2 and WE3 production 158
Figure VI - 3: Water uptake against atmosphere Partial Pressure of alpha cellulose 159
Figure VI - 4: ADF/NDF method scheme 162
Figure VI - 5: NF EN ISO 3167 1A specimen compression mold: schematics, first version 164
Figure VI - 6: Picture of the 4th 1A dog-bone specimen compression mold preheating in the MAPA 50 press 164
Figure VI - 7: 45 x 10 mm DMA specimens used for molding water resistance and esterification specimens 165
Figure VI - 8: Description of the press cycle (Chapter III) 166
Figure VI - 9: Flow test setup in Nagoya 167
Figure VI - 10: Flow test setup in Toulouse 168
Figure VI - 11: Example of flow test with the prototype made in Toulouse 168
Figure VI - 12: Transfer molding module for producing mechanical tests specimens 169
Figure VI - 13: Example of mounting of the transfer prototype / flow test built in Toulouse presented equipped with the transfer module. 169
Figure VI - 14: Picture obtained with the Digidrop and used for drop angle measurements in chapter IV 174

Table VI - 1: Parameters for pressurization speed evaluation in chapter (Chapter III) 166